



**Maynooth
University**
National University
of Ireland Maynooth

Application of tailored decadal predictions for Eastern North Atlantic

A dissertation submitted for the degree of
Doctor of Philosophy

By:

Catherine O'Beirne

Under the supervision of:

Dr. Gerard D. McCarthy

Dr. André Düsterhus

ICARUS, Geography Department
National University of Ireland Maynooth
Ollscoil na hÉireann, Má Nuad

February 2024

I would like to dedicate this thesis to my parents
Anne Marie and Stephen.

Declaration

I hereby declare that I have produced this manuscript without the prohibited assistance of any third parties and without making use of aids other than those specified.

The thesis work was conducted from December 2019 to February 2024 under the supervision of Dr. Gerard D. McCarthy and Dr. André Düsterhus in Department of Geography, ICARUS, National University of Ireland Maynooth.

Catherine O'Beirne.

Maynooth, Ireland,

February 2024.

Sponsor

Receiving funding from the Marine Institute Galway as a part of the A4 project until the completion of the research (PBA/CC/18/01).



Collaborations

Dr. Gerard D. McCarthy: As my supervisor, supervised and collaborated on the work of all chapters.

Dr. André Düsterhus: As my supervisor, supervised and collaborated on the work of all chapters.

Dr. Louise Vaughan: Collaborated on the work of Chapter 7 by providing the observational data.

Publications

The chapters contained in this thesis have been either published or submitted to peer-reviewed journals. Chapter 5 has been submitted to the journal *Climate Dynamics* and is currently under review.

Submitted articles (under review):

- O’Beirne, C., & Brune, S., & McCarthy, G. D., & Düsterhus, A. (2023). Decadal Prediction along the Western Irish Coast. Under review in the journal *Climate Dynamics*. *arXiv* preprint: <https://doi.org/10.21203/rs.3.rs-3177972/v1>.

Contents

Abstract	x
Acknowledgements	xi
List of Figures	xiii
List of Tables	xxvi
1 Application of tailored decadal predictions for Eastern North Atlantic Ocean	1
1.1 Introduction	1
1.2 What is prediction?	2
1.3 Interactions and predictability in the Eastern North Atlantic Ocean	6
1.4 Definition of the Atlantic multidecadal variability (AMV)	8
1.5 Definition of the Subpolar Gyre (SPG)	8
1.6 Case Study: Decadal Prediction along the Western Irish Coast	9
1.7 Application of tailored decadal predictions for Irish Fisheries	11
1.8 Effective communication of scientific research	14
1.9 Research Questions	14
1.10 Thesis Contributions	15
1.11 Thesis Structure	17
2 Literature Review	18
2.1 Introduction	18
2.2 Predictability of the physical mechanisms in the Eastern North Atlantic Ocean	19
	vi

2.2.1	Physical mechanisms in the Eastern North Atlantic Ocean . . .	20
2.2.2	Predictability of physical mechanisms	24
2.3	Tailoring of Decadal predictions for stakeholder needs	29
2.3.1	Fish stock management and sustainability	31
2.3.2	Sustainability	33
2.3.3	Environmental and Ecological pressures	36
2.3.4	Mackerel	38
2.4	Effective communication of scientific research	39
2.4.1	Different types of communication	41
2.4.2	Infographics	42
2.4.3	Challenges of communicating science	43
2.5	Summary	44
3	Models and Methods	46
3.1	The MPI-ESM model and components	46
3.1.1	What are ensembles and lead times	49
3.1.2	Initialised Hindcast	50
3.1.3	Uninitialised historical simulations (CMIP5 and CMIP6) . . .	51
3.2	Post-Processing Methods	52
3.3	Calculation of the Anomaly Correlation Coefficient	52
3.4	Investigation into the improvement of skill using sub-sampling. . . .	53
3.4.1	Calculation of AMV	54
3.4.2	Calculation of SPG	54
3.5	Tailoring of decadal predictions for observational data: Stage 1 egg density	55
4	Predictability of the Physical Mechanisms in the North Atlantic Ocean	57
4.1	Introduction	57
4.2	Simulations and methods	58
4.3	Predictability of Sea Surface temperature from the ECHAM6 model	59
4.4	Predictability of Sea Surface temperature from the MPIOM model .	62
4.5	Predictability of Potential temperature from the MPIOM model . .	65

4.6	Predictability of Salinity from the MPIOM model	68
4.7	Discussion	70
5	Case Study: Predictability at depth along the Irish coast	72
5.1	Introduction	72
5.2	Simulations and methods	75
5.3	Predictability of temperature and salinity in the North Eastern At- lantic	76
5.4	Water Mass Analysis in the model along the three transects	79
5.5	Predictability of Potential Temperature along the three transects	82
5.6	Predictability Sea Water Salinity along the three transects	89
5.7	Discussion	94
5.8	Conclusions	96
6	Investigation into improving prediction skill for the Eastern North Atlantic	98
6.1	Introduction	98
6.2	Simulations and methods	99
6.3	Improving prediction skill for potential temperature	101
6.4	Improving prediction skill for salinity	108
6.5	Discussion	114
7	Application of tailored decadal predictions	117
7.1	Introduction	117
7.2	Density and distribution of stage 1 eggs	119
7.3	Prediction skill for West and NE Atlantic northwest of Ireland up to 2014	127
7.4	Prediction skill for West and NE Atlantic northwest of Ireland upto 2019	132
7.5	Effective communicate of scientific research	139
7.6	Discussion	141
8	Conclusions	144
8.1	Introduction	144

8.2	Interactions and predictability in the Eastern North Atlantic Ocean	144
8.3	Investigation into improving prediction skills for the North Atlantic Ocean	145
8.4	Application of tailored decadal predictions for Irish Fisheries	146
8.5	Effective communication of scientific research	148
8.6	Overall Conclusions	149
8.7	Limitations	149
8.8	Thesis Contributions	150
8.9	Future Work	150
A	Appendix	153
	Bibliography	175

Abstract

Predictability is the result of both externally forced and internally generated variability on time scales such as seasonal, annual, and decadal (Meehl et al., 2014). There have been improvements in the field of global decadal prediction. This is in terms of a better understanding of the interactions that occur in our world and in the improvement of the models that are being used. While the consensus is that the models are accurate on a global scale, there is limited confidence in prediction skill on a regional scale. There have been studies conducted on the model components for target areas with some success. This is one of the motivators for this thesis, which investigates the benefits of developing targeted decadal predictions for stakeholder needs. The second motivator is how these predictions can be tailored to stakeholder needs. It will explore the predictability of the North Atlantic Ocean on a decadal time scale for oceanographic properties like ocean temperature, sea salinity, the subpolar gyre (SPG), and Atlantic Multidecadal Variability (AMV). Making this information usable on a regional scale for Ireland would allow tailoring for different applications such as fisheries. The fishery sector is of vast importance to the Irish economy. The ability to predict changes in future stock will support adaptation and fish stock management. The different stages of fish development are dependent on oceanic variables like temperature and salinity so decadal prediction skill for those variables would allow us to make statements on potential changes in fish stock for a species such as Mackerel.

Acknowledgements

First and foremost. I would like to express my appreciation to my supervisors Dr. André Düsterhus and Dr. Gerard D. McCarthy, whose unwavering support has been instrumental throughout my PhD journey. Whose invaluable patience and feedback encouraged me throughout the PhD, even with the numerous questions about coding mistakes. I am thankful for André and Gerard who have guided me through the research process helping me further develop my skills as an independent researcher, that there is no such thing as a stupid question. I would not be where I am today without your guidance and support. Additionally, this endeavour would not have been possible without the generous support from the Marine Institute, which financed my research.

To the staff and postgrads at the Department of Geography, ICARUS at Maynooth University I wish to express my sincere appreciation. Everyone In ICARUS created a welcoming environment. In particular, I would like to thank Corrine who patiently answered all my queries about forms and provided nice conversation on our lunch breaks.

I would like to thank Dr. Gerard McCarthy for applying for our funding and forming the A4 team. Being a part of the A4 team has been a wonderful experience. In particular, thank you to Maeve, André, Ashly, Guillaume, Stephen, Levke, Zoe, Fermin, Patrick, Sam H, Emmanuel, and Sam D. They helped me in my endeavours throughout the PhD, whether it be presentation prep or in the makings of a paper. Without this support, these aspects would have been a challenge.

Thank you to all my collaborators who helped me understand the importance of my work. From Hamburg Sebastian Brune and Leo . From the Marine Institute,

I would like to mention Dr. Louise Vaughan, for assisting the biological aspects of the research and for her kindness. Dr. André Düsterhus, is an amazing person who was willing to help at every opportunity, especially over the final months. I appreciate his guidance and generosity.

Finally, to my family and friends, I am incredibly lucky to have so many wonderful people in my life. A special thank you to my parents, siblings Louise and Mairéad, for all their support, encouragement and listening to me. My brother-in-law Robert and nephew Oisín. My partner Laragh for your love and support. Friends Emma, Aaron, Patrice, Niamh, Amanda, Danie who provided much-needed breaks and support.

List of Figures

1.1	Seasonal-to-decadal climate predictions (highlighted by the section between the grey dashed lines) proceed from an initial condition problem at shorter timescales to a forced boundary-value problem at longer timescales (from (Boer et al., 2016) Figure 1).	4
1.2	This figure shows an example of an Atlantic multidecadal variability (AMV) time series for the years (1880-2010). The red areas are warm phases and the blue areas are cold phases. (from (Vecchi and Delworth, 2017) Figure 1).	8
1.3	This figure shows an example of an subpolar gyre (SPG) index for the years (1960-2015). Time series of observed SPG indices, salinity (SAL) in the upper 500 m in the ENA (lines) and the NAO (bars). For all SPG indices, positive values represent a strong SPG (from (Koul et al., 2020) Figure 3).	9
2.1	Mechanisms that occur within the North Atlantic Ocean and how they interact on timescales generated from the literature. Provides a simplification of a selection of interactions in the North Atlantic Ocean that have an impact on both temperature and salinity.	24
3.1	The Max Plank Institute Earth system model (MPI-ESM) highlighting the 5 systems and how they interact with each other. ECHAM6 (atmosphere), MPIOM (ocean physics), JSBACH (terrestrial biosphere) and HAMOCC (ocean’s biogeochemistry). A separate coupling program, OASIS3, establishes the link between the different components, in which energy, momentum, water and CO2 can be exchanged (From DKRZ, 2021).	48

3.2	From the model three components are analysed; Assimilation Simulation (Internal Variability, External variability, Internal Observations), Uninitialised Historical Simulations (Internal Variability, External variability), Initialised Hindcast Simulations (Internal Variability, External variability, Internal Observations up to a initialisation then Internal Variability, External variability after initialisation). Internal Variability generates information from the climate model (Green box) and External Variability (Orange box).	49
4.1	Schematic representation of the Anomaly correlation coefficient (ACC) method for 16 ensemble members for the proposed variables in 1961-2008. The proposed variables are taken from 2 systems (ECHAM6, MPIOM) in the Max Plank Institute Earth system model (MPI-ESM). The uninitialised historical simulations are taken from the CMIP5 and CMIP6 simulations and the initialised hindcast simulations are taken from decadal prediction. The simulations undergo statistical analysis where for each ensemble member a 2 to 5 year mean is calculated for each year, followed by an ensemble mean. The final step is the ACC calculation where the variables for initialised hindcast simulation, uninitialised historical simulation evaluated against assimilation simulation.	59
4.2	Anomaly correlation coefficient (ACC) for SST (ECHAM6) for initialised hindcast simulation (a and d), uninitialised historical simulation (CMIP5(b), CMIP6 (e)) evaluated against assimilation at lead years 2-5. The difference between initialised hindcast simulation - uninitialised historical (CMIP5(c), CMIP6 (f)) simulation. Generated from the MPI-ESM-LR; 1966-2013; initialised each November; 2 to 5 years lead time; 16 ensemble members. The red is positive correlation, the blue is negatively correlated and the black dots show significance.	61

4.3	Anomaly correlation coefficient (ACC) for SST (MPIOM) for initialised hindcast simulation (a and d), uninitialised historical simulation (CMIP5 (b), CMIP6 (e)) evaluated against assimilation at lead years 2-5. The difference between initialised hindcast simulation - uninitialised historical (CMIP5 (c), CMIP6 (f)) simulation. Generated from the MPI-ESM-LR; 1966-2013; initialised each November; 2 to 5 years lead time; 16 ensemble members. The red is positive correlation, the blue is negatively correlated and the black dots show significance.	64
4.4	Anomaly correlation coefficient (ACC) for Potential Temperature (MPIOM) (6m) for initialised hindcast simulation (a and d), uninitialised historical simulation (CMIP5(b), CMIP6 (e)) evaluated against assimilation at lead years 2-5. The difference between initialised hindcast simulation - uninitialised historical (CMIP5(c), CMIP6 (f)) simulation. Generated from the MPI-ESM-LR; 1966-2013; initialised each November; 2 to 5 years lead time; 16 ensemble members. The red is positive correlation, the blue is negatively correlated and the black dots show significance.	67
4.5	Anomaly correlation coefficient (ACC) for Salinity (MPIOM) for initialised hindcast simulation (a and d), uninitialised historical simulation (CMIP5(b), CMIP6 (e)) evaluated against assimilation at lead years 2-5. The difference between initialised hindcast simulation - uninitialised historical (CMIP5(c), CMIP6 (f)) simulation. Generated from the MPI-ESM-LR; 1966-2013; initialised each November; 2 to 5 years lead time; 16 ensemble members. The red is positive correlation, the blue is negatively correlated and the black dots show significance.	69
5.1	The three sections are the EEL (dark orange line) most northward section, moving south the next section is along Porcupine Bank (PB, red line), and the most southerly section along Goban Spur (GS, navy line).	74

- 5.2 Shows the anomaly correlation coefficient initialised hindcast against assimilation for potential temperature (6m) (a) and seawater salinity (6m) (c) for the North Eastern Atlantic and the difference between initialised hindcast ACC and uninitialised CMIP6 ACC for the North Eastern Atlantic for potential temperature (6m) (b) and seawater salinity (6m) (d). The areas shaded in red highlight the regions that have good predictability, the orange line is the Extended Ellet Line, the yellow line is the Porcupine Bank transect, and the navy line is the Goban Spur. The red areas show that there is a positive skill, the blue shows that there is negative skill and the black dots show that they are significant. Generated from the MPI-ESM-LR; 1966-2013; initialised each November; 2 to 5 years lead time; 16 ensemble members. 78
- 5.3 Potential temperature-salinity diagram using the assimilation (a), initialised hindcast (b), uninitialised historical (CMIP5) (c), uninitialised historical (CMIP6) (d), for the EEL. The colours on the diagram indicate the depth which Orange (6 - 82m), Yellow (100-362m), Green (420 - 1085m), Blue (1220 - 2525m), Darkgreen (2785 - 5720m). Generated from the MPI-ESM-LR; 1966-2013; initialised each November; 2 to 5 years led time; 16 ensemble members. 80
- 5.4 Potential temperature-salinity diagram using the assimilation (a), initialised hindcast (b), uninitialised historical (CMIP5) (c), uninitialised historical (CMIP6) (d), for the Porcupine Bank. The colours on the diagram indicate the depth which Orange (6 - 82m), Yellow (100- 362m), Green (420 - 1085m), Blue (1220 - 2525m), Darkgreen (2785 - 5720m). On plots (c) and (d) show the water masses ENAW, and the LSW. Generated from the MPI-ESM-LR; 1966-2013; initialised each November; 2 to 5 years led time; 16 ensemble members. . 81

5.5	Potential temperature-salinity diagram using the assimilation (a), initialised hindcast (b), uninitialised historical (CMIP5) (c), uninitialised historical (CMIP6) (d), for the Goban Spur. The colours on the diagram indicate the depth which Orange (6 - 82m), Yellow (100- 362m), Green (420 - 1085m), Blue (1220 - 2525m), Darkgreen (2785 - 5720m). On plots (c) and (d) show the water masses ENAW, MOW, and the LSW. Generated from the MPI-ESM-LR; 1966-2013; initialised each November; 2 to 5 years led time; 16 ensemble members.	82
5.6	Potential temperature values from the model for the assimilation (a), initialised hindcast (b), uninitialised historical (CMIP5) (c), uninitialised historical (CMIP6) (d) simulations along the EEL transects. The red areas show that there is positive skill, the blue shows that there is negative skill and the black dots show that they are significant. Generated from the MPI-ESM-LR; 1966-2013; initialised each November; 2 to 5 years lead time; 16 ensemble members.	84
5.7	Potential temperature values from the model for the assimilation (a), initialised hindcast (b), uninitialised historical (CMIP5) (c), uninitialised historical (CMIP6) (d) simulations along the Porcupine Bank transects. The red areas show that there is positive skill, the blue shows that there is negative skill and the black dots show that they are significant. Generated from the MPI-ESM-LR; 1966-2013; initialised each November; 2 to 5 years lead time; 16 ensemble members.	85
5.8	Potential temperature values from the model for the assimilation (a), initialised hindcast (b), uninitialised historical (CMIP5) (c), uninitialised historical (CMIP6) (d) simulations along the Goban Spur transects. The red areas show that there is positive skill, the blue shows that there is negative skill and the black dots show that they are significant. Generated from the MPI-ESM-LR; 1966-2013; initialised each November; 2 to 5 years lead time; 16 ensemble members.	86

5.9	Anomaly correlation coefficient against assimilation for potential temperature at lead years 2 to 5, using the initialised hindcast (a-c), uninitialised historical (CMIP6) (d-f), hindcast - uninitialised historical (g-i) for the EEL, Porcupine Bank, and Goban Spur. The red areas show that there is positive skill, the blue shows that there is negative skill and the black dots show that they are significant. Generated from the MPI-ESM-LR; 1966-2013; initialised each November; 2 to 5 years lead time; 16 ensemble members.	88
5.10	Anomaly correlation coefficient against assimilation for potential temperature at lead years 2 to 5, using uninitialised historical (CMIP5) (a-c), hindcast - uninitialised historical (d-f) for the EEL, Porcupine Bank, and Goban Spur. The red areas show that there is positive skill, the blue shows that there is negative skill and the black dots show that they are significant. Generated from the MPI-ESM-LR; 1966-2013; initialised each November; 2 to 5 years lead time; 16 ensemble members.	89
5.11	Sea water salinity values from the model for the assimilation (a), hindcast (b), uninitialised historical (CMIP5) (c), uninitialised historical (CMIP5) (d) simulations along the EEL. Generated from the MPI-ESM-LR; 1966-2013; initialised each November; 2 to 5 years led time; 16 ensemble members.	90
5.12	Sea water salinity values from the model for the assimilation (a), hindcast (b), uninitialised historical (CMIP5) (c), uninitialised historical (CMIP5) (d) simulations along the Porcupine Bank. Generated from the MPI-ESM-LR; 1966-2013; initialised each November; 2 to 5 years led time; 16 ensemble members.	91
5.13	Sea water salinity values from the model for the assimilation (a), hindcast (b), uninitialised historical (CMIP5) (c), uninitialised historical (CMIP5) (d) simulations along the Goban Spur. Generated from the MPI-ESM-LR; 1966-2013; initialised each November; 2 to 5 years led time; 16 ensemble members.	92

5.14	Anomaly correlation coefficient against assimilation for sea water salinity at lead years 2 to 5, using the initialised hindcast (a-c), uninitialised historical (CMIP6) (d-f), hindcast - uninitialised historical (g-i) for the EEL, Porcupine Bank, and Goban Spur. The red areas show that there is positive skill, the blue shows that there is negative skill and the black dots show that they are significant. Generated from the MPI-ESM-LR; 1966-2013; initialised each November; 2 to 5 years lead time; 16 ensemble members.	93
5.15	Anomaly correlation coefficient against assimilation for sea water salinity at lead years 2 to 5, using uninitialised historical (CMIP5) (a-c), hindcast - uninitialised historical (d-f), for the EEL, Porcupine Bank, and Goban Spur. The red areas show that there is positive skill, the blue shows that there is negative skill and the black dots show that they are significant. Generated from the MPI-ESM-LR; 1966-2013; initialised each November; 2 to 5 years lead time; 16 ensemble members.	94
6.1	Schematic representation of the sub-sampling method 16 ensemble members for temperature and salinity from the initialised hindcast simulations in 1961-2008, for a 2 to 5 year lead time. The data is taken from the decadal prediction system where the full ensemble series undergoes statistical analysis, the assimilation simulation is used to create the two predictor time-series. The two predictor time-series are correlated with the Northeastern Atlantic Ocean at each location over the time frame. In every location and time we start with the output of the 16 ensemble members generated by initialised hindcast simulations and only select those members in which they agree with the predictor. Those selected ensemble members are then correlated with the Northeastern Atlantic Ocean at each location over the time frame. The final step highlighted three locations from the Northeastern Atlantic Ocean that had no skill through the 16 ensemble members, explored if the 8 sub-selected ensembles members improves skill. . . .	101

- 6.2 ACCs for Potential Temperature for initialised hindcast simulation (a, c), AMV (b), SPG (d) evaluated against assimilation at lead years 2-5. The difference between initialised hindcast simulation - uninitialised historical (CMIP5(c), CMIP6 (f)) simulation. Generated from the MPI-ESM-LR; 1966-2013; initialised each November; 2 to 5 years lead time; 16 ensemble members; depth mean 6m – 220m. The red is positive correlation, the blue is negatively correlated and the black dots show significance. The yellow hatching shows whether there is a positive or negative correlation between the initialised hindcast simulations (a, c) and the predictors (b, d). 103
- 6.3 Improvement of the prediction of Potential Temperature in the Eastern North Atlantic due to more accurate prediction of the AMV, SPG, and both. ACCs for Potential Temperature for initialised hindcast simulation (16 ensemble members) (a, d, g), Sub-sampled initialised hindcast simulation (8 ensemble members) (AMV (b), SPG (e), both(h)) evaluated against assimilation at lead years 2-5. The difference between initialised hindcast simulation sub-sampled initialised hindcast simulation (8 ensemble members) (SPG (c), AMV (f), both (i)) simulation. Generated from the MPI-ESM-LR; 1966-2013; initialised each November; 2 to 5 years lead time; depth mean 6m – 220m. The red is positive correlation, the blue is negatively correlated and the black dots show significance. Red dots in the right column indicate regions that became significant after sub-sampling. . 105

6.4	<p>Time series for Potential Temperature from the three yellow hatched areas (6.1), it was normalised and detrended. They will be referred to as South East (a-c), South West (d-f), and North (g-i). Each location correlates the initialised hindcast simulation (16 ensemble members) (a, d, g), Sub-sampled initialised hindcast simulation (8 ensemble members) (SPG (b, e, h), AMV (c, f, i)) against assimilation at lead years 2-5. The blue line is the ensemble mean for the assimilation simulation, the red line is the ensemble mean for the initialised hindcast simulation, and the grey dots are the ensemble members. The initialised hindcast (16 ensemble members) when correlated with the assimilation at each location is quite low, South East (-0.315), South West (0.007), North (0.225). The sub-sampled (SPG) initialised hindcast (8 ensemble members) when correlated with the assimilation at each location overall is poor, South East (-0.323), South West (-0.125), North (0.337). The sub-sampled (AMV) initialised hindcast (8 ensemble members) when correlated with the assimilation at each location has some improvement, South East (-0.177), South West (0.201), North (0.145). Generated from the MPI-ESM-LR; 1966-2013; initialised each November; 2 to 5 years lead time; depth mean 6m – 220m.</p>	107
6.5	<p>ACCs for Salinity for initialised hindcast simulation (a, c), AMV (b), SPG (d) evaluated against assimilation at lead years 2-5. The difference between initialised hindcast simulation - uninitialised historical (CMIP5 (c), CMIP6 (f)) simulation. Generated from the MPI-ESM-LR; 1966-2013; initialised each November; 2 to 5 years lead time; 16 ensemble members; depth mean 6m – 220m. The red is positive correlation, the blue is negatively correlated and the black dots show significance. The yellow hatching shows whether there is a positive or negative correlation in the initialised hindcast simulations (a, c) and the predictors (b, d).</p>	109

- 6.6 Improvement of the prediction of Salinity in the Eastern North Atlantic due to more accurate prediction of the AMV, SPG, and both. ACCs for Potential Temperature for initialised hindcast simulation (16 ensemble members) (a, d, g), Sub-sampled initialised hindcast simulation (8 ensemble members) (AMV(b), SPG (e), both(h)) evaluated against assimilation at lead years 2-5. The difference between initialised hindcast simulation - sub-sampled initialised hindcast simulation (8 ensemble members) (SPG(c), AMV (f), both (i)) simulation. Generated from the MPI-ESM-LR; 1966-2013; initialised each November; 2 to 5 years lead time; depth mean 6m – 220m. The red is positive correlation, the blue is negatively correlated and the black dots show significance. Red dots in the right column indicates regions that became significant after sub-sampling. 111
- 6.7 Time series for Potential Temperature from the three yellow hatched areas (6.5), it was normalised and detrended. They will be referred to as South East (a, b, c), South West (d, e, f), and North (h, i, j). Each location correlates the initialised hindcast simulation (16 ensemble members) (a, d, g), Sub-sampled initialised hindcast simulation (8 ensemble members) (SPG (b, e, h), AMV (c, f, i)) against assimilation at lead years 2-5. The blue line is the ensemble mean for the assimilation simulation, the red line is the ensemble mean for the initialised hindcast simulation, and the grey dots are the ensemble members. The initialised hindcast (16 ensemble members) when correlated with the assimilation at each location is quite low, South East (0.455), South West (-0.095), and North (0.507). The sub-sampled (SPG) initialised hindcast (8 ensemble members) when correlated with the assimilation at each location overall is poor, South East (0.361), South West (-0.231), North (0.428). The sub-sampled (AMV) initialised hindcast (8 ensemble members) when correlated with the assimilation at each location has some improvement, South East (0.505), South West (0.136), North (0.554). Generated from the MPI-ESM-LR; 1966-2013; initialised each November; 2 to 5 years lead time; depth mean 6m – 220m. 113

7.1	Schematic representation of how both the model data (1989-2015) and the observational data (1992-2014) is initial explored to determine the similarity between the two. Two regions have been identified for this study the NE Atlantic northwest of Ireland (Northern Territory) and the West of Ireland (Irish Territory). These regions under went statistical analysis. The model data undergoes time series analysis and is extended out to 2019, this time series is then compared to the observational data.	118
7.2	An illustration of the true extent of Ireland’s Territory in both land mass and ocean with the border highlighted by the red line. The majority of the territory is in the North Atlantic, on the shelf highlighted by the regions in orange and the deeper ocean highlighted by the darkening blue colours (From Marine Institute (2022))	119
7.3	Atlantic Mackerel (<i>Scomber Scombrus</i>) egg density data at each location for every 3 years from 1992 - 2016, were the size blue circle represents the density of eggs found and the red crosses shows that there have no eggs been found.	121
7.4	<i>Scomber Scombrus</i> (Atlantic Mackerel) egg density data at each location for every 3 years from 1992 - 2016, where each blue circle represents the number of eggs found and the red crosses shows that there have no eggs been found. The red box highlights the Irish territory and the black box highlights Northern territory with the potential increase in temperature.	123
7.5	<i>Trachurus Trachurus</i> (Horse Shoe Mackerel) egg density data at each location for every 3 years from 1998 - 2016, were the size blue circle represents the density of eggs found and the red crosses shows that there have no eggs been found.	124
7.6	<i>Trachurus Trachurus</i> (Horse Shoe Mackerel) egg density data at each location for every 3 years from 1992 - 2016, where each blue circle represents the number of eggs found and the red crosses shows that there have no eggs been found. The red box highlights the Irish territory and the black box highlights Northern territory with the potential increase in temperature.	125

7.7	West of Ireland: Time series of temperature and egg density 3 years from 1992 - 2016.	126
7.8	NE Atlantic northwest of Ireland: Time series of temperature and egg density 3 years from 1998 - 2016.	127
7.9	Anomaly correlation coefficient (ACC) for potential temperature (MPIOM) for initialised hindcast simulation evaluated against assimilation at lead years 2-5. Generated from the MPI-ESM-LR; 1991-2014; initialised each November; 2 to 5 years lead time; 16 ensemble members; depth mean 6-220m. The red is a positive correlation the black crosses show significance. The black lined box is the NE Atlantic northwest of Ireland and the red shows the West of Ireland.	129
7.10	Time series for potential temperature (MPIOM) for initialised hindcast simulation (black line) evaluated against assimilation (blue line) at lead years 2-5. Generated from the MPI-ESM-LR; 1989 -2014; initialised each November; 2 to 5 years lead time; 16 ensemble members; depth mean 6-220m. This was compared with the observational temperature data (red line) 1992 - 2014 for the a) NE Atlantic northwest of Ireland and 1998 - 2014 for the b) West of Ireland.	131
7.11	Time series for potential temperature (MPIOM) for initialised hindcast simulation (black line) evaluated against assimilation (blue line) at lead years 2-5. Generated from the MPI-ESM-LR; 1989 -2019; initialised each November; 2 to 5 years lead time; 16 ensemble members; depth mean 6-220m. This was compared with the observational temperature data (red line) 1992 - 2014 for the a) NE Atlantic northwest of Ireland and 1998 - 2014 for the b) West of Ireland.	133
7.12	Time series for potential temperature (MPIOM) for initialised hindcast simulation evaluated against assimilation at lead years 2-5. Generated from the MPI-ESM-LR; 1991-2019; initialised each November; 2 to 5 years lead time; 16 ensemble members; depth mean 6-220m. This was compared with the observational temperature data (red line) 1992 - 2019 for the a) NE Atlantic northwest of Ireland and 1998 - 2019 for the b) West of Ireland.	135

7.13 West of Ireland: Detrended time series for the initialised hindcast simulations (MPIOM) for initialised hindcast simulation evaluated against assimilation at lead years 2-5 (Red line). Generated from the MPI-ESM-LR; 1991-2019; initialised each November; 2 to 5 years lead time; 16 ensemble members; depth mean 6-220m, with error bars (Black lines). 136

7.14 NE Atlantic northwest of Ireland: Detrended time series for the initialised hindcast simulations (MPIOM) for initialised hindcast simulation evaluated against assimilation at lead years 2-5 (Red line). Generated from the MPI-ESM-LR; 1991-2019; initialised each November; 2 to 5 years lead time; 16 ensemble members; depth mean 6-220m, with error bars(Black Lines). 137

7.15 Time series for Egg Density data from the observational data from the ICES survey report for Atlantic mackerel. Plot a) shows the changes in egg density in the NE Atlantic northwest of Ireland for the time frame 1992-2019. Plot b) shows the changes in egg density in the West of Ireland for the time frame 1998-2019. 138

7.16 Info-graphic connecting the observational data from the ICES survey report with the model. Highlighting that the model can predict potential shifts in mackerel stock. 140

List of Tables

6.1	Summary of the different locations correlations for potential temperature for the initialised hindcast and the two-predictor sub-sampled ensemble members against the assimilation simulation	116
6.2	Summary of the different locations correlations for salinity for the initialised hindcast and the two-predictor sub-sampled ensemble members against the assimilation simulation	116

Application of tailored decadal predictions for Eastern North Atlantic Ocean

1.1 Introduction

The impacts of climate change have become clearer over the last few decades. Changes in the atmospheric mode of the North Atlantic Oscillation (NAO) can influence temperature on land resulting in warmer summers, in wintertime there is an increase in precipitation and storminess (Curtis et al., 2016; Fan et al., 2016; Dobrynin et al., 2018). There have been observations of warming sea surface temperatures (SST) (Brown et al., 2016) with a possibility of previously cool waters warming. There are a range of goods and services that humans obtain from the ocean; from economic (the fishery industry) (Payne et al., 2021) to recreational (Halpern et al., 2012). Climate variability strongly influences fish stocks with changes in productivity resulting in major consequences for socio-economic systems that rely on these resources (Koul et al., 2021). These include a shift in species abundance, distribution, and productivity, resulting in a complex and un-

even distribution of the fish stock that hurts coastal communities (Mason et al., 2021; Payne et al., 2021; Sandø et al., 2020). With an increasing threat of climate change, expanding on the understanding of the impact of climate variability has become more central (Koul et al., 2021).

Climate variability on inter-annual to decadal timescales can alter the size of ongoing long-term climate change (Koul et al., 2021). Human society and natural ecosystems are vulnerable to climate variability and change (Smith et al., 2019). Taking account of these changes in management systems can improve outcomes for fishery catches and in turn profits under most climate scenarios (Mason et al., 2021). The inclusion of climate information into the modelling of exploitable resources, aids in the understanding of ecological processes but also forecasts future states of the system on these timescales (Koul et al., 2021). A key aspect of climate-adaptive management is the inclusion of forecasting and incorporating future climate scenarios into management decisions (Mason et al., 2021). However, management systems can be restrictive to fishery companies that have access to the scientific and technical ability to adapt to climate change (Mason et al., 2021). Few sectors can make direct use from information from predictions besides scientists and policymakers (Dunstone et al., 2022).

1.2 What is prediction?

To start to answer this we first need to know the difference between prediction and predictability. Prediction is used for a forecast or projection. While predictability is the result of both externally forced and internally generated variability (Meehl et al., 2014). It is part of a physical and or mathematical system that characterises “its ability to be predicted” (Meehl et al., 2014; Boer et al., 2016). A variety of prediction systems have been around for a long time. This includes weather predictions and climate projections on a scale of up to 100 years. A new development is predictions of a few months to a few years ahead, called seasonal and decadal predictions. There are a variety of different designs of decadal prediction systems, they consist of either multi-member single-model suites or based on multi-model suites (Schuster et al., 2019). Skill is defined as the comparison of the observational data with the initialised hindcast or uninitialised historical simulations

over a common period (Sgubin et al., 2021). Initialised hindcasts are retrospective predictions initialised at a given past climate state (Sgubin et al., 2021).

Decadal predictions provide key information for a variety of sectors including agriculture, water management and others (Shaffrey et al., 2017; Mariotti et al., 2020). It is an active research field that is growing yearly with varying distinct types of models with a variety of applications that are socially relevant to suitable strategies for adaption (Volpi et al., 2017; Schuster et al., 2019). It makes a bridge between short seasonal to seasonal predictions and climate projections with a focus on annual, multi-annual to decadal time scales (Boer et al., 2016; Volpi et al., 2017). It should be noted that while there has been an increase in the demand for long term predictions. Challenges still exist in the development of skilful and statistically reliable climate predictions (Shaffrey et al., 2017).

These short time scales can range from weather predictions to monthly or seasonal predictions, the long-term time scales are climate change projections. Figure 1.1 is one such example of the breakdown of the different types of prediction scales up to climate projections. The weather predictions start with a first value problem and use these to predict the following day, week, month, and season. For long-term projections, these are mainly climate change focused, where they look beyond a decade to a century, and these are mainly forced boundary-value problem-based. These two regimes overlap for seasonal to decadal predictions, which incorporate time scales of a few months to multiple years. Incorporating both aspects of the other two-time scales to generate robust predictions. Seasonal to decadal predictions is an area that has so much potential and applications. There are a vast number of different prediction systems that exist and within each model, there are numerous different kinds of components that have various interactions with each other. The goal of these models is to attempt to replicate the state of the real-world environment, these are called assimilation simulations. They also generate prediction systems that are based on whether they are initialised or uninitialised, with the aim being that the initialisation generates an improvement in prediction skills. The model that will be used throughout this thesis is the Max Planck Institute earth system model (MPI-ESM-LR). In Chapter 4 the different components of the MPI-ESM and how they interact with each other will be explored.

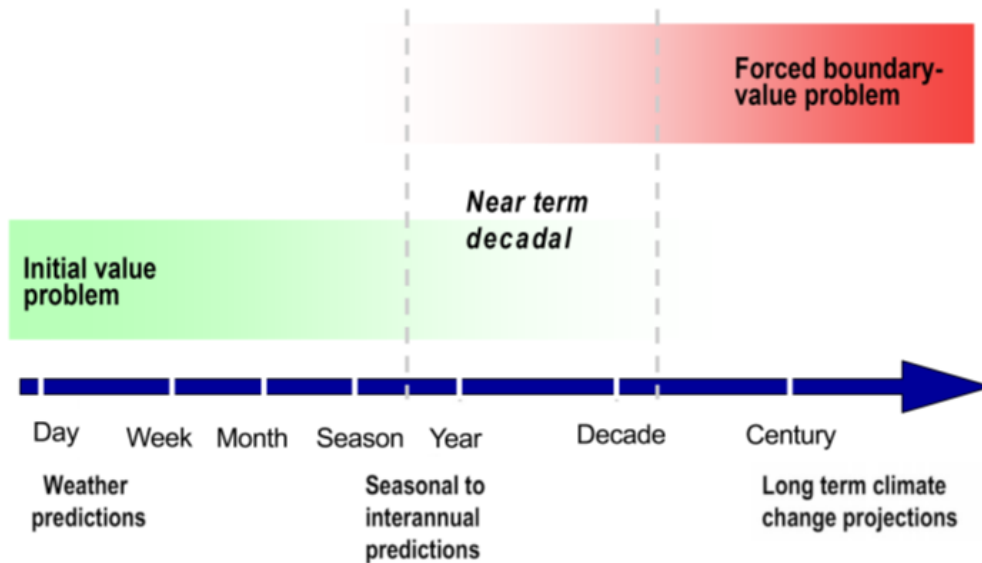


Figure 1.1: Seasonal-to-decadal climate predictions (highlighted by the section between the grey dashed lines) proceed from an initial condition problem at shorter timescales to a forced boundary-value problem at longer timescales (from (Boer et al., 2016) Figure 1).

The research will be divided into three parts, exploration into the understanding of the physics of the ocean, the statistics post-processing sub-sampling to improve prediction and the application of these predictions to fisheries. The first stage of this research will be understanding Atlantic variability and its connection to the Irish seas. This is the physical part that will identify predictors from the North Atlantic Ocean for the Irish climate. Mechanisms are identified to be applied as constraints within statistical post-processing including Atlantic sea surface temperature variations, AMV, and subpolar gyre variability, SPG. This will allow for advancing knowledge on Irish SST change and variability in an Atlantic context and focus the research further on the sub-sequential stages. I will investigate its effect on a selection of climate modes such as the AMV, and SPG, on ocean variables SST, and sea SSS at depth. This will begin the second stage of the statistical analysis to improve prediction. Including AMV and SPG in the improvement of the prediction, we see a positive effect on the prediction of temperature and salinity at depth. While there have not been many studies conducted that included the AMV as a mode in prediction systems. The investigation into the improvement

of decadal prediction skills in the North Atlantic Ocean has begun in terms of exploring the impact the SPG and AMV have on SST and SSS at depth. The first results show that there is some good prediction improvement, however SSS shows greater improvement than SST. The use of these mechanisms in prediction systems to improve the prediction skill for the North Atlantic Ocean. The identified mechanisms will then undergo statistical post-processing such as sub-sampling, which is a process that was developed to create better predictions on seasonal timescales. This method will be adapted within the thesis for the development of predictive capacity on decadal timescales. To use the understanding of the specific sources for decadal predictability from the North Atlantic Ocean and then use this information to tailor decadal predictions to stakeholder needs. Finally, how can this information be communicated to the stakeholders, this can be achieved through a simple infographic. But first, we need to get an understanding of the mechanism and predictability of the North Atlantic Ocean.

The Max Planck Institute Earth system model low resolution “MPI-ESM-LR” consists of 5 systems (ECHAM6, JSBACH, MPIOM, HAMOCC, and OASIS) that interact with each other and will be used in this thesis (Brune and Baehr, 2020). The initial exploration of decadal predictability was using the ECHAM6 data to explore the atmospheric/oceanic interaction in the North Atlantic Ocean. The MPIOM data contains just the ocean information which was explored at various depth levels. Many different statistical tools are used to identify the physical mechanisms in climate models, among them the Anomaly Correlation Coefficient (ACC;(Dobrynin et al., 2018, 2019; Borchert et al., 2018)) and composite plots (Borchert et al., 2018, 2019). The ACC is used to determine the prediction skill of model predictions compared to reanalyses or observations. The significance of each location of the predictions is determined using bootstrapping. Borchert et al. (2018) determined that there is an indication for significant ACC in the North Atlantic Ocean to be connected to low-frequency ocean dynamics, which break down when the atmosphere contributes significantly to SST variability. The composite plots used by Borchert et al. (2018, 2019) were used to distinguish between the effects of warm and cold Ocean Heat Transport phases or subpolar gyre SST phases on the surface SST over Europe.

The ocean modes identified above were fed into the model to determine if there was an improvement in prediction skill for SST and SSS at depth for the North Atlantic Ocean. This allowed for the generation of composite plots to determine if the SPG and the AMV had an impact on the prediction skill for both SST and SSS at depth. The initial analysis illustrated that the internal mechanisms in the model had more skill than taking the SPG, and the AMV into consideration. We aim to improve decadal prediction skills in the North Atlantic Ocean using the process of ensemble sub-sampling. Applying this methodology on seasonal scales has demonstrated improved prediction skills for other climate modes.

1.3 Interactions and predictability in the Eastern North Atlantic Ocean

In recent years there have been vast improvements in the field of decadal prediction on a global scale based on the understanding of the mechanisms that occur in the North Atlantic Ocean. The North Atlantic Ocean has already been shown to be predictable on decadal timescales (Marotzke et al., 2016). Understanding these interactions will allow for a greater understanding of how interconnected the various cycles that occur are. How they can influence temperature and salinity not only daily but on longer time scales such as multidecadal. This can be broken down into two sections the oceanographic and atmospheric components. The focus is the oceanographic components as they can be tailored for application for stakeholder needs such as fisheries. It is important to understand both aspects as they both contain drivers in the North Atlantic Ocean, with a key interest in the influence on Ireland. One atmospheric pattern with a large effect on the Irish climate is the North Atlantic Oscillation (NAO) (García-Serrano et al., 2015). Changes in the amplitude and sign of the winter NAO are strongly linked to the patterns of winter temperature, precipitation, and storminess (wave power/height) (Curtis et al., 2016; Fan et al., 2016; Dobrynin et al., 2018).

The oceanic patterns that need to be considered are the Atlantic Meridional Overturning Circulation (AMOC), the Subpolar Gyre (SPG), and Atlantic Multidecadal Variability (AMV), also referred to as the Atlantic Multidecadal Oscil-

lation (AMO). All of which interact with temperature and salinity on a longer time scale than their atmospheric counterparts. Some of the oceanic interactions that occur in the North Atlantic Ocean that influence temperature and salinity are AMOC, SPG, and AMV/AMO (Muir and Fedorov, 2015). Where variations of the AMOC are believed to be an important driver of decadal to multidecadal climate variability and play an important role in the climate system by transporting heat northwards in the Atlantic (Jackson et al., 2015; Muir and Fedorov, 2015). On a longer timescale temperature is often referred to as AMV/AMO where variations in the AMOC are suggested to have some control or contribution to the AMV/AMO, however, the physics behind the AMV/AMO remains uncertain and a matter for debate (Muir and Fedorov, 2015; Brown et al., 2016). One of the fundamental variables for the ocean circulation and global climate is salinity as it provides the density of water masses that take part in the upper branch of the AMOC (Friedman et al., 2017). There have been a variety of studies that point to the SPG being a key component in the North Atlantic decadal climate variability, with some of this variability being connected to the NAO (Born et al., 2015; Buckley and Marshall, 2016).

Understanding the mechanisms within the North Atlantic Ocean, and how they interact with both temperature and salinity is a key aspect of how they are represented in the model. Exploration of these variables will be conducted using the Max Planck Institute Earth System Model (MPI-ESM). The initial investigation will explore predictability at the surface for both temperature and salinity on a 2-to-5-year lead time for the period 1966-2013. This was completed for both temperature and salinity at depth for the initialised hindcast simulations and uninitialised historical simulations. This allows for a comparison to be made on whether there is an improvement in skill using an initialised simulation compared to uninitialised simulations.

Chapter 4 determines if there is prediction skill in the Eastern North Atlantic Ocean in the MPI-ESM for sea surface temperature and salinity also showing areas of significance. This will be completed for three types of sea surface temperature: the first from the atmospheric model (ECHAM6-Tas), and the oceanic model (MPIOM- Tos, Thetao).

1.4 Definition of the Atlantic multidecadal variability (AMV)

The first predictor that will be used in this thesis is the Atlantic multidecadal variability (AMV). Chapter 6 subsection 3.4.1 highlights the methodology I have employed for calculating the AMV. AMV is the term used to describe the decadal variability of North Atlantic SSTs, broadly characterised by decades of basin-wide warm or cool anomalies, relative to the global mean (Sutton et al., 2018). Some suggest that it arises from variations with the AMOC with influence from the North Atlantic winds (Vecchi and Delworth, 2017). Figure 1.2 is an example of the AMV for a longer time scale roughly 1880 to 2010. In this thesis a similar process is used, however the AMV will be for a shorter time frame 1960-2013.

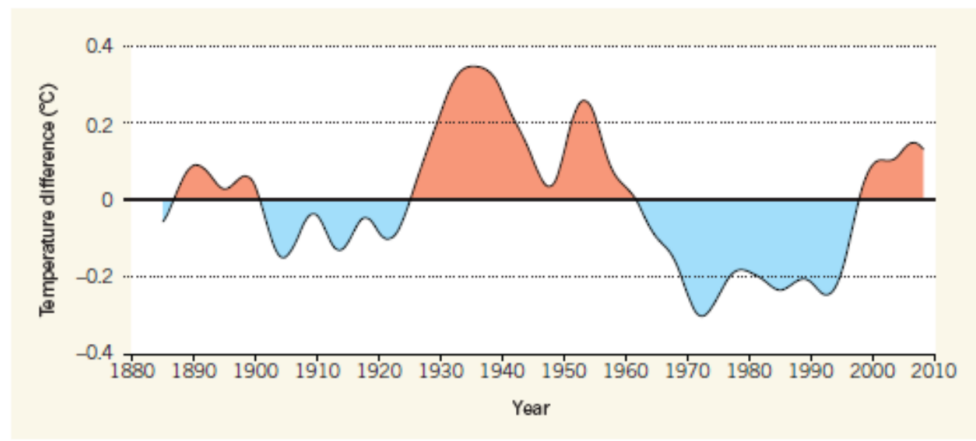


Figure 1.2: This figure shows an example of an Atlantic multidecadal variability (AMV) time series for the years (1880-2010). The red areas are warm phases and the blue areas are cold phases. (from (Vecchi and Delworth, 2017) Figure 1).

1.5 Definition of the Subpolar Gyre (SPG)

The second predictor that will be used in this thesis is the Atlantic multidecadal variability (AMV). Chapter 6 subsection 3.4.2 highlights the methodology I have employed for calculating the Subpolar gyre (SPG) index. Surface waters of the eastern subpolar gyre in the North Atlantic are exceptionally warm and salty compared to the surface waters at similar latitudes, leading to the supposition that

the subpolar gyre is primarily supplied by the similarly warm and salty waters of the subtropical gyre (Foukal and Lozier, 2016). The North Atlantic SPG is attributed mainly to the passive advection of surface salinity anomalies of remote origin (Born et al., 2016). Sea surface characteristics of the North Atlantic SPG provide the environment for density-driven overturning, the warm surface water loses heat to the atmosphere becomes denser and sinks to depth as it flows around the SPG (Foukal and Lozier, 2016). Figure 1.3 is an example of an SPGI for a similar time scale roughly 1960 to 2015. The SPGI that will be calculated in 6 will be for a similar time frame 1961-2013.

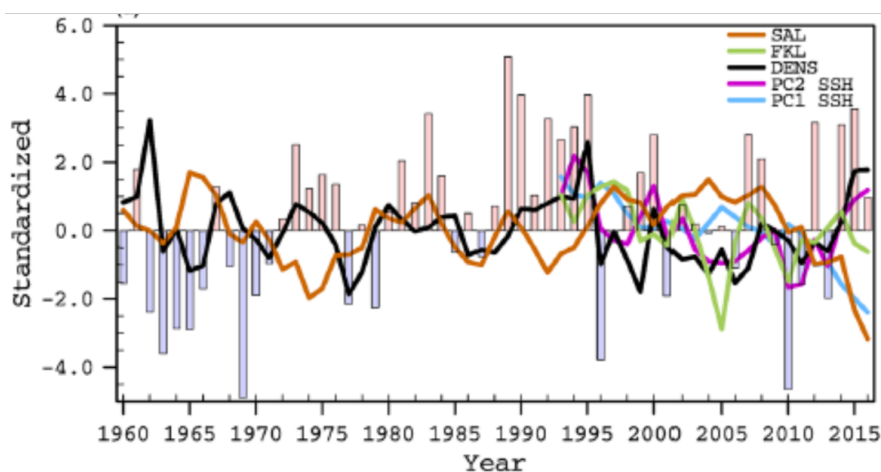


Figure 1.3: This figure shows an example of an subpolar gyre (SPG) index for the years (1960-2015). Time series of observed SPG indices, salinity (SAL) in the upper 500 m in the ENA (lines) and the NAO (bars). For all SPG indices, positive values represent a strong SPG (from (Koul et al., 2020) Figure 3).

1.6 Case Study: Decadal Prediction along the Western Irish Coast

In this case study the predictability of the surface of the ocean for both temperature and salinity were explored along the Western Irish coast. The results show that for this region, it is predictable and that the skill is significant. In this case study I wanted to go beyond the surface and determine if the model system could be skilful at depth and if it is significant. Studies have shown that both atmospheric (North Atlantic Oscillation) and oceanic processes (sub-polar gyre) can be

replicated within models in both initialised hindcast simulations and uninitialised historical simulations (Andrews et al., 2015; Athanasiadis et al., 2017; Barcikowska et al., 2018; Koul et al., 2019). However, there is limited research completed on the predictability of potential temperature and salinity at depth, both on a global and a regional scale just for the ocean. By having the ability to predict changes in climate variables such as temperature and salinity for a target region, informed decisions can be made about environmental and economic conditions.

Three transects were identified (Extended Ellett line, Porcupine Bank, Goban Spur) to explore temperature and salinity at depth for the initialised hindcast simulations and uninitialised historical simulations. This allows for a discussion to be made on whether there is an improvement in skill using initialisation. Two uninitialised historical simulations ("CMIP5", and "CMIP6") were used to highlight the potential improvements that have developed between the simulations. Allowing for a detailed examination of the different simulations and comment on the prediction skill obtained.

1. Does the model system have prediction skill at depth for temperature?
2. Does the model system have prediction skill at depth for salinity?
3. Does the model system have prediction skill at depth for both initialised and uninitialised simulations?

This study investigates the predictability within the Northeastern Atlantic at depth with an initialised decadal prediction system. Both temperature and salinity at the West Coast of Ireland are compared for 2 to 5 years ahead in a 16-member initialised decadal prediction system and in two 16-member uninitialised historical simulations from the Max Planck Institute Earth system model for the period 1966-2013. We find that there is predictability in the upper levels of the Northeastern Atlantic up to a depth of 1000m for temperature and salinity. For the same period, we analysed water mass properties and prediction skills along three transects (Extended Ellett line, Porcupine Bank, and Goban Spur).

1.7 Application of tailored decadal predictions for Irish Fisheries

There is a growing interest among many stakeholders in the coming decade, there is an increasing need for decadal climate predictions (Smith et al., 2019). For this Chapter 7, we begin to tailor the predictions more towards the use of the fishery sector. This is achieved by getting a mean over the depth of 6 - 220m for both temperature and salinity before the data undergoes analysis. At this depth, we capture the habitable zone for mackerel and the spawning level. Temperature and salinity are two important factors that influence the spawning habits of Atlantic and Horseshoe mackerel. Having the ability to predict changes in either will help create robust management strategies. To achieve this there first needs to be an understanding of the physical mechanisms that influence temperature and salinity. Then how are these variables represented in the model system and are they predictable on decadal timescales? We know that international fisheries are a massive source of both food and revenue generation from an area of the environment that is majority open access (Wilder, 1995). With a high demand for this source commercial fisheries are experiencing increasing pressure from environmental conservation and the higher demand from competing vessels (Symes et al., 2015). This demand could lead to unsustainable fishing practices which in turn can result in over-fishing or over-exploitation of the species (Olson, 2011). To attempt to reduce the economic impact this may have there was a move to privatise fishing rights where access to fishing grounds were limited, a variety of quota systems were implemented, and permit leasing (Olson, 2011). Observations have been made that when it comes to the oceans shifts in species distributions happen faster compared to those on land (Sumby et al., 2021). This has implications for fisheries as it can result in drastic changes in species abundance, this is due to changes in the reproductive or recruitment capacity (Sumby et al., 2021).

While prediction of such key global and large-scale indices is useful to scientists and policymakers, there are few sector end-users who can make direct use of this information in their operations (Dunstone et al., 2022). For many cultures and countries fishing has been an integral part of society, whether it be part of the food

sector or part of traditions that have been occurring for thousands of years. There is a high demand for what comes out of the oceans globally, where strict protocols are set in place to not only protect the species but also allow for the continuation of fishing as an economic sector. These range from major fishing corporations to smaller family-owned businesses. These processes by which the fishing sector must abide by no matter what size of the corporation are fish stock management. There have been a variety of practices that have been in place on a governance level in recent times to maintain fish stocks this is referred to as sustainability. Fishing is one of the oldest occupations where it was passed down generational from parent to child, it allows for the passing of traditions that guarantee the success of the enterprise from local ecological knowledge (Symes et al., 2015). With the opportunity of other jobs there, some local fisheries find it difficult to employ people from the area (Symes et al., 2015).

To help improve the biological health of fish stocks there was a reform in the European Common Fisheries Policy (CFP) was released in 2013, this brought the well-being of the species to the centre of European fisheries management (Fitzpatrick et al., 2017; Bresnihan, 2019). There is also a move towards sustainable practices where they aim to conserve both the fisheries and marine environments by market-based approaches (Konefal, 2013). However, this is a difficult task as successful governance of marine fisheries is a global issue that needs the support of the international community (Fitzpatrick et al., 2017). To date, there are very few examples of decadal climate services (tailored forecast products) for sector users. This is despite the skill now demonstrated by retrospective decadal predictions and the clear need of sector users for operational near-term climate predictions delivered in the format of useful climate services (Dunstone et al., 2022). Instead, end-users in different sectors typically require more regionally focused climate predictions of relevant variables, usually for a specific forecast range, period and/or season (Dunstone et al., 2022).

The environmental pressures that drive most fish species are sensitive to changes in salinity and temperature at depth (Mann and Drinkwater, 1994; Nelson et al., 2016). The changes in temperature and salinity of the water could drive species out of their normal living environments leading to a reduction in the amount available

for fisheries (Nelson et al., 2016). To understand where these sensitivities are coming from, they can be sourced back to the climatic factors originating from the difference in pressure between the Icelandic Low and the Azores High (Mann and Drinkwater, 1994). This difference is referred to as the North Atlantic Oscillation (NAO), changes in this system have been known to cause a wide range of effects within the marine systems (Marshall et al., 2001).

The NAO had the most influence in the winter months this resulted in an increase around sea ice and increases in the volume of cold water at depth (Mann and Drinkwater, 1994). One species this influence is the Atlantic cod, as these factors are known to have an impact on temperature and salinity conditions (Mann and Drinkwater, 1994). These are associated with poor growth and recruitment in spring and summer (Mann and Drinkwater, 1994).

The fishery sector is of vast importance to the Irish economy. In 2019 it generated €577 million and employed 16 thousand people. The ability to predict changes in the future stock will support adaptation and fish stock management. The different stages of fish development are dependent on oceanic variables like SST. Having the ability to determine stock changes several years ahead will allow for the adaptation of management strategies. Before the analysis of the model can be determined, exploration into the current state of the fish stock needs to be considered.

Chapter 2 will provide some insight into the change of the mackerel stage 1 eggs and the influence the variability of SST has on the density, and distribution has eggs. Building on what was completed in the previous chapters on prediction skills, I focus more on the Irish fishing grounds and the NE Atlantic northwest of Ireland. This will allow for a comparison between the egg density for each section to be compared to the predictability of each area for the time frame 1989 to 2014 with a 2 to 5-year lead time. From the MPI-ESM the initialised hindcast simulation will be used to extend this time frame up to 2019. With this information, I will be able to see in the following 5 years if there is a temperature change.

1.8 Effective communication of scientific research

It has become evident that there is an urgent and growing need for climate information that will inform governmental bodies to support the framework, e.g. for disaster risk reduction (Smith et al., 2019). Chapter 2 section 2.4 discusses the different aspects of how scientific information is communicated. It is a challenge that faces scientists, how can we effectively communicate our work to those who are not directly involved in the topic? Whether these are fellow scientists, or the public and the information being provided is credible (Smith et al., 2019). Care needs to be taken when communicating with audiences that have a mixed understanding of the concepts being discussed. As scientists, we strive to increase the public's knowledge and understanding of complex topics (Luisi et al., 2019). There are a variety of different methods that aid in the distribution and communication of scientific research, including presentations, posters, infographics, and community engagement events. In the thesis using the key results obtained an infographic was generated in chapter 7. An infographic was chosen as it allows of a balance of just the right amount of imagery with the relevant text. As it allows the reader to gain an understanding of such a complex topic in an easy-to-follow manner. Starting from the observations to the prediction systems to how this can inform us about the changes in the observations.

1.9 Research Questions

This thesis aims to establish that it is possible to tailor decadal predictions for stakeholders' needs. This thesis has 4 broad research questions:

1. What mechanisms that influence temperature and salinity in the North Atlantic Ocean, are these variables predictable?
2. Can the North Atlantic Ocean's predictive skill be improved using the sub-sampling method?
3. Can the predictive skill in the North Atlantic Ocean be tailored for stakeholder needs?

4. How can this information relate to the fisheries and be communicated effectively?

1.10 Thesis Contributions

While there have been improvements in how these predictions can be tailored to suit stakeholder needs. Including having a better understanding of the interactions that occur in our world and how these are represented in model environments that are being used to replicate the real world. While the consensus is that the models are confident on a global scale, there is limited confidence in prediction skills on a regional scale. I will explore the predictability of the North Atlantic Ocean on a decadal time scale for oceanographic properties like ocean temperature (SST), sea salinity (SSS), the subpolar gyre (SPG), and so Atlantic Multidecadal Variability (AMV). Making this information usable on a regional scale for Ireland would allow tailoring for different applications such as fisheries. The fishery sector is of vast importance to the Irish economy. Consequently, the ability to predict changes in the future stock will support adaptation and fish stock management. Different stages of fish development are dependent on oceanic variables such as temperature and salinity. Having the ability to predict changes for these variables would allow us to make statements on potential changes in fish stock for a species such as Mackerel. In this thesis, I investigate the possibility of tailoring these decadal predictions for both temperature and salinity for the Eastern North Atlantic Ocean.

Within this thesis, I explore how decadal predictions can be tailored to suit stakeholders' needs focusing on the Northeastern Atlantic Ocean. This is achieved through the identification of the key oceanic variables that are important to the stakeholders, how predictable they are and finally how predictable they are. Exploring the predictability of temperature and salinity for the northeastern Atlantic Ocean with a focus on Ireland. Using different models and outputs I evaluate the best simulations that provide the best potential for tailoring. Two uninitialised historical simulations and one initialised hindcast simulation are evaluated to determine the output with the best skill. This comparison between the uninitialised historical simulations highlights the change in skill between the CMIP5 and CMIP6 simulations to my knowledge has not been explored in this context.

This is achieved by exploring how well these simulations are predictable at depth this is discussed further in chapters 4 and 5. The results of this research were communicated to the stakeholders.

Following this initial investigation, I determined that the initialised hindcast simulation from the ocean model provided the best skill for tailoring. Using this simulation, three target areas were identified that had no skill. Using two predictors I had hoped to improve the skill for these areas. These results are discussed further in Chapter 6. Work conducted using this method has mainly been constrained to the atmosphere, I have focused on the ocean. While this has not been as successful, it shows promise as in certain areas there was an improvement in skill. While this was not a noticeable improvement it shows that this technique can be used within the ocean.

Communicating the findings of the predictability of both temperature and salinity with the stakeholders, it was agreed that the final investigation would focus on temperature. One of the reasons for this is that it is an important variable of the target species would be mackerel. They had noticed that there was a shift in the mackerel stock northwards in the last 30 years. I had asked to determine if this shift was due to a change in the temperature of the spawning grounds. Work on this topic mainly focused on using models and predictability to determine the changes in stocks months in advance. They use the model outputs to inform their biological models. In this contribution, I evaluate temperature from the initialised hindcast simulation to determine how temperature will change in the future. How this temperature change will impact egg density and distribution. This research takes a statistical approach, adding an understanding of the model aspects that can be incorporated into the biological models. Others that have explored similar research focus more on a seasonal or even monthly time scale, I extend this time scale to 1 year. This can allow for the development of biological models that can predicted up to multiple years in advance.

1.11 Thesis Structure

Chapter 2 discusses the mechanisms that occur in the North Atlantic Ocean and their predictability on decadal time scales. This chapter also discusses the connection of the AMV and SPG have with temperature and salinity. Whether they can aid in the improvement of prediction skills, following this the application of predictions is discussed as to why it is necessary. Chapter 3 presents the methods that I will use throughout this thesis.

Chapter 4 uses both the initialised and uninitialised versions of the MPI-ESM to explore the prediction skill for both temperature and salinity at the surface of the Eastern North Atlantic Ocean on the decadal time scale. A paper in the review in the journal *Climate Dynamics* summarizing the possibility of prediction skill at depth within the MPI-ESM is presented in chapter 5. In Chapter 6, I examine the possibility of improving predictability in areas of little or no skill and investigate whether SPG or AMV can improve skill in these areas. In Chapter 7 I use the prediction skill shown in the previous chapters to show potential changes in the fish stock Mackerel in two locations. The first location is the West of Ireland and the second is the NE Atlantic northwest of Ireland where the stock is potentially migrating. This chapter will also contain the infographic that will be sent to the stakeholders. Providing them with all the relevant information about the potential migration of the stock. Finally, in Chapter 8, we conclude the thesis by showing topics for future research.

Literature Review

2.1 Introduction

This chapter highlights the relevant literature connecting the physical environment with the model and how prediction can be tailored to the benefit of stakeholder needs. Before any tailoring can occur there needs to be an understanding of the physical mechanisms, the time scales that they interact and the predictability of temperature and salinity. Next an exploration into how these predictions have been tailored to suit the fishery industry that has been previously conducted. Finally, background information on the fishery industry in Ireland and the target species will be explored. The literature reviewed is necessarily selective given that the topic will focus on tailoring temperature and salinity for two mackerel species (Atlantic and horseshoe). This literature review is not limited to but focuses primarily on;

- **Literature:** Tailoring of decadal prediction skill of physical mechanisms in the Eastern North Atlantic Ocean.
- **Species and location:** Atlantic and horseshoe mackerel, Eastern North Atlantic Ocean.

- **Variables:** Sea surface temperature, salinity, and two predictors (AMV, SPG).

Section 2.2 discusses the literature on the connection between the physical mechanisms in the Eastern North Atlantic Ocean and how they are represented in the model on different timescales. Section 2.3 outlines how predictions have been tailored previously, management systems in place, sustainability, and environmental factors that impact fish stock. Section 2.4 explores how scientific research can be effectively communicated to stakeholders, how infographics are a useful tool in communication, and the challenges of scientific communication.

2.2 Predictability of the physical mechanisms in the Eastern North Atlantic Ocean

To understand the processes that go into decadal prediction it is necessary to understand the mechanisms of variability that occur in the North Atlantic Ocean. With a focus on temperature and salinity can be tailored for application for stakeholder needs such as fisheries. It is important to understand both aspects as they both contain drivers in the North Atlantic Ocean, with a key interest in the influence on fish stock. One atmospheric pattern with a large effect on Irish climate is the North Atlantic Oscillation (NAO). Changes in the amplitude and sign of the winter NAO are strongly linked to the patterns of winter temperature, precipitation, and storminess (wave power/height) (Curtis et al., 2016; Fan et al., 2016; Dobrynin et al., 2018). The oceanic patterns that need to be considered are the Atlantic Meridional Overturning Circulation (AMOC), the subpolar Gyre (SPG), and Atlantic Multidecadal Variability (AMV), also referred to as the Atlantic Multidecadal Oscillation (AMO). Which interact with temperature and salinity on a longer time scale than their atmospheric counterparts. An exploration into these patterns with the model and what decadal predictions can offer will be discussed.

2.2.1 Physical mechanisms in the Eastern North Atlantic Ocean

The North Atlantic Ocean basin shows remarkable variability over decadal to multidecadal timescales, which has received a considerable amount of attention as it provides a large source of natural climate variability (Sun et al., 2015b). On decadal to multidecadal timescales the North Atlantic Ocean basin exhibits variability (Sun et al., 2015b). In the upper ocean that feedback that is closely related is the Atlantic Multidecadal Variability (AMV) was found in surface potential temperature (Delworth et al., 1993). The observed AMV is associated with coherent multidecadal variations in the subpolar North Atlantic Ocean SST, sea surface salinity, and upper heat/salt content (Yan et al., 2019). In the deeper ocean what connects the large-scale circulation of the atmosphere in the polar and subpolar North Atlantic Ocean is the oceanic SPG and deep convection zones (Marshall et al., 2001). This process in turn controls the strength and variability of the AMOC in the ocean and also determines large parts of the multidecadal AMOC variability (Yeager, 2015). The subtropical gyre and the subpolar gyre are two current systems that form the complex European Boundary Current System that influences the circulation along the European continental slope (Moritz et al., 2021). The North Atlantic Ocean current connects the subtropical gyre where the warm and saline water masses move northward and the SPG where colder fresher water masses move southward (Holliday et al., 2020; Moritz et al., 2021). It widens as it crosses the North Atlantic Ocean, separating into branches east of the Mid-Atlantic Ridge that flow into the Iceland Basin, the Rockall Trough, and southward to re-join the STG (Holliday et al., 2020). Understanding the connection of these processes aids in the predictability of the North Atlantic Ocean.

The NAO is a large-scale atmospheric circulation pattern and is the dominant mode of atmospheric inter-annual variability over the North Atlantic Ocean, it emerges from a dipole oscillation in normalized sea level pressure that occurs between the Icelandic Low and the Azores high (Hurrell, 1995; Davini and Cagnazzo, 2014; Herceg-Bulić and Kucharski, 2014; Chen et al., 2015; Cropper et al., 2015; Sun et al., 2015a; Xin et al., 2015; Fan et al., 2016; Madrigal-González et al., 2017; Dobrynin et al., 2018; Önskog et al., 2018). The NAO is shown to have large inter-

annual and decadal variability over the last 50 years, switching from a negative phase (1960's) to a strong positive phase (1980's, 1990's)(Zhai et al., 2014). The NAO is influenced by the sea surface temperature (SST) and the North Atlantic Ocean SST by the NAO. While some studies such as Herceg-Bulić and Kucharski (2014) describe that variations in SST in the North Atlantic Ocean may influence NAO variability, others, like Gastineau and Frankignoul (2014), state the NAO mainly forces North Atlantic Ocean SST. When there are persistent anomalies in the NAO it can force some wind stress and heat flux anomalies that can amplify or weaken the formation of the North Atlantic Deep Water masses, in turn, can lead to a reinforcement or weakening of the AMOC with a couple years lag (Zhai et al., 2014; Peings et al., 2016). Dobrynin et al. (2019) investigate the wintertime NAO and its relationship with wave dynamics. They discuss that the better representation of active wave generation leads to better prediction skills in regions of direct NAO impact. The leading mode of variability in the large-scale circulation over the North Atlantic Ocean in winter is the NAO, which strongly impacts the weather and climate in the Euro-Atlantic sector (Parker et al., 2019). The winter NAO dominates the inter-annual atmospheric variability in the Euro-Atlantic sector and largely contributes to regional surface climate variability (García-Serrano et al., 2015). It is frequently regarded as the regional expression of the Arctic Oscillation or northern annular mode (García-Serrano et al., 2015).

The various large-scale atmosphere-ocean interactions that occur in the Earth's climate can be separated using different timescales (Brune and Baehr, 2020). Examples of this large-scale atmosphere-ocean feedback on these decadal time scales are the AMV and the Pacific decadal oscillation (PDO) (Brune and Baehr, 2020). The oceanic interactions that occur in the North Atlantic Ocean that influence temperature and salinity are AMOC, SPG, and AMV/AMO (Muir and Fedorov, 2015). The contribution of the AMV to global sea surface temperature (SST) variability over the observational record is second only to El Niño-Southern Oscillation (Brown et al., 2016). On a longer timescale temperature is often referred to as AMV/AMO where variations in the AMOC are suggested to have some control or contribution to the AMV/AMO, however, the physics behind the AMV/AMO remains uncertain and a matter for debate (Muir and Fedorov, 2015; Brown et al.,

2016; Peings et al., 2016). Where variations of the AMOC are believed to be an important driver of decadal to multidecadal climate variability and play an important role in the climate system by transporting heat northwards in the Atlantic (Jackson et al., 2015; Muir and Fedorov, 2015). The leading mechanism of the observed AMV was originally linked to the low-frequency variability of the AMOC, some suggest that it is a direct response of the North Atlantic SST to changes in external radiating forcings (Gastineau and Frankignoul, 2014; Yan et al., 2019). Yan et al. (2019) explored this within the CMIP5 project and determined that these external forcings were not the dominating observed AMV but were linked to the multidecadal variations in the AMOC. One of the fundamental variables for ocean circulation and global climate is salinity as it provides the density of water masses that take part in the upper branch of the AMOC (Friedman et al., 2017). The AMOC is the Atlantic component of the global thermohaline circulation, this is driven by the temperature and salinity gradients in the ocean that modulate deep convection in high latitudes (Peings et al., 2016). The connection between the AMOC and the NAO shows that a reinforcement of the AMOC is generally seen with a persistent positive phase in the winter NAO (Peings et al., 2016). One of the key components in North Atlantic Ocean decadal climate variability points to the Atlantic subpolar gyre (SPG) (Born et al., 2015). There have been a variety of studies that point to the SPG being a key component in the North Atlantic Ocean decadal climate variability, with some of this variability being connected to the NAO (Born et al., 2015; Buckley and Marshall, 2016).

AMV is a mode of climate variability affecting SST characterised by fluctuations between anomalously warm and anomalously cool phases, with enhanced energy in the inter-decadal band (Sun et al., 2015b; Sutton et al., 2018; Sgubin et al., 2021). At low frequencies the SST in the North Atlantic Ocean shows a lot of variability, it experiences alternating basin-wide warming and cooling with an approximate periodicity of 70 years known as the AMV (Gastineau and Frankignoul, 2014). The AMV is modulated to some extent by the fluctuations in the strength of the AMOC which together with the North Atlantic Ocean subpolar gyre is influenced by deep ocean density anomalies, particularly in the Labrador Sea; these influences contribute to the especially high multiyear predictability in the North Atlantic

Ocean (Sun et al., 2015b; Vecchi and Delworth, 2017; Merryfield et al., 2020). The AMV is found to be closely related to climate variations over the Atlantic basin and adjacent continents (Sun et al., 2015b; Moat et al., 2019). These impacts involve decadal variations in temperature and rainfall patterns, hurricane activity, and sea level changes (Sutton et al., 2018). In some cases, the magnitude of these impacts is sufficient that, on time scales up to a few decades, the AMV influence may dominate over the influence of longer-term climate change (Sutton et al., 2018). Variations in the AMOC modulate a north-ward movement of near-surface warm water and a compensating southward movement of deep, colder waters, driving changes in ocean temperature (Vecchi and Delworth, 2017). Strong changes in North Atlantic SST/AMV are linked to important climate impacts, including the number of hurricanes, and the surface climate over the surrounding continents (Ghosh et al., 2017; Robson et al., 2018). The origin of the AMV is not confined to the ocean (Vecchi and Delworth, 2017). Shifts in the strength and position of North Atlantic winds (NAO), can strengthen or weaken the AMOC and result in multidecadal temperature swings in the Atlantic (Vecchi and Delworth, 2017). Modelling suggests that Atlantic Ocean circulation responds to external forcing, either through decadal variations in surface radiative forcing or through changes in the NAO (Vecchi and Delworth, 2017).

Sea surface salinity is a fundamental variable for ocean circulation and global climate (Friedman et al., 2017). Resulting from the combined effects of evaporation, precipitation, land surface runoff, oceanic advection, vertical mixing, and melting and freezing ice (Friedman et al., 2017). As large-scale variations are thought to reflect the net surface freshwater flux, which is difficult to measure directly, sea surface salinity has been considered an indirect ocean rain gauge (Friedman et al., 2017). Global trends since the 1950s show that salinification in saltier regions and freshening in fresher regions provide evidence for such an intensification (Friedman et al., 2017). In the North Atlantic Ocean, it is of particular importance as it contributes to the density of water masses that take part in the upper branch of the AMOC (Friedman et al., 2017). Variations in salinity also contribute to North Atlantic Ocean regional sea level change and Atlantic marine biodiversity (Friedman et al., 2017).

2.2. Predictability of the physical mechanisms in the Eastern North Atlantic Ocean

The interactions that were identified in the North Atlantic Ocean are illustrated in Figure 2.1, involved in the processes are the NAO in the atmosphere, the Subpolar Gyre (SPG), the AMOC and the AMV. Where these components interact with each other in different ways on different timescales.

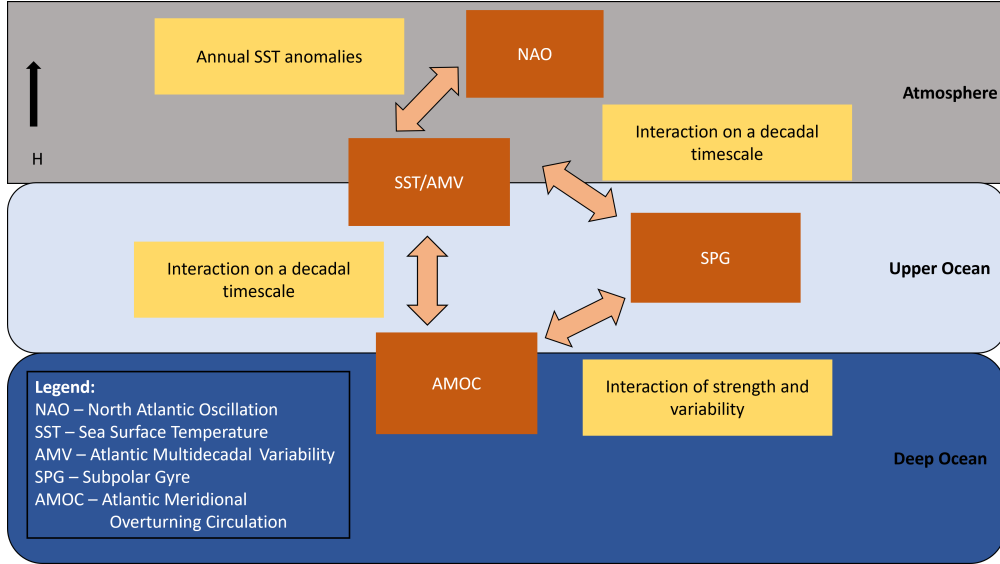


Figure 2.1: Mechanisms that occur within the North Atlantic Ocean and how they interact on timescales generated from the literature. Provides a simplification of a selection of interactions in the North Atlantic Ocean that have an impact on both temperature and salinity.

2.2.2 Predictability of physical mechanisms

There have been rapid advances in the observation and the modelling of the earth system allowing for a revolution in our ability to forecast our planet’s weather and climate, in decadal prediction there has been increasing scientific and public attention (Borchert et al., 2019; Payne et al., 2017). The North Atlantic Ocean has been identified as a key region that has pronounced forecast skill for different parameters such as surface air temperatures or OHC (Kröger et al., 2018). Early coupled global circulation models (CGCMs) revealed that intrinsic, low-frequency SST surface air temperature and SLP variations in the North Atlantic Ocean and Arctic Ocean were consistently associated with variations in the strength of the AMOC, and in particular its slow thermohaline circulation component (Yeager

and Robson, 2017). However, regarding surface temperature, there is generally weak over continental regions and high over the ocean (Borchert et al., 2018). For the North Atlantic SPG region, high forecast skill for SST and OHC arises from the correct initialisation of the ocean flow. However, there are some limitations as direct observations of oceanic flow are sparse (Kröger et al., 2018). One area that has seen the most impressive results is in the oceanic domain, this is due to the slow dynamics and the long memory of the ocean that readily lend themselves to forecast timescales dramatically longer than in the atmosphere (Payne et al., 2017). Allowing for the skilful forecast on an annual and even decadal scale for temperature, upper ocean heat, and salt content (Payne et al., 2017). These are not without fault, generating forecasts of biological systems is not straightforward, with many models having the ability to produce forecasts of physical variables like the ones mentioned previously, instead of the variables that have a direct interest in marine resource management and ecosystem applications (Payne et al., 2017). Using the Max Planck Institute for Meteorology Earth system model (MPI-ESM-MR) Dobrynin et al. (2019) used a 10-member seasonal prediction system based on the mixed resolution Coupled Model Intercomparison Project Phase 5 to correlate (prediction skill) the observed and forecasted NAO index. Ocean general circulation models (OGCMs) employing hindcast simulations have been used to study the response of the ocean to changes in the NAO (Zhai et al., 2014). While progress has been made with the OGCMs they are still limited due to the lack of observations as well as the complexity of the model itself (Zhai et al., 2014). An additional source of seasonal to decadal predictability is variations in radiative forcing, which provide significant skill on multiyear time scales (Merryfield et al., 2020). Much of this skill arises from changes in greenhouse gases, but anthropogenic aerosols may force decadal variations in AMV and PDV (Merryfield et al., 2020). Solar variability, volcanic eruptions including through their influence on ENSO and possibly AMV, and the NAO affect climate on seasonal to decadal time scales and are potentially important sources of predictability (Merryfield et al., 2020).

Within decadal predictability there are limitations of AMV as the influence of external factors is removed, the main source of predictability of the climate at a decadal to multidecadal time scale is the slow oceanic fluctuations (Peings et al.,

2016). This is most evident when it comes to predicting SST, sea ice and oceanic heat content in the subpolar North Atlantic gyre (Peings et al., 2016). Focusing on the predictive skill of SST for the North Atlantic Ocean, one area that has shown an improvement of skill is through initialisation (Meehl et al., 2014). The externally forced response of the historical climate simulations does not capture well the observed multidecadal sea surface variations in the subpolar North Atlantic Ocean that are coherent with the observed AMV (Yan et al., 2019). While this is the case, providing predictions of how Atlantic SST might change over the years to decades ahead still is an important challenge for climate prediction (Robson et al., 2018). On a sub-decadal time scale, the improvement of skill in the North Atlantic Ocean region from this initialisation of SST, can in part be linked to the skilful prediction of the AMOC from initialisation (Meehl et al., 2014). On the decadal time scale, SST that occurs in the North Atlantic Ocean is often referred to as the AMV or AMO and is linked with the AMOC (Meehl et al., 2014; Wen et al., 2016; Yan et al., 2019; Merryfield et al., 2020). On decadal time scales climate variability is largely modulated by the AMV and the NAO (Sgubin et al., 2021). The variability of the AMV is not fully understood or constrained to the change in the AMOC but also external forcings and the natural variability of the atmosphere (Wen et al., 2016; Yan et al., 2019; Merryfield et al., 2020; Sgubin et al., 2021). Due to a lack of long-term records, it is hard to connect the AMOC, SST, and the atmosphere in observations (Wen et al., 2016; Peings et al., 2016). Peings et al. (2016) found that the AMOC was reinforced followed by the warming of the SPG and a buildup of the positive phase of the AMV, which also causes a reduction in the AMOC. The connection between the AMV and the AMOC does have variation between the models, this is in the anomalies and the timing of maximum correlation.

The North Atlantic Ocean SPG represents an important part of the widely studied AMV, as a region it may experience important shifts which may impact the climate (Menary and Hermanson, 2018). The SPG of the North Atlantic Ocean is a cyclonically circulating oceanic gyre that exhibits pronounced decadal-to-multidecadal variability in its properties (Koul et al., 2022). Over the last sixty years, periods of strong decadal trends in surface temperature of the SPG have been observed cooling in the 1960s, warming in the 1990s and the recent cooling

in the 2000s (Koul et al., 2022). The region may be predictable up to a decade ahead, good initialisation of the North Atlantic SPG has shown to be important in providing potential predictability in other regions (Menary and Hermanson, 2018). The North Atlantic Ocean and particularly the North Atlantic SPG is a region where hindcasts (retrospective climate predictions), which are initialised from observations, are found to have significant skill in capturing past variations of SST (Robson et al., 2018). To build confidence that future predictions will remain skilful, it is important to understand why hindcasts are successful, and if the dominant mechanisms are robust (Robson et al., 2018). Process-based analysis of hindcast has shown that skill is not simply due to the thermal inertia of the SPG (Robson et al., 2018). Rather, the initialisation of ocean circulation plays an important role for hindcasts to capture the major shifts in the SPG heat content (Robson et al., 2018). Although there is significant skill at capturing previous shifts in North Atlantic Ocean temperatures in current prediction systems, there are still significant uncertainties (Robson et al., 2018). The majority of models used for initialised climate prediction have also used low-resolution models (ocean resolution $>1^\circ$), which may not capture all the relevant processes in the North Atlantic Ocean (Robson et al., 2018). The strength of ocean-atmosphere coupling and the time scale of ocean adjustment may differ in high-resolution models compared to low-resolution (Robson et al., 2018). To ensure that the best information is available to assess the robustness of predictions, and to guide model development, it is important to understand the sensitivity of skill and mechanisms to the underlying model used (Robson et al., 2018). SST in the North Atlantic Ocean including the SPG can impact climate both locally and remotely (Menary et al., 2021). They are potentially predictable on decadal timescales and successfully initialising them can provide skill elsewhere (Menary et al., 2021). Analysis of the CMIP6 archive has shown improvement since CMIP5 in multi-annual skill in SST in the NA SPG, in both uninitialised and initialised simulations (Borchert et al., 2021; Menary et al., 2021).

Several regions, such as the North Atlantic and Pacific Oceans, are characterised by their variations on decadal to inter-decadal timescales, which are manifested in substantial changes in sea surface temperature and ocean heat storage (van

Oldenborgh et al., 2012). An important advantage of decadal climate predictions compared to centennial climate projections is that their credibility can be assessed by performing retrospective forecasts (also known as hindcasts) of the historical period and comparing them against subsequent observations (Smith et al., 2019). Because of their potentially large socio-economic impact, climate predictions over interannual to decadal time scales have recently gained increased attention (van Oldenborgh et al., 2012). Pohlmann et al. (2013) explored the improvement of forecast skill in the tropics using the MPI-ESM in both its low-resolution and high-resolution format. They found that for hindcast averaged over years 2 to 5 years lead time an additional improvement is achieved in the tropical pacific with the higher model resolution. The ensemble mean generally outperforms individual ensemble members (Pohlmann et al., 2013). Müller et al. (2012) analyse the predictive skill of the baseline-0 (b0) system. They show that the initialization of MPI-ESM improves forecast skill with respect to the uninitialized experiment predominantly over the North Atlantic for all lead times and over parts of Europe for multiyear seasonal means. Although previous assessments have shown high skill in decadal forecasts of surface temperature, confidence in predictions of precipitation and atmospheric circulation, which are vital for many climate impacts, is much lower (Smith et al., 2019). Recent developments in seasonal forecasting have highlighted the need for very large ensembles to achieve skilful predictions, especially for precipitation and atmospheric circulation (Smith et al., 2019). Show that decadal prediction can capture many aspects of regional changes, including precipitation over land and atmospheric circulation in addition to surface temperatures Smith et al. (2019).

There have been vast improvements in the field of decadal prediction skill, one area that has shown significant improvement is the introduction of the initialised hindcast. These are based on the re-forecasting of observational data that is known in the models as assimilation runs. This initialised hindcast showed good prediction skill and proved a good starting point for the improvement of predictability in the North Atlantic Ocean. Identifying and understanding the mechanisms that are involved in the North Atlantic Ocean and determining if there is a possibility that they could be used as potential predictors. The results that Yeager and Robson

(2017) have produced after investigating the subpolar gyre can improve decadal prediction in the North Atlantic Ocean when looking at initialised hindcast. They were looking at sea surface temperature and it shows that there is promise that there is good prediction skill in the Northeastern Atlantic when looking at temperature and the SPG. This will be expanded on in the work that I will be conducting where both temperature and salinity will be explored at depth and compared to the SPG/AMV to see if there is an improvement in decadal prediction at a 2-to-5-year lead time. Both the SPG and the AMV were identified and calculated within the models and then compared with the initialised hindcast to determine if there was an improvement in the prediction skill in the area.

2.3 Tailoring of Decadal predictions for stakeholder needs

To date, there have been a variety of different ways in which models have been used in the fishery industry to detect changes in the density and distribution of fish stock and egg larvae (Bartsch, 2005; Bruge et al., 2016; Koul et al., 2022; Payne et al., 2022). Decadal predictions of the ocean could be invaluable in supporting climate adaptation and sustainable development in coastal communities and nations, particularly in the Global South where ocean dependency and climate risk are higher (Payne et al., 2022). With the majority using environmental attributes for these studies (Koul et al., 2022; Payne et al., 2022), some explore ecological attributes such as prey distribution (Bartsch, 2005). Individual-based models (IBMs) are one approach that takes into consideration both the environmental variables and the ecological attributes. The development of sophisticated circulation models allows for IBMs to be a useful tool in the study of dispersal, growth, and mortality of marine populations (Bartsch, 2005). A study conducted by Koul et al. (2022) explored the decadal predictability of the SPG and how it can influence cod stock in the Barents Sea. Payne et al. (2022) combined existing biological habitat models characterising the species' environment preferences with predictions of the physical environment from existing climate prediction systems to produce decadal-scale habitat predictions. Bruge et al. (2016) highlighted that both the spawning activity distribution and the thermal spawning niche of

North-East Atlantic mackerel (NEAM) have shifted northward between 1992 and 2013. The NEAM supports one of the most valuable fisheries in Europe and recent distribution shifts into Icelandic and Greenlandic waters have driven the aforementioned conflict over fishing rights (Payne et al., 2022). It suggests that the NEAM has tracked its thermal spawning niche in response to sea warming, although the warming is not the only cause of this shift (Bruge et al., 2016).

When it comes to climate change a better understanding of spawning habitat characteristics is necessary to be able to predict the impact on different fish species (Ibaibarriaga et al., 2007). This needs to be considered in a multi-species context because it is not always known to what extent different species share spawning habitats or whether conditions that are detrimental for one species can be favourable for another (Ibaibarriaga et al., 2007). Longer climate scale projections allow for managers and practitioners to evaluate risk and plan for future losses or gains in suitability. This in turn informs longer-term decision-making processes such as national legislation or international negotiations (Mason et al., 2021). Forecasting fish abundance depending on decadal climate variability is necessary to devise timely interventions to ensure sustainable use of resources (Koul et al., 2021). There are still some limitations when it comes to the application of climate models to predict ecosystem processes at decadal timescales (Koul et al., 2021). The climate has been shown to influence fish directly or indirectly through recruitment, food availability, fecundity, growth, and migration (Koul et al., 2021). With this being the case, climate variables are rarely included in the management-oriented modelling and forecasting of fish populations (Koul et al., 2021). This is due to the historically large impact of fishing mortality on commercial stock biomass and due to forecasting being complicated by frequent transient and non-stationary properties of climate impacts on fish stocks (Koul et al., 2021). In addition to the climatic factors, fish experience the cumulative impacts of different drivers; fishing pressures and climate can have combined effects inducing non-linear dynamics in fish stocks (Koul et al., 2021). International conflicts over fishing rights can also arise as shifting fish stock starts to straddle international jurisdictions, an issue that is only expected to worsen: transboundary stocks impact as many as 40% of exclusive economic zones in the future (Payne et al., 2022).

Conflicts are already being seen, one such instance is the so-called North Atlantic Ocean "mackerel war" between the European Union, Norway and Iceland, and the Faroe Islands over access to Atlantic mackerel (*Scomber scombrus*) and is a leading cause of international disputes between democracies (Payne et al., 2022). The ability to foresee such shifts can therefore potentially hold the key to both avoiding conflict and adapting marine fisheries to a changing climate (Payne et al., 2022).

2.3.1 Fish stock management and sustainability

Climate change and other environmental pressures are not the only things that need to be considered ecological pressures need to be included to a degree, climate change is having an impact on marine organisms and ecosystem functions (Pitois et al., 2012; Mason et al., 2021). Alongside the urgent need for bold action to reduce GHG emissions is needed for adaptive management approaches to maintain desired fishery outcomes under changing and novel conditions (Mason et al., 2021). It is a concept that the relationship between predator and prey influence each other's distribution is an ancient one (Rose and Leggett, 1990). This predation on prey needs to be examined also. This occurs at all phases throughout the fish species life cycle (Paradis et al., 1996). It cannot be ignored that the death of the larval is the result of two different causes, these being starvation and predation (Paradis et al., 1996). Starvation occurs in a short time frame when the species has not reached full maturity, giving the predation factor a greater source of mortality (Paradis et al., 1996). At each developmental stage, the vulnerability to predation changes depending on the size of the fish and the distribution of the fish (Paradis et al., 1996). One way the larval fish can overcome this specific type of predator is the process of rapid growth, this reduces the time in which the larval fish is in a vulnerability window (Paradis et al., 1996). To promote biodiversity and sustainability within fisheries, the expansion of the knowledge and understanding of how climate variability influences this early stage of fish species and the connection to their environment (Pitois et al., 2012). As it stands, European fisheries are highly exploited, and many are vulnerable to the effect climate change will have on the ecosystem (Lynam et al., 2010). It is well known that fish usually have spawning seasons these are certain times of the year and spawning habitats which are specific places, these provide the suitable conditions for the offspring to

survive (Miesner and Payne, 2018). If these conditions are compromised likely under climate change reproductive success is likely to be at risk as spawning habitat temperatures will exceed the tolerance limit of the most sensitive life stage, this can then force species to reproduce at different times and/or places (Miesner and Payne, 2018). One way in which climate change affects marine ecosystems is the profound impact on the distributions of marine fishery resources (Dahlke et al., 2020). There has been observed shifts in the spatial distributions of marine species that have been observed in response to both gradual warming and extreme events, and there is a need to understand how ecosystem factors, such as temperature, can influence the current and future distributions of natural resources in the ocean (Dahlke et al., 2020).

Fish stock management systems are the processes by which governments regulate and monitor the amount of resources available in the seas. For hundreds of years, the sea has been an area of exploitation where its resources have been a providing a constant source of wealth for the international community (Wilder, 1995). However, the extent of this exploitation is becoming increasingly evident as the state of global fisheries is considered in a “crisis” (Urquhart et al., 2013). A more interdisciplinary approach is needed to help get a better view of the state of the stocks, the environmental processes and the ecological interactions (Zimmermann et al., 2019). By identifying these the hope is that they will help in the explanation of the fish population dynamics, determining the key drivers behind the dynamics can be used to improve the predictability of recruitment (Zimmermann et al., 2019). It has been reported that 85 of marine fish stocks are under one of the following categories; fully exploited, over-exploited, depleted or recovering (Urquhart et al., 2013). In the last 50 years there has been a movement to develop more sustainable fishing practices, an example of this is the Common Fisheries Policy developed by the EU (Wilder, 1995; Bresnihan, 2019). Initially introduced in 1983, a shared management system that all conservation measures are determined at the community level was subsequently reformed in 2013 bringing the well-being of species into centre focus (Wilder, 1995; Bresnihan, 2019). On a European level the community collectively manages all the stocks that are within 200 miles of the member states (Wilder, 1995). For those who have access to adequate

scientific and technical capacity the incorporation of forecasts is a key aspect of climate adaptive management (Mason et al., 2021). Understanding ecosystems in general and environmental effects on the variability in abundance and distribution of exploited fishery stocks in particular, are keys for future management strategies (Denis et al., 2002).

2.3.2 Sustainability

A key consideration is the connection between the economic side of fish stock management and how this interacts with the sustainability of fish species. Small-scale fisheries (marine and inland) are estimated to account for over half of the world's fish catches and employ more than 90% of the world's 35 million fishers (Urquhart et al., 2013). These contribute not only economically, but socially and culturally to society; however, these livelihoods are under threat from lack of poverty (Urquhart et al., 2013). 88% of European quota stocks are considered overfished (Urquhart et al., 2013). According to the UN, approximately "57% of fish stocks are fully exploited and roughly 30% are overexploited" (Silver and Hawkins, 2017). On a European scale, coastal fisheries are under pressure from external and internal pressures for change, in terms of approaches to fisheries management (Symes et al., 2015). On a local scale, the Irish seafood sector can be divided into 3 distinct areas, a commercial fishing sector, an aquaculture sector and a seafood processing sector (Vega et al., 2014). Among the 27 member states Ireland is ranked eighth when it comes to the contribution to the overall value added of sea fisheries (Vega et al., 2014). However, smaller fisheries are usually the first to feel the effects of any policy changes, causing a lot more to go out of business as they cannot compete with the larger companies. Outside of the EU changes to the management style could negatively impact the implementation of quotas, while these are more beneficial for sustainability, they may drive smaller fisheries out of business. The over-exploitation of fish is not one that is inherently obvious it is something that will be seen over several decades (Hannesson, 1996). An example of this is in the period a fish species catches had increased fivefold from 20 million tonnes to in excess of 80 million tonnes (Hannesson, 1996). One example of a fish stock that has almost completely depleted is the northeast Atlantic herring, which has been in decline for many years (Hannesson, 1996).

Quotas are one way in which fisheries are attempting to regulate the main output of the industry (Wilder, 1995). Some of the possible ways to regulate the amount of stock that has been harvested is by placing total allowable catch (TAC) or a catch limit on a fishery (Wilder, 1995; Brox, 1996). This sets a limit on the amount that a species can be harvested and once this is reached activity must stop, this keeps the species within sustainable limits (Wilder, 1995; Brox, 1996). For these quotas to work it is necessary to determine what is the level of exploitation that ensures that the resource is sustainable (Wilder, 1995) i.e. the amount of fish that can potentially be caught from a self-regenerating stock year after year without it impacting the industry or the average size of the stock (Wilder, 1995). The highest catch rate is known as the maximum sustainable yield (MSY), with the goal of maintaining the productivity of the oceans by limiting the number of fish to the number that can be replaced by the annual rate of new recruits (Wilder, 1995). Other examples of the different types of quotas are boat quotas, group quotas, company quotas, individual quotas, trade-able quotas, and area regulations (Brox, 1996). While not all of these quota systems worked when it came to capital and sustainability, they did provide insight into where there was a monopoly in the sector. An example of this is company quotas where those who had larger fleets benefited compared to those who only had a couple of boats (Brox, 1996). The larger fleets would be able to catch a larger amount leading to a greater investment in boats and high-end equipment that would all for a greater yield (Brox, 1996). This would lead to smaller fishing companies unable to compete with these larger companies. To create a more equitable system individual quotas were put in place where the TAC was equally divided among all the fishermen, yet this was not a popular option (Brox, 1996). Tradeable quotas where companies, fishermen or boats could buy and sell the number of fish they were allowed to catch (Brox, 1996). With these quotas in place, it does not guarantee that the number of fish that are caught will be the correct species they are looking to catch (Bresnihan, 2019). One way to improve this system is to work with scientists and fishermen to expand the knowledge of fish behaviour, their patterns and distribution, and their improvement of fishing equipment and fishing practices (Bresnihan, 2019). This will eliminate the uncertainty that is associated with fishing, but it will account for some of it (Bresnihan, 2019).

Other approaches that have been implemented are market-based, community-based or co-management approaches (Olson, 2011). These are very different approaches with the market-based placing stakeholders in the fisheries above everyone else, compared to the community-based or co-management where the focus is more on the fishery as a cornerstone of the economy and a part of life in general (Olson, 2011). If there is a move towards the privatisation of fisheries it would create a divide between “economic efficiency versus culture and community” (Olson, 2011). One thing that is evident is that there needs to be a reduction of overcapacity in order for any sort of sustainability (Pauly et al., 2002). When done correctly the reduction of fleet size, should in theory lead to an increase of benefits from the resources (Pauly et al., 2002). There are a variety of different studies of human-environment adaptation, these have found that the natural resource policies and programs that are promoted by both government and private sectors lack the understanding of the value of local knowledge, and social relations but instead, they highlight technical fixes (Brewer, 2013). In an ideal world, the flow of information from science to policy and practice would inform the managing environmental systems (Dale et al., 2019). This information would be generated from a multidisciplinary approach from both the social and natural sciences, including political systems, and would inform policy (Dale et al., 2019). Taking the multi-discipline approach requires that information be easily accessible between the scientist, the fisheries and governments, however not everyone is willing to hand over information that they want to analyse themselves. When there is cooperation amongst the 3 areas more robust adaptation policies could be put in place in terms of sustainability and allow for planning if there are changes in fish species.

A lot of work needs to be done in terms of sustainability in the fishery sector, there is a heavy reliance on the use of quotas as a way of combating overfishing. While there have been improvements such as making the well-being of the fish species a part of policy as a way of improving fish stocks. To get a more detailed image of all the factors that are influencing the fish stocks, there needs to be an investigation of the impacts of both the environmental and ecological factors.

2.3.3 Environmental and Ecological pressures

Other ways adaptation could be made is in the use of earth system models where changes in spawning distributions can be predicted up to 5 years in advance (Miesner and Payne, 2018). Environmental and ecological pressure impacts fish stocks naturally without the added pressures of human activity. While overfishing is always associated with fisheries or governments, it may not be the only reason for the decline in fisheries (Hamilton, 2007). Besides the human pressure that is impacting fish species, there are also environmental pressures, such as wind, which also impacts fishing operations and biological processes such as plankton production (Lindegren and Brander, 2018). Climate change adaptation is necessary for both biological systems as well as human ones, the human aspect is regarding how fisheries and the associated management will adapt (Lindegren and Brander, 2018). These adaptations intersect in healthy marine ecosystems, and productive fisheries, allowing fisheries production to be maximized (Lindegren and Brander, 2018). Climate change is another factor that needs to consider that will have an impact on food systems (Nelson et al., 2016). Other factors need to be considered such as environmental variation, and species interaction such as the predator/prey relationship (Hamilton, 2007).

The environmental pressures that drive most fish species are sensitive to changes in salinity and temperature at depth (Nelson et al., 2016). The changes in temperature and salinity of the water could drive species out of their normal living environments leading to a reduction in the amount available for fisheries (Nelson et al., 2016). However, the spatial and temporal spawning distributions of many fish species are out of the coverage capability of most research cruises, which limits the understanding of the factors controlling spawning (Ibaibarriaga et al., 2007). Even the limits of factors as basic as temperature are difficult to determine if the cruise coverage does not expand over the whole spawning area and farther (Ibaibarriaga et al., 2007). To understand where these sensitivities are coming from, they can be sourced back to the climatic factors originating from the difference in pressure between the Icelandic Low and the Azores High (Mann and Drinkwater, 1994). This difference is referred to as the NAO, changes in this system have been known to cause a wide range of effects within the marine systems

(Marshall et al., 2001). One species with this influence is the Atlantic cod, as these factors are known to have an impact on temperature and salinity conditions (Mann and Drinkwater, 1994). These are associated with poor growth and recruitment in spring and summer (Mann and Drinkwater, 1994).

Climate change and other environmental pressures are not the only things that need to be considered ecological pressures need to be included to a degree. It is a concept that the relationship between predator and prey influence each other's distribution is an ancient one (Rose and Leggett, 1990). This is the predation on prey also needs to be examined also, this occurs at all phases throughout the fish species life cycle (Paradis et al., 1996). It cannot be ignored that the death of the larval is the result of two different causes, these being starvation and predation (Paradis et al., 1996). Starvation occurs in a short time frame when the species has not reached full maturity, giving the predation factor a greater source of mortality (Paradis et al., 1996). At each developmental stage the vulnerability to predation changes depending on the size of the fish and the distribution of the fish (Paradis et al., 1996). One way the larval fish can overcome this specific type of predator is the process of rapid growth, this reduces the time in which the larval fish is in a vulnerability window (Paradis et al., 1996). While this works for the most part the relationship that exists between the two means that predators are drawn to areas where the prey are most dense, this is completed by the prey they try to avoid areas where the predator density is high (Rose and Leggett, 1990). In the prey species the predation risk can induce the fight or flight response, while this is well known among land animals there is very little information on the effect on aquatic animals (Johnsson et al., 2001). An experiment on the effect of the exposure of predators to prey showed that juvenile Atlantic salmon had an increased beat rate and rainbow trout showed flight response (Johnsson et al., 2001). The predation factor needs to be considered when producing a fish stock management system when determining the volume of a catch. Taking into consideration that the ecological processes are influenced by climatic conditions they have a link between the predator and prey relationship (Stenseth et al., 2002). An example of this connection is the match mismatch hypothesis where the growth and survival of cod larvae depend on how well their main food source has reproduced (Stenseth et al., 2002). This highlights

that all the levels of the food chain are interconnected and are sensitive to changes in the environment.

2.3.4 Mackerel

The seas around Ireland are among the most productive and biologically sensitive areas in EU waters (Marine Institute). Atlantic mackerel and horseshoe mackerel are among the most productive and valuable fish species for Irish Fisheries, in 2022 Atlantic mackerel sold approximately €78 million and horseshoe mackerel approximately €17 million (Marine Institute). Atlantic mackerel is one of the most abundant and widely distributed migratory fish species in the North Atlantic Ocean (Jansen and Gislason, 2013). They live their entire life in the pelagic environment (Jansen and Gislason, 2013). Mackerel is able to spawn in a wide range of temperatures (8–18°C), and migrate in temperatures ranging from 5 to 15°C but prefer temperatures between 9 and 13°C (Reid, 2001; dos Santos Schmidt et al., 2023). However, the most suitable temperature for egg development seems to range from 11 to 13°C (Ibaibarriaga et al., 2007; dos Santos Schmidt et al., 2023). The distribution of mackerel is closely linked to these optimal ambient temperatures, differing between the development stage (dos Santos Schmidt et al., 2023). Early life stages (eggs and young larvae) drift passively with the currents until they start undertaking vertical migrations (Jansen and Gislason, 2013). Young juveniles begin to migrate horizontally, and mature adult individuals perform extensive horizontal migrations between overwintering spawning and feeding areas (Jansen and Gislason, 2013).

The Northeastern mackerel spawn from the Mediterranean Sea in the south to the Faroe Island in the North and from Hatton in the west to Kattegat in the east (Jansen and Gislason, 2013). Spawning starts in January in the Mediterranean Sea, February off the Portuguese coast, and ends in July north of Scotland and in the North Sea (Jansen and Gislason, 2013). During the spawning season, the fish are found along the whole European shelf break, from the Hebrides in the north to the Cantabrian Sea in the south (Beare and Reid, 2002). Atlantic mackerel spawn along the European shelf-edge from the Iberian Peninsula to the west of Scotland (Bartsch, 2005). Spawning typically starts in January/February in the south and

then moves progressively north following the seasonal warming, ending around July to the west of Scotland (Bartsch, 2005). Usually, eggs take about 1 week to hatch into larvae, at this stage eggs essentially drift passively (Bartsch, 2005). Ocean warming is expected to continue to affect North-East Atlantic mackerel spawning activity over the 21st century, with displacements toward the northwest and differences in amplitude according to emission scenario and time frame (Bruge et al., 2016). Consequences for the survival of early life stages could certainly be detrimental when aberrant drift occurs in combination with these changes (Bruge et al., 2016). Bruge et al. (2016) projections aim to allow the fishing industry to anticipate the future distribution of mackerel shoals during the spawning period, the implications in terms of future international management of the stock, adaptation, and the planning of future ICES egg surveys.

Working in conjunction with the Marine Institute it was determined that the fish species that will be of interest will be Atlantic mackerel (*Scomber scombrus*) and horseshoe mackerel (*Trachurus trachurus*). This section will discuss the life cycle of mackerel with the main focus on the egg stage. It will also discuss previous studies that have been conducted on this species and what they have done. In my approach, I will utilize the skill of the initialized hindcast simulations to determine if there will be any change in the distribution of the mackerel fish stock. This will be explored through the movement of the stock northward. This will be highlighted in Chapter 7.

2.4 Effective communication of scientific research

Scientists communicate to stimulate public understanding of science, including the process and the result, our data (Coffin, 2021). Communication increases public support for science (Coffin, 2021). We communicate so our findings can influence policy, such as testifying at a hearing about anthropogenic sound regulations and whale migration (Coffin, 2021). A starting point in improving scientific communication in a public forum is speaking with confidence and reducing apprehension (Luisi et al., 2019). Recognising that the target audiences do not often come

equipped with the vocabulary, experiences, at times the motivation to understand and value the messages that STEM scientists want to convey (Luisi et al., 2019). Having the awareness that science communication is more effective when considering the diversity within audiences, persuasive devices, audience attitudes and beliefs, access to information, and empowerment strategies (Luisi et al., 2019). It has become apparent that those with communication training as part of their education are better prepared to communicate their research to various audiences (Luisi et al., 2019). Communicating with the public focuses the attention on a specific issue that requires a decision that would benefit from understanding the related science (Luisi et al., 2019). When communicating research findings with the public a problem arises with the broad range of specialities that occur (Jamieson, 1996). Finding a balance between two extremes: a warning that is issued too early based on weak data may scare people and discredit science; a warning that is issued too late may be useless for preventing a problem or mitigating its effects (Jamieson, 1996).

At the social level, the success of scientists' communication depends on their awareness of the role that their work plays in the public discourse (Fischhoff and Scheufele, 2013). Although scientists may know more than anyone about the facts and uncertainties, applications of that science can raise complex ethical, legal, and social questions, regarding which reasonable people may disagree (Fischhoff and Scheufele, 2013). As a result, if scientists want to be effective in their communication, they must understand and address the perspectives of interest groups, policymakers, businesses, and other players in debates over decisions that require scientific expertise (Fischhoff and Scheufele, 2013). The social, behavioural, and decision sciences have documented the many ways in which intuitions about others and the effectiveness of communication can go wrong—and how those biases grow with the distance between the parties (Fischhoff and Scheufele, 2013). The unique ways of looking at the world that make scientists such indispensable sources of information may also distance them from non-scientists (Fischhoff and Scheufele, 2013). Making the most of what science has to offer society requires the give-and-take of two-way communication with lay people (Fischhoff and Scheufele, 2013). Those interactions can be direct, as in classrooms and social settings, or indirect,

through the mediation of research helping scientists to understand the public and vice versa (Fischhoff and Scheufele, 2013). Ineffective communication can be costly to science as well as to society (Fischhoff and Scheufele, 2013).

2.4.1 Different types of communication

There are a variety of ways in which science can be effectively communicated, such as public forums (i.e. presentations oral and poster), reports in news or through research articles, and infographics. The scientific information that the public receives can come from various actors and sources (e.g., scientists, science PR, science journalists) via various media/channels (e.g., newspapers, TV, press releases, social media) (Weingart and Guenther, 2016). All of these have different target audiences in mind but what needs to be clear in all forms is the uncertainties within the research and approachable at all levels (Coffin, 2021). Using storytelling or narratives could be one way of tailoring the information to suit the public, through using a simplified version of the research yet still retaining the main message (Negrete and Lartigue, 2004; Dahlstrom, 2014). However, storytelling is often viewed as baseless or even manipulative (Dahlstrom, 2014). Narratives are easier to comprehend, and audiences find them more engaging than traditional logical-scientific communication (Dahlstrom, 2014). The sources from which non-experts receive most of their science information are already biased toward narrative formats of communication (Dahlstrom, 2014). Storytelling may provide an accurate way of representing and communicating knowledge, an effective emotional trigger, a lasting memory structure, an enjoyable medium and a powerful aid for learning (Negrete and Lartigue, 2004). To present scientific information through stories, novels, comics and plays should be regarded as an important means to transmit information in the repertoire of both science teachers and communicators (Negrete and Lartigue, 2004). Using YouTube for science and environmental communication has various advantages: it does allow passive consumption of the users, but it also allows building communities and establishing dialogues with various audiences (Allgaier, 2019).

2.4.2 Infographics

Infographics can take various shapes and forms but may be grouped into three main types of data graphics, maps, and diagrams (Otten et al., 2015). Infographics can be static, animated or interactive and seek to educate, inform, or persuade the target audience (Beecher et al., 2023). The data visualizations range from simple graphs in elementary school classrooms to depictions of uncertainty in election forecasts in news media, to complex data displays used by scientists and analysts (Franconeri et al., 2021). Infographics may also address challenges in health communication to lay audiences with lower levels of literacy or language barriers (Beecher et al., 2023). Multiple data visualizations, maps, or diagrams can be combined into an overall visual composition with illustrations and selected text to convey a larger story or narrative (Otten et al., 2015). Such large posters, panels, or scrolling images are commonly considered to be infographics, although they might also be called “story graphics” because they impose a narrative flow on the data (Otten et al., 2015). When designed effectively, these displays leverage the human visual system’s massive processing power, allowing rapid foraging through patterns in data and intuitive communication of those patterns to other viewers (Franconeri et al., 2021). It has been estimated that 56% of the total world population currently uses the internet compared with only 5% in 2000 (Kunze et al., 2021). The internet and particularly social media have become essential means of obtaining information, with a recent study estimating that approximately 75% of patients make medical decisions influenced by online sources (Kunze et al., 2021). The widespread use of social media in this context led to the development of altmetrics (also known as “alternative metrics”), a tool that measures and quantifies the impact of research shared on social media (Kunze et al., 2021). Viewers of infographics should read them out of interest but turn their attention toward the original article or a source of more detailed information before making changes in clinical decision-making or practice, as they can be oversimplified (Kunze et al., 2021).

2.4.3 Challenges of communicating science

One of the challenges that face scientist is how can our work be effectively communicated to those who are not directly involved in the field. Whether these are fellow scientists or the general public. Care needs to be taken when communicating with audiences that have a mixed understanding of the concepts being discussed. As scientists, we strive to increase the public's knowledge (Luisi et al., 2019). However, there is a tendency to forget that not everyone has the same level of knowledge (Luisi et al., 2019). There is a risk of the public being under-informed or even misinformed when it comes to scientific issues. Misinformation can be broadly defined as information that is incorrectly spread to others, possibly by accident. Disinformation has sometimes been used to denote a specific type of misinformation that is intentionally false. There is a fine line between being misinformed and uninformed. Being misinformed is believing in incorrect or counterfactual claims, while uninformed is not having any awareness of the facts (Scheufele and Krause, 2019). The process by which we gather information about the state of the world is characterised by assumptions, limitations, extrapolations, and generalisations (Van Der Bles et al., 2020). This brings imprecision and uncertainties to the facts, numbers, and scientific hypotheses that express our understanding of the world around us (Van Der Bles et al., 2020). Even though scientists and other producers of knowledge are usually well aware of the uncertainties around their findings, these are often not communicated clearly to the public and other key stakeholders (Van Der Bles et al., 2020). This lack of transparency could potentially compromise important decisions people make based on scientific or statistical evidence (Van Der Bles et al., 2020). Being open and transparent has both risk and reward, it can restore public trust in science but will also invite criticism (Van Der Bles et al., 2020). There are two kinds of uncertainty: epistemic uncertainty (uncertainty due to limitations of the sample or methodology) vs. uncertainty about the future that arises because we cannot know (i.e., randomness, chance; we cannot know for certain what will happen tomorrow) (Van Der Bles et al., 2020). Although uncertainty about the future is a widely acknowledged aspect of forecasts and predictions, epistemic uncertainty about the past and present is equally important yet often overlooked in communication (Van Der Bles et al., 2020).

One example where scientific communication fell short is the vaccination rate in the United States (Luisi et al., 2019). Through repeated communications recommending vaccines and pointing out the millions of lives they save, this was not enough to convince people to get them (Luisi et al., 2019). This method of communicating is not enough, messages need to be designed to include evidence in a way that is understandable and appealing to target audiences (Luisi et al., 2019).

2.5 Summary

To tailor predictions for stakeholders' needs, the identification of what they are looking for needs to be completed. In this case, working with the Marine Institute, they identified that they wanted to try to determine if there was a northward shift in the mackerel stock in the Eastern North Atlantic if this was associated with a temperature change. As the time scale in which the thesis is decadal, I want to know if there is prediction skill with the variables. The first step is to find out what influences temperature and salinity and the time scales that are associated with it. How the variables react within the model framework. The second step is to determine what has been done before in terms of using predictions for fisheries. The timescales on which previous work has been conducted are on a lesser time scale than what I am working with. This holds the potential for the development of better models. Finally, how can this information be effectively communicated to stakeholder needs?

From the literature review in section 2.2 the main influences on temperature are NAO etc. The decadal variability seen in temperature is referred to as the AMV. Salinity is influenced by and on longer time scales is the AMOC. The AMOC is one of the leading drivers in the North Atlantic however the influence it has on temperature or salinity would not be as evident as using the SPG and AMV. Further detail on the influence on skill they will have can be found in Chapter 6. Knowing the drivers that impact temperature is an important factor in the spawning of mackerel. While it is not the only factor that influences mackerel for this study I take a statistical approach, the environmental and ecological were explored to get an idea of what else is happening with the stock. it can be forgotten how these predictions can be used, this is the management of fish stock within private fishing

companies, as evidenced in the better regulation of policies surrounding the fishing industry. while trying to factor in every aspect of the fish's life cycle, the analysis of temperature on a decadal time scale provides the basis for further research to be conducted at a later date. It is important how this information is communicated as it could easily be misinterpreted by those who are not familiar with such work. while there has been usually a negative reaction to storytelling or narratives, they can be very useful in communicating scientific research when done right. One of the easiest yet challenging ways to communicate is through infographics. getting the balance between visuals and text is often a challenge. After identifying how each of the variables are represented within prediction systems the final task is to determine how they are in decadal predictions. Some other information is the various components that go into these systems that aid in providing prediction skill, these include ensembles. As discussed, initialisation. It should also be noted that how these systems are put together and run also impacts the. This will be further explored in Chapter 3.

Models and Methods

3.1 The MPI-ESM model and components

There is a wide range of earth system models that exist, and these have mainly been developed through government funding institutes that have the resources to dedicate time in the improvement. Among these is a group called initialised Earth System prediction, these have their set up conditions set to close to observations and allowed to run for up to 10 years (Meehl et al., 2021). The model that will be used for this thesis is the Max Planck Institute Earth system model low resolution “MPI-ESM-LR” which consists of 5 systems that interact with each other (Brune and Baehr, 2020). These are ECHAM6, JSBACH, MPIOM, HAMOCC, and OASIS which can be seen in Figure 3.1. ECHAM6 is the atmospheric model, MPIOM is the oceanic physics model, JSBACH is the terrestrial biosphere, and HAMOCC is the oceans biochemistry. OASIS3 is a separate coupling program that establishes the link between the different components, where energy, momentum, water, and CO₂ can be exchanged. The initial exploration of decadal predictability was using the ECHAM6 data to explore the atmospheric/oceanic aspect of the research, this was isolated to the MPIOM data which was explored various depth levels.

The Hamburg Ocean Model, MPI-OM is the successor of the Hamburg Ocean Primitive Equation (HOPE) model and has undergone significant development in

recent years (Wetzel et al., 2004). The most notable change is in the treatment of horizontal discretisation which has undergone transition from a staggered E-grid to an orthogonal curvilinear C-grid (Wetzel et al., 2004). The treatment of the sub-grid scale mixing has been improved by the inclusion of a new formulation of bottom boundary layer slope convection, an isopycnal diffusion scheme, and a Gent and McWilliams style eddy-induced mixing parameterisation (Wetzel et al., 2004). The MPI-OM is an ocean general circulation model (OGCM) based on the primitive equations representing thermodynamic processes (Wetzel et al., 2004). It can simulate the oceanic circulation from small scales to gyre scales, in response to atmospheric forcing fields (Wetzel et al., 2004). For an application on horizontal scales smaller than 1 km, the hydrostatic assumption is no longer valid, and the model must be reformulated in parts (Wetzel et al., 2004). The use of an ocean circulation model requires a comprehensive understanding of ocean physics and the numerical formulation (Wetzel et al., 2004). Many physical processes in the ocean are still not well understood and therefore only crudely parameterised (Wetzel et al., 2004).

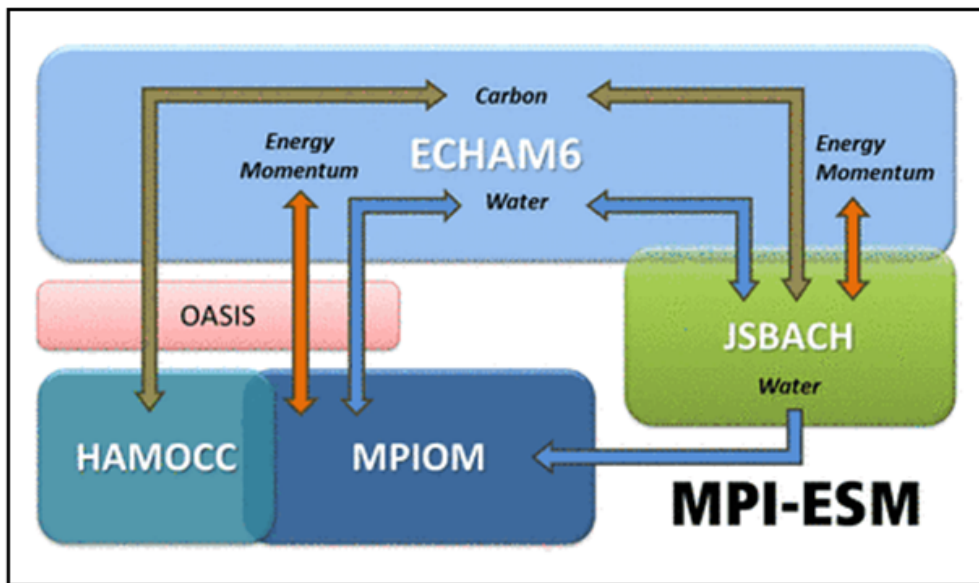


Figure 3.1: The Max Plank Institute Earth system model (MPI-ESM) highlighting the 5 systems and how they interact with each other. ECHAM6 (atmosphere), MPIOM (ocean physics), JSBACH (terrestrial biosphere) and HAMOCC (ocean's biogeochemistry). A separate coupling program, OASIS3, establishes the link between the different components, in which energy, momentum, water and CO₂ can be exchanged (From DKRZ, 2021).

From this model, the following simulations are used assimilation, initialised hind-cast, and uninitialised historical simulations. These simulations are taken from the MPI-ESM-LR MPIOM model and are visible in Figure 3.2. Figure 3.2 also highlights how each of the components are generated from the model and observations. The initialised simulations are generated from observational data and allowed to run for a period of 10-30 years (Schuster et al., 2019). Through initialisation from the observational data decadal predictions have shown to provide more skill than climate projections, this is through the exploitation of the arising from internal variability from the observation data (Volpi et al., 2017). One of the key aspects of these time-evolving climate predictions is the ability to internally generate the naturally occurring variability with the natural system (Meehl et al., 2021). When model components are brought into close correspondence with the observed state this is referred to as initialisation, the predictions that are started from these states are referred to as initialised predictions (Meehl et al., 2021).

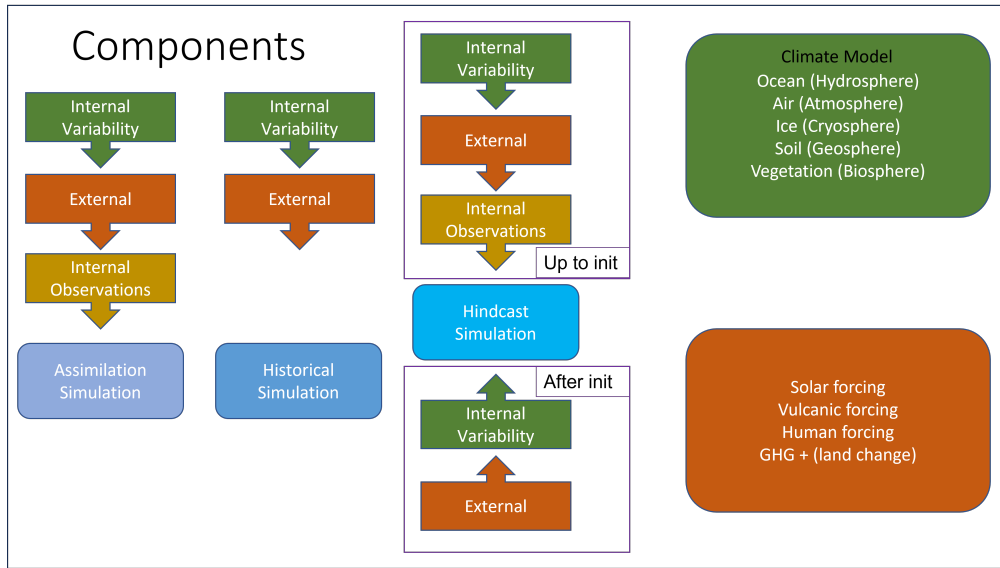


Figure 3.2: From the model three components are analysed; Assimilation Simulation (Internal Variability, External variability, Internal Observations), Uninitialised Historical Simulations (Internal Variability, External variability), Initialised Hindcast Simulations (Internal Variability, External variability, Internal Observations up to a initialisation then Internal Variability, External variability after initialisation). Internal Variability generates information from the climate model (Green box) and External Variability (Orange box).

3.1.1 What are ensembles and lead times

Models use a range of ensembles, forcings, and initialisation which are combined that allow for a variety of different results and predictions. One of these aspects that is important in predictive skill and reliability is ensemble size, they range from anything between 10 and 50 for most prediction systems (Meehl et al., 2021). Ensembles are generated from the model, were it runs several times using slightly different starting conditions generating a varying number of members to the ensemble. Typically, the greater the number of ensembles the higher the anomaly correlation coefficient (ACC) (Meehl et al., 2021). The initialisation is the integration of a vast amount of observational information into an Earth System Model (ESM) which is central to s2d prediction (Meehl et al., 2021). Within the model components the atmosphere is an area that has the most advanced data assimilation techniques implemented, coupled ocean-atmospheric shows promise (Meehl

et al., 2021). The coupling has the ability to reduce "initialisation shock" and improve forecast prediction (Meehl et al., 2021). The lack of observations still remains an obstacle, a way to get around this is to nudge reanalysis products in the ocean and atmosphere to use as assimilation simulations (Meehl et al., 2021). Despite limitations for decadal forecasts, it is possible to estimate the forecast skill of numerical models by applying statistical methods (Thoma et al., 2015). Lead-time is defined as the length of time from the issuing of the forecast to the middle of the running mean window (Payne et al., 2022). In this study the the 2 to 5 year lead times are used to generate multi-year averages. For the initialisation year 1961 the multi-year average is generated for the time span of 1963-1966. This is completed for the time frame 1961 to 2008 for both the 4, 6 Chapters and 7 Chapter.

3.1.2 Initialised Hindcast

In recent times there have been vast improvements in the field of decadal prediction skill, one area that has shown significant improvement is the development of initialised hindcast simulations. Initialised hindcast simulations are retrospective forecasts that are used to assess the ability of the model systems to predict climate variability on inter-annual to decadal time scales (Schuster et al., 2019). Forecast skill is measured by comparing initialized forecasts with observations and indicates the "ability to predict" the actual evolution of the climate system (Boer et al., 2016). Initialisation is the process of integrating a vast amount of observational data into an ESM, this is central to the seasonal to decadal predictions (Schuster et al., 2019; Meehl et al., 2021). They are allowed to run for a period of 10-30 years, combining forecast elements from weather and seasonal forecast divisions (initial conditions) as well as from long-term climate projections (boundary conditions) (Schuster et al., 2019). Initialised products that have the longest forecast range available are decadal prediction ensembles, which supply climate information up to 10 years into the future (Befort et al., 2022). They can be made with a single model or with multiple models (preferably). Also provides information, together with targeted simulations, for understanding the physical mechanisms that govern climate variation, and this is important for the science as well as for engendering confidence in the forecasts (Boer et al., 2016).

There are obstacles with initialised simulations, one being the lack of observations. One way around this issue is to nudge reanalysis products in the ocean and atmosphere to use as assimilation simulations (Meehl et al., 2021). Another is model limitations, where the ability of models to reproduce the observed climate that can lead to model biases (Thoma et al., 2015). If the model is initialised in the best possible way, the model forecast can be obscured by the drift toward the model’s own inherent climate (Thoma et al., 2015). One way to take advantage of the added value of the initialisation carried by decadal predictions is by selecting those projections that are close to the ensemble mean (Befort et al., 2022). Befort et al. (2020) highlighted this through constraining projection ensembles there is significantly more skill at predicting near-surface air temperatures over the North Atlantic Gyre region compared to the unconstrained climate projection ensemble. The advantage of using sub-sampling approaches is that the resulting constrained ensembles are physically consistent as they are based solely on climate projections which are available for the entire period from the present up to the end of the century (Befort et al., 2022).

3.1.3 Uninitialised historical simulations (CMIP5 and CMIP6)

The differences in the CMIP6 experimental protocol compared to that of CMIP5 include more frequent hindcast start dates and larger ensembles of hindcasts for each start date intended to provide robust estimates of skill (Boer et al., 2016). Compared with CMIP5, the atmospheric and ocean resolution of CMIP6 improved; it also includes new and more complex processes, including more complex land surface processes, ice fields, and permafrost which improve the hydrological processes (Guo et al., 2022). CMIP6 has improved the simulation performance of runoff compared with CMIP5. However, GCMs still have great potential of further improvement in arid regions. Although the deviation still exists, it is gradually decreasing (Guo et al., 2022). It shows that with the development of the climate model, it is increasingly suitable to analyse the changes on a large scale (Guo et al., 2022). In CMIP5, skill improvement through initialization was particularly high in the North Atlantic subpolar gyre (SPG) region (Borchert et al., 2021). Predic-

tions of decadal SPG SST variations were found to improve because initialization synchronized modelled fluctuations in the Atlantic Meridional Overturning Circulation (AMOC) and associated ocean heat transport with observations (Borchert et al., 2021).

3.2 Post-Processing Methods

For this initial investigation, we analysed simulations with the Max Planck Institute Earth system model (Giorgetta et al., 2013; Mauritsen et al., 2019) in its low-resolution setup (MPI-ESM-LR) for the time period 1961-2013. In MPI-ESM-LR, the oceanic component (MPIOM, Jungclaus et al., 2013) is set up with a nominal horizontal resolution of 1.5° globally, actually corresponding to $\approx 1^\circ$ in the Northeastern Atlantic, and 40 levels vertically. The atmospheric component (ECHAM6, Stevens et al., 2013) is configured with a spectral resolution T63, corresponding to $\approx 1.9^\circ$ horizontal resolution globally, and 47 levels in the vertical. In this thesis hindcasts and both uninitialised simulations ("CMIP5", "CMIP6") are analysed for both potential temperature and salinity at the surface. Annual mean values of model output variables are computed and then used to generate a 2-to-5-year lead year time series for the time frame 1958-2013 for each member. For all simulations, we compute the 16-member ensemble mean.

3.3 Calculation of the Anomaly Correlation Coefficient

Many different statistical tools are used to identify physical mechanisms in climate models, among them the Anomaly Correlation Coefficient (ACC) seen in equation 1; (Dobrynin et al., 2018, 2019; Borchert et al., 2018) and composite plots (Borchert et al., 2018, 2019). It is a measure of how well the forecast anomalies have represented the observed anomalies. In this instance, the forecast is the uninitialised and initialised simulations (v) with the observed being the assimilation simulation (o) for a given period of time (i). It highlights how well the predicted values from the forecast model “fit” with the real-life data. The values obtained range from +1 to -1. Where approaching +1 shows there is a good agreement and the forecast anomaly has had value. Approaching -1 the agreement is in anti-phase and the

forecast is unreliable. Anything around 0 there is poor agreement, and the forecast has had no value.

$$ACC = \frac{\sum_{i=1}^n (v_i - \bar{v})(o_i - \bar{o})}{\sqrt{\sum_{i=1}^n (v_i - \bar{v})^2 (o_i - \bar{o})^2}} \quad (1)$$

The initialised and uninitialised simulations quality of the ensemble mean is assessed by calculating skill based on ACCs (Kröger et al., 2018). ACCs of the initialised and uninitialised simulations are defined with respect to the assimilation simulation (Kröger et al., 2018). Borchert et al. (2018) determined that there is an indication for significant ACC in the North Atlantic to be connected to low-frequency ocean dynamics, which break down when the atmosphere contributes significantly to SST variability. We also calculate the differences of the resulting ACCs between the hindcasts and the uninitialised simulations. Typically, the greater the number of ensembles the higher the anomaly correlation coefficient (ACC) (Meehl et al., 2021). The composite plots used by Borchert et al. (2018, 2019) were used to distinguish between the effects of warm and cold Ocean Heat Transport phases or subpolar gyre SST phases on the surface temperature over Europe. Uncertainty is estimated by a bootstrapping of 500 repetitions with a significance level of 5% (Wang et al., 2014).

3.4 Investigation into the improvement of skill using sub-sampling.

The next step is the improvement of prediction skill. One method of improving the prediction skill is a method known as subsampling. The sub-sampling method was introduced by Dobrynin et al. (2018) and subsequently used by Dobrynin et al. (2019) and Düsterhus (2020), who used this algorithm to increase prediction skill of model prediction. It is an algorithm applied during post-processing that helps in the improvement of prediction skill in regions where the simulations lack skill. A predictor is needed that is relevant to the region either atmospheric or oceanic indices for the region that can aid in the improvement of skill. The sub-selection of members from hindcast ensembles is based on statistically predicted on chosen

indices (Dalelane et al., 2020). For the North Atlantic Ocean, I have identified two predictors that may help in the improvement of skill the SPG, and the AMV. They both have decadal trends in the North Atlantic Ocean which will improve the prediction skill on both temperature and salinity at depth. The calculations of each predictor are outlined in the subsections 3.4.1 and 3.4.2. Two time series is generated of the target region from the initialised hindcast simulation one with the ensemble mean and the other containing the individual member means. These time series are compared with the predictors, the 16 members, which are closest to the predictors are then selected for a sub-sampled average. This was completed for the AMV, SPG, and a combination of the two. Then the subsampled grids were subtracted from the initialised hindcast leaving areas of improvement from the predictors. Three areas (Southeast, Southwest, and North) from the initialised hindcast simulation, with little prediction skill underwent further analysis to determine if the predictors could improve skill in these areas. These sites were analysed using the assimilation simulation and the initialised hindcast simulation which were compared to the time series of the SPG and AMV individually. Generated from the MPIOM component from MPI-ESM-LR for the time frame 1966-2013 with a 2 to 5 years lead time for a depth mean of 6m – 220m for the initialised hindcast simulation.

3.4.1 Calculation of AMV

The AMV was generated from the assimilation data from the MPI-ESM-LR. Where the sea surface temperature (SST) was taken from the North Atlantic region ($60^{\circ}\text{N}, 0^{\circ}, 0^{\circ}, -75^{\circ}\text{W}$) and a field mean was created. What this means is that every grid point of the same field is weighted by area weights obtained by the input field.

3.4.2 Calculation of SPG

The SPG was calculated using the principal coefficients of empirical orthogonal function (EOFs) of sea surface height for the subpolar gyre region ($60^{\circ}\text{N}, 40^{\circ}\text{S}, 40^{\circ}\text{E}, -75^{\circ}\text{W}$). The EOFs were calculated from the anomalies, from these EOFs the principal coefficients were calculated. A time series of these principal coefficients of EOFs was created that will be used in the analysis. The initialised hindcast simulation,

AMV and SPG were correlated with the assimilation simulation to determine if there was skill based on the initialisation or through the predictors.

3.5 Tailoring of decadal predictions for observational data: Stage 1 egg density

The data required for this type of estimate are the abundance of stage I mackerel eggs, and the water temperature over the whole spawning area and season for this species (Beare and Reid, 2002). In the context of the western spawning component of the Northeast Atlantic Mackerel, this covers the western, shelf-edge area from the corner of the Bay of Biscay to the North of Scotland, and the period from March to July inclusive (Beare and Reid, 2002). In the context of the western spawning component of the Northeast Atlantic Mackerel, this covers the western, shelf-edge area from the corner of the Bay of Biscay to the North of Scotland, and the period from March to July inclusive (Beare and Reid, 2002). The ICES triannual Atlantic mackerel and horse mackerel egg survey, conducted from January to July covering south Portugal to the north of Scotland (Reid, 2001; Ibaibarriaga et al., 2007). The primary analysis is dedicated to mackerel and horse mackerel eggs, the survey also provides samples of eggs and larvae for a range of other species, while these are not routinely sorted and counted (Ibaibarriaga et al., 2007).

Data were available from nine triannual (1992, 1995, 1998, 2001, 2004, 2007, 2010, 2013, 2016, 2019) Mackerel and horse mackerel egg surveys (MEGS, 1992-2019). The surveys covered the same basic sampling area with some variation between years in their detail. This survey area has generally been extended over the years to cover changes in the perception of the spatial scope of mackerel spawning. In the first three years of the surveys (1992, 1995, 1998) very few samples were collected north of 55 but the samples extend up to 65 in the final three surveys (2010, 2013, 2016). Data that obtained from these surveys also included surface temperature, temperature at 20m, salinity at 20m, the species, number, egg per m^2 . It also holds the ICES haul ID, survey, country, survey period, ship, depth upper and lower, this is not as important.

For this analysis two species of mackerel were identified, the first Atlantic (Scomber

3.5. Tailoring of decadal predictions for observational data: Stage 1 egg density

scombrus) and the second Horseshoe (*Trachurus trachurus*). For each species of mackerel, the density (egg per m^2) and distribution were examined to determine changes in the range of the stage 1 eggs. The absence of eggs was also considered. Once this was obtained two areas were highlighted to roughly show the Northern fishing grounds and a section to the north where the stock could potentially be spawning. These two areas allowed for the exploration into the mean annual temperature changed compared to that of the density of the fish stocks.

The next step was to explore these two target areas in the initialised hindcast simulations in within the MPIOM for a grouped depth of 6m to 220m. Where an ensemble mean is generated, and this is what is used in the generation of the ACC plots. The model was initialised each November from 1989 – 2014 with a 2-to-5-year lead time and contain 16 ensemble members and was detrended. Following on from this the initialised hindcast simulation was extended forward five years to 2019, where error bars were added.

Finally, the last step was communicating this information to the stakeholders and relevant individuals who do not necessarily have a background in models and predictions. An infographic was developed that contained the key pieces of information that is needed from both the observations and the model.

Predictability of the Physical Mechanisms in the North Atlantic Ocean

4.1 Introduction

Through consultation with stakeholders, the environmental factors that influence spawning activity are temperature and salinity. This chapter aims to answer the first question posed in the 1 chapter. Specifically, whether temperature and salinity are predictable for the North Atlantic Ocean. In this research, temperatures will be compared from two models an ocean model and an atmospheric model. From the ocean model temperature was analysed in two forms the first from sea surface temperature and the second from the depth profile of 6m. The purpose of this is to narrow down which model that will be used further in the thesis. The first half of this question dealing with the mechanism in the North Atlantic Ocean was dealt with in the 2 chapter.

1. What mechanisms that influence temperature and salinity in the North Atlantic Ocean, are these predictable?

4.2 Simulations and methods

This chapter explores the predictability of the North Atlantic Ocean for temperature and salinity through the analysis of the data highlighted in Figure 4.1. The variables are analysed on a 2-to-5-year lead time average for the time period 1961 to 2008 with a 16-ensemble member mean. The temperature in this region was broken down into three different versions of the variable, the first is from the atmospheric model (ECHAM6) and the other two from the ocean model (MPIOM). The ocean model consists of the SST that contains the atmospheric interactions and the second is the potential temperature oceanic interactions, from the depth data this will be from 6m. The salinity is from the MPIOM depth data where the 6m was also used at the near-surface salinity. This initial exploration into the data will allow us to determine what is predictable in this region and if there is skill, it will also allow for a comparison between the different types of temperature data this will allow for the exploration into the variability of the different models. Within each of the different models, there will also be a comparison between initialised simulations and uninitialised simulations, this will allow us to see if there is an improvement in skill from the initialisation. What is expected is that there will be a skill for SST amongst all the models and little or no skill for the salinity.

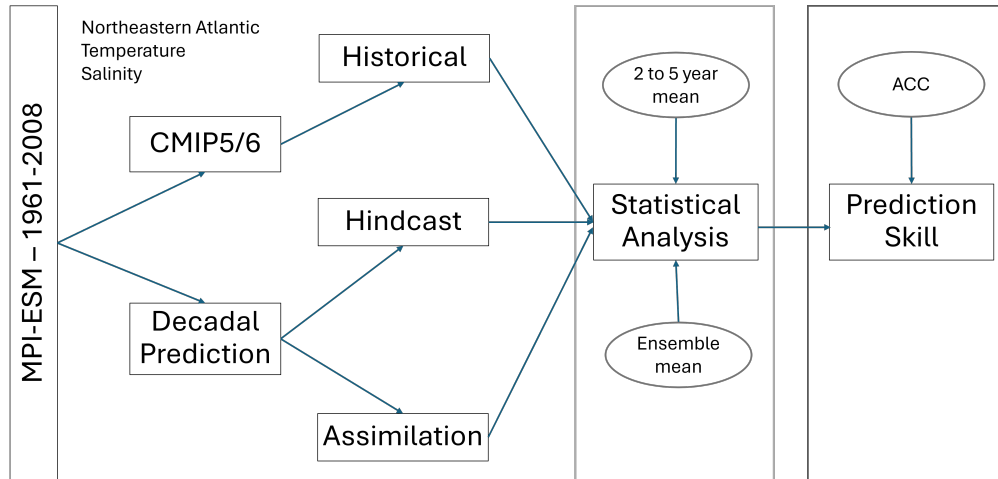


Figure 4.1: Schematic representation of the Anomaly correlation coefficient (ACC) method for 16 ensemble members for the proposed variables in 1961-2008. The proposed variables are taken from 2 systems (ECHAM6, MPIOM) in the Max Plank Institute Earth system model (MPI-ESM). The uninitialised historical simulations are taken from the CMIP5 and CMIP6 simulations and the initialised hindcast simulations are taken from decadal prediction. The simulations undergo statistical analysis where for each ensemble member a 2 to 5 year mean is calculated for each year, followed by an ensemble mean. The final step is the ACC calculation where the variables for initialised hindcast simulation, uninitialised historical simulation evaluated against assimilation simulation.

4.3 Predictability of Sea Surface temperature from the ECHAM6 model

The first variable that was looked at was the SST from the atmospheric model (ECHAM6), this was an initial exploration into what is capable within the model and to determine if there was a difference between the ocean model (MPIOM). I have analysed predictability for one initialised hindcast simulation and two uninitialised historical simulations ("CMIP5", "CMIP6") for the eastern North Atlantic Ocean where the assimilation simulation was removed from each only leaving the prediction skill, the results of the analysis are found in Figure 4.2. The initialised hindcast simulation shows skill for the majority of the eastern North Atlantic Ocean this is highlighted by the areas in red, and the areas in blue show that there is little or no skill for that region (Figure 4.2 a and d). Both the uninitialised his-

torical simulations show very few areas of skill compared to the initialised hindcast simulations, I will first discuss the CMIP5 results followed by the CMIP6 results. Uninitialised CMIP5 simulation (Figure 4.2 b) skill in the subpolar North Atlantic region. Figure 4.2 c) shows the initialised hindcast simulations compared to the uninitialised historical simulation CMIP5 and the difference between the two. The uninitialised CMIP5 simulations have less skill over Eastern North Atlantic with a small section of skill between Greenland and Iceland. When the initialised hindcast simulations are compared to the uninitialised CMIP5 simulations through initialisation there is an improvement of skill in this region. Uninitialised CMIP6 simulation (Figure 4.2 e) has some skill in the subpolar North Atlantic region, but this is not significant. Figure 4.2 f) shows the initialised hindcast simulations compared to the uninitialised historical simulation CMIP6 and the difference between the two. While this does look promising there is little significant skill for Eastern North Atlantic, the two main areas that show significant skill are over Greenland and off Eastern Canada. This is what we would expect from this model as it is more skilful over large land masses with some skill in small sections of the ocean. This is clear for West of Ireland, it does show that there is an improvement in the North Atlantic Ocean using initialised hindcast simulations. When these results are compared with initialised hindcast simulations it is clear that the uninitialised CMIP6 simulation is outperformed the CMIP5 simulation.

This allows for an initial investigation into the model systems and how predictability in the atmospheric model is represented. While for this thesis the main focus will now be shifted to the ocean model (MPIOM), this will allow for the predictions be tailored to the fishery industry. To do this a decision needs to be made on whether the MPIOM SST will be used or the potential temperature (6m) alongside the salinity (6m) in chapter 7.

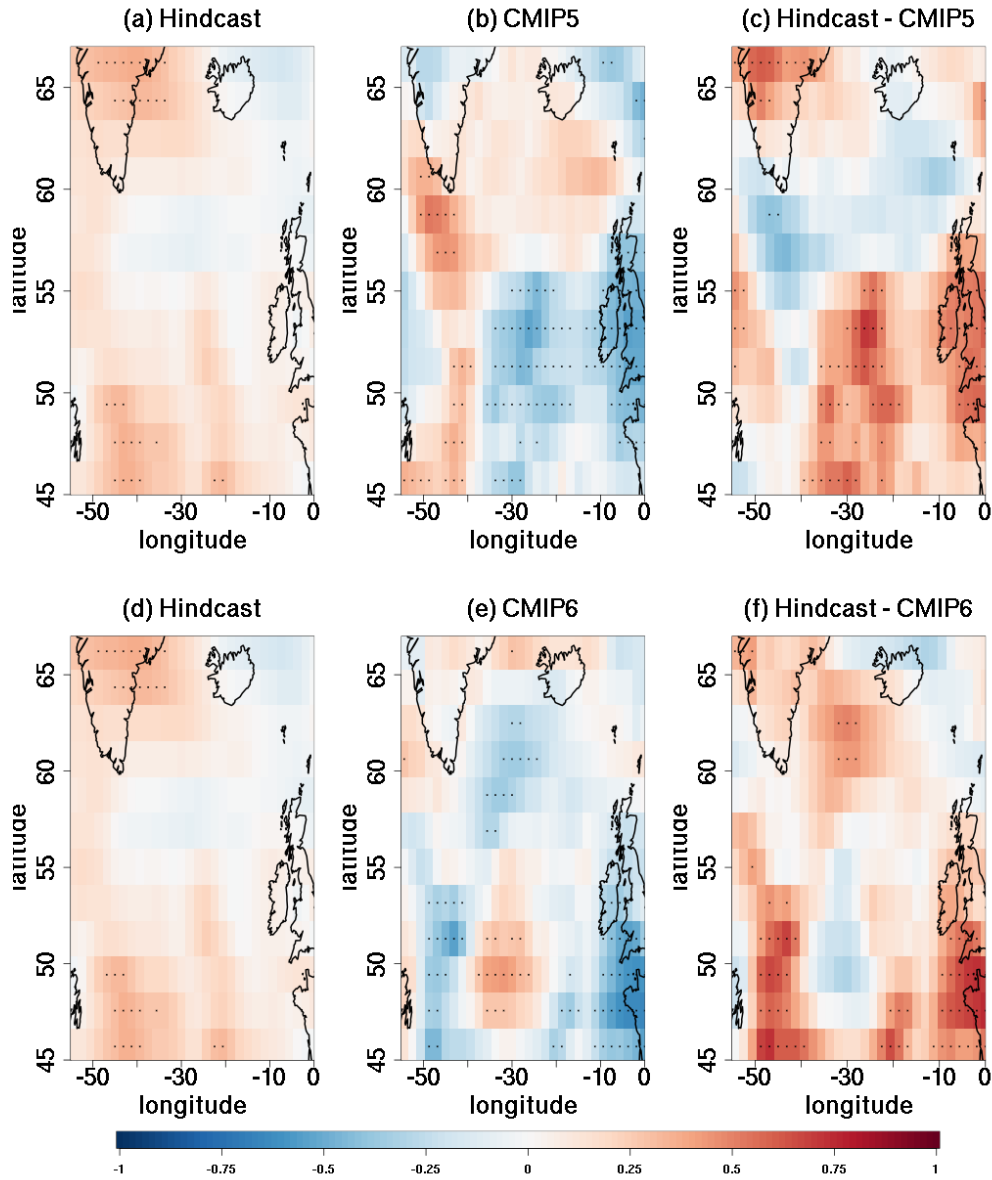


Figure 4.2: Anomaly correlation coefficient (ACC) for SST (ECHAM6) for initialised hindcast simulation (a and d), uninitialised historical simulation (CMIP5(b), CMIP6 (e)) evaluated against assimilation at lead years 2-5. The difference between initialised hindcast simulation - uninitialised historical (CMIP5(c), CMIP6 (f)) simulation. Generated from the MPI-ESM-LR; 1966-2013; initialised each November; 2 to 5 years lead time; 16 ensemble members. The red is positive correlation, the blue is negatively correlated and the black dots show significance.

4.4 Predictability of Sea Surface temperature from the MPIOM model

Alternative to the atmospheric SST is the ocean SST from the MPIOM, this has the ability to generate finer resolution. For this variable I explored the predictability for the eastern North Atlantic Ocean for initialised hindcast simulations and two uninitialised historical simulations ("CMIP5", "CMIP6"). These are illustrated in Figure 4.2 below where the initialised hindcast simulations are Figure 4.2 a and d, the two uninitialised historical simulations ("CMIP5", "CMIP6") Figure 4.1 b and e respectively, the difference between the initialised simulation and the uninitialised simulation Figure 4.2 c and f respectively.

The initialised hindcast simulation result for the eastern North Atlantic Ocean shows significant skill for the majority of the region, with a few areas with little or no skill (Figure 4.3 a). Taking a closer look at Ireland and the surrounding sea there is significant skill in the northwest region, as you move southward along the European shelf there is little or no skill. Moving westward from France towards Canada there is also reduced skill, a final area that does not show skill is in the Norwegian Sea. The uninitialised historical simulation CMIP5 shows a completely different picture, it is mixed more with areas that have particularly good skill and areas that have little or no skill (Figure 4.3 b). These uninitialised CMIP5 simulations do have areas that have improved skill over the initialised hindcast simulation, which is visible around Ireland and France where there was little or no skill now has significant skill (Figure 4.3 c). The same can be seen in the area to the north of Iceland, but just as there is improvements there is also little to no skill around Canada and Greenland where there was previously significant skill. When these two simulations are compared to each other the initialisation has improved over the uninitialised CMIP5 simulation in the north and the CMIP5 performs better to the southeast (Figure 4.3 c). The uninitialised CMIP6 simulations have quite good significant skill for the region with small areas that have little or no skill (Figure 4.3 e). Similar to the CMIP5 simulation it performs better around Iceland and Ireland. With a small area in the middle of the North Atlantic Ocean that has little or no skill, this also occurs around Canada and Greenland. When

the initialised hindcast simulations and the uninitialised CMIP6 simulations are compared it shows that the main improvement occurs in the ocean with little or no skill around Ireland, Iceland and at the bottom of the region from France to Canada (Figure 4.3 f).

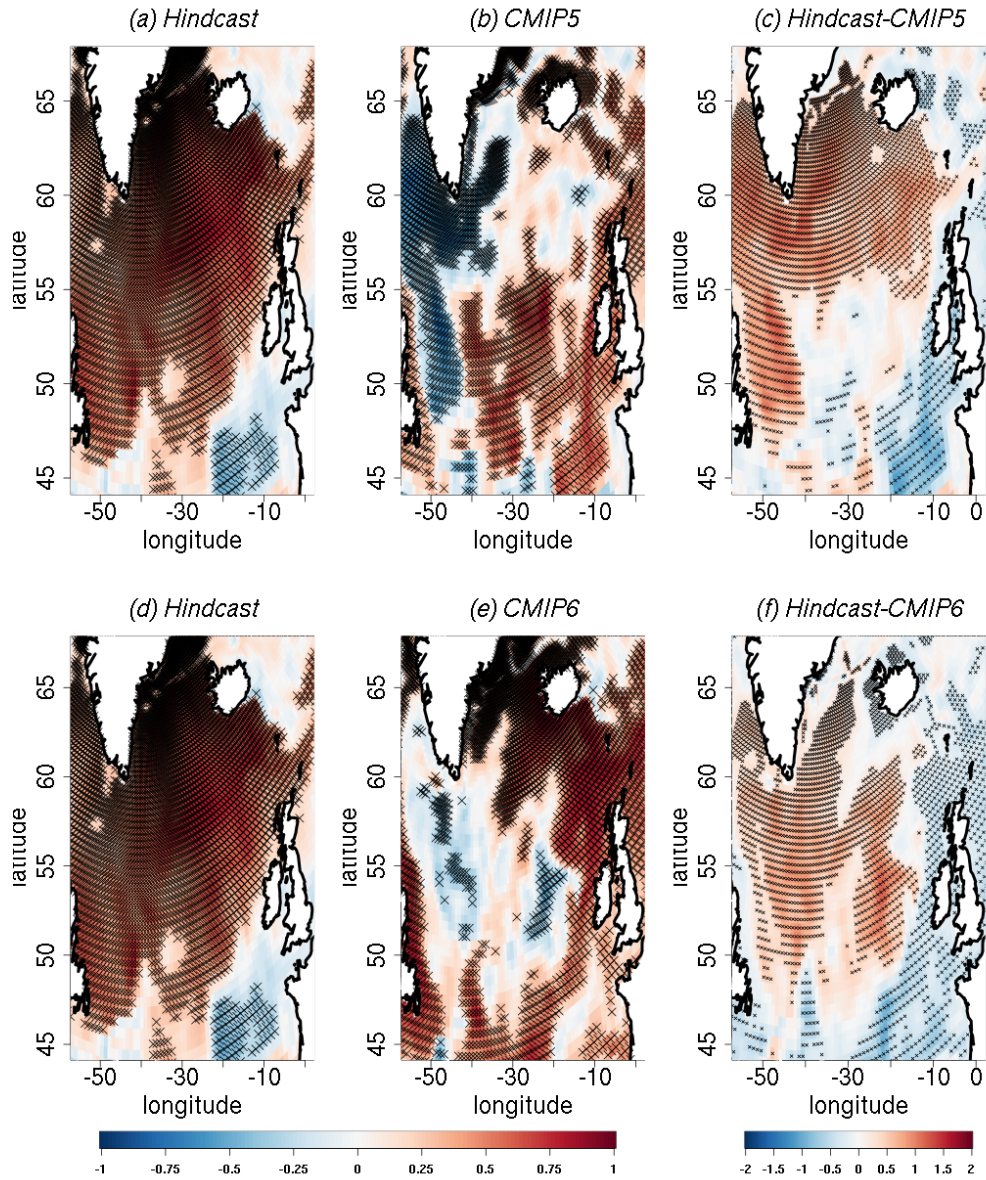


Figure 4.3: Anomaly correlation coefficient (ACC) for SST (MPIOM) for initialised hindcast simulation (a and d), uninitialised historical simulation (CMIP5 (b), CMIP6 (e)) evaluated against assimilation at lead years 2-5. The difference between initialised hindcast simulation - uninitialised historical (CMIP5 (c), CMIP6 (f)) simulation. Generated from the MPI-ESM-LR; 1966-2013; initialised each November; 2 to 5 years lead time; 16 ensemble members. The red is positive correlation, the blue is negatively correlated and the black dots show significance.

4.5 Predictability of Potential temperature from the MPIOM model

The final version of the temperature variable that will be discussed is the potential temperature at 6m this is the closest to SST that is available from the depth data. This main reason to explore this is to get an idea of the similarity to the other SST from the MPIOM and then in chapters 6, and 7 this variable will be used. Predictability of potential temperature (6m) for the eastern North Atlantic Ocean was explored for initialised hindcast simulations and two uninitialised historical simulations ("CMIP5", "CMIP6"). These are illustrated in Figure 4.4 below where the initialised hindcast simulations are Figure 4.4 a and d, the two uninitialised historical simulations ("CMIP5", "CMIP6") Figure 4.4 b and e respectively, the difference between the initialised simulation and the uninitialised simulation Figure 4.4 c and f respectively.

The results obtain for potential temperature (6m) (Figure 4.4) is almost identical to the SST of the MPIOM model (Figure 4.3), this is what was expected. The initialised hindcast simulation result for the eastern North Atlantic Ocean shows significant skill for majority of the region, with a few areas with little or no skill (Figure 4.4 a and d). Taking a closer look at Ireland and the surround sea there is significant skill in the northwest region, as you move southward towards France there is little or no skill. Moving westward from France towards Canada there is also reduced skill, a final area that does not show skill is north of Iceland. The uninitialised historical simulation CMIP5 shows a completely different picture, it is mixed more with areas that have particularly good skill and areas that have little or no skill (Figure 4.4 b). This uninitialised CMIP5 simulations does have areas that has improved skill over the initialised hindcast simulation, the is visible around Ireland and France where there was little or no skill now has significant skill (Figure 4.4 c). The same can be seen in the area to the north of Iceland, but just as there is improvements there is also little to no skill around Canada and Greenland where there was previously significant skill. When these two simulations are compared to each other the initialisation has improvement over the uninitialised CMIP5 simulation in the north and the CMIP5 preforms better to the southeast.

The uninitialised CMIP6 simulations has quite good significant skill for the region with small areas that have little or no skill (Figure 4.4 e). Similar to the CMIP5 simulation it performs better around Iceland and Ireland. With a small area in the middle of the North Atlantic Ocean that has little or no skill, this also occurs around Canada and Greenland. When the initialised hindcast simulations and the uninitialised CMIP6 simulations are compared it shows that the main improvement occurs in the ocean with little or no skill around Ireland, Iceland and at the bottom of the region from France to Canada (Figure 4.4 f).

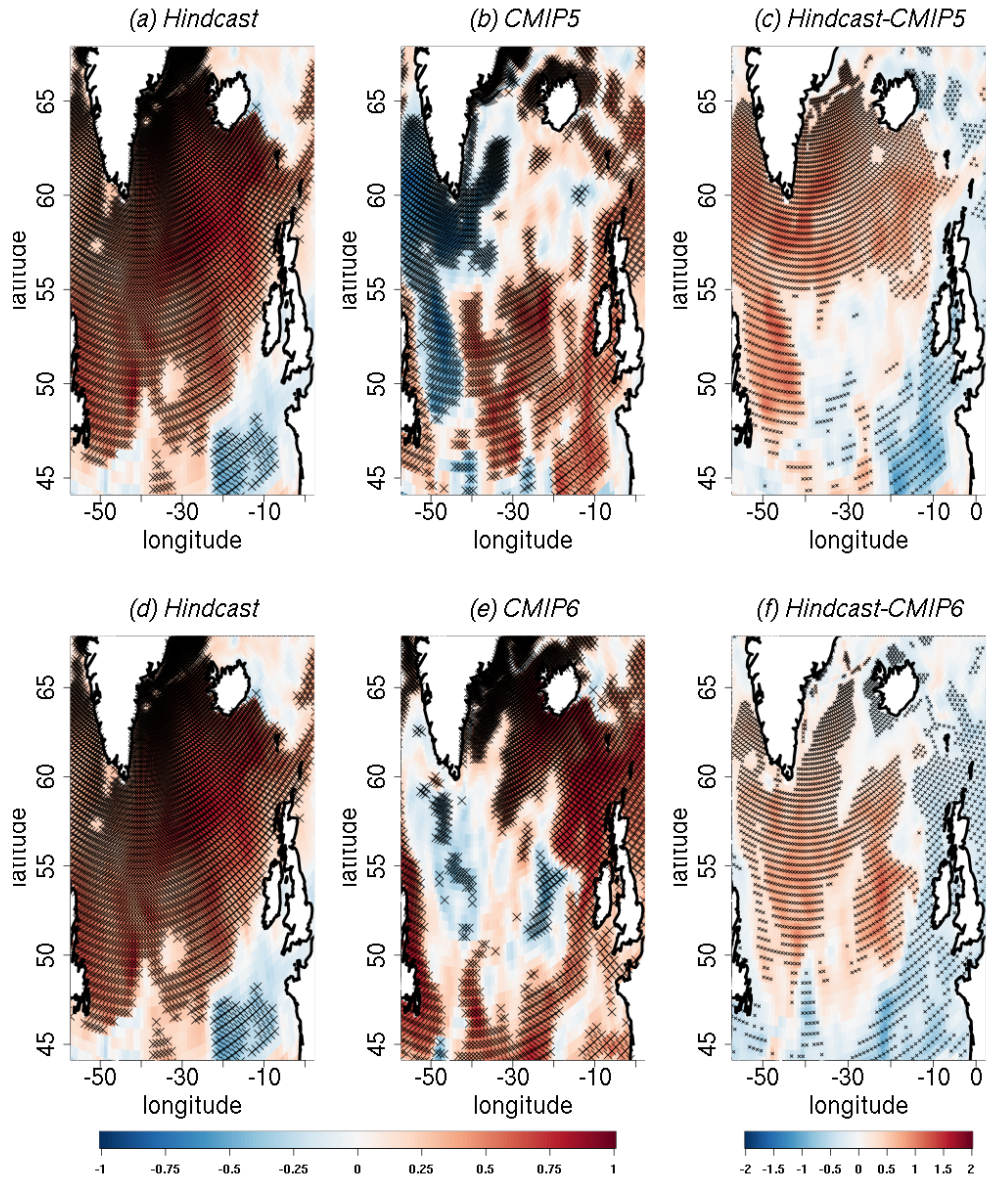


Figure 4.4: Anomaly correlation coefficient (ACC) for Potential Temperature (MPIOM) (6m) for initialised hindcast simulation (a and d), uninitialised historical simulation (CMIP5(b), CMIP6 (e)) evaluated against assimilation at lead years 2-5. The difference between initialised hindcast simulation - uninitialised historical (CMIP5(c), CMIP6 (f)) simulation. Generated from the MPI-ESM-LR; 1966-2013; initialised each November; 2 to 5 years lead time; 16 ensemble members. The red is positive correlation, the blue is negatively correlated and the black dots show significance.

4.6 Predictability of Salinity from the MPIOM model

The final variable that is of importance for the Eastern North Atlantic is salinity, this was taken from the depth data of the MPIOM model where an initial depth of 6m was explored. This is to give an insight into what predictability is like for this variable and in the following chapters (6, 7) further analysis will be conducted. The predictability of salinity (6m) for the eastern North Atlantic Ocean was explored for initialised hindcast simulations and two uninitialised historical simulations ("CMIP5", "CMIP6"). These are illustrated in Figure 4.5 below where the initialised hindcast simulations are Figure 4.5 a and d, the two uninitialised historical simulations ("CMIP5", "CMIP6") Figure 4.5 b and e respectively, the difference between the initialised simulation and the uninitialised simulation Figure 4.4 c and f respectively.

The initialised hindcast simulation result for salinity in the eastern North Atlantic Ocean shows a similar picture to that of the temperature results of the MPIOM, there is significant skill for most of the area with small areas of little or no skill (Figure 4.5 a). These are found north of Iceland, near Canada and Greenland, for Ireland and its surrounding seas there is a good significant skill. The uninitialised CMIP5 simulation shows very little skill at all, with the only areas that have significant skill being north of Iceland, between Ireland and England (Figure 4.5 b). When you compare the initialised hindcast simulation to that of the uninitialised CMIP5 simulation it is clear that for salinity (6m) initialisation has a vast improvement in skill (Figure 4.5 c). For the uninitialised CMIP6 simulation, the majority of the region shows little or no skill at all, with the exception of a few areas that have some significant skill (Figure 4.5 e). Notably between Ireland and the UK, there is significant skill, also between the UK and Iceland there are areas of skill with some being significant. Overall when the uninitialised CMIP6 simulations are compared with the initialised hindcast it highlights the benefit of the initialisation process, as the uninitialised simulations have very little skill compared to the initialised hindcast simulations which have skill for majority of the region (Figure 4.5 f).

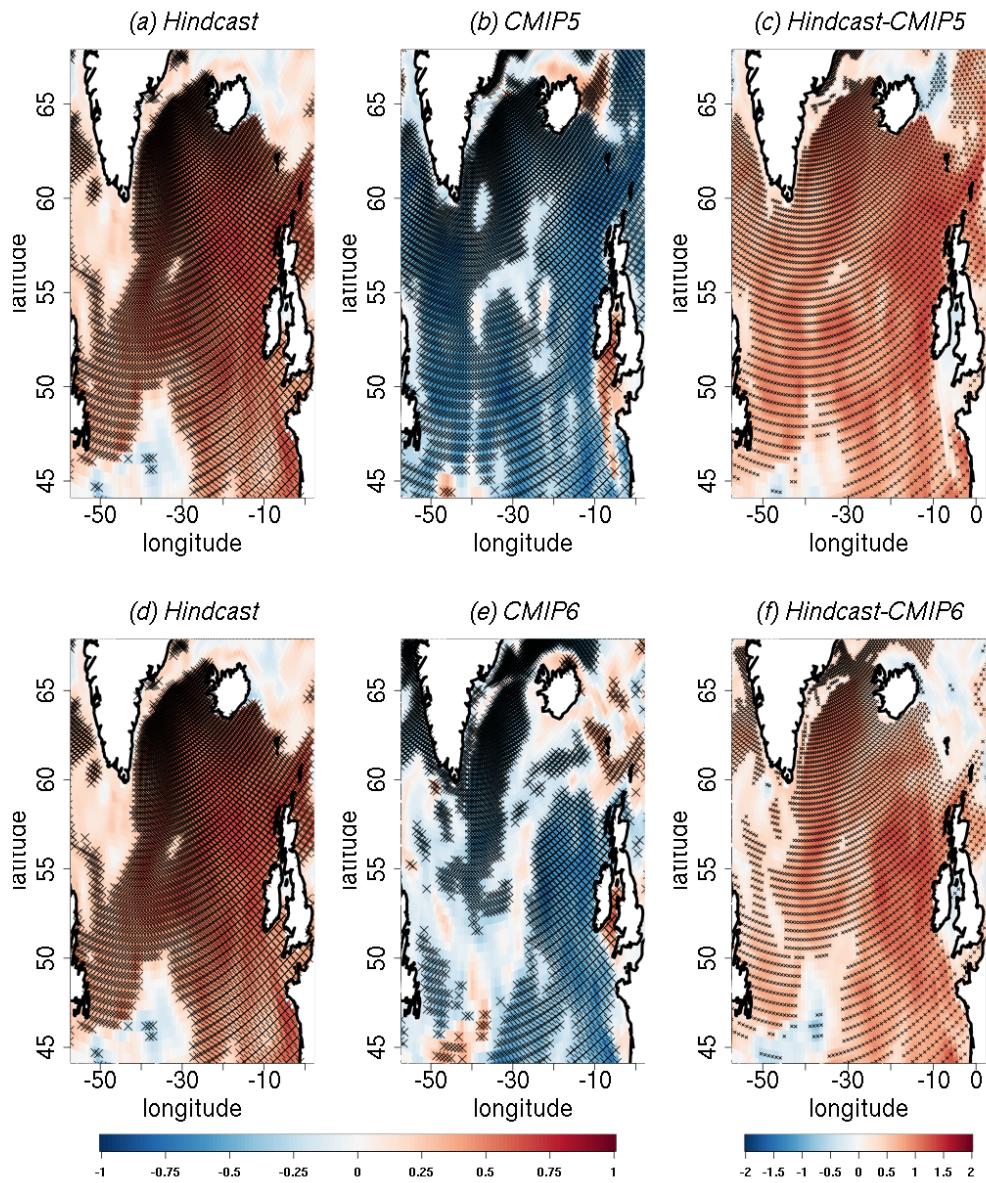


Figure 4.5: Anomaly correlation coefficient (ACC) for Salinity (MPIOM) for initialised hindcast simulation (a and d), uninitialised historical simulation (CMIP5(b), CMIP6 (e)) evaluated against assimilation at lead years 2-5. The difference between initialised hindcast simulation - uninitialised historical (CMIP5(c), CMIP6 (f)) simulation. Generated from the MPI-ESM-LR; 1966-2013; initialised each November; 2 to 5 years lead time; 16 ensemble members. The red is positive correlation, the blue is negatively correlated and the black dots show significance.

4.7 Discussion

In this Chapter 4 SST and salinity are shown to have predictability in the Eastern North Atlantic in the MPI-ESM-LR and that it is skillful. This is the case for both initialised hindcast and uninitialised historical ("CMIP6", "CMIP5") simulations. I show predictability on a 2-5-year lead time in the Northeastern Atlantic for potential temperature and salinity. The salinity initialised hindcast simulations have good skill for the Eastern North Atlantic, SST showed a varying result amongst the two different models. ECHAM6 SST initialised hindcast simulation shows some skill but would require further analysis to improve skill in the Eastern North Atlantic. MPIOM SST initialised hindcast simulations show that there is skill and that the Eastern North Atlantic is predictable.

Prediction of Eastern North Atlantic Ocean SST ("ECHAM6", "MPIOM"), potential temperature 6m and salinity 6m can be improved with initialisation as in some areas the initialised hindcast out-perform the uninitialised CMIP5/CMIP6 simulations. This can be seen in the comparison plots between the initialised hindcast and uninitialised historical simulations for both temperature and salinity for the four variables. In Figures 4.2 and 4.3 the last column shows that salinity outperforms the initialisation on prediction skill compared to that of the uninitialised historical simulations ("CMIP5", "CMIP6"). In the uninitialised historical simulations, there was very little or no prediction skill from the model at this depth. The improvement in skill between the CMIP5 and CMIP6 simulations obtained in our results is what was also observed by [Boer et al. \(2016\)](#) and [Guo et al. \(2022\)](#).

The first step was to analyse temperature and salinity from the MPI-ESM model and determine if there was predictability for the Eastern North Atlantic Ocean. This was explored using the simulations discussed where I can compare initialised and uninitialised simulations to determine if there is an advantage in one over the other. From here I can identify regions of poor predictability and use these in Chapter 6 where they can undergo the sub-sampling process. The results from this study feed into the sequential chapters where they can be tailored to the Irish seas. Understanding what decadal predictions will help in how these can be tailored in Chapter 7 for stakeholders' needs. Understanding the physical mechanisms in the

North Atlantic Ocean will help identify interactions that might be useful in Chapter 6 when I am looking at the improvement in prediction skill of both temperature and salinity. Before either of these can occur, I first to determined if they are found within the model.

Through this comparison, of the two model outputs, the initialised hindcast simulations outperform the uninitialised historical simulations. The results shown in this section were communicated to the stakeholders and through discussion I had recommended a further exploration of both temperature and salinity. The first was through an investigation into the predictability at depth as seen in Chapter 5. The following step was to determine if it is possible to improve skill as seen in Chapter 6. That there is no need to further look at the atmospheric model and that all further analysis will be conducted using the MPIOM initialised hindcast simulation and the assimilation simulation.

Case Study: Predictability at depth along the Irish coast

5.1 Introduction

The North Atlantic is an extensively studied region regarding the climatological features involved within the ocean and how they interact with the atmosphere. Studies have shown that both atmospheric climate variability pattern (North Atlantic Oscillation) and oceanic climatological features (subpolar gyre) are well represented within models in both initialised hindcast simulations and uninitialised historical simulations ([Andrews et al., 2015](#); [Athanasiadis et al., 2017](#); [Barcikowska et al., 2018](#); [Koul et al., 2019](#)). However, there is limited research completed on the predictability of potential temperature and salinity at depth, both on a global and a regional scale. Having the ability to predict changes in climate variables such as temperature and salinity for a target region, informed decisions can be made about environmental and economic conditions. [Koul et al. \(2019\)](#) demonstrated that uninitialised historical simulations with the Max Planck Institute Earth system model (MPI-ESM) as part of the Coupled Model Intercomparison Project Phase 5 (CMIP5, [Taylor et al., 2012](#)), are well representing large-scale ocean dynamics and atmosphere-ocean interaction. The simulations used in [Koul et al.](#)

(2019) form the first part of the Max Planck Institute Grand Ensemble (Maher et al., 2019). Koul et al. (2019) examined subsurface salinity on three sections in the North Eastern Atlantic (Rockall Trough, Faroe-Scotland Channel, and North Sea entrance). It showed that in their uninitialised historical simulations, atmospheric variability eventually influences the evolution of North Sea salinity (Koul et al., 2019).

Previous work that was conducted on the North Eastern Atlantic was focused on the Rockall Trough and in particular the Extended Ellett line (Holliday et al., 2015; Humphreys et al., 2016; Jones et al., 2018). I will use the full length and depth of the Extended Ellett line, which will act as our most northwest section. Porcupine Bank West and Goban Spur Southwest comprise two other sections along the west coast of Ireland as seen in Figure 5.1. All three sections begin on parts of the continental shelf two being off the west coast of Ireland, Porcupine Bank and Goban Spur head out to the open ocean (de Graciansky and Poag, 1985; O'Reilly et al., 2022). All three sections are influenced by both the North Atlantic and different water masses. The Extended Ellett line is a multidecadal hydrographic transect that is an extension of the Ellett line that is located between Scotland and Iceland. It runs through the Rockall Trough, Hatton-Rockall Basin, and Iceland Basin (Holliday et al., 2015; Humphreys et al., 2016; Jones et al., 2018). The Porcupine Bank has surface salinities that are about 0.05 PSU less than surface values in deeper water on either side (White, 1997; O'Reilly et al., 2022). Goban Spur is a submarine plateau 250km southwest of Ireland in the southwestern Celtic Sea and into the deeper ocean (Dingle and Scrutton, 1979; de Graciansky and Poag, 1985; Huthnance et al., 2001; Moritz et al., 2021). The Extended Ellett line captures the surface flow of warm, salty water from the North Atlantic into the Nordic Seas and half of the returning deep, cold overflow current (Humphreys et al., 2016). In turn, warm and saline pass through the Rockall Trough water to the Nordic Seas, transforming it into fresh southward flowing deep water (Holliday et al., 2020). Several water masses circulate around the Porcupine Bank and Goban Spur that influence both temperature and salinity along the shelf. The main water masses that influence both are Eastern North Atlantic Water (ENAW, 200-700m), and Mediterranean Outflow Water (MOW,

800-1000m) moving the high saline water mass northward and then returning as denser water southward (Huthnance et al., 2001; O'Reilly et al., 2022). Lower Deep Water is thought to circulate cyclonically around Goban Spur, Porcupine Bank and the entrance to Rockall Trough (Huthnance et al., 2001).

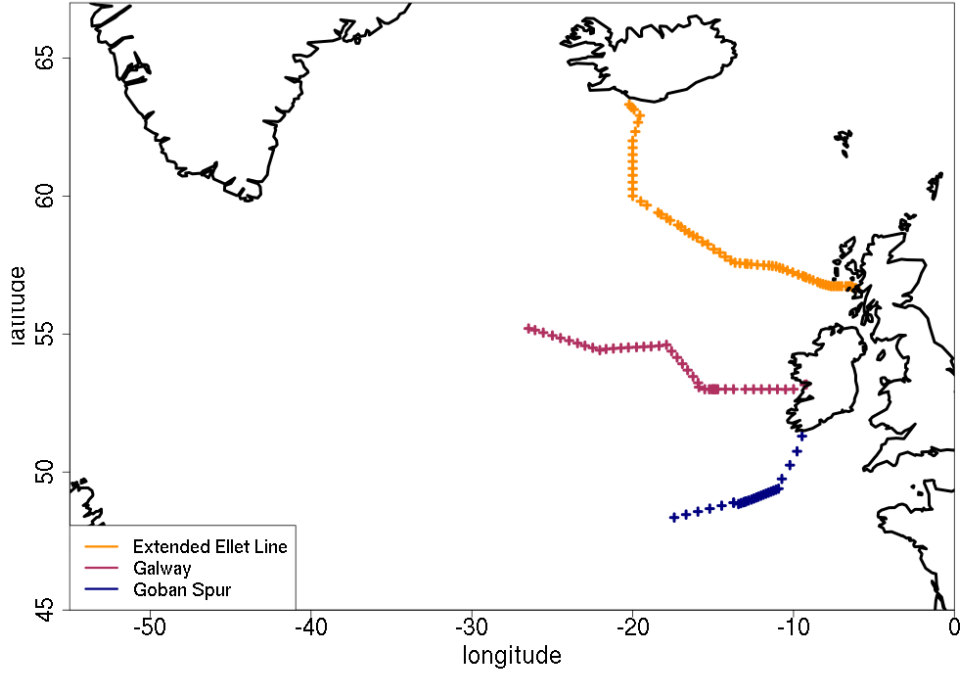


Figure 5.1: The three sections are the EEL (dark orange line) most northward section, moving south the next section is along Porcupine Bank (PB, red line), and the most southerly section along Goban Spur (GS, navy line).

Large-scale atmosphere-ocean feedback that occurs in the North Atlantic gives the ability to improve decadal predictability (Koul et al., 2020; Borchert et al., 2021). Some studies suggest that the predictability improves on scales of 2-8 years and others for even up to 10 years into the future (Borchert et al., 2018, 2019; Brune and Baehr, 2020). The leading cause of inter-annual to decadal variability in salinity is linked with the variability in the sub-polar gyre (Koul et al., 2020), one of the regions in the North Atlantic that showed skill improvement with initialisation in CMIP5 (Borchert et al., 2021).

To expand on prediction in the North Eastern Atlantic, the uninitialised historical simulations from both CMIP5 and CMIP phase 6 (CMIP6, [Eyring et al., 2016](#)) from MPI-ESM will be explored, as well as initialised decadal predictions. I will explore the predictability on a 2-5-year lead time. For this I analyse potential temperature and salinity at depth along the Irish coast for the Extended Ellett line, Porcupine Bank, and Goban Spur. The aim is to demonstrate the capability of a state-of-the-art decadal prediction system to predict the three transects along the West of Ireland.

5.2 Simulations and methods

For this study I analysed simulations with the Max Planck Institute Earth system model ([Giorgetta et al., 2013](#); [Mauritsen et al., 2019](#)) in its low-resolution setup (MPI-ESM-LR) for the time period 1961-2013. In MPI-ESM-LR, the oceanic component (MPIOM, [Jungclauss et al., 2013](#)) is setup with a nominal horizontal resolution of 1.5° globally, actually corresponding to $\approx 1^\circ$ in the North Eastern Atlantic, and 40 levels vertically. The atmospheric component (ECHAM6, [Stevens et al., 2013](#)) is configured with a spectral resolution T63, corresponding to $\approx 1.9^\circ$ horizontal resolution globally, and 47 levels in the vertical.

I use the assimilation simulation with MPI-ESM-LR ([Hövel et al., 2022](#); [Brune and Baehr, 2020](#)), which covers the time period 1958-2019, both as a reference and for the initialisation of predictions. Oceanic temperature and salinity profiles from EN4 ([Good et al., 2013](#)) are assimilated monthly with a 16-member oceanic ensemble Kalman filter ([Brune et al., 2015](#); [Polkova et al., 2019](#)) using the Parallel Data Assimilation Framework (PDAF, [Nerger and Hiller, 2013](#)). Simultaneously, monthly mean atmospheric temperature, vorticity, divergence (all only above 900hPa), and sea level pressure from ERA40 ([Uppala et al., 2005](#)), ERA-Interim ([Dee et al., 2011](#)), and ERA5 ([Hersbach et al., 2020](#)) are nudged into ECHAM6. CMIP6 external forcing ([Eyring et al., 2016](#)) is applied throughout the whole assimilation, with historical forcing until 2014, and scenario forcing SSP2-45 thereafter.

For the purpose of our study, I use a 16-member ensemble of initialised predictions

("hindcasts") that have been started November 1st each year initialised between 1961-2008 from the assimilation with a 2-to-5-year lead time (Hövel et al., 2022). Thus our analysis time period is between 1966 and 2013. Similar to the assimilation, CMIP6 external forcing is applied to these hindcasts correspondingly.

Uninitialised simulations with MPI-ESM-LR have been part of both CMIP5 (Taylor et al., 2012) and CMIP6 (Eyring et al., 2016) model intercomparisons. In this study, I use the first 16 members of the CMIP5 MPI Grand Ensemble (Maher et al., 2019), with CMIP5 historical external forcing until 2005, and CMIP5 scenario RCP4.5 external forcing starting with 2006. I also use the first 16 members of the CMIP6 MPI Grand Ensemble (Olonscheck et al., 2023), with the same CMIP6 external forcing as in assimilation and hindcasts.

I analyse the hindcasts and both uninitialised simulations ("CMIP5", "CMIP6") for both potential temperature and salinity at depth. Annual mean values of model output variables are computed and then used to generate a 2-to-5-year lead time series for each member. For all simulations, I compute the 16-member ensemble mean.

For the comparison of the simulations, the time series were detrended, and an anomaly correlation coefficient (ACC) was estimated, with reference to the assimilation. I also calculate the differences of the resulting ACCs between the hindcasts and the uninitialised simulations. Significance is estimated by a bootstrapping of 500 repetitions and a significance level of 5% (Wang et al., 2014). The same approach is used for estimating the skill along the transects.

5.3 Predictability of temperature and salinity in the North Eastern Atlantic

I first investigate surface predictability of potential temperature and salinity within the MPI-ESM on a lead time of 2 to 5 years for the North Eastern Atlantic. The ACC is used to assess skill in both potential temperature and salinity for uninitialised historical and initialised hindcast simulations of the MPI-ESM-LR. Then the initialised hindcast simulations are compared with the uninitialised histori-

cal simulations (CMIP6) to determine if there was an improvement in skill due to the initialisation. Initialised hindcast simulations for potential temperature (Figure 5.2 a) demonstrate that the North Eastern Atlantic shows to have good predictability apart from a small area of low predictability southwest of Ireland. The salinity results (Figure 5.2 c) show that for the initialised hindcast simulation the predictability has greater skill compared to the uninitialised historical simulation. For the potential temperature (Figure 5.2 b) highlights that there are advantages for the initialised prediction for the open ocean, while the uninitialised simulation performs better over the continental shelf close to the Irish coast. In contrast, for salinity (Figure 5.2 d) the initialisation provides better predictability for both the open ocean and the continental shelf around the Irish coast.

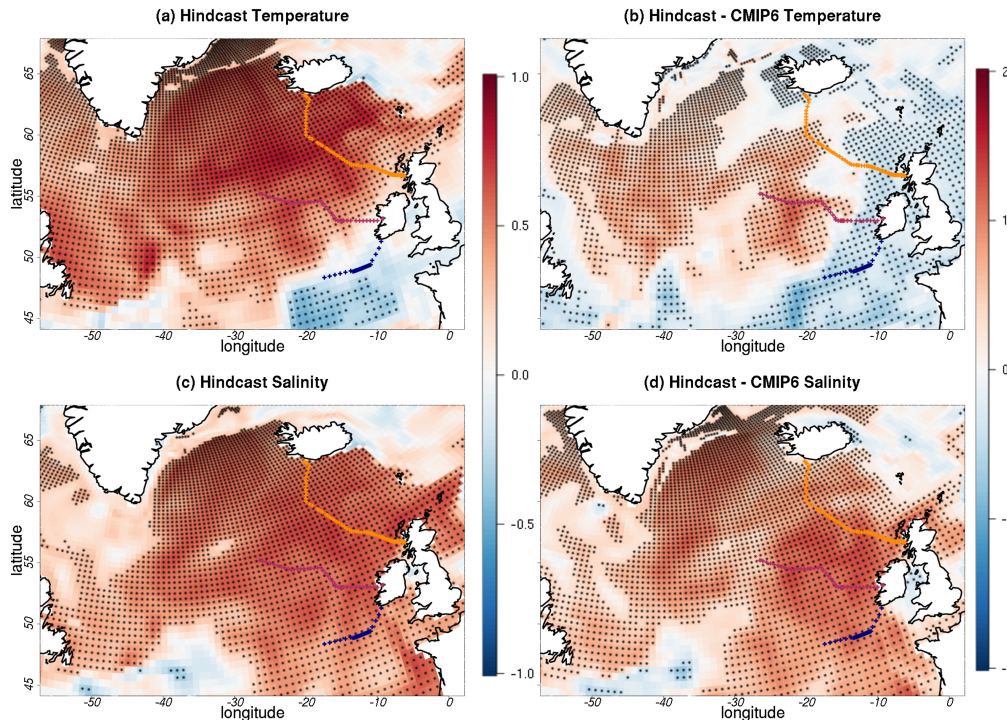


Figure 5.2: Shows the anomaly correlation coefficient initialised hindcast against assimilation for potential temperature (6m) (a) and seawater salinity (6m) (c) for the North Eastern Atlantic and the difference between initialised hindcast ACC and uninitialised CMIP6 ACC for the North Eastern Atlantic for potential temperature (6m) (b) and seawater salinity (6m) (d). The areas shaded in red highlight the regions that have good predictability, the orange line is the Extended Ellet Line, the yellow line is the Porcupine Bank transect, and the navy line is the Goban Spur. The red areas show that there is a positive skill, the blue shows that there is negative skill and the black dots show that they are significant. Generated from the MPI-ESM-LR; 1966-2013; initialised each November; 2 to 5 years lead time; 16 ensemble members.

A common approach for predictions at depth is to calculate a mean over a group of target depths. In this study I take an alternative approach and analyse predictability for three sections off the Irish coast: Extended Ellet Line (EEL), Porcupine Bank (PB), and Goban Spur (GS). The three sections are highlighted in Figure 5.1, together with the surface prediction skill at each of the locations. Overall there is predictability (using the assimilation as reference) in both temperature and salinity along the West of Ireland as seen in Figure 5.1, this can give an in-

sight into what I could expect to see in the transects. In the next step, I investigate the three transects at depth.

5.4 Water Mass Analysis in the model along the three transects

The temperature-salinity diagrams for the three locations (EEL Figure 5.3, Porcupine Bank Figure 5.4, Goban Spur Figure 5.5) highlight that the initialised hindcast simulations differ from the uninitialised simulations. These initialised hindcasts are closer to the assimilation than uninitialised historical simulations for all three transects. However, the CMIP5 and CMIP6 simulations show that they are potentially picking up the MOW and Labrador Sea water movements at the transect of the PB (Figure 5.4) and the GS (Figure 5.5). The uninitialised historical simulations show a more chaotic pattern in the upper ocean. While assimilation and initialised hindcast simulations are not identical, they do show that at the surface the water potential temperatures are higher and more saline compared to lower depths. The salinity range is confined to a particular range for the assimilation and hindcast simulations, but for the uninitialised ("CMIP5", "CMIP6") simulations the range is much larger. From Figures 5.3, 5.4, 5.5 I observe that it is clear that the long-term memory could be assigned to water masses in the area and this can be potentially beneficial to the initialised hindcast simulations for increasing the prediction skill.

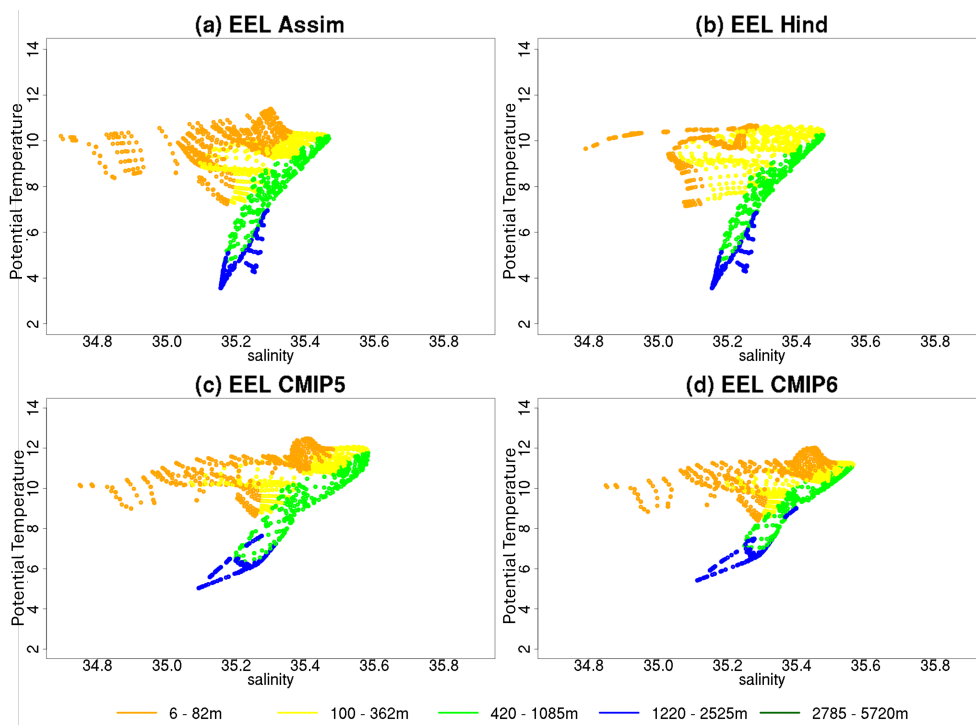


Figure 5.3: Potential temperature-salinity diagram using the assimilation (a), initialised hindcast (b), uninitialised historical (CMIP5) (c), uninitialised historical (CMIP6) (d), for the EEL. The colours on the diagram indicate the depth which Orange (6 - 82m), Yellow (100- 362m), Green (420 - 1085m), Blue (1220 - 2525m), Darkgreen (2785 - 5720m). Generated from the MPI-ESM-LR; 1966-2013; initialised each November; 2 to 5 years led time; 16 ensemble members.

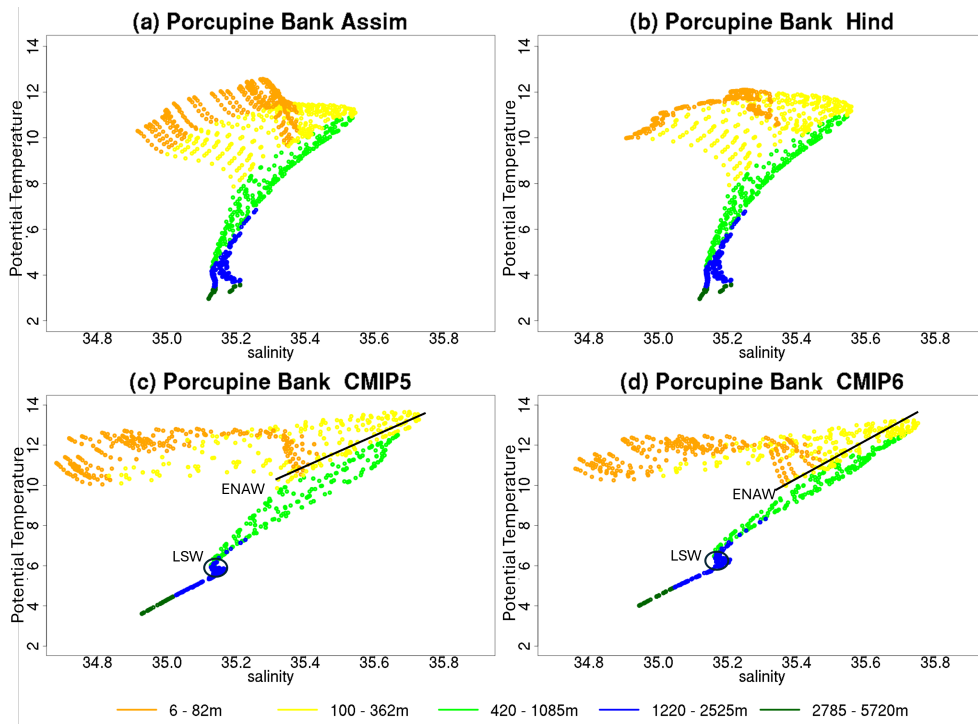


Figure 5.4: Potential temperature-salinity diagram using the assimilation (a), initialised hindcast (b), uninitialised historical (CMIP5) (c), uninitialised historical (CMIP6) (d), for the Porcupine Bank. The colours on the diagram indicate the depth which Orange (6 - 82m), Yellow (100- 362m), Green (420 - 1085m), Blue (1220 - 2525m), Darkgreen (2785 - 5720m). On plots (c) and (d) show the water masses ENAW, and the LSW. Generated from the MPI-ESM-LR; 1966-2013; initialised each November; 2 to 5 years led time; 16 ensemble members.

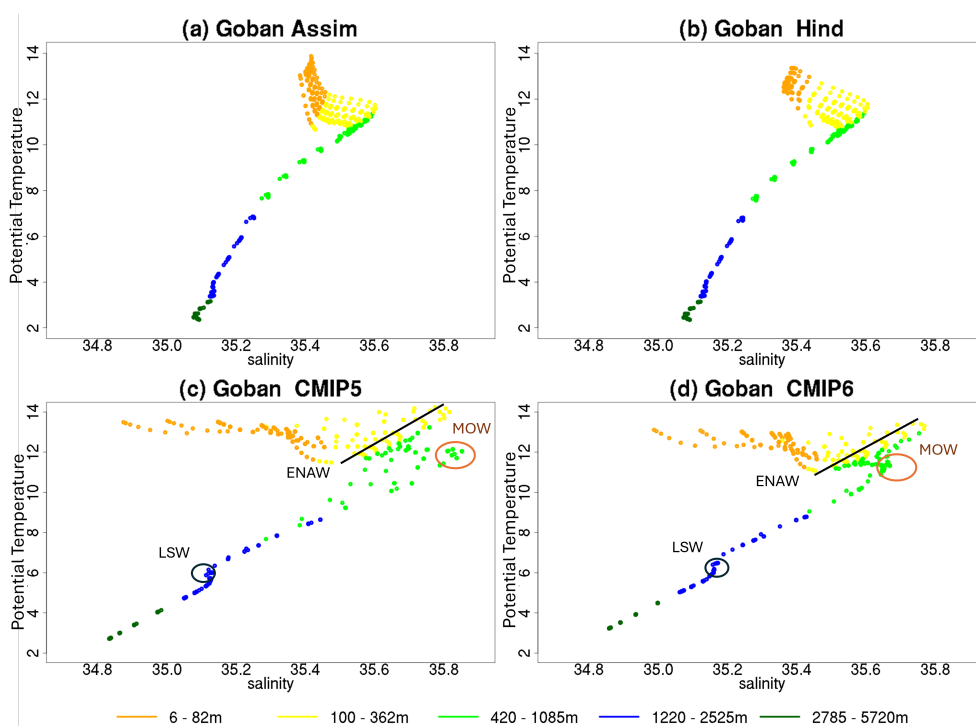


Figure 5.5: Potential temperature-salinity diagram using the assimilation (a), initialised hindcast (b), uninitialised historical (CMIP5) (c), uninitialised historical (CMIP6) (d), for the Goban Spur. The colours on the diagram indicate the depth which Orange (6 - 82m), Yellow (100- 362m), Green (420 - 1085m), Blue (1220 - 2525m), Darkgreen (2785 - 5720m). On plots (c) and (d) show the water masses ENAW, MOW, and the LSW. Generated from the MPI-ESM-LR; 1966-2013; initialised each November; 2 to 5 years led time; 16 ensemble members.

5.5 Predictability of Potential Temperature along the three transects

Building on the water mass analysis and the predictability of the surface I investigate whether the model can reproduce the potential temperature values in the regions. I know that temperatures will decrease towards the north and west. Near 49°N the temperatures can reach about 16°C at the surface. At depth, the values range in winter from 10-11°C to up to about 700 m. Below that they decrease steadily to below 4°C at 2000 m (Huthnance et al., 2001). The closest section that is at this slope is that of the Goban Spur. I expect that while the water

moves north- and westward (away from the slope) the potential temperature will decrease.

To estimate the capability of the model, I compare the absolute values of the potential temperature from the assimilation simulation, which by design is the closest to the observations, with the uninitialised historical ("CMIP5", "CMIP6") and initialised hindcast simulations. The results of the three sections are illustrated in Figures 5.6,5.7,5.8. Overall results show that the model is within the limits of values that have been observed for the regions, that as water is moving northward there is a decrease in temperature. Across the three transects the hindcast simulations are almost identical with the assimilation simulations with the upper ocean showing a warmer temperature. Both the uninitialised historical ("CMIP5", "CMIP6") simulations overestimate potential temperature by approximately 1.5 degrees Celsius above the assimilation for the EEL. At PB, all the simulations appear to be within 0.5 degrees Celsius of the assimilation. Similarly, the same is true for the GS section except that the CMIP5 results are approximately 2 degrees warmer compared to the other results for this section. It is possible that uninitialised historical simulations could be overestimating the potential temperature for these regions. Due to their initialisation, the hindcast is slightly more accurate than the uninitialised historical simulations. Following on from this, I want to determine if there is an improvement in prediction skill between the two simulations because of this initialisation.

5.5. Predictability of Potential Temperature along the three transects

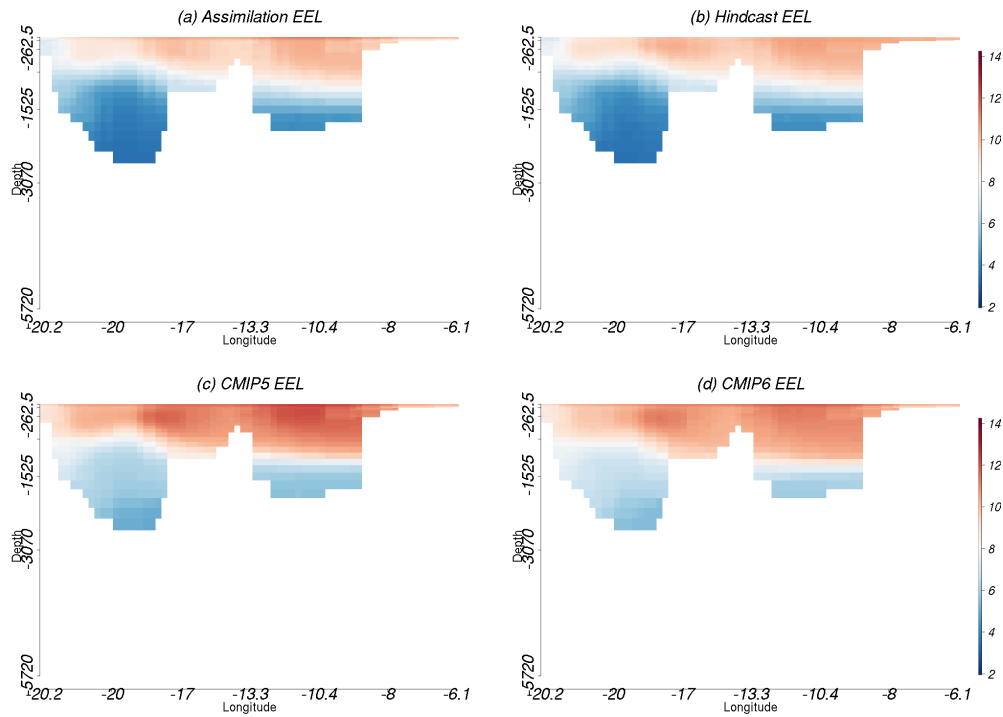


Figure 5.6: Potential temperature values from the model for the assimilation (a), initialised hindcast (b), uninitialised historical (CMIP5) (c), uninitialised historical (CMIP6) (d) simulations along the EEL transects. The red areas show that there is positive skill, the blue shows that there is negative skill and the black dots show that they are significant. Generated from the MPI-ESM-LR; 1966-2013; initialised each November; 2 to 5 years lead time; 16 ensemble members.

5.5. Predictability of Potential Temperature along the three transects

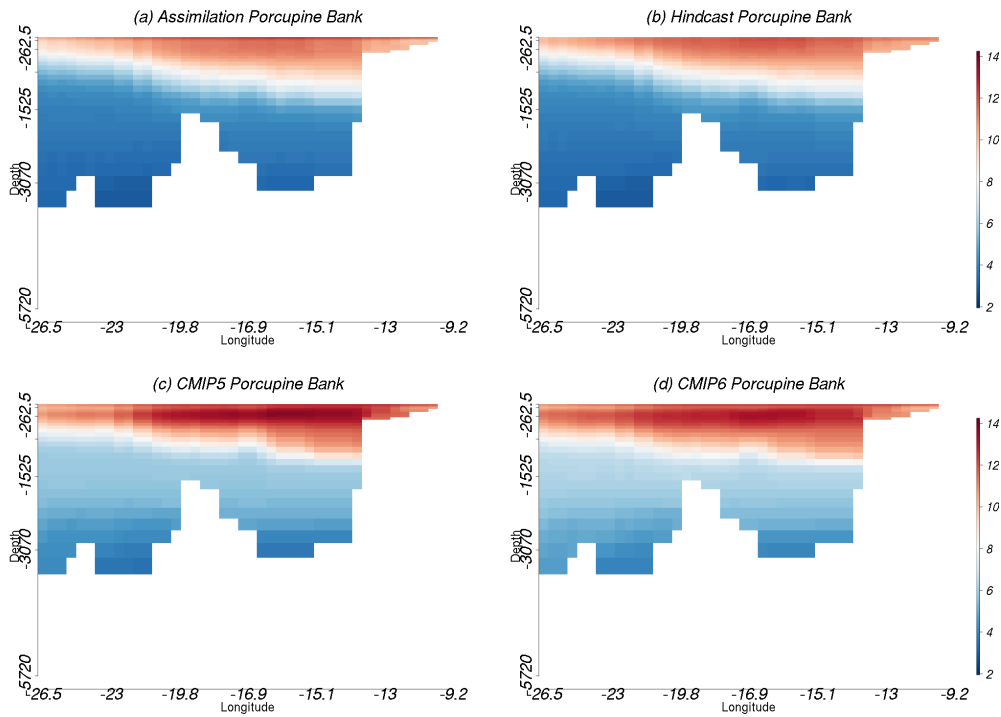


Figure 5.7: Potential temperature values from the model for the assimilation (a), initialised hindcast (b), uninitialised historical (CMIP5) (c), uninitialised historical (CMIP6) (d) simulations along the Porcupine Bank transects. The red areas show that there is positive skill, the blue shows that there is negative skill and the black dots show that they are significant. Generated from the MPI-ESM-LR; 1966-2013; initialised each November; 2 to 5 years lead time; 16 ensemble members.

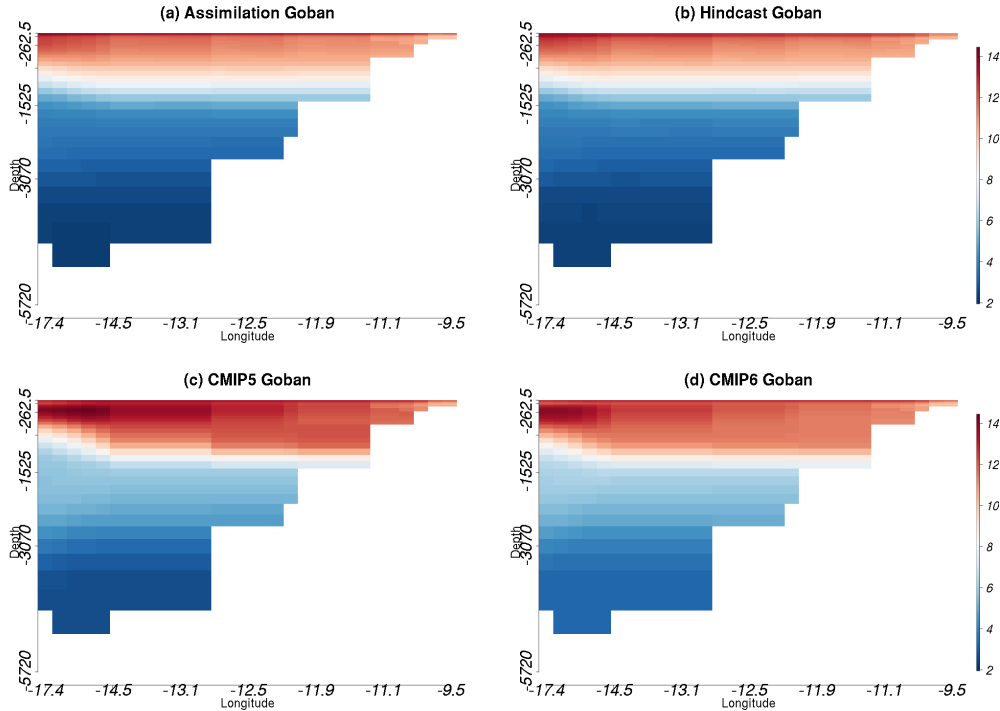


Figure 5.8: Potential temperature values from the model for the assimilation (a), initialised hindcast (b), uninitialised historical (CMIP5) (c), uninitialised historical (CMIP6) (d) simulations along the Goban Spur transects. The red areas show that there is positive skill, the blue shows that there is negative skill and the black dots show that they are significant. Generated from the MPI-ESM-LR; 1966-2013; initialised each November; 2 to 5 years lead time; 16 ensemble members.

In a next step I analyse the predictability for the three transects, at the EEL (Figure 5.9 a, d, g), the PB (Figure 5.9 b, e, h), and the GS (Figure 5.9 c, f, i). A common theme for the initialised hindcast simulation for the three transects is the predictability at depth. Starting with the EEL (Figure 5.9 a) there is a region of lower predictability in the depth of about 1200 m. Above this level and in the Iceland basin also partly below this level, the predictability is high. In the CMIP6 simulation (Figure 5.9 d), I find high predictability only in the upper 1000 m, with even higher values than in the initialised simulation (Figure 5.9 g). At the PB, the initialised simulations (Figure 5.9 b) show a clear region of predictability for the upper 300 to 400 m, and below 1500 m. In between these depths, the predictability is lower. In the uninitialised CMIP6 simulations (Figure

5.9 e) the main areas of high predictability can be found just below the surface layer. Consequently, comparing the two simulations (Figure 5.9 h) shows that initialisation is mainly beneficial for the surface layer and the depth. For the GS (Figure 5.9 c), the initialised simulations show consistently high predictability for most depths, while in the uninitialised CMIP6 simulation, high predictability is confined to the upper 1400 m only (Figure 5.9 f). Consequently, initialisation is beneficial to a higher prediction skill below 1400 m (Figure 5.9 i).

5.5. Predictability of Potential Temperature along the three transects

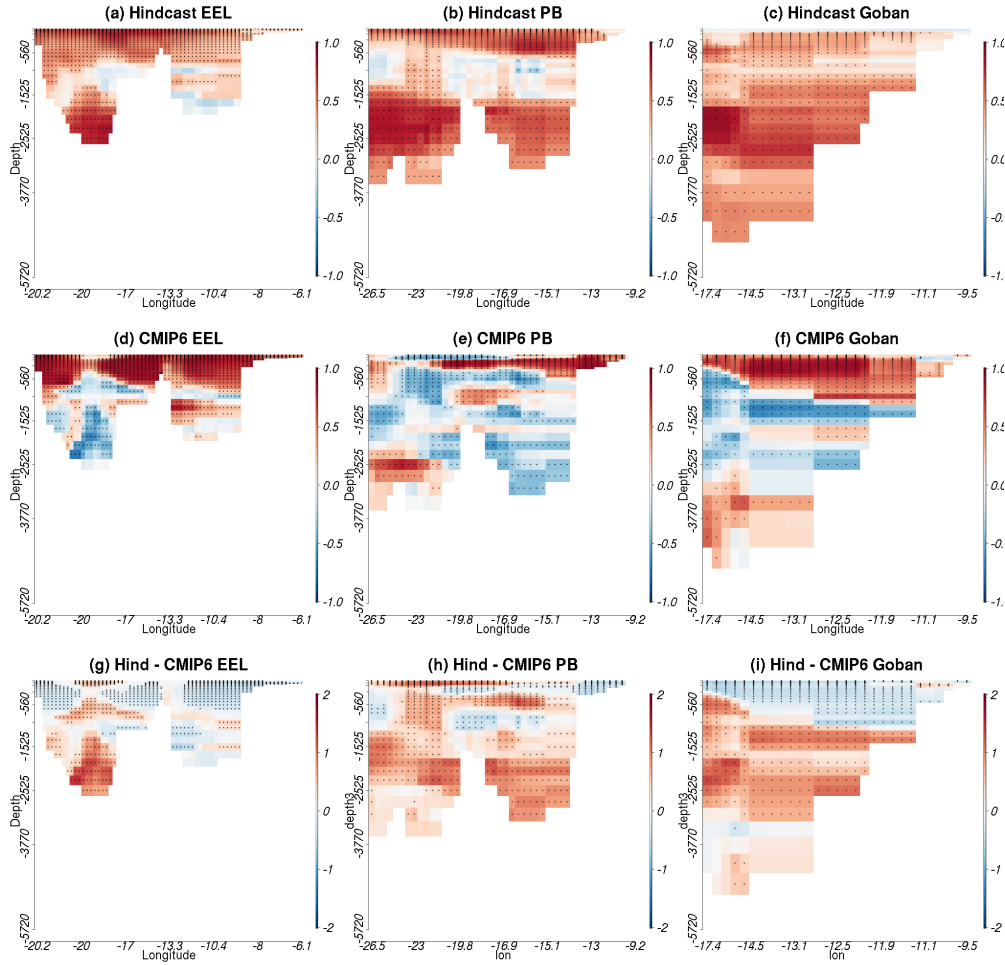


Figure 5.9: Anomaly correlation coefficient against assimilation for potential temperature at lead years 2 to 5, using the initialised hindcast (a-c), uninitialised historical (CMIP6) (d-f), hindcast - uninitialised historical (g-i) for the EEL, Porcupine Bank, and Goban Spur. The red areas show that there is positive skill, the blue shows that there is negative skill and the black dots show that they are significant. Generated from the MPI-ESM-LR; 1966-2013; initialised each November; 2 to 5 years lead time; 16 ensemble members.

When I investigate the uninitialised CMIP5 simulations Figure 5.10 I see that their results are generally similar to the uninitialised CMIP6 simulations (Figure 5.9). The main difference is that the upper layer of predictability for the PB and the GS (Figure 5.10 b, c) extends deeper, but with smaller values. Compared to the initialised simulation again the initialised hindcast dominates in the depth, while

in the upper layers, an inconsistent picture emerged (Figure 5.10 d, e, f).

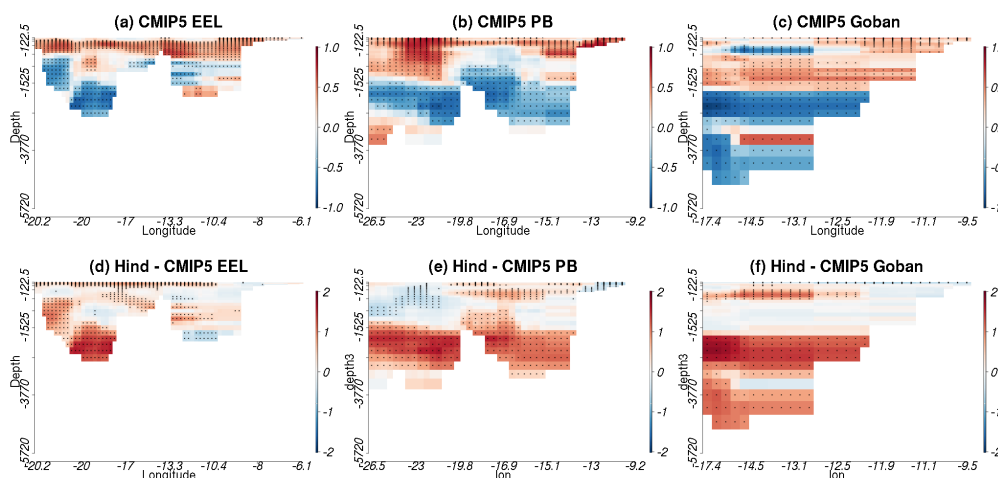


Figure 5.10: Anomaly correlation coefficient against assimilation for potential temperature at lead years 2 to 5, using uninitialised historical (CMIP5) (a-c), hindcast - uninitialised historical (d-f) for the EEL, Porcupine Bank, and Goban Spur. The red areas show that there is positive skill, the blue shows that there is negative skill and the black dots show that they are significant. Generated from the MPI-ESM-LR; 1966-2013; initialised each November; 2 to 5 years lead time; 16 ensemble members.

5.6 Predictability Sea Water Salinity along the three transects

I investigate whether the model could reproduce the salinity values that occur in these regions. I expect that the water at the most southern transect (GS) will be the most saline of the three transects. Salinity should be reducing when the water moves further north through the PB towards the EEL.

What the salinity values (Figures 5.11, 5.12, 5.13) show that as the water moves northward, it does become slightly less saline for assimilation, initialised hindcast and uninitialised historical (CMIP5/6) simulations. The hindcast simulations (Figure 5.11 b, 5.12 b, 5.13 b) for the three sections are the ones that are for salinity almost identical to the assimilation simulations (Figure 5.9 a, 5.10 a, 5.11 a). For the EEL the CMIP5 (Figure 5.11 c) and CMIP6 (Figure 5.11 d) simulation

also closely replicate the assimilation with the lowest depths being a bit fresher. This also follows for PB transect where it is fresher at lower levels but a broader saline range. Goban CMIP5 (Figure 5.13 c) and CMIP6 (Figure 5.13 d) results show a more saline region in the upper ocean. In contrast to the initialised simulations which have a high saline depth of roughly less than 1000 m, both of the uninitialised historical simulations extended to a depth of about 1300 m. The initialised hindcasts are highly saline to the west at the surface, for the uninitialised historical simulations show this area to be a fresher region.

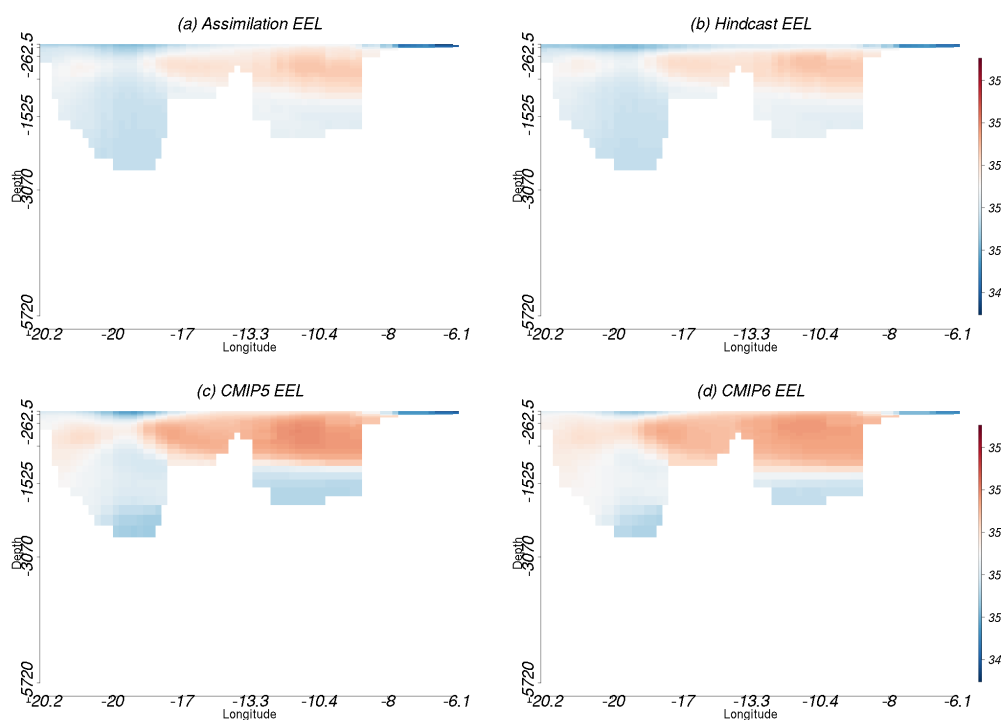


Figure 5.11: Sea water salinity values from the model for the assimilation (a), hindcast (b), uninitialised historical (CMIP5) (c), uninitialised historical (CMIP5) (d) simulations along the EEL. Generated from the MPI-ESM-LR; 1966-2013; initialised each November; 2 to 5 years led time; 16 ensemble members.

5.6. Predictability Sea Water Salinity along the three transects

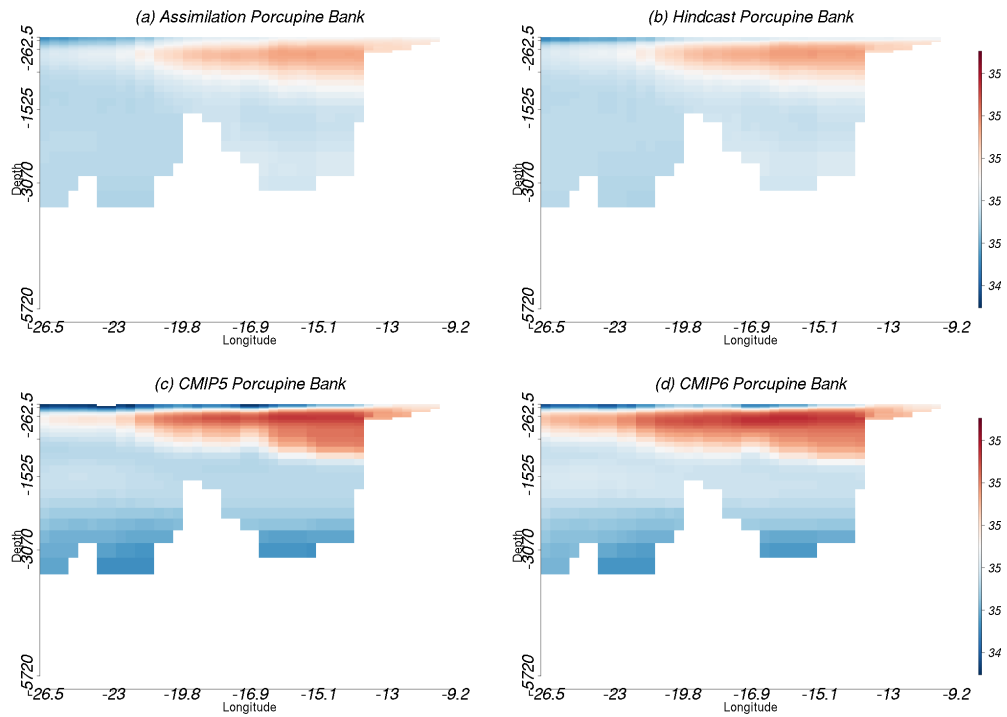


Figure 5.12: Sea water salinity values from the model for the assimilation (a), hindcast (b), uninitialised historical (CMIP5) (c), uninitialised historical (CMIP5) (d) simulations along the Porcupine Bank. Generated from the MPI-ESM-LR; 1966-2013; initialised each November; 2 to 5 years led time; 16 ensemble members.

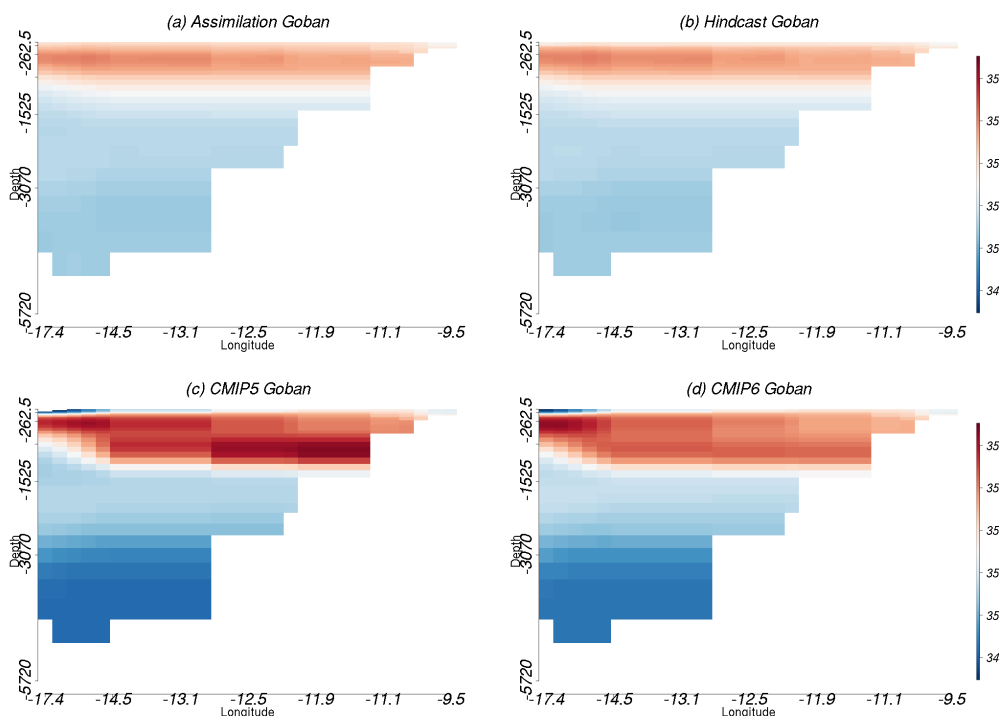


Figure 5.13: Sea water salinity values from the model for the assimilation (a), hindcast (b), uninitialised historical (CMIP5) (c), uninitialised historical (CMIP5) (d) simulations along the Goban Spur. Generated from the MPI-ESM-LR; 1966-2013; initialised each November; 2 to 5 years led time; 16 ensemble members.

Similar to the potential temperature, the salinity values are compared for the initialised hindcasts, the CMIP6 (Figure 5.14) and CMIP5 (Figure 5.15) simulations. The initialised hindcasts for the three transects (EEL, PB, GS) (Figure 5.14 a, b, c) highlight that there is skill at most depth levels. Initialised hindcasts for EEL (Figure 5.14 a) show a region with little or low skill at a depth of about 1200 m, but besides that they demonstrate a consistently high predictability along the depth range. In contrast to this, the uninitialised CMIP6 simulation has little skill in the surface layer and at depth (Figure 5.15 d). Comparing the two simulations shows (Figure 5.15 g) that the initialised hindcasts perform better in the upper couple of hundred metres and in the deeper depths. Along the PB (Figure 5.15 b) the initialised hindcasts have significant skill for the majority of the transect except for its central part. The same transect within the CMIP6 simulation (Figure 5.15 e)

shows two bands with high prediction skill in the upper layers. The difference (Figure 5.15h) between the initialised hindcast and the CMIP6 simulation illustrates that initialisation outperforms the uninitialised simulations everywhere apart from the two distinct bands. For the GS (Figure 5.15 c) there is a high predictability of overall depth in the initialised prediction. In contrast, the CMIP6 results for the GS (Figure 5.15 f) show low predictability in the surface layer, and at a depth of about 1400 m. In the comparison (Figure 5.14 i) I see that the initialisation benefits prediction skill in these two layers.

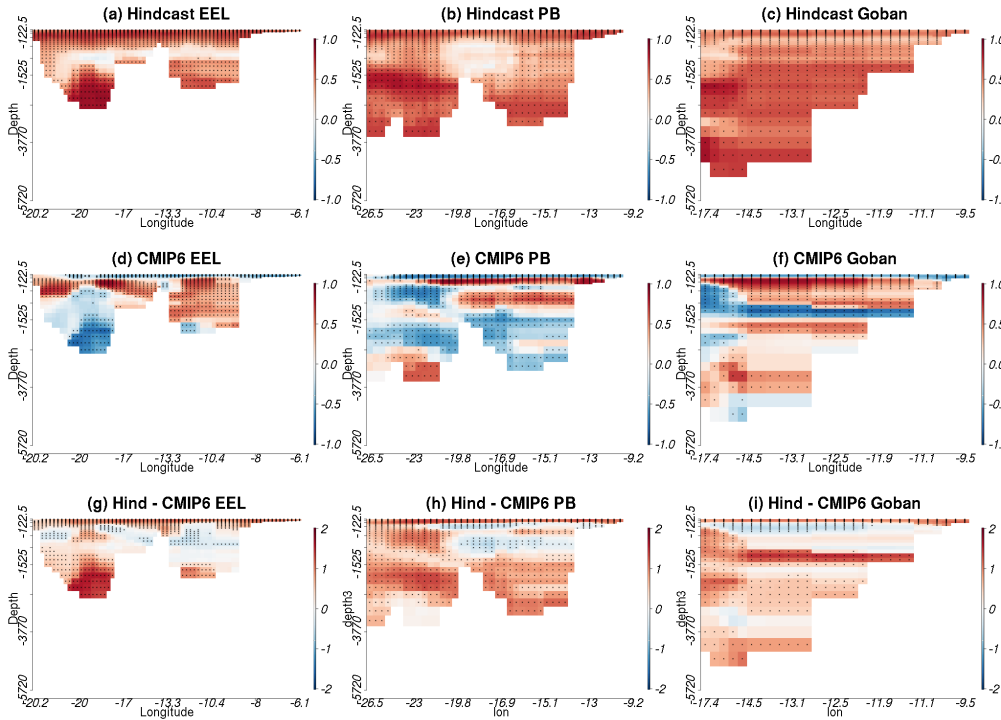


Figure 5.14: Anomaly correlation coefficient against assimilation for sea water salinity at lead years 2 to 5, using the initialised hindcast (a-c), uninitialised historical (CMIP6) (d-f), hindcast - uninitialised historical (g-i) for the EEL, Porcupine Bank, and Goban Spur. The red areas show that there is positive skill, the blue shows that there is negative skill and the black dots show that they are significant. Generated from the MPI-ESM-LR; 1966-2013; initialised each November; 2 to 5 years lead time; 16 ensemble members.

Figure (5.15 a, b, c) shows the ACC results for the CMIP5 simulation along the three transects. There is very little skill at the surface, but high skill at depths

down toward 1400 m. In comparison with the initialised hindcasts at the EEL (Figure 5.15 d), the main increase in skill due to initialisation can be found in the depth and at the surface. For the PB (Figure 5.15 e) and the GS (Figure 5.15 f) I find a similar result. In general it can be said that between the CMIP5 and CMIP6 simulation the general pattern of skill improvement by initialisation is comparable, but in the details it shows considerable differences. Especially it shows that the CMIP5 simulation has much less consistent skill in that area than the CMIP6.

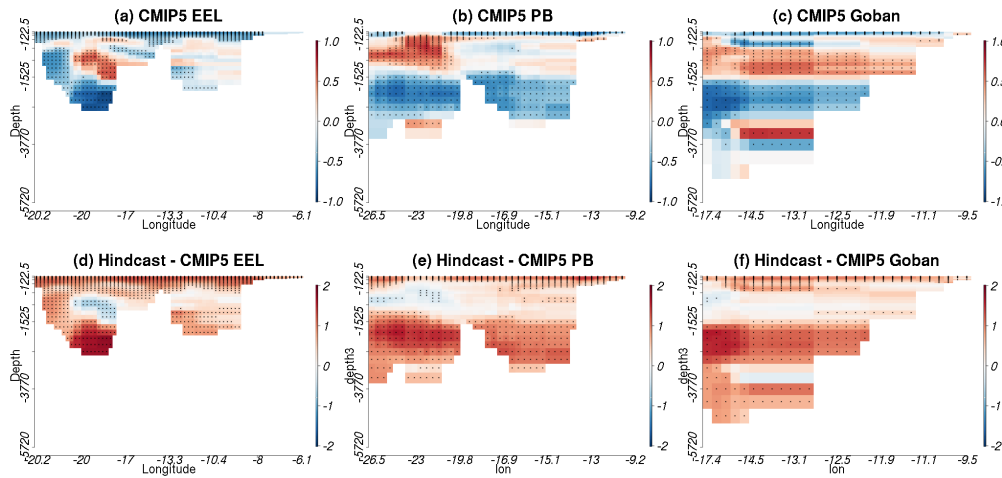


Figure 5.15: Anomaly correlation coefficient against assimilation for sea water salinity at lead years 2 to 5, using uninitialised historical (CMIP5) (a-c), hindcast - uninitialised historical (d-f), for the EEL, Porcupine Bank, and Goban Spur. The red areas show that there is positive skill, the blue shows that there is negative skill and the black dots show that they are significant. Generated from the MPI-ESM-LR; 1966-2013; initialised each November; 2 to 5 years lead time; 16 ensemble members.

5.7 Discussion

The main aim for the study is to determine if the predictability seen for surface variables in the North Atlantic can be replicated for potential temperature and salinity in the North Eastern Atlantic at depth. Using two uninitialised historical simulations and one set of initialised hindcast simulations I have assessed the predictability at depth for the three transects (EEL, PB, and GS) using MPI-

ESM. I show that there is predictability on a 2-5-year lead time in the North Eastern Atlantic for potential temperature and salinity.

Prediction of North Atlantic potential temperature and salinity can be improved with initialisation as in some areas the initialised hindcast outperforms the CMIP5/CMIP6 simulations. This can be seen in the comparison plots between the initialised hindcast and uninitialised historical simulations for both temperature and salinity along the three transects. Three areas of importance were identified as the Extended Ellett line in the north, the Porcupine Bank transect in the west, and Goban Spur to the south along the Irish coast. The last row of plots on Figures 5.9 and 5.10 show that for temperature the main improvements due to initialisation occur at the lower depths and that the upper ocean is well represented in all of the simulations. For salinity (Figures 5.12 and 5.13) the results show that improvements in prediction skill due to initialisation are not confined to larger depths, but also show up at the surface. Taking a look at the absolute values temperature (Figures 5.6, 5.7, 5.8), salinity (Figures 5.11, 5.12, 5.13), and the temperature-salinity diagram (Figures 5.3, 5.4, 5.5) show a better representation for both variables by the initialised simulation. This is especially at the surface in the North Eastern Atlantic. Overall the results show that there is an improved predictability and representation at depth for both variables with the initialisation, with better performance for salinity than temperature.

The results that I obtained for near-surface potential temperature are in line with the current research. Borchert et al. (2018) explored this region looking at the sea surface temperature (SST) and its connection with the ocean heat transport and the Atlantic Multidecadal Variability and how they are interconnected with each other. It was determined that on longer timescales SST is influenced and impacted by ocean heat transport. Koul et al. (2019) explored uninitialised historical simulations to show that open-ocean circulation can have an impact on North Sea inflow. While Koul et al. (2019) investigated the historical simulations I went a step further to determine if there is predictability along our three transects, by using initialised hindcast and uninitialised historical simulations. These simulations were compared with the assimilation simulation, as a first step I looked at the values that each simulation had generated followed by the temperature-salinity

diagram then moved on to the prediction skill. This has produced results that have highlighted that initialised simulations generally have improved predictability compared with uninitialised simulations. By extending our analysis further to the south compared to [Koul et al. \(2019\)](#), I show that also in these regions, the potential temperature and salinity are well represented in the model. I analysed a time period of 1961 to 2013, on a 2-to-5-year lead time to compare the results with two uninitialised simulations. A future target would be to extend the time frame as well as lead times. While these results look promising it should be noted that due to limited observations, any references for the sub-surface ocean prior to 2004 might not be as reliable as they are since then with the Argo observational network in place ([Wong et al., 2020](#)). Nevertheless, the results showed promising insights into the ability of initialised simulations, even when discussions about the benefit of initialisation are getting more traction ([Borchert et al., 2021](#)).

The ability to predict changes in the future fish stock will support adaptation for its management, which is of vast importance for international coastal communities. Through the analysis of both temperature and salinity at depth, I can identify habitable zones and spawning grounds that may be predictable. It will also support a better understanding of the life cycle and distribution of future fish habitats. Its potential has already been demonstrated for the blue whiting ([Miesner and Payne, 2018](#)) and cod ([Koul et al., 2021](#)) in the wider North Eastern Atlantic context.

5.8 Conclusions

In this study, I explored the predictability within the Eastern North Atlantic at depth using three transects the Extended Ellett Line, the Porcupine Bank, and Goban Spur. To achieve this I first determined validity in the temperature/salinity-space of the initialised and uninitialised simulations by comparing it to an assimilation simulation. I followed this by determining the predictability of the two categories of simulations and determining the impact of initialisation for the three transects. I found that;

1. there is multi-year memory in the water mass properties of the initialised predictions

2. that prediction skill depends on variable, depth, and external forcing scheme
3. that improvements in prediction skill in the initialised system over uninitialised simulations are mostly in the upper ocean above 300 m depth and in the deep ocean below 1500 m depth
4. that these improvements are more pronounced in salinity than in temperature

Investigation into improving prediction skill for the Eastern North Atlantic

6.1 Introduction

In chapters 4 the first investigation explored predictability in the Eastern North Atlantic for surface temperature and salinity. Using the initialised hindcast simulations from MPI-ESM-LR, the first step in the improvement of skill was to see, if expanding the depth profile could be beneficial. Using the initialised hindcast simulations a mean of temperature and salinity was obtained over 6m to 220m for the Eastern North Atlantic. The second step is to determine how correlated (against the assimilation simulation) the predictors are. The AMV is highly correlated in the Eastern North Atlantic and the SPG is highly correlated in the Norwegian Sea. When talking about improving prediction skill, it is important to understand that when referring to the correlation of the predictors it is the connection at that location. Initialised hindcast simulations can have skill (which is measured with ACC and the significance thereof), while the combination is the improved skill

(or not improved, depending). The goal of this section encompasses two distinct aspects of improving predictability in the Eastern North Atlantic.

1. Can the prediction skill of the initialised hindcast simulation be improved upon using two predictors?
2. Can the prediction skill of the initialised hindcast simulation be improved upon using grouped depth mean?

6.2 Simulations and methods

To answer these questions, I will be using both temperature and salinity from the initialised hindcast simulation like what was completed in Chapter 4. I use a mean of a group depth (6-220m) to determine if there was an improvement in skill. Where they undergo the ACC and will highlight any areas that have skill because of the initialisation. Next, there needs to be an understanding of how the two predictors are correlated with the Eastern North Atlantic. For each location, the predictor was correlated with the assimilation simulation to determine if it is connected. I will answer the two questions posed by looking at the potential temperature first followed by salinity.

The investigation into the potential improvement of prediction skills in the Eastern North Atlantic Ocean has begun in terms of exploring the impact the SPG and AMV have on temperature and salinity at depth. While it is important to determine if a grouped depth mean of 6-220m can provide an improvement compared to using one level i.e. the surface. This was completed using the initialised hindcast simulations. The initialised hindcast simulations have shown to have skill in the North Atlantic Ocean and this is also significant. There are a few regions that do appear to have little skill. Using the regions identified with little skill they will undergo the sub-sampling process Figure 6.1. The sub-sampling method was introduced by [Dobrynin et al. \(2018\)](#), and subsequently used by [Dobrynin et al. \(2019\)](#) and [Düsterhus \(2020\)](#), who used this algorithm to increase prediction skill of model prediction. It occurs during post-processing which helps in the improvement of prediction skills. With the identification of those ensemble members

who promise a better prediction skill on a climatic variable. This is achieved by creating statistical predictors for each single prediction, which are then compared to the ensemble members. The members, which are closest to the predictors are then selected for a sub-sampled average.

To get into further detail on the change of predictability based on the predictors the initial investigation explored the correlation between initialised hindcast simulations versus assimilation simulations, followed by one of the predictors (SPG, AMV) versus assimilation simulations, then the difference between the two. This should highlight areas in which the predictor performs the initialised hindcast simulations and potentially be used in the improvement of skill in a target area. Three areas were identified with little or no skill in the initialised hindcast simulations; two were in the south on either side of the North Atlantic Ocean, and the final area was to the north around Iceland. At these locations, the predictors do show some promise.

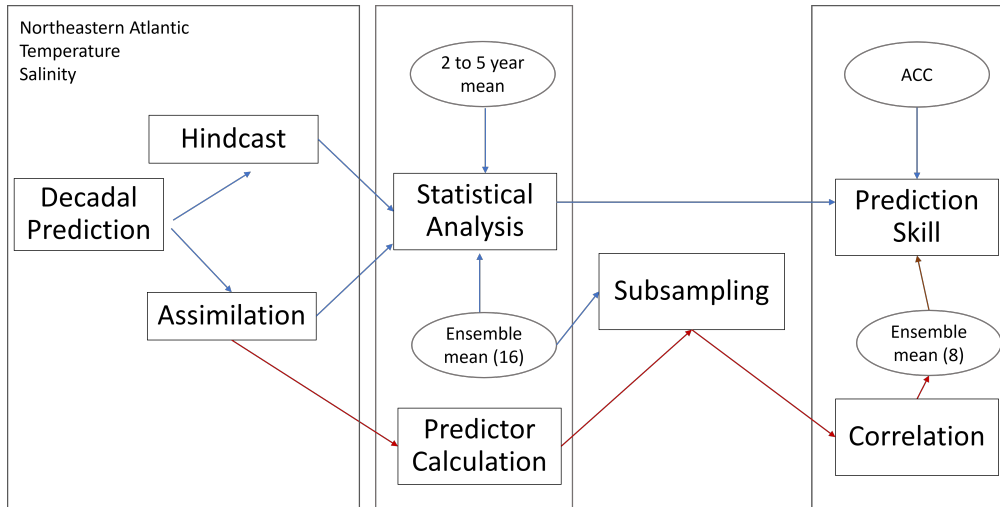


Figure 6.1: Schematic representation of the sub-sampling method 16 ensemble members for temperature and salinity from the initialised hindcast simulations in 1961-2008, for a 2 to 5 year lead time. The data is taken from the decadal prediction system where the full ensemble series undergoes statistical analysis, the assimilation simulation is used to create the two predictor time-series. The two predictor time-series are correlated with the Northeastern Atlantic Ocean at each location over the time frame. In every location and time we start with the output of the 16 ensemble members generated by initialised hindcast simulations and only select those members in which they agree with the predictor. Those selected ensemble members are then correlated with the Northeastern Atlantic Ocean at each location over the time frame. The final step highlighted three locations from the Northeastern Atlantic Ocean that had no skill through the 16 ensemble members, explored if the 8 sub-selected ensembles members improves skill.

6.3 Improving prediction skill for potential temperature

The initialised hindcast simulation was evaluated against the assimilation simulation from the MPI-ESM-LR for the time frame 1966-2013 on a 2 to 5 year lead time. Next I the correlation between the two predictors (SPG and AMV) with the assimilation simulation. These results can be found in figure 6.2, I will discuss the initialised hindcast simulation, then AMV followed by the SPG. The initialised hindcast (figure 6.2 a, c) already shows to be quite skillful and this is significant. The AMV shows that the majority of the region has good skill and that this is

significant. Some areas have little or no skill there is a large section off the coast of Greenland. The SPG plot shows a different story. There was a smaller area of significant positive skill mainly in the southern section, on the shelf and Norwegian Sea. For the open Atlantic Ocean, there was very little or low skill. From figure 6.2, some small areas are highlighted in the yellow boxes show to have that have little or no skill, two in the south of the region and one in the north for the initialised hindcast simulations. The two in the south will be referred to as the Southeast which is negatively correlated and the Southwest. The north area is the region in the Norwegian Sea, these will be further analysed to determine if there is any improvement in skill through sub-sampling. While there appears to be some improvement in these areas through using either of the predictors. Before that is completed, I will explore how the sub-selection using both of these predictors has an impact on the prediction skill compared to the initialised hindcast for the North East Atlantic Ocean.

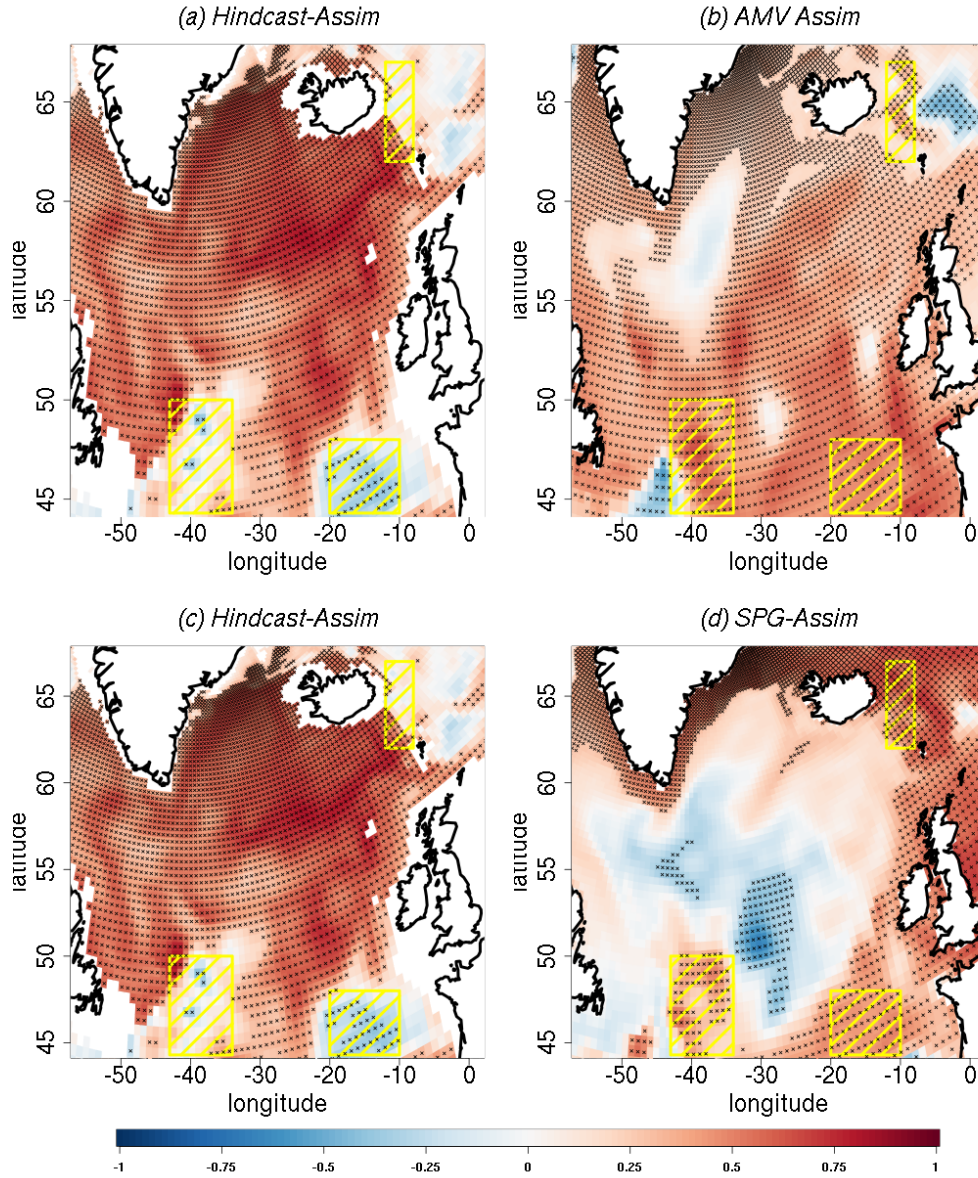


Figure 6.2: ACCs for Potential Temperature for initialised hindcast simulation (a, c), AMV (b), SPG (d) evaluated against assimilation at lead years 2-5. The difference between initialised hindcast simulation - uninitialised historical (CMIP5(c), CMIP6 (f)) simulation. Generated from the MPI-ESM-LR; 1966-2013; initialised each November; 2 to 5 years lead time; 16 ensemble members; depth mean 6m – 220m. The red is positive correlation, the blue is negatively correlated and the black dots show significance. The yellow hatching shows whether there is a positive or negative correlation between the initialised hindcast simulations (a, c) and the predictors (b, d).

The next step of the analysis was to determine if the sub-sampled temperature field (8 ensemble members), based on the predictors (SPG, AMV) showed any improvement on the initialised hindcast simulations (16 ensemble members). From the figure 6.3 it is clear that for this region there is a lot of significant skill for this region for the initialised hindcast simulation. To get an idea of how correlated the sub-sampled SPG is with the assimilation simulation this is highlighted in figure 6.3 b. There is a high correlation the for the majority of the Eastern North Atlantic, there are a few areas in which skill is very low these being in the south and a bit to the west. When this sub-sampled SPG is compared with the initialised hindcast simulation figure 6.3 (c), it highlights the areas that show some improvement. One such area is in the Norwegian Sea, with some skill improvement in the south. Figure 6.3 (e) shows the correlation between the assimilation simulation and the sub-sampled AMV for the Eastern North Atlantic. It shows that there is good skill for the areas with little or low correlation. Figure 6.3 (f), is the sub-sampled AMV compared with the initialised hindcast simulations. What it highlights is that for the Eastern North Atlantic, the sub-sampled ensemble provides a slight improvement in skill. Knowing that the sub-sample ensembles can improve skill in certain areas of the Eastern North Atlantic on their own. The final step is to determine if the combination of both predictors can improve skill. Where for each coordinate it chooses the closest 8 ensemble members from either the SPG or the AMV this is highlighted in figure 6.3 (g, h, i). Figure 6.3 (g) is the initialised hindcast simulation (16 ensembles), and figure 6.3 (h) is the combined sub-sample (SPG + AMV). What this combination of 8 ensembles highlights is that this duo does not work for the improvement of skill (Figure 6.3 i). Moving forward this combination will not be considered when trying to improve the skill in the three locations highlighted in figure 6.3.

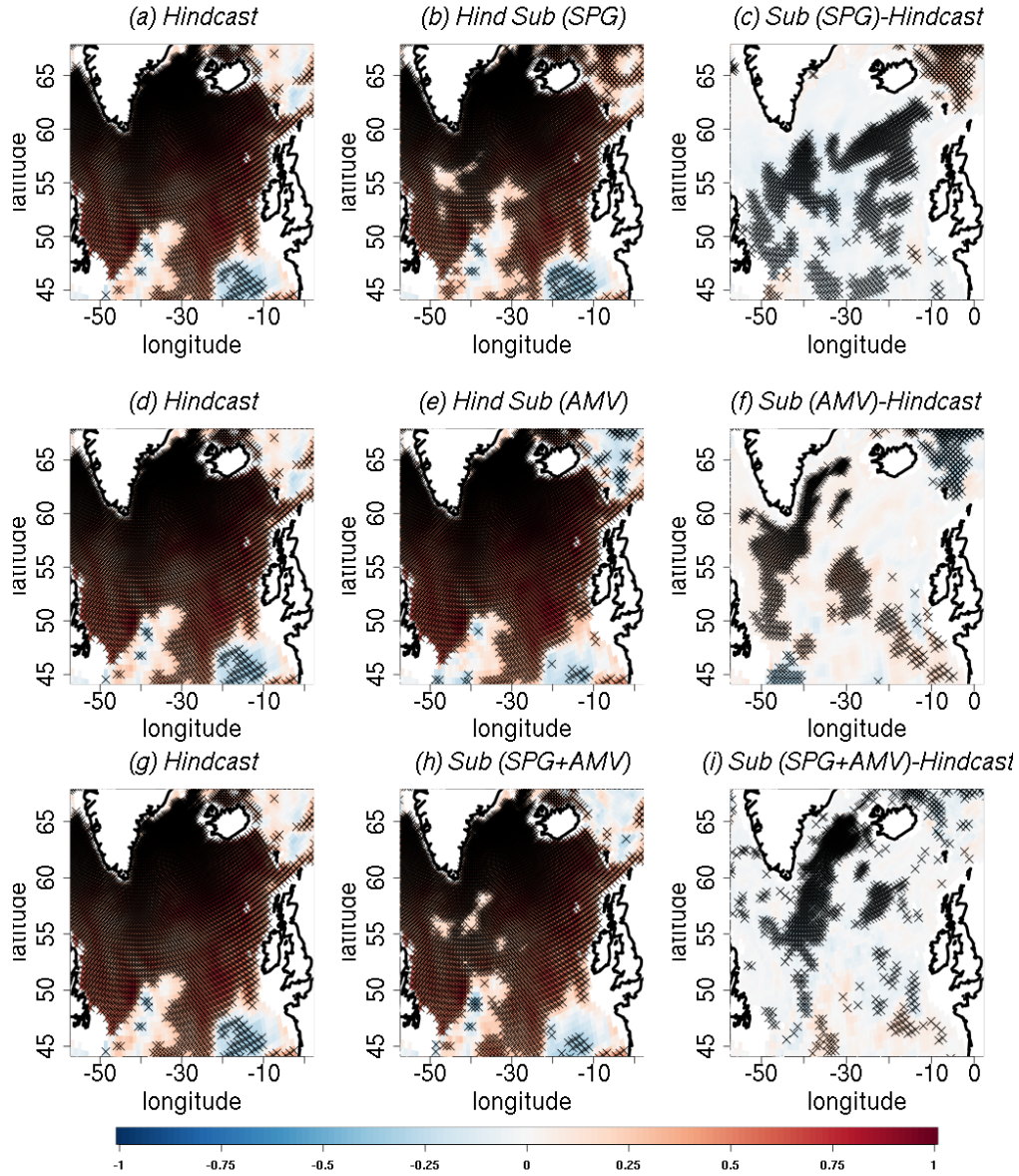


Figure 6.3: Improvement of the prediction of Potential Temperature in the Eastern North Atlantic due to more accurate prediction of the AMV, SPG, and both. ACCs for Potential Temperature for initialised hindcast simulation (16 ensemble members) (a, d, g), Sub-sampled initialised hindcast simulation (8 ensemble members) (AMV (b), SPG (e), both(h)) evaluated against assimilation at lead years 2-5. The difference between initialised hindcast simulation sub-sampled initialised hindcast simulation (8 ensemble members) (SPG (c), AMV (f), both (i)) simulation. Generated from the MPI-ESM-LR; 1966-2013; initialised each November; 2 to 5 years lead time; depth mean 6m – 220m. The red is positive correlation, the blue is negatively correlated and the black dots show significance. Red dots in the right column indicate regions that became significant after sub-sampling.

The potential temperature results are highlighted in figure 6.4 with the first column being the comparison between the assimilation simulation and the initialised hindcast simulation, the middle column being the SPG compared with the assimilation simulation and the last column being the AMV compared to the assimilation simulation. Figure 6.4 (a, b, c) shows the results for the southeast location, the comparison shows that the two correlate -0.315. This is quite a poor correlation and shows that the initialised hindcast simulations have no skill along this section as previously discussed. When the sub-sampled SPG time series is compared to the assimilation simulation it shows no improvement in the skill going up to -0.323. The AMV time series shows some promising results with a correlation of -0.177, while this is not a great improvement in skill it is still an improvement over the initialised hindcast simulations. The southwest (figure 6.4 d, e, f) results show that the comparison between the assimilation simulation and the initialised hindcast simulation has a correlation value of 0.007. This is an improvement on the previous site which was negatively correlated and this site is slightly positively correlated. While this result is promising I can see if I can improve upon the skill using the SPG and the AMV, following the previous site I expect the AMV to show improvement over the SPG. The SPG result for the site shows a correlation of -0.125 which follows the same as the previous site where the skill has declined compared to the initialised hindcast. Similar to the previous site the AMV shows an improvement in skill compared to the initialised hindcast, with a correlation of 0.201. For the North section (figure 6.4 g, h, i) of the sub-sampling, the initialised hindcast simulations have an improved correlation with the assimilation simulation of 0.225. The sub-sampled SPG time series when correlated with the assimilation simulations has a result of 0.337. When this value is compared to that of the initialised hindcast it is clear that there is some improvement in the prediction skill. The sub-sampled AMV time series when correlated with the assimilation simulated has a result of 0.145. Unlike previous sections, this result does not improve the prediction skill of the region. From what is seen in the correlation, the northern section is most impacted by the SPG index and the two lower sections are impacted by the AMV. The correlations have been summarised and discussed further in the discussion section (6.1).

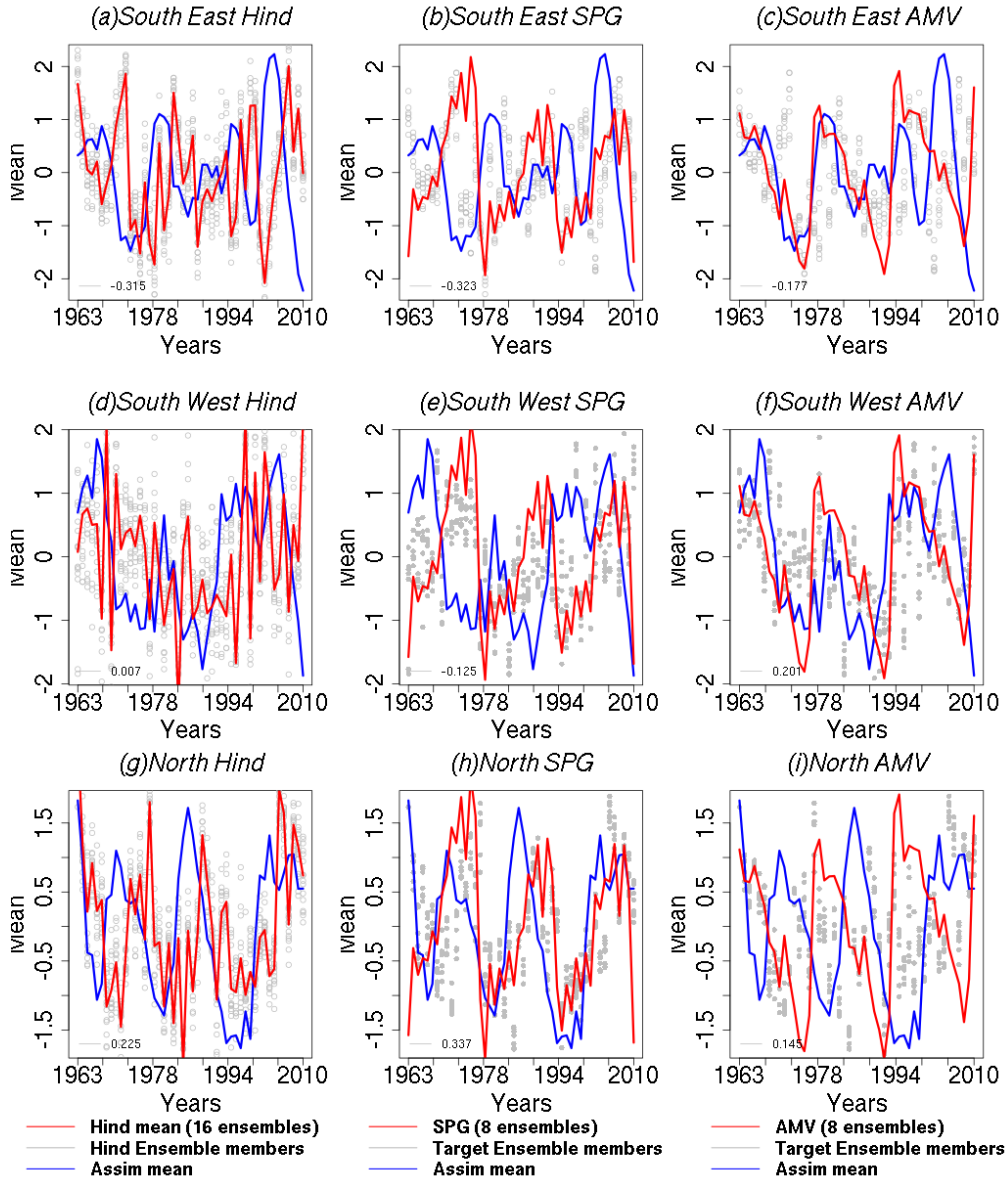


Figure 6.4: Time series for Potential Temperature from the three yellow hatched areas (6.1), it was normalised and detrended. They will be referred to as South East (a-c), South West (d-f), and North (g-i). Each location correlates the initialised hindcast simulation (16 ensemble members) (a, d, g), Sub-sampled initialised hindcast simulation (8 ensemble members) (SPG (b, e, h), AMV (c, f, i)) against assimilation at lead years 2-5. The blue line is the ensemble mean for the assimilation simulation, the red line is the ensemble mean for the initialised hindcast simulation, and the grey dots are the ensemble members. The initialised hindcast (16 ensemble members) when correlated with the assimilation at each location is quite low, South East (-0.315), South West (0.007), North (0.225). The sub-sampled (SPG) initialised hindcast (8 ensemble members) when correlated with the assimilation at each location overall is poor, South East (-0.323), South West (-0.125), North (0.337). The sub-sampled (AMV) initialised hindcast (8 ensemble members) when correlated with the assimilation at each location has some improvement, South East (-0.177), South West (0.201), North (0.145). Generated from the MPI-ESM-LR; 1966-2013; initialised each November; 2 to 5 years lead time; depth mean 6m – 220m.

6.4 Improving prediction skill for salinity

The initialised hindcast simulation for group salinity depth (6m – 220m) provides an improvement in skill compared to the single layer discussed in the previous chapter. The majority of the Northeast Atlantic Ocean shows to be quite skilful and also significant. There are still some areas that have little or no skill, these include areas in the north, around the European shelf, the Labrador Sea and the Continental shelf. When the AMV is correlated with the assimilation simulation there is good skill for a lot of the region with a few areas with little or no skill. There is a small area along the continental shelf that has little skill highlighted by the blue colour, there is also a band of little skill off the Labrador Sea and Norwegian Sea. This is not the case when it comes to the SPG correlated with the assimilation simulation. The majority of the Eastern North Atlantic has very little skill, with only small areas of significant skill. Around the Labrador Sea and Norwegian Sea have skill and this is significant, there is also an area off the Continental shelf that has some significant skill.

Figure 6.5 there are some small areas (highlighted in the yellow boxes) that have little or no skill in the initialised hindcast simulations. The two are in the south of the Eastern North Atlantic and one in the north in the Norwegian Sea. The two in the south will be referred to as the southeast where it is negatively correlated and the southwest is located off the coast of the Continental shelf. The north area is the region of the Norwegian Sea, these will be further analysed to determine if there is any improvement in skill through sub-sampling. While there appears to be some improvement in these areas through using either of the predictors. Before that is completed, I will explore how the sub-selection using both predictors has an impact on the prediction skill compared to the initialised hindcast for the Eastern North Atlantic. The AMV is correlated with the assimilation simulation for each coordinate showing that for the Eastern North Atlantic, there is skill and that this is significant (Figure 6.5 b). When the same is completed for the SPG, the correlation is not as skilful or significant (Figure 6.5 d). The Nordic region shows to have skill and this is significant.

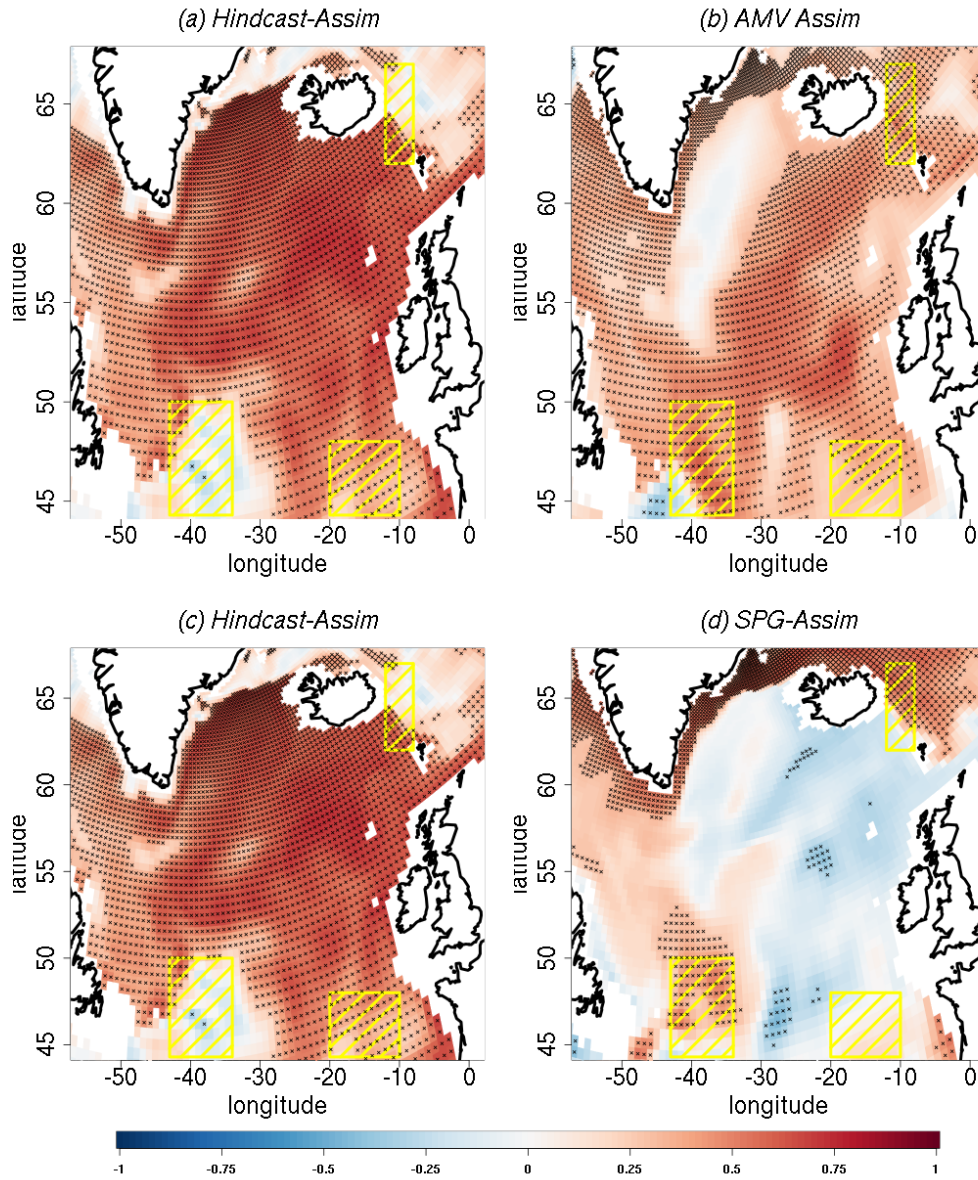


Figure 6.5: ACCs for Salinity for initialised hindcast simulation (a, c), AMV (b), SPG (d) evaluated against assimilation at lead years 2-5. The difference between initialised hindcast simulation - uninitialised historical (CMIP5 (c), CMIP6 (f)) simulation. Generated from the MPI-ESM-LR; 1966-2013; initialised each November; 2 to 5 years lead time; 16 ensemble members; depth mean 6m – 220m. The red is positive correlation, the blue is negatively correlated and the black dots show significance. The yellow hatching shows whether there is a positive or negative correlation in the initialised hindcast simulations (a, c) and the predictors (b, d).

Before a more detailed investigation occurs into these areas of yellow boxes I wanted to explore the impact of sub-sampling using the two predictors (SPG, AMV) on the initialised hindcast. The next step is to determine if the sub-sampled temperature field using the predictors (8 ensembles) can improve the skill of the initialised hind simulations (16 ensembles). This sub-sampled ensemble is based on the initialised hindcast simulations. Figure 6.6 (a, d, g) shows the initialised hindcast simulations (16 ensembles) before any sub-sampling has occurred. Figure 6.6 (b, e, h) shows the sub-sampled initialised hindcast simulations using either the SPG or the AMV or the combination of both the AMV and SPG. Figure 6.6 (c, f, i) shows the difference between the two plots with the sub-sampled plots subtracted from the initialised hindcast simulations, any areas that remain red have some skill and the crosses show that they are significant. The initialised hindcast has only two small areas that do not have any significant skill, one being in the North in the Norwegian Sea and the second on the Continental shelf (Figure 6.6 a, d, g). The sub-sampled salinity field with the predictor SPG (8 ensembles) initialised hindcast simulation is almost identical to that of the initialised hindcast simulation (figure 6.6 B). The skill remains the same in the three areas that I am trying to improve. This is evident in the comparison plot where you get some improvement in the Norwegian Sea, but this is not significant (figure 6.6 c). There is also some improvement in the south that is significant, but this is already quite skilful, the area of the Continental shelf does show a slight improvement with a small area of significant skill. The sub-sampled salinity field AMV initialised hindcast simulation this similar to that of the initialised hindcast simulation with reduced skill to the northeast of the Norwegian Sea and a section off the Labrador Sea (Figure 6.6 e). When this sub-sample salinity field AMV (8 ensembles) is compared to the initialised hindcast simulation (16 ensembles) it highlights the areas that are improved upon, these being the red areas and the black crossed means that these locations are significant (Figure 6.6 f). The final step in the sub-sample of the salinity field is the combination of the two predictors (Figure 6.6 h, i), this combination does not work. The full 16 ensembles of initialised hindcast simulations have better skill compared to the 8 ensembles of the predictors.

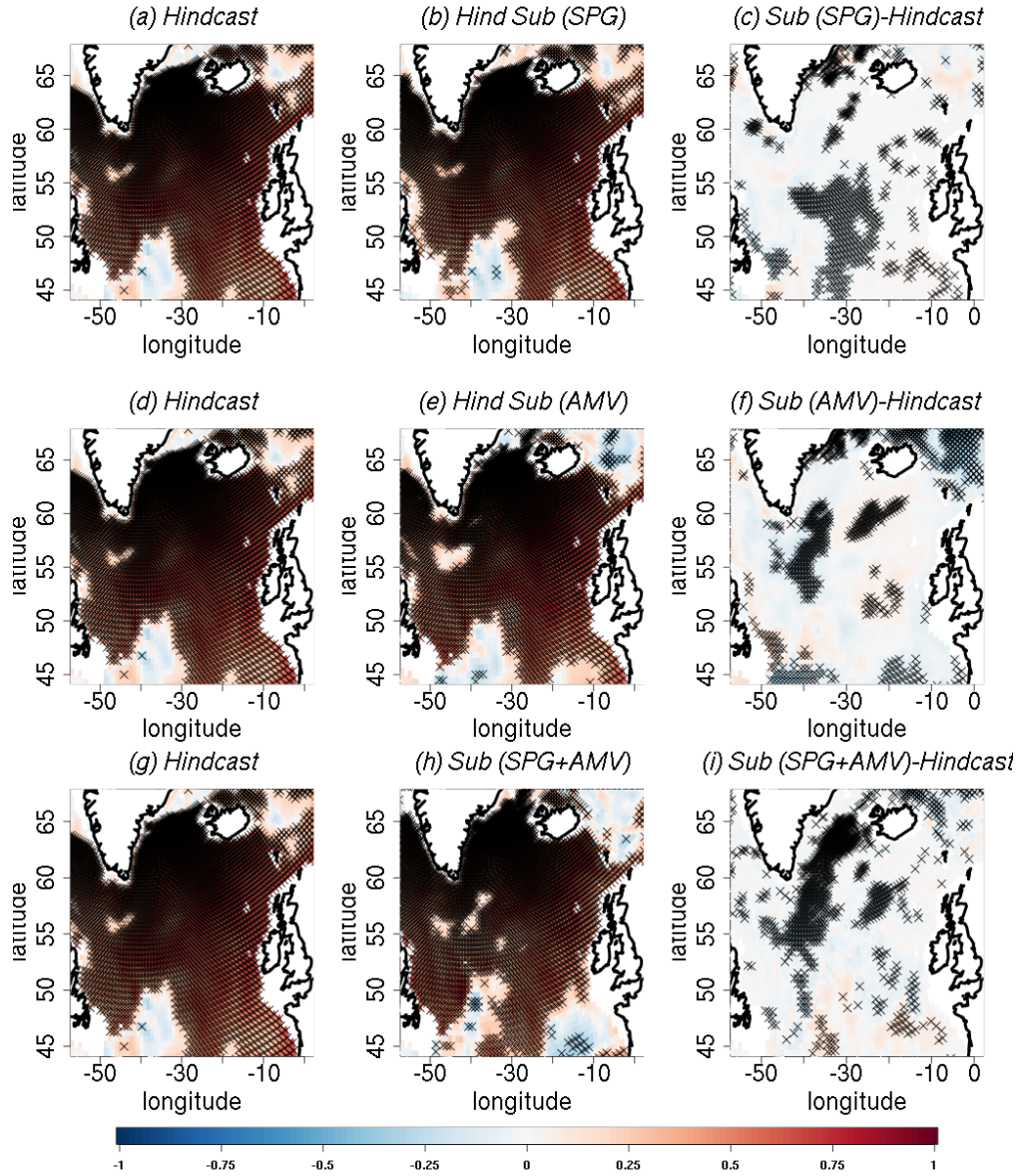


Figure 6.6: Improvement of the prediction of Salinity in the Eastern North Atlantic due to more accurate prediction of the AMV, SPG, and both. ACCs for Potential Temperature for initialised hindcast simulation (16 ensemble members) (a, d, g), Sub-sampled initialised hindcast simulation (8 ensemble members) (AMV(b), SPG (e), both(h)) evaluated against assimilation at lead years 2-5. The difference between initialised hindcast simulation - sub-sampled initialised hindcast simulation (8 ensemble members) (SPG(c), AMV (f), both (i)) simulation. Generated from the MPI-ESM-LR; 1966-2013; initialised each November; 2 to 5 years lead time; depth mean 6m – 220m. The red is positive correlation, the blue is negatively correlated and the black dots show significance. Red dots in the right column indicates regions that became significant after sub-sampling.

Similar to the temperature results the salinity sections have been taken from the same locations with two locations in the south and one in the North (Figure 6.7). Figure 6.7 (a, d, g) is the comparison of the initialised hindcast with the assimilation simulation. Figure 6.7 (b, e, h) the comparison of the sub-selected ensembles of the initialised hindcast simulations based on the SPG. Figure 6.7 (c, f, i) the comparison of the sub-selected ensembles of the initialised hindcast simulations based on the AMV. I will discuss each location individually to determine if there is any improvement in skill using this sub-selected time series. The first location that will be discussed is the southeast location with the assimilation simulations correlated to the initialised hindcast simulation, this results in a value of 0.455 (Figure 6.7 a). The sub-sampled SPG time series when correlated to the assimilation simulation has a value of 0.361, this is similar to the result found in the temperature results. The correlation of the AMV time series with the assimilation simulation results in a value of 0.505 which gives a slightly better result than that of the initialised hindcast simulation. For this location, the AMV provides a better result than that of the full ensemble of initialised hindcast simulations and the sub-sampled SPG time series. The next location that was explored was the southwest when the initialised hindcast was correlated with the assimilation simulation it gave a value of -0.095, this highlights that for this section there is little or no skill with the initialised hindcast simulations. Using the SPG sub-sampled time series the aim was to improve on this negative skill however the SPG did not have the desired impact and performed worse than the initialised hindcast simulation resulting in a value of -0.231. Using the other predictor sub-sample time series of AMV showed to have an improvement in skill for this location with a value of 0.136.

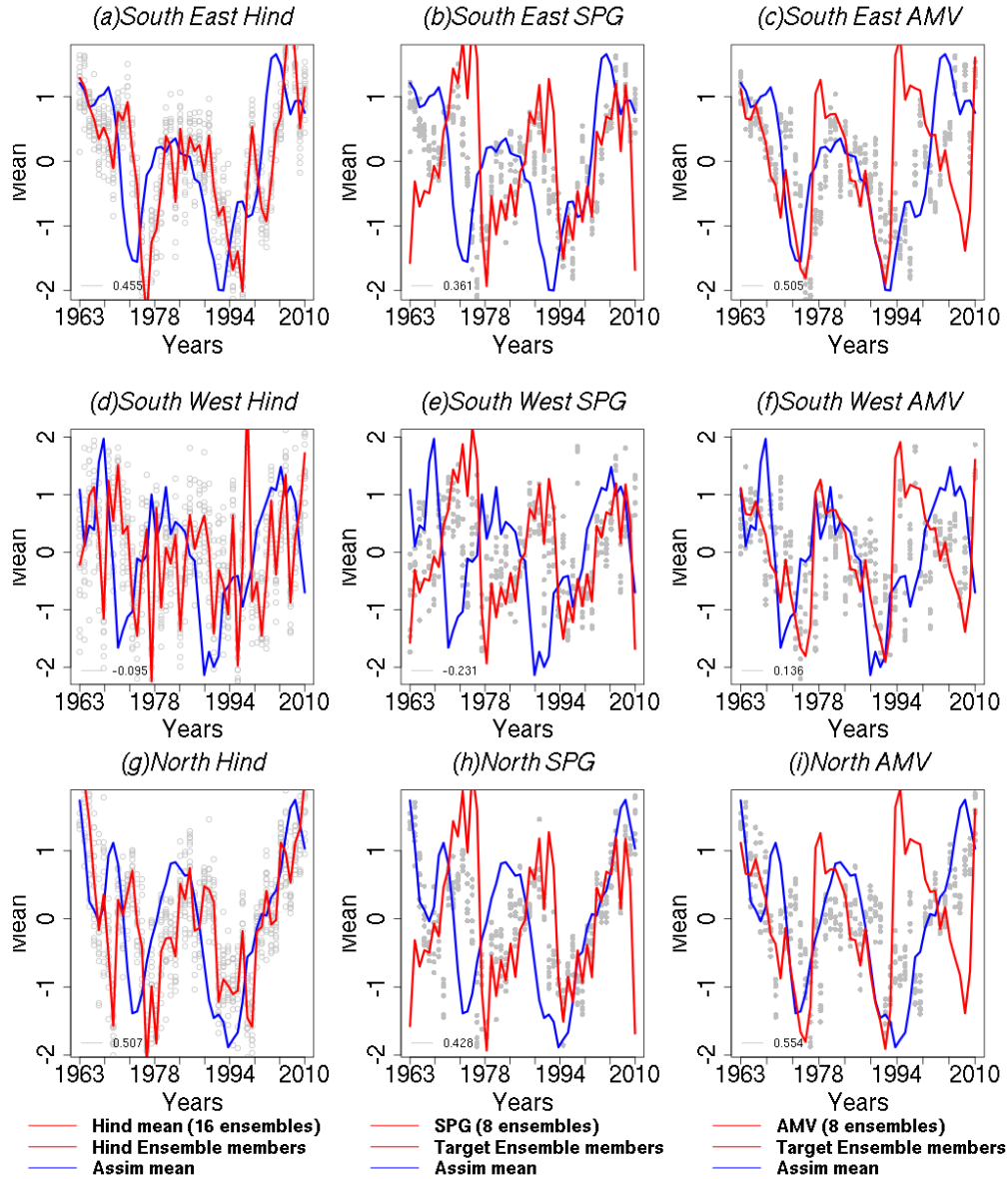


Figure 6.7: Time series for Potential Temperature from the three yellow hatched areas (6.5), it was normalised and detrended. They will be referred to as South East (a, b, c), South West (d, e, f), and North (h, i, j). Each location correlates the initialised hindcast simulation (16 ensemble members) (a, d, g), Sub-sampled initialised hindcast simulation (8 ensemble members) (SPG (b, e, h), AMV (c, f, i)) against assimilation at lead years 2-5. The blue line is the ensemble mean for the assimilation simulation, the red line is the ensemble mean for the initialised hindcast simulation, and the grey dots are the ensemble members. The initialised hindcast (16 ensemble members) when correlated with the assimilation at each location is quite low, South East (0.455), South West (-0.095), and North (0.507). The sub-sampled (SPG) initialised hindcast (8 ensemble members) when correlated with the assimilation at each location overall is poor, South East (0.361), South West (-0.231), North (0.428). The sub-sampled (AMV) initialised hindcast (8 ensemble members) when correlated with the assimilation at each location has some improvement, South East (0.505), South West (0.136), North (0.554). Generated from the MPI-ESM-LR; 1966-2013; initialised each November; 2 to 5 years lead time; depth mean 6m – 220m.

6.5 Discussion

This chapter was to explore whether skill could be improved in the North Atlantic through the inclusion of two predictors on the variable fields. To the best of my knowledge the first application of sub-sampling on decadal timescales. The two oceanic processes that have the greatest influence in this region are the SPG and AMV. Using the initialised hindcast simulation as a starting point, the prediction skill was determined using the ACC. From this analysis three areas of where the initialised hindcast did not perform too well. One of these sections were in the Northern area and two more southern on either side of the North Atlantic. Before a targeted analysis can occur the predictors were compared with the assimilation simulation to determine how skillful they were. This did show that there was an improvement in these three areas for either one of the predictors. Using this information the targeted analysis was conducted. To make the most of the possibility of improving skill a mean was made of the grouped depth to maximise the ability to potentially improve the skill. This was completed for both temperature and salinity for the years 1966-2013 on a 2 to 5 year lead time.

It is known that through initialisation there is an improvement in skill ([Müller et al., 2012](#); [Pohlmann et al., 2013](#)) which was highlighted previously at a surface level. Taking a slightly different approach was undertaken, this was in the form of a mean over the depth. With this approach, the aim is to increase the prediction skill for this region. If this does not have the desired effect then the inclusion of the predictors will take place. The initialised hindcast simulation (16 ensemble members) of both temperature and salinity shows to have skill and that this is significant in the Eastern North Atlantic. However, three locations were chosen from the section above from the initialised hindcast where there was little or no skill, from the initial exploration into the correlation of the two individual indices shows that these regions have an improvement in skill. These locations were then isolated out as a time series for further analysis to be conducted, using both SPG and AMV time series for both these regions. The first variable that I have looked at is the temperature followed by salinity at each of the locations, from henceforth will be referred to as Southeast, Southwest and North. These sites were analysed using the assimilation simulation and the initialised hindcast which were compared

to the time series of the SPG and AMV individually.

The majority of the North Atlantic Ocean has shown to be quite skillful with a few areas with little skill. Through the sub-sampling process on three of these areas, it was found that there was an improvement with one or the other of the predictors. It was expected that the northern area would be improved using the SPG and this was shown to be true, the same with the AMV in the two southern areas table 6.1 and table 6.2. The tables (6.1 and 6.2) highlight the different location correlations for both variables for the initialised hindcast and the two-predictor sub-sampled ensemble members with the assimilation simulation.

Table 6.1 shows the temperature correlations between the full 16 ensemble members of the initialised hindcast simulations and the 8 ensemble members of initialised hindcast simulations based on the predictors. It shows that there is an improvement of skill using the sub-sampled ensembles of the AMV for the two of the three locations. While the sub-sampled ensembles of the SPG for the two of three locations does not show any improvement in skill. Table 6.2 Shows the salinity correlations between the full 16 ensemble members of the initialised hindcast simulations and the 8 ensemble members of initialised hindcast simulations based on the predictors. It shows that there is an improvement of skill using the sub-sampled ensembles of the AMV for the three locations. While the sub-sampled ensembles of the SPG for the three locations does not show any improvement in skill.

Overall, the salinity results show that the initialised hindcast simulations correlated better than the temperature results. For both variables, results highlight the two south locations show improvement with the AMV and the North shows improvement using the SPG. This is not surprising as the Northern section of the Atlantic Ocean is more affected by the SPG and the south is more affected by the AMV. As a method sub-sample does show promise in its capabilities as a method of improving skill. That moving forward in the tailoring of decadal predictions (Chapter 7) it is more beneficial to use the mean grouped depth (6-220m) initialised hindcast simulations of temperature rather than just the SST.

In this instance it is clear that there is great potential for the sub-sampling method,

however there was no great improvement in skill. For such a method to work effectively the predictors chosen must relate to the areas. The two predictors chosen in this case relate the North Atlantic Ocean and can impact temperature or salinity, the results clearly show that they have no impact. While this was a more generalised approach, it highlights the skill that the initialised hindcast simulation in the Northeast Atlantic over the subsampling method. What did show potential for the improvement of skill is moving from using the surface data to a mean over a number of depth levels. Moving forward this will be referred to as the mean depth and the range (6-220m) has been agreed upon with stakeholders.

Potential Temperature			
	Southeast	Southwest	North
Hindcast (16 members)	-0.315	0.007	0.225
SPG (8 members)	-0.323	-0.125	0.337
AMV (8 members)	-0.177	0.201	0.145

Table 6.1: Summary of the different locations correlations for potential temperature for the initialised hindcast and the two-predictor sub-sampled ensemble members against the assimilation simulation

Salinity			
	Southeast	Southwest	North
Hindcast (16 members)	0.445	-0.095	0.507
SPG (8 members)	0.361	-0.231	0.428
AMV (8 members)	0.505	0.136	0.554

Table 6.2: Summary of the different locations correlations for salinity for the initialised hindcast and the two-predictor sub-sampled ensemble members against the assimilation simulation

Application of tailored decadal predictions

7.1 Introduction

In chapters 4 and 6 the Eastern North Atlantic was found to be predictable on a 2 to 5 year lead time. The analysis in Chapter 4 explored the time frame 1961 - 2013 for temperature and salinity highlighting there was skill in the Eastern North Atlantic using initialised hindcast simulation. In this same time frame, a grouped depth mean of 6-220m for initialised hindcast simulations was shown to have skill in this same region to determine if there was any improvement in skill (Chapter 6). Wanting to exploit this skill seen in the Eastern North Atlantic to tailor for stakeholder needs, the methods employed in this chapter are highlighted in Figure 7.1. In this contribution the exploration shift in the distribution and density of Atlantic (Scomber Scombrus) and horseshoe (Trachurus Trachurus) mackerel is influenced by changes in temperature. To achieve this there are a few questions that need to be answered;

1. Has there been a northward shift in the Mackerel stock in the last 20 years?

2. Can the initialised simulation be used to predict changes in temperature up to 2019?
3. How can this information be effectively communicated to stakeholders?

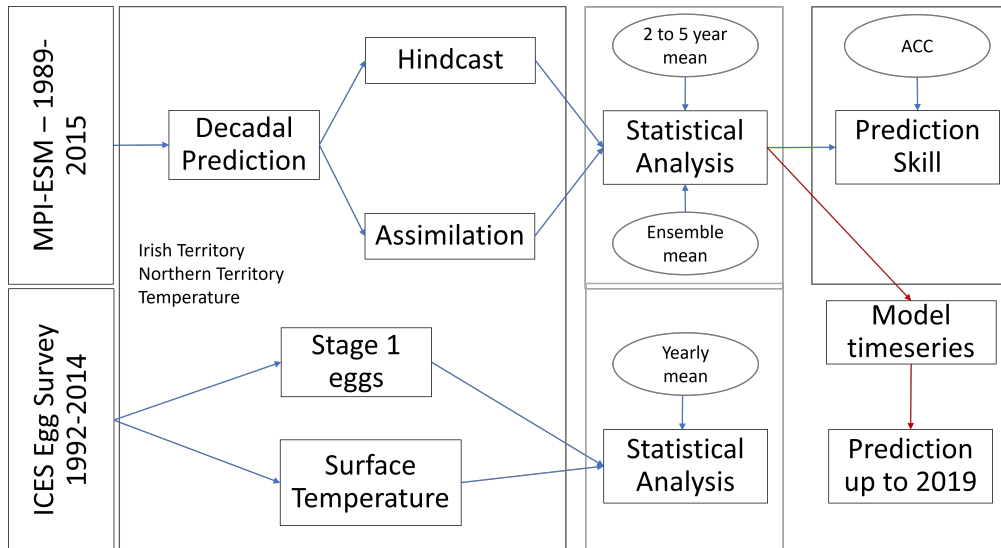


Figure 7.1: Schematic representation of how both the model data (1989-2015) and the observational data (1992-2014) is initial explored to determine the similarity between the two. Two regions have been identified for this study the NE Atlantic northwest of Ireland (Northern Territory) and the West of Ireland (Irish Territory). These regions under went statistical analysis. The model data undergoes time series analysis and is extended out to 2019, this time series is then compared to the observational data.

Identifying if there has been a northward shift in mackerel previously is the initial step in the tailoring process. Using the observational data from the ICES survey report stage 1 egg, two areas were identified. The first area identified was the West of Ireland (Figure 7.2) and the section of the NE Atlantic northwest of Ireland. In these two sections, the change in temperature and egg density was investigated. Allowing for a comparison to the initialised hindcast simulations of temperature for these two areas. Taking advantage of the predictability of the grouped depth (6-220m) temperature on a shorter time frame 1989-2014 with a 2 to 5-year lead time. This is roughly in line with the observational data from the ICES survey

report for Atlantic and horseshoe mackerel in the time frame 1992-2014 and 1998-2014 respectively. Two time series from MPI-ESM-LR were compared to evaluate if the value obtained from initialised hindcast simulation and assimilation simulation with the observational temperature data. The initialised hindcast simulation was then extended to 2019, to determine if it was possible to predict temperature changes. If this temperature change will impact the density and distribution of the mackerel eggs. The final step is how to effectively communicate this information to the stakeholders.

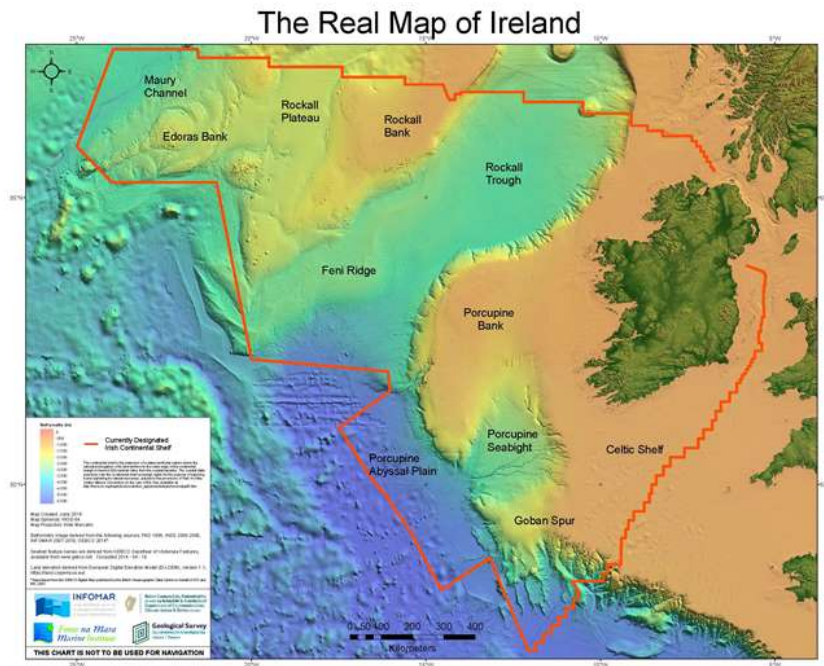


Figure 7.2: An illustration of the true extent of Ireland’s Territory in both land mass and ocean with the border highlighted by the red line. The majority of the territory is in the North Atlantic, on the shelf highlighted by the regions in orange and the deeper ocean highlighted by the darkening blue colours (From Marine Institute (2022))

7.2 Density and distribution of stage 1 eggs

The first step is to evaluate the changes in the distribution of both the Atlantic mackerel and horseshoe mackerel. Determining if there is a northward shift in

the spawning regions in the time frame 1992 to 2016. From 1992 the distribution of the eggs has changed dramatically, this is highlighted in Figure 7.3. From the years 1992 to 2004 the density of the stage 1 eggs is thinning as they were highly compacted around Spain all the way up to Ireland. There also appears to be movement northward of the spawning grounds. This is made clearer in the surveys that occur between 2007 to 2016 where there has been an increase in the egg density around Scotland and Iceland that was not observed in the previous years. From 1992 to 1995 there is a reduction in the presence of eggs highlighted by the areas in red but the density of the eggs has increased around the coast of Ireland compared to the southern area. Similar is observed when moving onto 1998 there appears to be a slight movement northward of the stock but this is in low density with the higher density of stock spawning on the Spanish Coast. 2001 we see a rise in the presence of stage 1 eggs this being a lower density than that has been observed previously, it is also clear that the stock has moved further northward to the top of Scotland. While 2004 we see a reduction in the distribution of the stock and in density, after this year there appears to be a resurgence in the stock. 2007 is the first year in which we see the stock moving and expanding further north but also westward. This also shows a higher density around Ireland compared to previous years. The trend continues on in the following survey of 2010 where there seems to be an explosion with a string increase of eggs Northward around Scotland and Iceland. There is a slight reduction as you move southward from Ireland towards France. While this is the case the density of the eggs is as they are more spread out. Moving forward to 2013 what was expected to see is the increase in density in the NE Atlantic northwest of Ireland but this is not the case. There is a wider spread of eggs in this region but this is not as dense. More eggs in the southern section compared to the previous year. The final year that was observed is 2016. It shows a reduction in the distribution of the stock through all areas. The section around Spain and France shows a decline over the last 20 plus year. This is similar with around Ireland where they also seem to be in lower density. The eggs can be found in front of the Scottish coast, but no longer extend towards Iceland. However, the density found in these regions has increased.

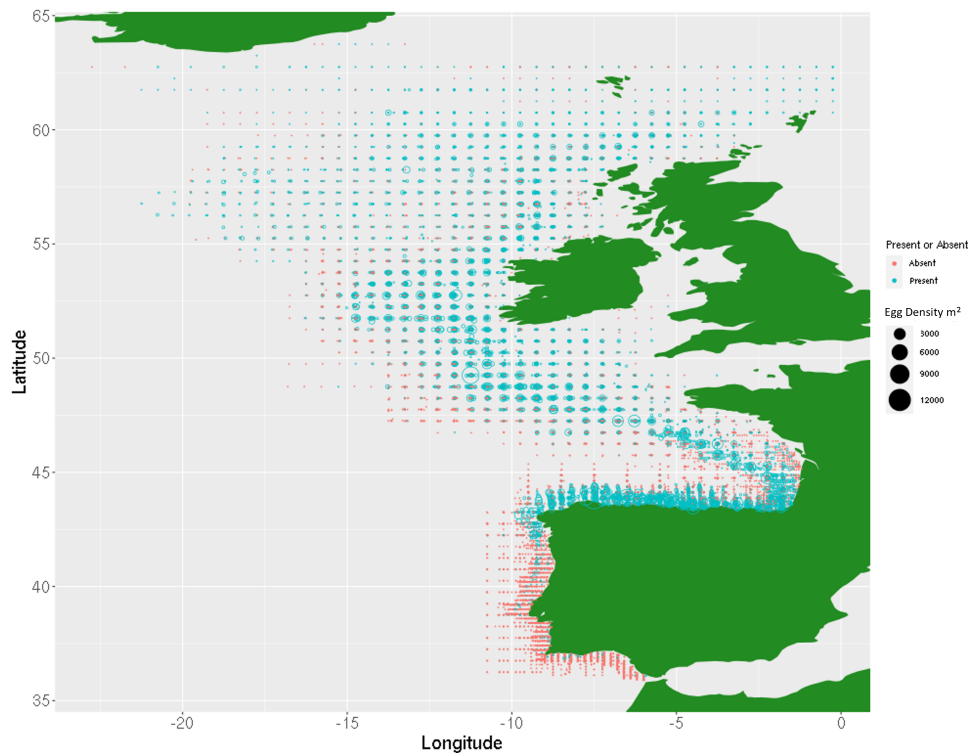


Figure 7.3: Atlantic Mackerel (*Scomber Scombrus*) egg density data at each location for every 3 years from 1992 - 2016, where the size blue circle represents the density of eggs found and the red crosses show that there have no eggs been found.

There are obvious changes in the distribution in the form of a northward shift from the beginning till the end of the time frame. The density changes as well, which is highlighted in Figure 7.4, where two areas of interest are identified. The first highlighted in red being the West of Ireland and the second highlighted in black is the NE Atlantic northwest of Ireland where the stock has potentially moved to. In this section I explore the changes on a roughly 9 year period with the first plot being 1992, the second plot being 2001 and the third plot being 2010. The fourth plot shows six years after this as it is the last available year. The 1992 data set shows for the West of Ireland the Atlantic Mackerel covers the majority of the area and the density is quite high. At this moment in time this stock has slightly moved out of the fishing ground in the north east sector towards Scotland. Jumping forward to 2001 the fish stock begins to show signs of a reduction in both distribution and density in the stock found in the West of Ireland. This is

highlighted by the red crosses on the Figure 7.4. The move of the stock northward is more evident as it extends up and beyond Scotland with higher density than what was seen previously. Moving forward to 2010, the West of Ireland saw a sharp decline in the density of the fish stock, but the distribution has remained similar to previous years. The biggest difference can be seen in the 2016 time series where the stock in the West of Ireland has moved back towards the Irish coast. Here, an increase of locations that have no eggs. There has also been a decrease in the density of the stock. In the NE Atlantic northwest of Ireland is an increase in the density of the stock but the distribution is not as extensive as the previously seen. Between 1992 and 2001 there is a shift in the distribution towards Scotland while this density is quite low between these two time frames. Focusing on Ireland it is clear that there in the time span there is a lower density of eggs but also there begins to show areas where they no longer find eggs that were previously found in the area. Moving forward to the 2010 and 2016 years there is a dramatic change in the distribution of the eggs compared to the previous two years. In the West of Ireland there is a clear change in the spread of the eggs found and in the density that they occur, particularly in 2016. Looking at the NE Atlantic northwest of Ireland it shows that between these two time frames that the distribution went from Scotland to Iceland then in 2016 it did not extend as far. Nevertheless, the density was higher compared to the 2010 survey.

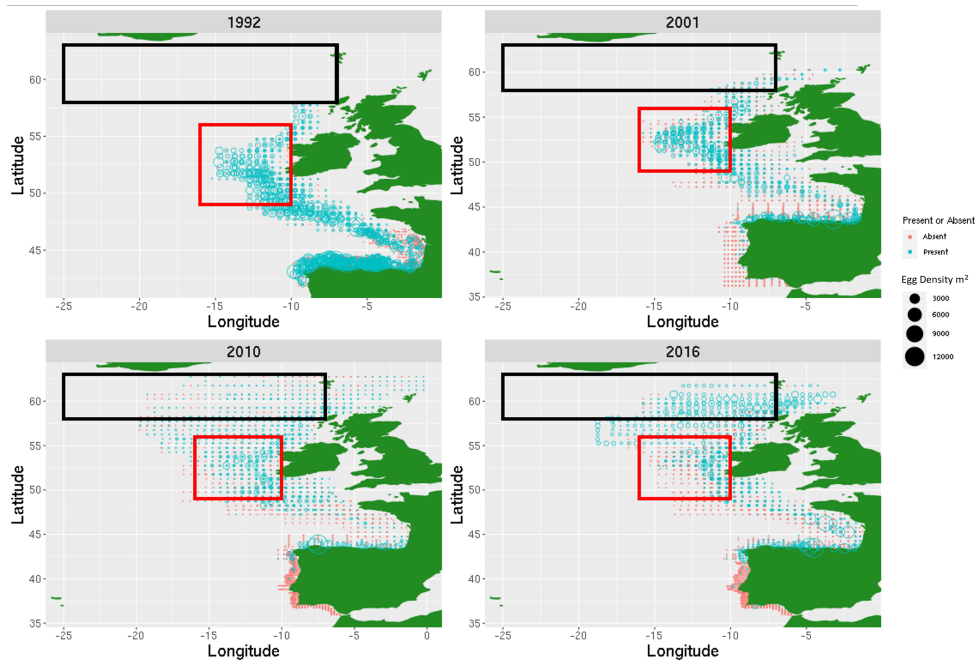


Figure 7.4: *Scomber Scombus* (Atlantic Mackerel) egg density data at each location for every 3 years from 1992 - 2016, where each blue circle represents the number of eggs found and the red crosses shows that there have no eggs been found. The red box highlights the Irish territory and the black box highlights Northern territory with the potential increase in temperature.

The second species of interest is the horseshoe mackerel, shown in 7.5 for the time frame 1998 - 2016. What is immediately obvious by looking at the individual years that there is a decline in the stage 1 eggs. At the beginning of the time frame 1992 the distribution of the stage 1 eggs ranges from the Spanish coast to just past Ireland. There are some sampling sites that did not contain any of these eggs at all. Moving forward to 1995 the sample area has been extend to include around Portugal. It shows that the stock does extend that far south but there is a reduction in the distribution and density of eggs. The decline is seen in 1998 where the stock still ranges from Portugal to just beyond Ireland. Stage 1 eggs where only found in half in the surveyed area the density was also reduced in this time frame. In 2001 the survey has shown that for most of the area there were either low egg density or no eggs found at all. This is similar for 2004. 2007 there appears to be a resurgence of the stage 1 eggs especially around Ireland and the

Spanish coast, while the density does not seem to be as high as previous years. The years 2010 and 2013 show a decline in the stage 1 eggs across the survey area the density of the eggs is also quite variable in the but not as high as seen previously. Where there is a real difference between the start and end of this time frame is in 2016. In the survey area there is very few eggs found and the density is quite low.

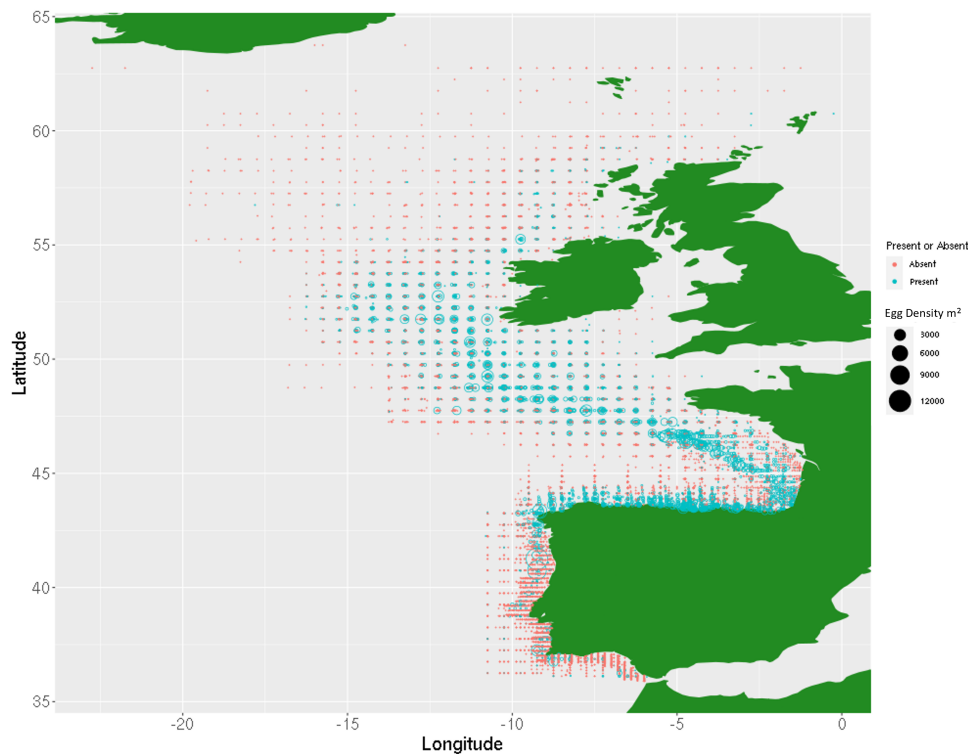


Figure 7.5: *Trachurus Trachurus* (Horse Shoe Mackerel) egg density data at each location for every 3 years from 1998 - 2016, where the size blue circle represents the density of eggs found and the red crosses show that there have no eggs been found.

There change in the density in the stage 1 eggs for horseshoe mackerel, this is highlighted in 7.6. I will explore these changes for the West of Ireland highlighted in red. The 1992 the stage 1 eggs are distributed evenly within the West of Ireland, with the highest density being in the lower section. The year 2001 shows an increase in the density of the eggs in this area and they take up a lot more of the area, there was also more locations where the eggs were not found at all. This does not change much in 2010 with exception to a slight reduction in the density

of the eggs. The largest difference is in 2016 where there are little or no eggs in the West of Ireland.

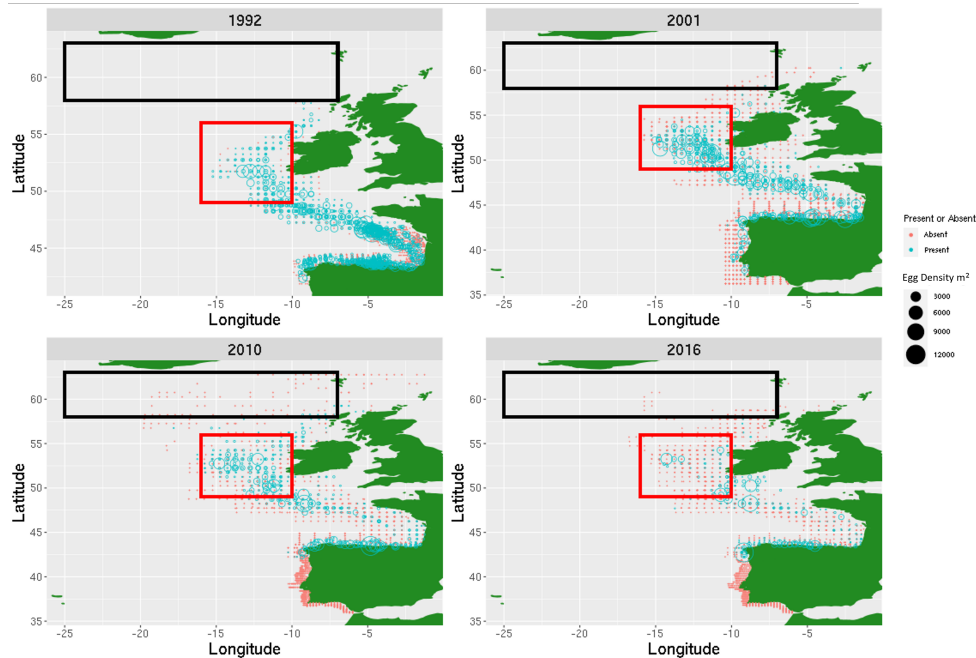


Figure 7.6: *Trachurus Trachurus* (Horse Shoe Mackerel) egg density data at each location for every 3 years from 1992 - 2016, where each blue circle represents the number of eggs found and the red crosses shows that there have no eggs been found. The red box highlights the Irish territory and the black box highlights Northern territory with the potential increase in temperature.

It is evident that there have been changes in the stage 1 egg for both of the mackerel species from 1992 to 2016, whether this been in a reduction in the eggs themselves or a change in the spawning grounds. One of the reasons for this is a change in the optimal range in temperature for spawning. To get an idea if this temperature for both regions highlighted in figures (7.2 and 7.6) was compared to the density. The results are highlighted in figure 7.7 for the West of Ireland and figure 7.8 for the NE Atlantic northwest of Ireland (Scotland and Iceland). For the West of Ireland the temperature ranges from 13 degrees Celsius to below 11 degrees Celsius and the Scottish fishing grounds the temperature ranges from about 12 degrees down to about 9.5 degrees Celsius.

Focusing on the West of Ireland first (figure 7.7) the beginning of the time series (1992) has the highest egg density compared to the following years the temperature for this year is approximately 13 degrees Celsius. This is the highest temperature seen where it begins to decline until 2004 where it reaches approximately 11.5 degrees Celsius, what is also seen is that the egg density also reduces. 2007 - 2013 sees an approximate 1 degree Celsius increase in temperature this co-insides with an increase in the egg density. After this year there is once again a decline in temperature not as low as the previous years. In 2015 there is an increase in egg density. This is the lowest temperature of the time frame comparable to 1998 but the temperature seen at this year is also higher. Finally 2016 sees and increase to approximately 12.5 degrees Celsius and this is also the lowest egg density that is observed.

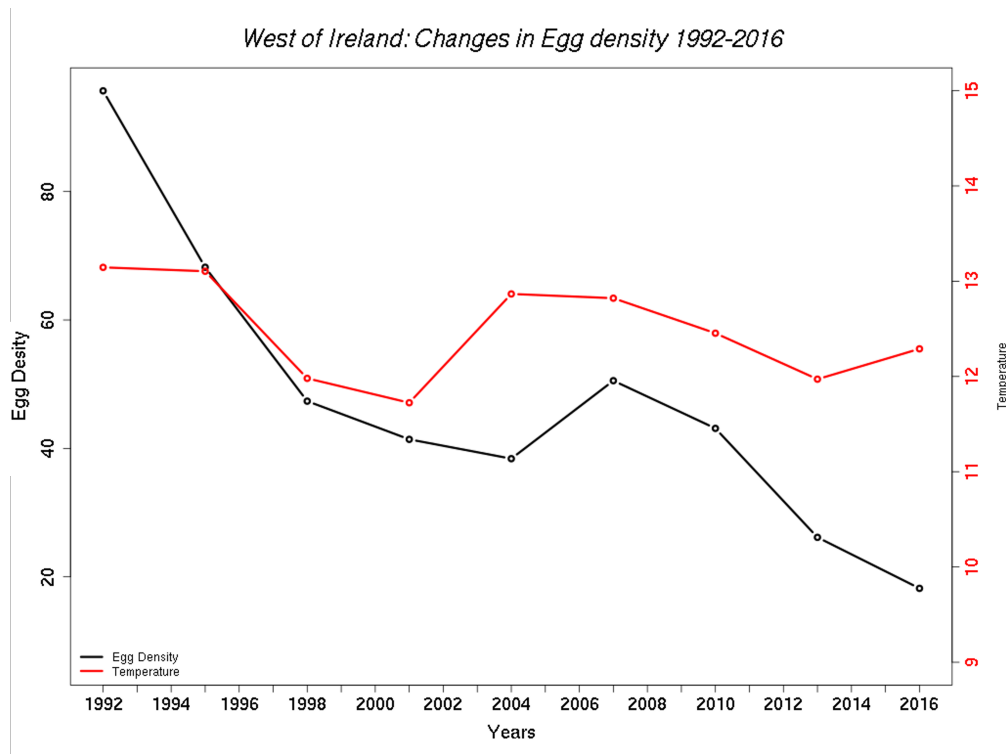


Figure 7.7: West of Ireland: Time series of temperature and egg density 3 years from 1992 - 2016.

Figure 7.8 Highlights the changes in both temperature and egg density for the

potential NE Atlantic northwest of Ireland, this section is slightly short as observations only began in 1998. For majority of the time frame the egg density is in the range about 20 eggs per m^2 and the temperature ranges between 10 - 12 degrees Celsius. In 2016 there is a massive spike in the egg density found in the region to almost 4 times what was seen previously and in this year the temperature is approximately 9.5 degrees Celsius.

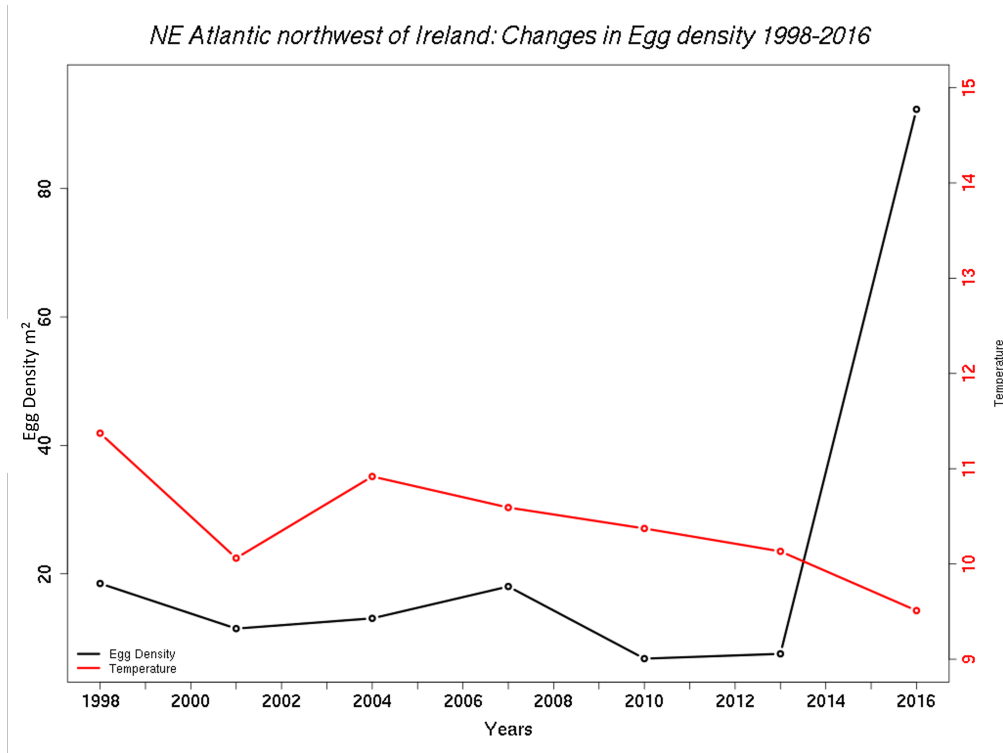


Figure 7.8: NE Atlantic northwest of Ireland: Time series of temperature and egg density 3 years from 1998 - 2016.

7.3 Prediction skill for West and NE Atlantic northwest of Ireland up to 2014

Chapter 4 has demonstrated that the Eastern North Atlantic is predictable on a decadal time scale and for the most part there is significant skill for this region. Wanting to build further on this we explored the predictability of this region for the time frame 1989 - 2014. Allowing for a comparison with the stage 1 egg density

data. This is a considerably shorter time frame from the previous investigation that looked at the time frame 1966 - 2013. In this instance there appears to be change in the predictability of the Eastern North Atlantic, while the overall picture still shows good skill for most of the region there has been a notable drop off of skill in some areas. In the subpolar North Atlantic the predictability remains relatively unchanged, the key difference is that skill is reduced in the southern section. Figure 7.9 highlights the results of this time frame along with the identification of the West of Ireland (red box) and the NE Atlantic northwest of Ireland (black box). The West of Ireland is a rough estimation of the fishing grounds and the major activity zone for spawning of the stage 1 eggs. Within this region the prediction skill is low. There is only a small section that contains any significant skill. A reason for this is that most of the region is on the shelf where the skill is limited. The NE Atlantic northwest of Ireland is a rough estimation in which the mackerel stage 1 eggs have been found in the later 3 years (2010, 2013, 2016) of the observational data from the ICES survey report. This region shows to have more promise, for the most part there is significant skill. Both regions are of interest in this study with a focus on the NE Atlantic northwest of Ireland as it will help determine if the shift in mackerel stock will be more likely to happen.

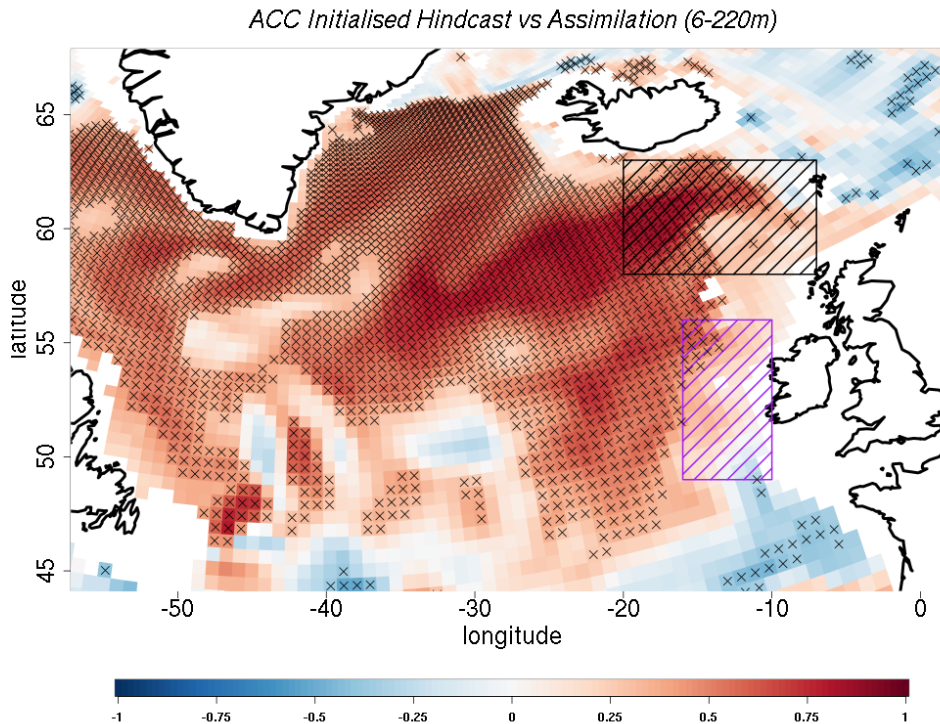


Figure 7.9: Anomaly correlation coefficient (ACC) for potential temperature (MPIOM) for initialised hindcast simulation evaluated against assimilation at lead years 2-5. Generated from the MPI-ESM-LR; 1991-2014; initialised each November; 2 to 5 years lead time; 16 ensemble members; depth mean 6-220m. The red is a positive correlation the black crosses show significance. The black lined box is the NE Atlantic northwest of Ireland and the purple shows the West of Ireland.

Having highlighted the predictability of the West of Ireland and the NE Atlantic northwest of Ireland, a time series can be made of each location. Using the initialised hindcast and assimilation simulation for temperature a grouped mean (6-220m) was compared with the two observational data (Figure 7.10 a, b). For both locations it is evident that there has been an over estimation of the temperature value for the two simulations. Figure 7.10 a, shows the West of Ireland comparing the simulations with the observations the overall trend is still present. That there is a decrease in temperature from 1992 till 2000, followed by an increase to 2005 then a steady decline. Figure 7.10 b, show the NE Atlantic northwest of Ireland comparing the observational data with the simulations, they still over estimate the

temperature values. However, these values are closer to the observational data. Mackerel have only been observed since 1998, so there is only temperature values from 1998. The two simulations do capture the trend that is observed in the observations for change in temperature. The West of Ireland remains the ideal temperature range for the development of stage 1 eggs and the NE Atlantic northwest of Ireland is in the range that is suitable for spawning.

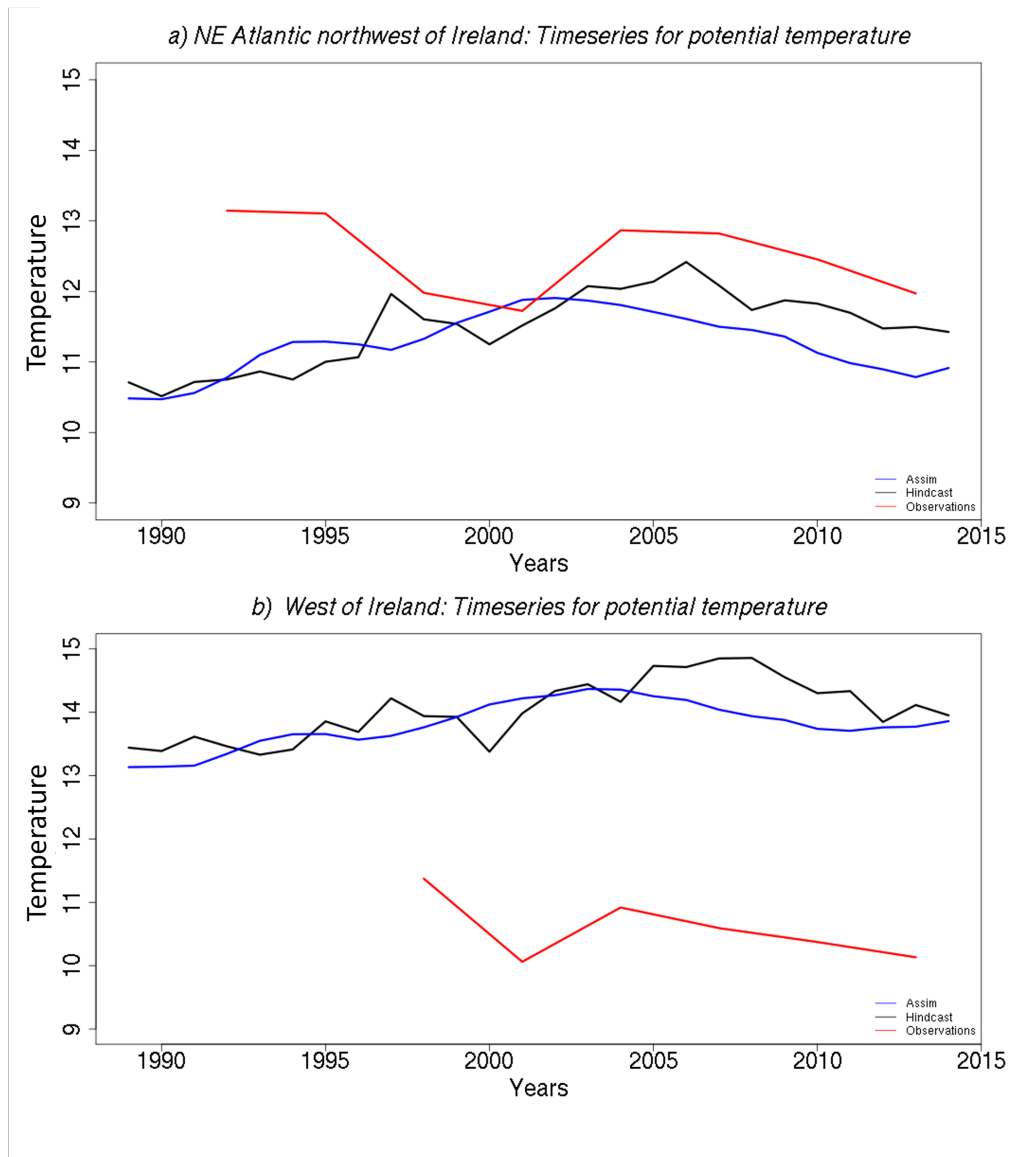


Figure 7.10: Time series for potential temperature (MPIOM) for initialised hind-cast simulation (black line) evaluated against assimilation (blue line) at lead years 2-5. Generated from the MPI-ESM-LR; 1989 -2014; initialised each November; 2 to 5 years lead time; 16 ensemble members; depth mean 6-220m. This was compared with the observational temperature data (red line) 1992 - 2014 for the a) NE Atlantic northwest of Ireland and 1998 - 2014 for the b) West of Ireland.

7.4 Prediction skill for West and NE Atlantic northwest of Ireland upto 2019

Having identified the key target regions further exploration into the predictability for the future was completed using the initialised hindcast simulations. The initialised hindcast simulations for both territories are extending out to 2019 in to determine what the change in temperature will be. This gives an actual value of temperature from the model that can be compared with observations. This value gives an insight to what the temperature of the region will be and how this could influence the spawning changes. Figure 7.11 shows that for the both of the locations the initialised hindcast simulations and observational simulations over estimate the observational data. The time series for the West of Ireland (Figure 7.11 a) starts at a similar value, then they diverge but they do follow the trends. When the initialised hindcast is extended out to 2019 it shows that there will be an decrease in temperature. The time series for the NE Atlantic northwest of Ireland (Figure 7.11 b) shows that between 2016 to 2019 there will be an increase in temperature. In turn we can determine that for the West of Ireland there might be a decrease in the density of eggs as the temperature exceeds the limits for development. For the NE Atlantic northwest of Ireland tory the temperature range there will be an increase in the density of eggs. As we have the observational data from the ICEs report we can determine if the initialised hindcast simulation does track the change in temperature (Figure 7.12) and the egg density (Figure 7.13).

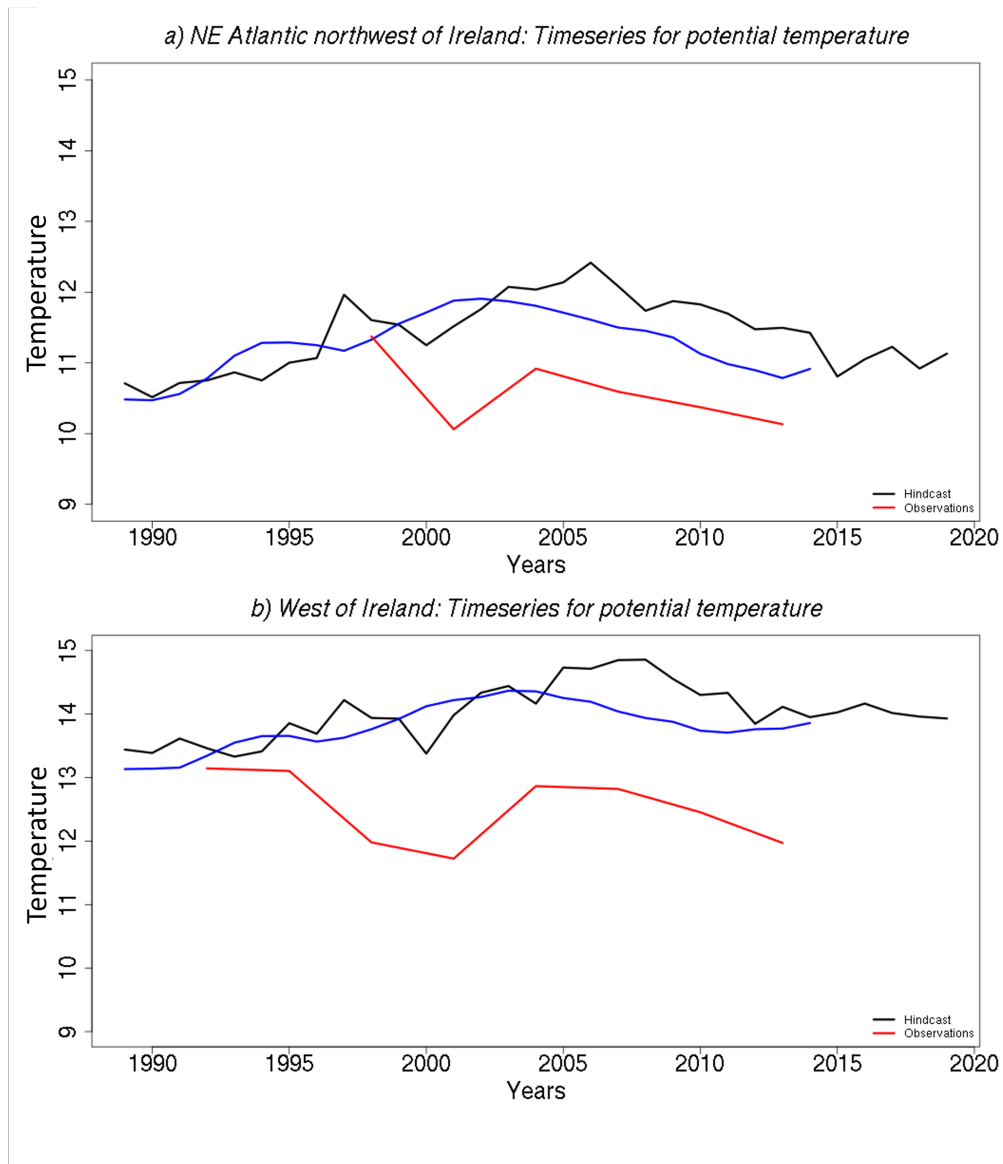


Figure 7.11: Time series for potential temperature (MPIOM) for initialised hind-cast simulation (black line) evaluated against assimilation (blue line) at lead years 2-5. Generated from the MPI-ESM-LR; 1989 -2019; initialised each November; 2 to 5 years lead time; 16 ensemble members; depth mean 6-220m. This was compared with the observational temperature data (red line) 1992 - 2014 for the a) NE Atlantic northwest of Ireland and 1998 - 2014 for the b) West of Ireland.

The results of this are highlighted in figure 7.12 with the West of Ireland being on top and the NE Atlantic northwest of Ireland being below. At the beginning of the

the time series the initialised hindcast simulation, assimilation simulation closely tracks with the observational data. Post 1995 the simulation time series divert away from the observations. When the initialised hindcast simulation is extended out to 2019 for the West of Ireland Figure 7.12 a, shows a decrease in temperature. Post 1998 the simulation time series divert away from the observations. When the initialised hindcast simulation is extended out to 2019 for the NE Atlantic northwest of Ireland Figure 7.12 b, shows an increase in temperature. This is in line with what is observed in the observational data. This means that the West of Ireland will keep at the higher range for egg development and the NE Atlantic northwest of Ireland will maintain the temperature for spawning.

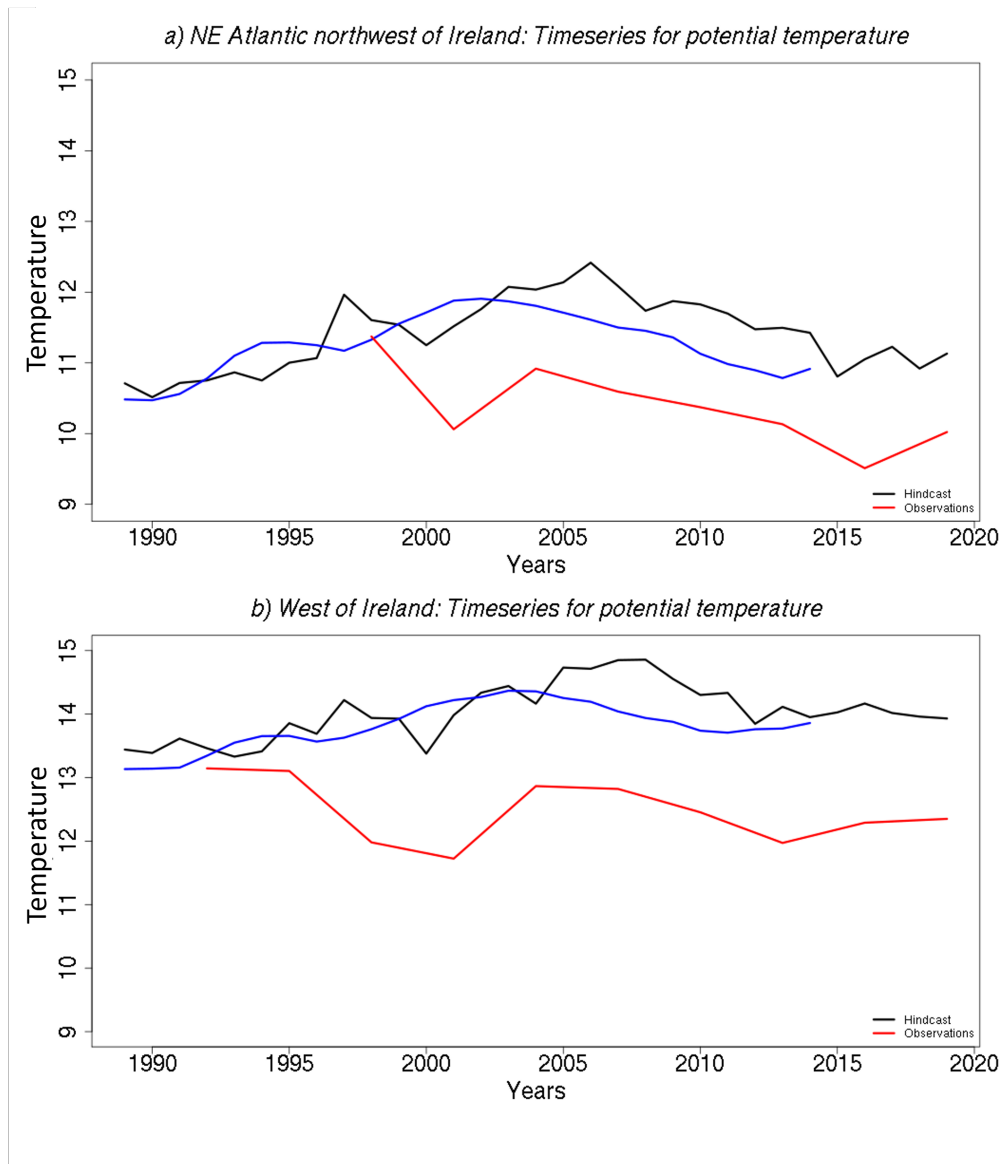


Figure 7.12: Time series for potential temperature (MPIOM) for initialised hindcast simulation evaluated against assimilation at lead years 2-5. Generated from the MPI-ESM-LR; 1991-2019; initialised each November; 2 to 5 years lead time; 16 ensemble members; depth mean 6-220m. This was compared with the observational temperature data (red line) 1992 - 2019 for the a) NE Atlantic northwest of Ireland and 1998 - 2019 for the b) West of Ireland.

Knowing the values that have been obtained from the initialised hindcast simulations in the prediction up to 2019. The next step is to determine the confidence of

these results. This was achieved by detrending the time series and calculating the uncertainties, the results can be found in Figure 7.13 for the West of Ireland and Figure 7.14 for the NE Atlantic northwest of Ireland. Figure 7.13 shows for the early years 1989-1994 and then for 2012-2019 are below zero. The years 1995-2011 is variable is mostly positive.

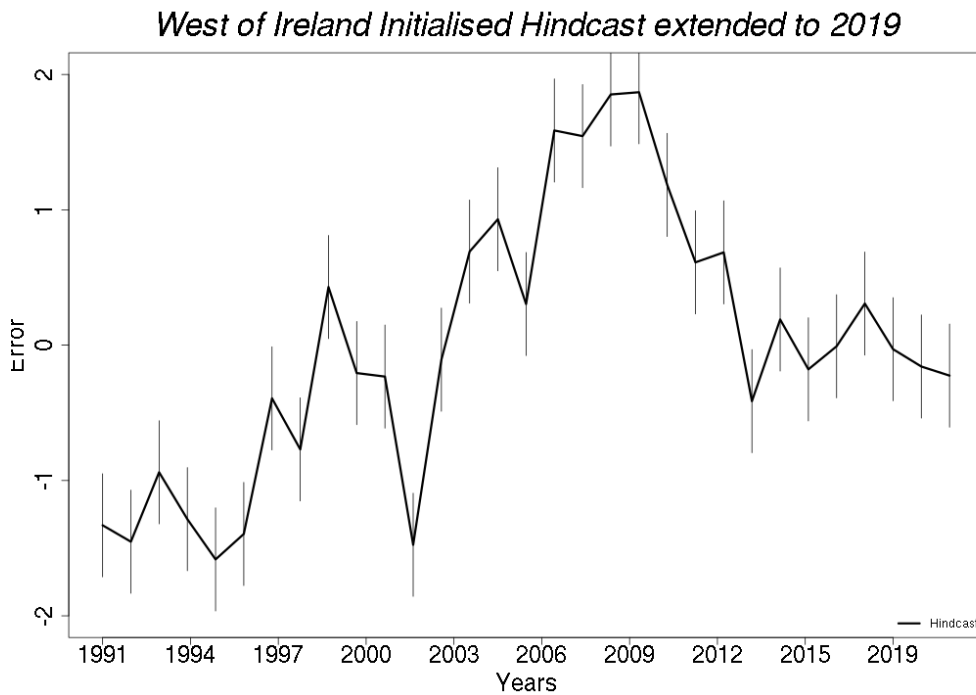


Figure 7.13: West of Ireland: Detrended time series for the initialised hindcast simulations (MPIOM) for initialised hindcast simulation evaluated against assimilation at lead years 2-5 (Red line). Generated from the MPI-ESM-LR; 1991-2019; initialised each November; 2 to 5 years lead time; 16 ensemble members; depth mean 6-220m, with error bars (Black lines).

Figure 7.14 shows for the early years 1989-1996 and then for 2012-2019 are below zero. The years 1997-2011 is variable is mostly positive.

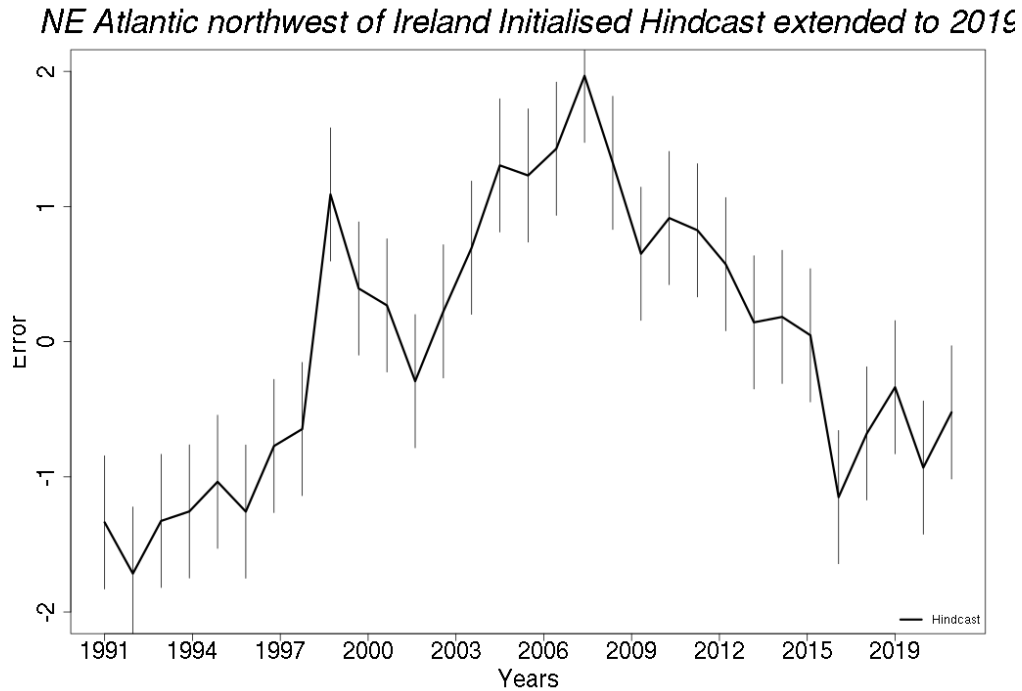


Figure 7.14: NE Atlantic northwest of Ireland: Detrended time series for the initialised hindcast simulations (MPIOM) for initialised hindcast simulation evaluated against assimilation at lead years 2-5 (Red line). Generated from the MPI-ESM-LR; 1991-2019; initialised each November; 2 to 5 years lead time; 16 ensemble members; depth mean 6-220m, with error bars(Black Lines).

From the initialised hindcast simulations, I can determine that there will be a shift northward with the Atlantic mackerel stock. As the West of Ireland temperature range is on the higher end of the scale for ideal egg development. The NE Atlantic northwest of Ireland shows warming within range of the ideal spawning grounds. Figure 7.5 shows the change in egg density for the West of Ireland (figure 7.15 a) and the NE Atlantic northwest of Ireland (Figure 7.15 b). The West of Ireland shows a decline in egg density since 1992 with the lowest amount in 2016 with a slight increase in 2019. The NE Atlantic northwest of Ireland shows very little spawning occurring in these waters up to 2013, with a spike in 2016 and a decrease in 2019. However, the amount of eggs found in 2019 in the NE Atlantic northwest of Ireland is still double the amount found in the West of Ireland for the same

year.

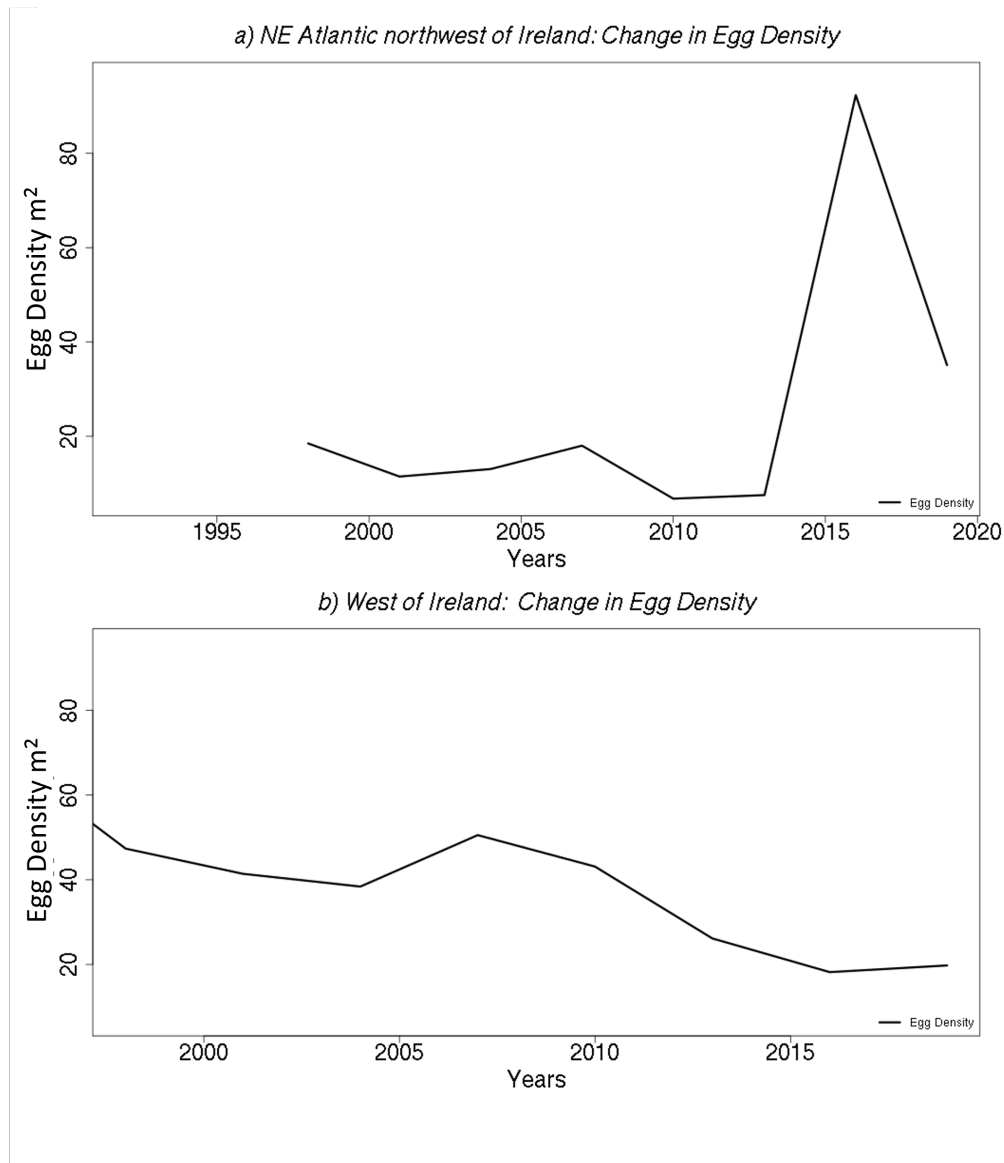


Figure 7.15: Time series for Egg Density data from the observational data from the ICES survey report for Atlantic mackerel. Plot a) shows the changes in egg density in the NE Atlantic northwest of Ireland for the time frame 1992-2019. Plot b) shows the changes in egg density in the West of Ireland for the time frame 1998-2019.

7.5 Effective communicate of scientific research

One aspect of this project is how can this information be communicated to those who do not necessarily have a background on this topic. To achieve this an info-graphic is developed that includes all the key information. How do we get from the observations to the model to the prediction and what does all of this mean? Using the information above I have compiled the main takeaway from the observations, and the predictions system found in the info-graphic (Figure 7.16). The info-graphic starts with the title (Potential Migration of Mackerel into the NE Atlantic northwest of Ireland) this sets the tone of the main message. This being the change in spawning locations from the West of Ireland to the NE Atlantic northwest of Ireland. However it does leave out any potential indication of what causes this change, with the aim of guiding the reader to go through the info-graphic to get the answer. This story was told using the the essential results and connected using arrows which show the path in which the data should be reviewed. Starting with the change in egg distribution, followed by skill of the initialised hindcast simulations in the Eastern North Atlantic, ending with if this skill can detect changes in temperature. The final message being that using initialised hindcast simulations can predict the temperature. That from this prediction, it can detect the changes in the egg distribution and density up to 2019.

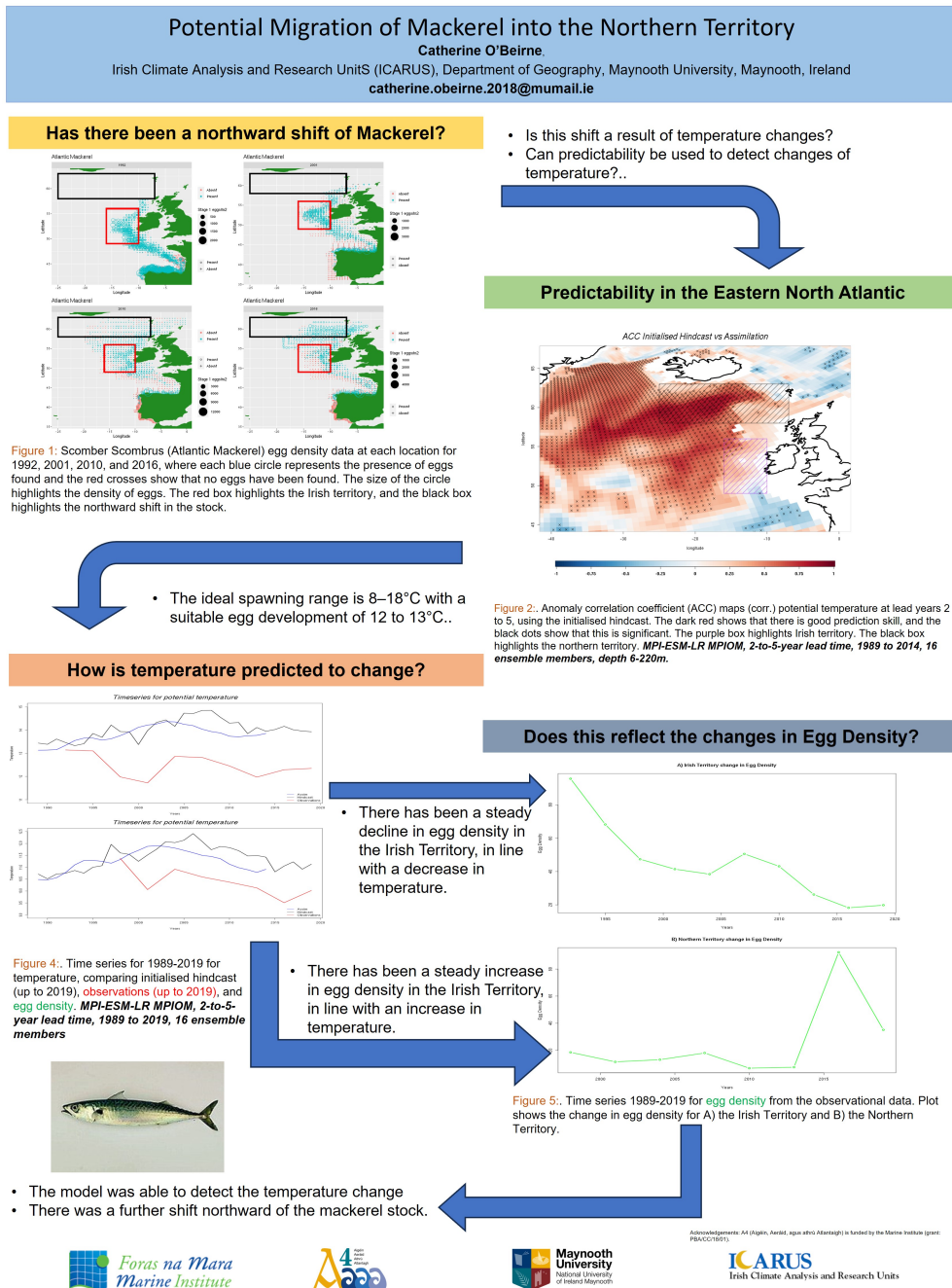


Figure 7.16: Info-graphic connecting the observational data from the ICES survey report with the model. Highlighting that the model can predict potential shifts in mackerel stock.

7.6 Discussion

This chapter demonstrated that there is a shift of the stock towards the north within the observations. One of the main driving forces for this shift is the change in temperature of the spawning grounds. What the observations tell us is that the fish stock is moving northward between each survey. That horseshoe mackerel even seems to be a decline in the numbers. While these are every three years it could be that there be some missing information in the years between. Previous chapters 4 and 6 have shown that the temperature pattern in the North Atlantic is robust within the MPI-ESM-LR. In this section, I will discuss the results from the MPI-ESM-LR can capture the temperature change and even have skill in the change of temperature which impacts the stock. I will finally discuss how this information can be put together to effectively communicate the findings with the stakeholders.

The first task was to determine if there was any change in the mackerel stock in the observations. Through plotting out the egg density and distribution changes over the years it is clear the the for both Atlantic mackerel and horseshoe mackerel has shifted. It is noted from 1998 that there is a northward shift. The observations for this data are collected every 3 years and the NE Atlantic northwest of Ireland was only recently (from 1998) included in the sampling locations. [Beare and Reid \(2002\)](#) has explored this data set from 1997-1998, to investigate the spatio-temporal change in spawning activity. The focus was the change around the West of Ireland, showing that since 1977 the fish stock has been making a northward shift. In part, they attributed this shift to the rate at which sea surface temperature increased in the spawning season. The temperature range in the West of Ireland maintains the ideal egg development temperature of 12 to 13°C ([Ibaibarriaga et al., 2007](#)). But the NE Atlantic northwest of Ireland has now become in range for as a suitable spawning site, mackerel are able to spawn at a range of temperature (8–18°C) ([Reid, 2001](#)).

Knowing that temperature is the main driving force for spawning the focus from MPI-ESM-LR was temperature from the initialised hindcast simulations. This has previously shown to good skill in the NE Atlantic northwest of Ireland and some

skill in the West of Ireland up to 2014. When this time series is extended out to 2019 through the initialised hindcast simulations, the NE Atlantic northwest of Ireland is showing that temperature will increase in the region but not as high as it was around 2019. Making this region ideal a spawning ground but not one for the development of the eggs. In contrast the West of Ireland appears to decrease in temperature back towards the higher range of temperature for egg development. What is expected that after 2014 the egg density in the NE Atlantic northwest of Ireland should see a increase in eggs and the West of Ireland see a decrease. When the egg density data is reviewed past 2014 to 2019 this is what is seen.

While there are some challenges with comparing the observational data (ICES - Mackerel and horse mackerel egg surveys (MEGS, 1992-present)) and the model (Initialised hindcast and assimilation simulations), this being in terms of the length of the time series. The ICES study is only conducted every three years and is limited to roughly the spawning season. Some inferences can be made on the time series of the temperature and the egg data, this being in the rough changes they have had over time. There is the potential to be missing some key changes in temperature or the areas where there might be a sharp increase could be connected to variability in the month in which the temperature reading was collected. One thing that could have also been changed is the methods in which the temperature was recorded or if it was recorded at all. Trying to make a yearly mean out of a few months' worth of observational data while does give insight, it can be difficult to compare to a time series that has full yearly means. While the model data has shown to be quite skillful, it too is also not perfect. This data is predicted up to 2019 using the initialised hindcast simulation on a 2 to 5 year lead time, to my knowledge this has not been conducted before. [Koul et al. \(2021\)](#) explores the skilful prediction of cod stocks using initialised hindcast simulations with lead year 1, lead year 4 and lead year 10. By completing a lead time analysis skill began to decline after lead year 5. Similarly to the work presented here it does show that it is possible to provide extended predictions that are in a usable fashion for fisheries. The final challenge will be how to effectively communicate this information to stakeholders. The info-graphic [Figure 7.16](#) has a balance of keeping the information to a generalised audience, which is difficult in some aspects with the complicated

model information. Through the use of figure descriptions is one way to get around it, and the arrows provide the questions that will explained in each plot.

Overall this sections does show that it is possible to tailor decadal predictions for stakeholder needs. Chapters 4 and 6 providing the understanding of what is predictable, can this be improved upon. At each stage of this thesis the results obtained helped guide the decision making for the following chapter. These results where summarised into an infographic that was communicated with informed stakeholders. Further discussion will be help with stakeholders to improve this infographic for a wider audience. This thesis also provides the necessary background and methodology on how decadal predictions can be useful in place of observational data.

Conclusions

8.1 Introduction

This thesis explores the tailoring of decadal temperature and salinity predictions in the Eastern North Atlantic region. In Chapter 1, I put forward four questions concerning whether it is possible to exploit the predictability of the Eastern North Atlantic to detect potential shifts northward in mackerel stock. In this chapter, I will answer these questions individually, and then conclude the findings presented. Each step will use the previous information to make informed decisions on how the approach will be in this case. Finally, I will conclude with future work.

8.2 Interactions and predictability in the Eastern North Atlantic Ocean

In Chapter 4, we explored the predictability within the Eastern North Atlantic at the surface level for both temperature and salinity from the MPI-ESM. From this model, three versions of the temperature were used, one from ECHAM6 (SST) and two from MPIOM (SST, potential temperature), and salinity. To achieve this we first determined validity in the temperature/salinity-space of the initialised hind-cast and uninitialised historical ("CMIP6", "CMIP5") simulations by comparing it to an assimilation simulation. We followed this by determining the predictability

of the two categories of simulations and determining the impact of initialisation for the variables. To get a better understanding of the origin of the predictability the physical mechanisms of the North Atlantic were explored in chapter 2, along with how these are present in the models. The decadal SST and salinity prediction skill shown in chapter 4 and an exploration of the predictability of SST and salinity at depth was discussed in chapter 5. Through these chapters, I answer the research question of this chapter:

- What are the mechanisms in the North Atlantic that influence temperature and salinity and are these predictable on a decadal timescale?

We found that there was skill from the initialisation hindcast simulations most notable for the salinity, the uninitialised historical simulations show that at the surface there was little skill. While the temperature also showed to be skillful for initialised hindcast simulation and the uninitialised historical simulations also had skill in this region. Between the two different versions of the uninitialised historical simulations, there have been improvements. The CMIP5 simulations show that in the subpolar region, there is little skill. Compared to the CMIP6 counterpart this region now shows to have significant prediction skill. Through this analysis, the second section of the question has been answered. Both temperature and salinity are found to be predictable at a 2 to 5 year lead time.

8.3 Investigation into improving prediction skills for the North Atlantic Ocean

The main aim of this section is to explore the possibility of improvement of prediction skill for three target areas that have little skill in the North Atlantic. The initialised hindcast simulation shows to have the most promise in this region in terms of skill for SST and salinity. Moving forward temperature and salinity were analysed using the initialised hindcast and utilising two predictors (SPG and AMV). In this approach a grouped depth mean was obtained (6-220m) to determine if this could also aid in answering the question;

- Can the skill in the North Atlantic be improved upon using the sub-sampling method?

The initial investigation conducted in Chapter 4 shows that there was prediction skill in the Eastern North Atlantic Ocean for SST and salinity. In Chapter 6, the first step in the improvement of skill was to see if expanding the depth profile could be beneficial. Using the initialised hindcast simulations a mean of temperature and salinity was obtained over 6m to 220m for the Eastern North Atlantic. It is evident that this grouped mean (6-220m) figure 5.8 (a, c) has improvement in skill compared to just looking at the SST figure 4.1, most notably along the shelf edge. The second step is to determine how correlated (against the assimilation simulation) the predictors are. The AMV is highly correlated in the Eastern North Atlantic and the SPG is highly correlated in the Norwegian Sea. However, there are still regions that have little skill with the initialised hindcast simulations this is where the predictors (AMV, SPG) come in. For two of the locations, the sub-sampling of the AMV shows to improve the skill for temperature and the three locations for salinity. While the sub-sampled SPG only showed improvement in one of the locations for temperature and showed no improvement for salinity. Depending on the region, sub-sampling can be of benefit to improve prediction skill, when the right predictors are chosen. The AMV has proven beneficial for most of the region while SPG had its limits to the Northern NEA. While in the target sub-sample sites there was an improvement in skill, they do not represent the fishery industry sites. Moving forward it would be more beneficial to use the grouped mean of the initialised hindcast simulations with the grouped depth mean compared to the predictors.

8.4 Application of tailored decadal predictions for Irish Fisheries

While both temperature and salinity are important factors for the spawning of Mackerel, the change rate of temperature is felt more immediately than salinity. Chapter 7 aims to determine if there may be a shift in Mackerel stock due to the temperature change and can the MPI-ESM-LR detect this change. Working in

conjunction with the Marine Institute Climefish project, observational data from the ICE's survey was obtained for both species of mackerel. Henceforth referred to as the observational data. Using the skill of initialised hindcast simulations of SST from Chapter 6 we aim to answer the following question;

- Can the prediction skill in the Eastern North Atlantic Ocean be tailored to stakeholder needs?

The ACC plot of the initialised hindcast (Figure 6.6) shows that for the West of Ireland there is some skill in this region but it is not significant. Similarly the same can be said for the NE Atlantic northwest of Ireland where the ACC of the initialised hindcast (Figure 6.6) shows to have skill and that this is significant. Meaning that there is not as much confidence in the West of Ireland results compared to the NE Atlantic northwest of Ireland. They aid in showing what is possible for areas where the skill is significantly better.

From the observational data stage 1 egg data showed that there was a northward shift in the mackerel stock in the mid-2000s to 2014. Within the MPI-ESM-LR on the 1989-2014 time frame, the initialised hindcast simulation for temperature there is good skill in the northward section and skill around Ireland. The focus is on the northward section a time series analysis of this area was conducted from 1989 - 2014 and then projected up to the year 2019. When compared with the observational egg data the initialised hindcast simulation follows the temperature trend yet overestimates the value in the West of Ireland. What this means is that for the West of Ireland, the initialised hindcast simulation can detect the temperature change and that there should be an increase in the egg density. The NE Atlantic northwest of Ireland is predicted to increase in temperature post-2014, this is in line with what is seen in the observational temperature data. What this means is that there is the possibility of seeing an increase in the egg distribution in the area, this was seen in 2016 when there was an increase in egg density. In 2019 the egg density was almost half what was seen previously in the NE Atlantic northwest of Ireland, that same year in the West of Ireland the egg density was almost half.

This has answered the question of whether the prediction skill in the Eastern Atlantic Ocean can be tailored, in this case, to detect changes in the Mackerel stock.

8.5 Effective communication of scientific research

Finding an effective way to communicate research to a wide target audience is not always the easiest of tasks for scientists. Focusing on developing these skills is now becoming an integral aspect within universities. There are a variety of ways in which scientific information is communicated, the main form is through presentations. Other mediums are posters, papers, info-graphics, and community meetings. While mostly these are within the specific target audience having the ability to tailor these to suit the knowledge level of all attendees is difficult. Finding the best way to communicate what the predictions mean with their implications led me to ask;

- How can this information relate to the fisheries and be communicated effectively?

Knowing that the model can catch the change in temperature in both the West of Ireland and the NE Atlantic northwest of Ireland and that this matches with the observations found in the regions. How can this complex topic be simply but effectively communicated with the stakeholders? A presentation would be too detailed, while an info-graphic allows for the information to be condensed to highlight the main points of the research. The main talking point from the research that needs to be conveyed to the stakeholders is that there is a shift northward in the stock. In both the initialised hindcast simulations and the observations up to 2019. The info-graphic mainly contains plots of these results, starting with observation, moving to the predictability in the model (2014) to the predicted (2019). The idea of this was to show that this northward shift has been evident in the observation and the initialised hindcast simulations. Building confidence in the prediction up to 2019 that shows the same shift in the optimal range of

temperature for egg development. The plots contain explanations of what the viewer is looking at with arrows guiding them to the next part of the story.

8.6 Overall Conclusions

By breaking it down into these topics we get an understanding of the physical mechanisms that occur in this region and how they influence each other in the real world. This aids in the understanding of how the variables can be predictable within the model. Once a determination on the predictability for the region has been identified, sub-sampling can be applied to improve prediction skill in areas with low skill. The next stage of the process is the connection to the stakeholders. In this case, stage 1 mackerel egg data was analysed. Using the stage 1 egg information we can track the change over the years in both density and distribution. While there was temperature and salinity data from the ships, it is very inconsistent. From the observational data, the Irish fishing grounds and the NE Atlantic northwest of Ireland were identified. These regions were then explored in the model environment. The final stage of this work is to communicate the model information in a useful and applicable way. In conclusion, this thesis has demonstrated the chain from the prediction of climatological factors towards the application towards the fishing industry and the scientific communication of the results towards the stakeholders. I will finish on how this work can be furthered.

8.7 Limitations

While the focus of this research was the application of tailored decadal predictions, this mainly focused on the modelled produced data. The observational data that was obtained was limited to the ICES data from the Marine Institute. This data is triannual, with any temperature or salinity data not completely compatible with the model data. This work does attempt to breach these gaps between the observed and modelled world. The work conducted in Chapter 4 used the modelled-based observations (assimilation simulation), this could indirectly cause a bias in the results.

Further investigation into sub-sampling (Chapter 6) could aid in the improvement of skill in the West of Ireland. There could be greater inclusion of the biological

components with these statistical components moving forward. This will allow for greater insight into what could be causing this shift northward. It can not be ignored that the human element could also have a negative impact on the survival of the stock. Incorporation of other types of models and using observational data instead of assimilation.

8.8 Thesis Contributions

The work that has been conducted throughout this thesis has several contributions, of which some will be published. The first is the changes in skill between the initialised hindcast versus uninitialised historical simulations moving from CMIP5 to CMIP6 versions of models. This was explored in Chapters 4 and in 5, with the latter being prepared for resubmission. That these simulations can also be explored on a regional scale, with a degree of confidence in the skill.

The approach in this thesis was from the statistical analysis of a prediction system on a singular variable. The work conducted in Chapter 7, is in preparation for a paper in conjunction with the marine institute. Using the MPI-ESM-LR initialised hindcast simulations for temperature shows great promise in the shift of mackerel northward. This is still a great leap forward as previous study that explored the spawning distribution of blue whiting mainly focused on monthly data (Miesner and Payne, 2018). This study could bridge the gap between the seasonal predictions into the decadal predictions as a tool to inform fish stock management decisions.

8.9 Future Work

Fish stock management must not just consider the human aspect but also the environmental and ecological influences that impact fish catch and their sustainability. The human aspect is having a massive impact on the number of fish within the oceans with several tonnes of fish being removed each year. A lot more needs to be done in terms of policy to protect what remains in the ocean and a new system other than quotas needs to be put in place as their application is not sufficient. However, what needs to be taken into consideration is that the policies will impact greater, the smaller community fisheries which may not be able to compete with

larger corporations. This may lead to the loss of local knowledge and traditional fishing practices, which are usually far more sustainable than mass commercial fishing. What is also needed to make informed decisions is the availability of quality data with long records. These records can be obtained from fishing vessels that routinely track sea temperature and to an extent salinity. From here it is clear that there is a need for a link between the fisheries and scientists who can use this data to develop models that could be used to predict potential changes in environmental factors. Which in turn influences the effectiveness of spawning and density distribution in either a positive manner or negative depending on the accuracy of the models. Understanding the mechanisms involved there is the hope that we will gain great insight into the change in the density and distribution of species. It is clear that by understanding the environmental and ecological factors they have the greatest impact on the fish species at the larval stage. It should be noted that this is also the stage in which the larval fish are under the greatest threat from predation. It would stand to reason that this is the key stage at which the fish should be protected or maintained; this could be using the process known as fish farming. This is usually an inland process where fish species are matured in a controlled environment allowing for maximum yield of adults without any risk of predation (Silver and Hawkins, 2017). However, this process is still highly contested, over the benefits, cost, and its future (Silver and Hawkins, 2017). As it stands there is no clear answer on how to improve the sustainability of fish stocks without a drastic overhaul of the fishing industry itself.

One clear thing is that there is great potential on this topic whether it is on the side of natural or political science. On the natural science side, the identification of the key drivers and habitable zones associated with fish productivity could be used to develop models that can predict potential changes in the density and distribution of the fish species. To achieve this access to earth system models and larval data is needed, which would require cooperation with the relevant bodies. This will allow to get an insight into the potential predictability of important species for the Irish fisheries sector and with it the possibility of improving the current fish stock management systems in Ireland. The application for such research would allow countries such as Ireland to develop a climate service that could revolutionise the

sector.

On the political side, there is a need for an in-depth analysis of all the current policies in place and at what level they are currently having the most impact. It would identify where there is a possibility for change in these policies and find out where they are falling short. The natural science side must translate the scientific information across to those who would not be familiar with models and the uncertainty that surrounds them. This would then allow for decisions about fish stock management to be made with the highest quality information available.

APPENDIX **A**

Appendix



This form is to accompany the submission of a PhD that contains research reported in published or unpublished work. **Please include one copy of this form for each co-authored work.** This form along with the published work should, under normal circumstances, appear in an Appendix.

Authorship Declaration Form

Publication Details:

Thesis Chapter/Pages	Chapter 4
Publication title	Decadal Prediction along the Western Irish Coast
Publication status	Submitted (Under Review/Preprint)
Type of publication	Journal Article
Publication citation	Catherine O'Beirne, Sebastian Brune, Gerard D. McCarthy et al. Decadal Prediction along the Western Irish Coast, 21 July 2023, PREPRINT (Version 1) available at Research Square [https://doi.org/10.21203/rs.3.rs-3177972/v1]

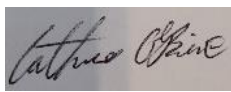

Nature/extent of my contribution to the work detailed above is as follows:



Nature/Extent of Contribution	Lead author
For this paper, I aided in the concept and design, carried out the analysis of the simulation data and the writing of the paper.	<input checked="" type="checkbox"/> Yes <input type="checkbox"/> No

The following co-authors contributed to the work (all contributing co-authors):

Name	Nature of contribution
Sebastian Brune	Provision of model data, proof reading, edits to the original text
Gerard D. McCarthy	Concept and design, proof reading, edits to the original text
André Düsterhus	Concept and design, proof reading, edits to the original text

The undersigned hereby certify that the above declaration correctly reflects the nature and extent of the student's and co-author's contribution to this work

	Name	Signature	Date
Student	Catherine O'Beirne		2024/02/08
Co-author 1	Sebastian Brune		2023/10/21

Co-author 2	Gerard D. McCarthy		8/2/2024
Co-author 3	André Düsterhus		2023/10/22

Decadal Prediction along the Western Irish Coast

Catherine O’Beirne^{1*}, Sebastian Brune², Gerard D. McCarthy¹ and André Düsterhus¹

^{1*}Irish Climate Analysis and Research UnitS (ICARUS),
Department of Geography, Maynooth University, Maynooth,
Ireland.

²Institute of Oceanography, Center for Earth System Research
and Sustainability, Universität Hamburg, Hamburg, Germany.

*Corresponding author(s). E-mail(s):

catherine.obeirne.2018@mumail.ie;

Contributing authors: ; ; ;

Abstract

This study investigates the predictability within the North Eastern Atlantic at depth with an initialised decadal prediction system. For both temperature and salinity at the West Coast of Ireland are compared for 2-to-5-years ahead in a 16-member initialised decadal prediction system and in two 16-member uninitialised historical simulations from the Max Planck Institute Earth system model for the time period 1966-2013. We find that there is predictability in the upper levels of the North Eastern Atlantic up to a depth of 1000m for temperature and salinity. For the same time period we analyse water mass properties and prediction skill along three transects (Extended Ellett line, Porcupine Bank, Goban Spur). Along these transects, we find (1) that there is multi-year memory in the water mass properties of the initialised predictions, (2) that prediction skill depends on variable, depth, and external forcing scheme, (3) that improvements in prediction skill in the initialised system over the uninitialised simulations are mostly in the upper ocean above 300m depth and in the deep ocean below 1500m depth, and (4) that these improvements are more pronounced in salinity than temperature.

Keywords: Decadal Prediction, Earth System Model, North Eastern Atlantic, Potential Temperature, Salinity

001
002
003
004
005
006
007
008
009
010
011
012
013
014
015
016
017
018
019
020
021
022
023
024
025
026
027
028
029
030
031
032
033
034
035
036
037
038
039
040
041
042
043
044
045
046

047 **1 Introduction**

048

049 The North Atlantic is an extensively studied region in terms of the processes
050 involved within the ocean and how they interact with the atmosphere. Studies
051 have shown that both atmospheric (North Atlantic Oscillation) and oceanic
052 processes (sub-polar gyre) can be replicated within models in both initialised
053 hindcast simulations and uninitialised historical simulations ([Andrews et al, 2015](#);
054 [Athanasiadis et al, 2017](#); [Barcikowska et al, 2018](#); [Koul et al, 2019](#)).
055 However, there is limited research completed on the predictability for potential
056 temperature and salinity at depth, both on a global and a regional scale just for
057 the ocean. By having the ability to predict changes in climate variables such as
058 temperature and salinity for a target region, informed decisions can be made
059 about environmental and economic conditions. [Koul et al \(2019\)](#) demonstrated
060 that uninitialised historical simulations with the Max Planck Institute Earth
061 system model (MPI-ESM) as part of the Coupled Model Intercomparison
062 Project Phase 5 (CMIP5, [Taylor et al, 2012](#)), are well representing large scale
063 ocean dynamics and atmosphere-ocean interaction. The simulations used in
064 [Koul et al \(2019\)](#) form the first part of the Max Planck Institute Grand Ensem-
065 ble ([Maher et al, 2019](#)). [Koul et al \(2019\)](#) examined subsurface salinity on
066 three sections in the North Eastern Atlantic (Rockall Trough, Faroe-Scotland
067 Channel, and North Sea entrance), and showed that in their uninitialised his-
068 torical simulations atmospheric variability eventually influences the evolution
069 of North Sea salinity.

070

071 Previous work that was conducted on the North Eastern Atlantic was
072 focused on the Rockall Trough and in particular the Extended Ellett line. We
073 will use the full length and depth of the Extended Ellett line, which will act
074 as our most northwest section. Porcupine Bank west, and Goban Spur south-
075 west make up two other sections along the west coast of Ireland as seen in
076 figure 1. All three sections lie on parts of the continental shelf off the west
077 coast of Ireland, with the Porcupine bank and Goban Spur heading out to
078 the open ocean. All three sections are influenced by both the North Atlantic
079 Ocean and different water masses. The Extended Ellett line is a multidecadal
080 hydrographic transect that is an extension of the Ellett line that is located
081 between Scotland and Iceland. It runs through the Rockall Trough, Hatton-
082 Rockall basin, and Iceland basin ([Holliday et al, 2015](#); [Humphreys et al, 2016](#);
083 [Jones et al, 2018](#)). The Porcupine Bank has surface salinities that are about
084 0.05 PSU less than surface values of that in deeper water either side ([White,](#)
085 [1997](#); [O'Reilly et al, 2022](#)). Goban Spur is a submarine plateau 250km that
086 extends away south-west of Ireland in the southwestern Celtic Sea, and into
087 the deeper ocean ([Dingle and Scrutton, 1979](#); [de Graciansky and Poag, 1985](#);
088 [Huthnance et al, 2001](#); [Moritz et al, 2021](#)). The Extended Ellett line captures
089 the flow of warm, salty water from the North Atlantic into the Nordic Seas
090 and half of the returning deep, cold overflow current ([Humphreys et al, 2016](#)).
091 In turn the Rockall Trough supplies warm and saline water to the Nordic
092 Seas, where it is transformed into fresh southward flowing deep water ([Hol-
liday et al, 2020](#)). There are several water masses that circulate around the

Porcupine Bank and Goban Spur that influence both temperature and salinity 093
along the shelf. The main water masses that influence both are North Eastern 094
Atlantic Water, and Mediterranean Outflow Water (MOW) moving the high 095
saline water mass northward and then returning as denser water southward 096
([Huthnance et al, 2001](#); [O'Reilly et al, 2022](#)). Lower Deep Water is thought to 097
circulate cyclonically around Goban Spur, Porcupine Bank and the entrance 098
to Rockall Trough ([Huthnance et al, 2001](#)). 099

Large-scale atmosphere-ocean feedback that occurs in North Atlantic 100
Ocean gives the ability to improve decadal predictability ([Koul et al, 2020](#); 101
[Borchert et al, 2021](#)). Some studies suggest that the predictability improves on 102
scales of 2-8 years and others for even up to 10 years into the future ([Borchert 103
et al, 2018, 2019](#); [Brune and Baehr, 2020](#)). The leading cause of inter-annual 104
to decadal variability in salinity is linked with the variability in the sub-polar 105
gyre ([Koul et al, 2020](#)), one of the regions in the North Atlantic that showed 106
skill improvement with initialisation in CMIP5 ([Borchert et al, 2021](#)). 107

To expand on prediction in the North Eastern Atlantic, the uninitialised 108
historical simulations from both CMIP5 and CMIP phase 6 (CMIP6, [Eyring 109
et al, 2016](#)) from MPI-ESM will be explored, as well as initialised decadal 110
predictions. We will explore the predictability on a 2-5-year lead time. For this 111
we analyse potential temperature and salinity at depth along the Irish coast 112
for the Extended Ellett line, Porcupine Bank, and Goban Spur. The aim is to 113
demonstrate the capability of a state-of-the-art decadal prediction system to 114
predict the waters on the West of Ireland. 115

2 Simulations and methods 117

For this study we analysed simulations with the Max Planck Institute Earth 118
system model ([Giorgetta et al, 2013](#); [Mauritsen et al, 2019](#)) in its low-resolution 119
setup (MPI-ESM-LR) for the time period 1961-2013. In MPI-ESM-LR, the 120
oceanic component (MPIOM, [Jungclaus et al, 2013](#)) is setup with a nominal 121
horizontal resolution of 1.5° globally, actually corresponding to $\approx 1^\circ$ in the 122
North Eastern Atlantic, and 40 levels vertically. The atmospheric component 123
(ECHAM6, [Stevens et al, 2013](#)) is configured with a spectral resolution T63, 124
corresponding to $\approx 1.9^\circ$ horizontal resolution globally, and 47 levels in the ver- 125
tical. 126

We use a weakly coupled assimilation with MPI-ESM-LR ([Hövel et al, 2022](#); 128
[Brune and Baehr, 2020](#)), which covers the time period 1958-2019, both as a 129
reference and for the initialisation of predictions. Oceanic temperature and 130
salinity profiles from EN4 ([Good et al, 2013](#)) are assimilated monthly with a 131
16-member oceanic ensemble Kalman filter ([Brune et al, 2015](#); [Polkova et al, 132
2019](#)) using the Parallel Data Assimilation Framework (PDAF, [Nerger and 133
Hiller, 2013](#)). Simultaneously, monthly mean atmospheric temperature, vortic- 134
ity, divergence (all only above 900hPa), and sea level pressure from ERA40 135
([Uppala et al, 2005](#)), ERA-Interim ([Dee et al, 2011](#)), and ERA5 ([Hersbach 136
et al, 2020](#)) are nudged into ECHAM6. CMIP6 external forcing ([Eyring et al, 137](#)

138

139 2016) is applied throughout the whole assimilation, with historical forcing until
140 2014, and scenario forcing SSP2-45 thereafter.

141 For the purpose of our study, we use a 16-member ensemble of initialised
142 predictions ("hindcasts") that have been started November 1st each year ini-
143 tialised between 1961-2008 from the assimilation with a 2-to-5-year lead time
144 (Hövel et al, 2022). Thus our analysis time period is between 1966 and 2013.
145 Similar to the assimilation, CMIP6 external forcing is applied to these hind-
146 casts correspondingly.

147 Uninitialised simulations with MPI-ESM-LR have been part of both CMIP5
148 (Taylor et al, 2012) and CMIP6 (Eyring et al, 2016) model intercomparisons.
149 In this study, we use the first 16 members of the CMIP5 MPI Grand Ensem-
150 ble (Maher et al, 2019), with CMIP5 historical external forcing until 2005,
151 and CMIP5 scenario RCP4.5 external forcing starting with 2006. We also use
152 the first 16 members of the CMIP6 MPI Grand Ensemble (Olonscheck et al,
153 2023), with the same CMIP6 external forcing as in assimilation and hindcasts.
154 We analyse the hindcasts and both uninitialised simulations ("CMIP5",
155 "CMIP6") for both potential temperature and salinity at depth. Annual mean
156 values of model output variables are computed and then used to generate a
157 2-to-5-year lead year time series for each member. For all simulations we com-
158 pute the 16-member ensemble mean.

159 For the comparison of the simulations a detrended anomaly correlation coeffi-
160 cient (ACC) is estimated, with reference to the assimilation. We also calculate
161 the differences of the resulting ACCs between the hindcasts and the unini-
162 tialised simulations. Uncertainty is estimated by a bootstrapping of 500
163 repetitions and a significance level of 5% (Wang et al, 2014). The same
164 approach is used for estimating the skill along the transects.

165

166 **3 Results**

167

168 **3.1 Predictability of temperature and salinity in the** 169 **North Eastern Atlantic**

170

171 We first investigate surface predictability of potential temperature and salin-
172 ity within the MPI-ESM on a lead time of 2-to-5-years for the North Eastern
173 Atlantic. The ACC is used to assess skill in both potential temperature and
174 salinity for uninitialised historical and initialised hindcast simulations of the
175 MPI-ESM-LR. Then the initialised hindcast simulations are compared with
176 the uninitialised historical simulations (CMIP6) to determine if there was any
177 improvement in skill due the initialisation. Initialised hindcast simulations
178 for potential temperature (Figure 2a) demonstrate that the North Eastern
179 Atlantic shows to have good predictability apart from a small area of low pre-
180 dictability southwest of Ireland. The salinity results (Figure 2c) show that for
181 the initialised hindcast simulation the predictability has an improvement over
182 that of the potential temperature. Comparing the initialised hindcast predic-
183 tion with the uninitialised historical simulation for the potential temperature
184 (figure 2b) highlights that there are advantages for the initialised prediction

for the open ocean, while the uninitialised simulation performs better over the continental shelf close to the Irish coast. In contrast, for salinity (figure 2d) the initialisation provides better predictability for both the open ocean and the continental shelf around the Irish coast.

A common approach for predictions at depth is to calculate a mean over a group of target depths. In this study we take an alternative approach and analyse predictability for three sections off the Irish coast: Extended Ellet Line (EEL), Porcupine Bank (PB), and Goban Spur (GS). The three sections are highlighted in figure 2, together with the surface prediction skill at each of the locations. Overall there is predictability (using the assimilation as reference) in both temperature and salinity along the West of Ireland as seen in figure 2, this can give an insight to what we could expect to see in the transects. In a next step we investigate the three transects at depth.

3.2 Water Mass Analysis in the model along the three transects

The temperature-salinity diagram (figure 3) highlights that the initialised hindcast simulations differ from the uninitialised simulations. These initialised hindcasts are closer to the assimilation than uninitialised historical simulations for all three transects. However, the CMIP5 and CMIP6 simulations show that they are potentially picking up the MOW and Labrador Sea water movements at the transect of the PB (figure 3h,k) and the GS (figure 3i,l). The uninitialised historical simulations show a more chaotic pattern in the upper ocean. While assimilation and initialised hindcast simulations are not identical, they do show that at the surface the water potential temperatures are higher and more saline compared to lower depths. The salinity range is confined to a particular range for the assimilation and hindcast simulations, but for the uninitialised ("CMIP5", "CMIP6") simulations the range is much larger. From figure 3 we observe that it is clear that the long-term memory could be assigned to water masses in the area and this can be potentially beneficial to the initialised hindcast simulations for increasing the prediction skill.

3.3 Predictability of Potential Temperature along the three transects

Building on the water mass analysis and the predictability of the surface we investigate whether the model can reproduce the potential temperature values in the regions. We know that temperatures will decrease towards the north and west. Near 49°N the temperatures can reach about 16°C at the surface. At depth the values range in winter from 10-11°C to up to about 700 m. Below that they decrease steadily to below 4°C at 2000 m (Huthnance et al, 2001). The closest section that is at this slope is that of the GS. We expect that while the water moves north- and westward (away from the slope) the potential temperature will decrease.

231 To estimate the capability of the model, we compare the absolute values of
232 the potential temperature from the assimilation simulation, which by design
233 is the closest to the observations, with the uninitialised historical ("CMIP5",
234 "CMIP6") and initialised hindcast simulations. The results of the three sections
235 are illustrated in figure 4. In the first column is the EEL (figure 4a,d,g,j), in
236 the second column the PB (figure 4b,e,h,k) and the last column the GS (figure
237 4c,f,i,l). Overall results show that the model is within the limits of values that
238 have been observed for the regions, that as water is moving northward there is
239 a decrease in temperature. Across the three transects the hindcast simulations
240 are almost identical with the assimilation simulations with the upper ocean
241 showing a warmer temperature. Both the uninitialised historical ("CMIP5",
242 "CMIP6") simulations overestimate potential temperature by approximately
243 1.5 degrees Celsius above the assimilation for the EEL. At PB, all the simu-
244 lations appear to be within 0.5 degrees Celsius of the assimilation. Similarly,
245 the same is true for the GS section except that the CMIP5 results are approxi-
246 mately 2 degrees warmer compared to the other results for this section. It is the
247 possibility that uninitialised historical simulations could be overestimating the
248 potential temperature for these regions. Due to their initialisation, the hind-
249 cast are slightly more accurate than the uninitialised historical simulations.
250 Following on from this, we want to determine if there is any improvement on
251 prediction skill between the two simulations because of this initialisation.

252 In a next step we analyse the predictability for the three transects, at the
253 EEL (figure 5a,d,g), the PB (figure 5b,e,h), and the GS (figure 5c,f,i). A com-
254 mon theme for the initialised hindcast simulation for the three transects is the
255 predictability at depth. Starting with the EEL (figure 5a) there is a region
256 of lower predictability in the depth of about 1200 m. Above this level and in
257 the Iceland basin also partly below this level, the predictability is high. In the
258 CMIP6 simulation (figure 5d), we find high predictability only in the upper
259 1000 m, with even higher values than in the initialised simulation (figure 5g). At
260 the PB, the initialised simulations (figure 5b) show a clear region of predictabil-
261 ity for the upper 300 to 400 m, and below 1500 m. In between these depths,
262 the predictability is lower. In the uninitialised CMIP6 simulations (figure 5e)
263 the main areas of high predictability can be found just below the surface layer.
264 Consequently, comparing the two simulations (figure 5h) shows that initialisa-
265 tion is mainly beneficial for the surface layer and the depth. For the GS (figure
266 5c), the initialised simulations show consistently high predictability for most
267 depths, while in the the uninitialised CMIP6 simulation high predictability is
268 confined to the upper 1400 m only (figure 5f). Consequently, initialisation is
269 beneficial to a higher prediction skill below 1400 m (figure 5i).

270 When we investigate the uninitialised CMIP5 simulations (figure 6) we see
271 that their results are generally similar to the uninitialised CMIP6 simulations
272 (figure 5). The main difference is that the upper layer of predictability for
273 the PB and the GS (figure 6b,c) is extending deeper, but with smaller values.
274 Compared to the initialised simulation again the initialised hindcast dominate

275
276

in the depth, while in the upper layers an inconsistent picture emerged (figure 277
6d,e,f). 278

3.4 Predictability Sea Water Salinity along the three 280 transects 281

We investigate whether the model could reproduce the salinity values that 283
occur in these regions. We expect that the water at the most southern transect 284
(GS) will be the most saline of the three transects. Salinity should be reducing 285
when the water moves further north through the PB towards the EEL. 286

What the salinity values (figure 7) show that as the water moves north- 287
ward, it does become slightly less saline for assimilation, initialised hindcast 288
and uninitialised historical (CMIP5/6) simulations. The hindcast simulations 289
(figure 7d,e,f) for the three sections are the ones that are for salinity almost 290
identical to the assimilation simulations (figure 7a,b,c). For the EEL the 291
CMIP5 (figure 7g) and CMIP6 (figure 7j) simulation also closely replicate the 292
assimilation with the lowest depths being a bit fresher. This also follows for PB 293
transect where it is fresher at lower levels but a broader saline range. Goban 294
CMIP5 (figure 7i) and CMIP6 (figure 7l) results show a more saline region in 295
the upper ocean. In contrast to the initialised simulations which have a high 296
saline depth of roughly less than 1000 m, both of the uninitialised historical 297
simulations extended to a depth of about 1300 m. The initialised hindcasts 298
are highly saline to the west at the surface, for the uninitialised historical 299
simulations show this area to be a fresher region. 300

Similar to the potential temperature, the salinity values are compared for 301
the initialised hindcasts, the CMIP6 (figure 8) and CMIP5 (figure 9) simula- 302
tions. The initialised hindcasts for the three transects (EEL, PB, GS) (figure 303
8a,b,c) highlight that there is skill at most depth levels. Initialised hindcasts 304
for EEL (figure 8a) show a region with little or low skill at a depth of about 305
1200 m, but beside that they demonstrate a consistent high predictability 306
along the depth range. In contrast to this the uninitialised CMIP6 simulation 307
has little skill in the surface layer and at depth (figure 8d). Comparing the 308
two simulations shows (figure 8g) that the initialised hindcasts perform bet- 309
ter in the upper couple of hundred metres and in the deeper depths. Along 310
the PB (figure 8b) the initialised hindcasts have significant skill for the major- 311
ity of the transect except for its central part. The same transect within the 312
CMIP6 simulation (figure 8e) shows two bands with high prediction skill in the 313
upper layers. The difference (figure 8h) between the initialised hindcast and the 314
CMIP6 simulation illustrates that initialisation out-performs the uninitialised 315
simulations everywhere apart from the two distinct bands. For the GS (figure 316
8c) there is high predictability over all depth in the initialised prediction. In 317
contrast, the CMIP6 results for the GS (figure 8f) shows low predictability in 318
the surface layer, and at a depth of about 1400 m. In the comparison (figure 319
8i) we see that the initialisation benefits prediction skill in these two layers. 320

Figure (9a,b,c) shows the ACC results for the CMIP5 simulation along the 321
three transects. There is very little skill at the surface, but high skill at depths 322

323 down toward 1400 m. In comparison with the initialised hindcasts at the EEL
324 (figure 9d), the main increase in skill due to initialisation can be found in the
325 depth and at the surface. For the PB (figure 9e) and the GS (figure 9f) we
326 find a similar result. In general it can be said that between the CMIP5 and
327 CMIP6 simulation the general pattern of skill improvement by initialisation is
328 comparable, but in the details it shows considerable differences. Especially it
329 shows that the CMIP5 simulation has much less consistent skill in that area
330 than the CMIP6.

331

332 4 Discussion

333

334 The main aim for the study is to determine if the predictability seen for surface
335 variables in the North Atlantic can be replicated for potential temperature
336 and salinity in the North Eastern Atlantic at depth. Using two uninitialised
337 historical simulations and one set of initialised hindcast simulations we have
338 assessed the predictability at depth for the three transects (EEL, PB, and GS)
339 using MPI-ESM. We show that there is predictability on a 2-5-year lead time
340 in the North Eastern Atlantic for potential temperature and salinity.

341 Prediction of North Atlantic potential temperature and salinity can be
342 improved with initialisation as in some areas the initialised hindcast out-
343 perform the CMIP5/CMIP6 simulations. This can be seen in the comparison
344 plots between the initialised hindcast and uninitialised historical simulations
345 for both temperature and salinity along the three transects. Three areas of
346 importance were identified as Extended Ellett line in the north, the Porcupine
347 Bank transect in the west, and Goban Spur to the south along the Irish coast.
348 The last row of plots on figures 5 and 6 show that for temperature the main
349 improvements due to initialisation occur at the lower depths and that the upper
350 ocean is well represented in all of the simulations. For salinity (figures 8 and 9)
351 the results show that improvements in prediction skill due to initialisation are
352 not confined to larger depths, but also show up at the surface. Taking a look
353 at the absolute values (figures 4 and 7) and the temperature-salinity diagram
354 (figure 3) show a better representation for both variables by the initialised
355 simulation, especially at the surface in the North Eastern Atlantic. Overall
356 the results show that there is an improved predictability and representation
357 at depth for both variables with the initialisation, with better performance for
358 salinity than temperature.

359

360 Results that we obtained for near surface potential temperature are in line
361 with the current research. [Borchert et al \(2018\)](#) explored this region look-
362 ing at the sea surface temperature (SST) and its connection with the ocean
363 heat transport and the Atlantic Multidecadal Variability and how they are
364 interconnected with each other. It was determined that on longer timescales
365 SST is influenced and impacted by ocean heat transport. [Koul et al \(2019\)](#)
366 explored uninitialised historical simulations to show that open-ocean circu-
367 lation can have an impact on North Sea inflow. While [Koul et al \(2019\)](#)
368 investigated the historical simulations we went a step further to determine if

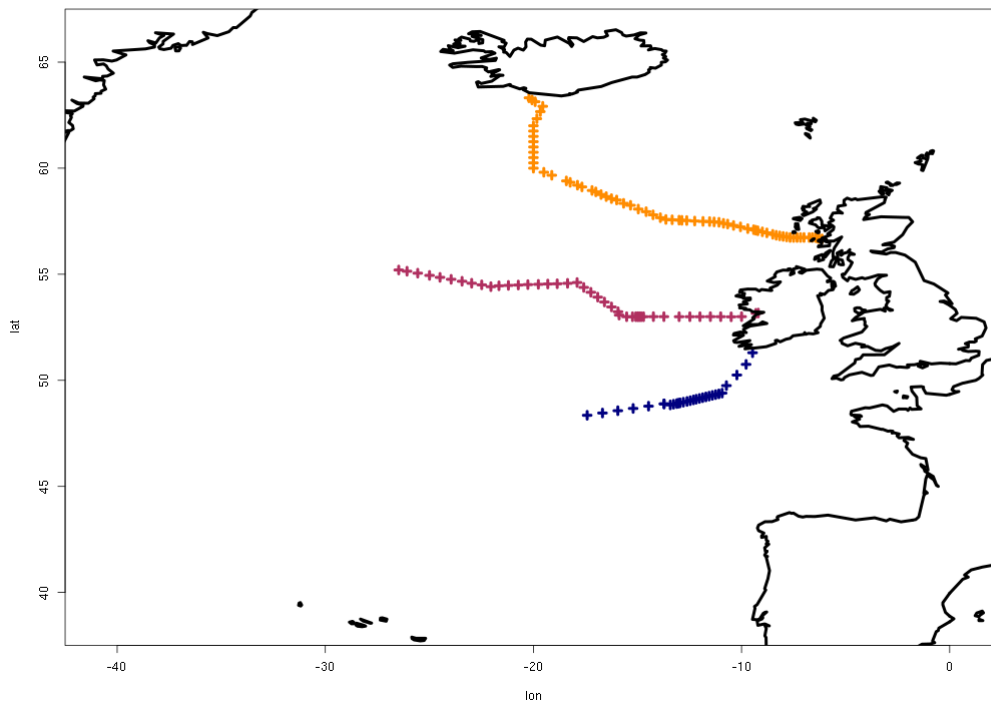
there is any predictability along our three transects, by using initialised hind-cast and uninitialised historical simulations. These simulations were compared with the assimilation simulation, as a first step we looked at the values that each simulation had generated followed by the temperature-salinity diagram then moving onto the prediction skill. This has produced results that have highlighted that initialised simulations generally have improved predictability compared with uninitialised simulations. By extending our analysis further to the south compared to [Koul et al \(2019\)](#), we show that also in these region, the potential temperature and salinity are well represented in the model. We analysed a time period of 1961 to 2013, on a 2-to-5-year lead time to compare the results with two uninitialised simulations. A future target would be to extend the time frame as well as lead times. While these results look promising it should be noted that due to limited observations any references for the subsurface ocean prior to 2004 might not be as reliable as they are since then with the Argo observational network in place ([Wong et al, 2020](#)). Nevertheless, the results showed promising insights into the ability of initialised simulations, even when discussions about the benefit of initialisation are getting more traction ([Borchert et al, 2021](#)).

The ability to predict changes in the future fish stock will support adaptation for its management, which is of vast importance for international coastal communities. Through the analysis of both temperature and salinity at depth we can identify habitable zones and spawning grounds that may be predictable. It will also support the better understanding of the life cycle and distribution of future fish habitats. Its potential has already been demonstrated for the blue whiting ([Miesner and Payne, 2018](#)) and cod ([Koul et al, 2021](#)) in the wider North Eastern Atlantic context.

5 Conclusions

In this study we explored the predictability within the Eastern North Atlantic at depth using three transects the Extended Ellett Line, the Porcupine Bank, and Goban Spur. To achieve this we first determined validity in the temperature/salinity-space of the initialised and uninitialised simulations by comparing it to an assimilation simulation. We followed this by determining the predictability of the two categories of simulations and determined the impact of initialisation for the three transects. We found that (1) there is multi-year memory in the water mass properties of the initialised predictions, (2) that prediction skill depends on variable, depth, and external forcing scheme, (3) that improvements in prediction skill in the initialised system over uninitialised simulations are mostly in the upper ocean above 300 m depth and in the deep ocean below 1500 m depth, and (4) that these improvements are more pronounced in salinity than in temperature.

415
416
417
418
419
420
421
422
423
424
425
426
427
428
429
430
431
432
433



434 **Fig. 1** The three sections are the EEL (dark orange line) most northward section, moving
435 south the next section is along Porcupine Bank (PB, red line), and the most southerly section
436 along Goban Spur (GS, navy line).

437
438

6 Figures

439
440
441
442
443
444

Acknowledgments. COB, GDM and AD were funded by the Marine Institute Galway, A4 project (Aigéin, Aeráid, agus athrú Atlantaigh—Oceans, Climate, and Atlantic Change), PBA/CC/18/01. SB was supported by Copernicus Climate Change Service, funded by the EU, under Contract C3S2-370.

445 Declarations

446
447
448
449
450
451
452
453
454
455
456
457
458
459
460

- Conflict of interest/Competing interests (check journal-specific guidelines for which heading to use) The authors have no relevant financial or non-financial interests to disclose
- Availability of data and materials
The output from the decadal prediction system can be accessed via [Brune et al \(2021\)](#). The output of MPI-GE CMIP6 historical simulations is available from <https://esgf-data.dkrz.de/search/cmip6-dkrz/>, under Institution ID MPI-M. The output of MPI-GE CMIP5 historical and RCP4.5 simulations is available from <https://esgf-data.dkrz.de/search/mip-ge/>. The variable names are "thetao" for potential temperature and "so" for salinity, respectively.
- Authors' contributions All authors contributed to the study conception and design. The analysis was performed by Catherine O'Beirne, who also wrote

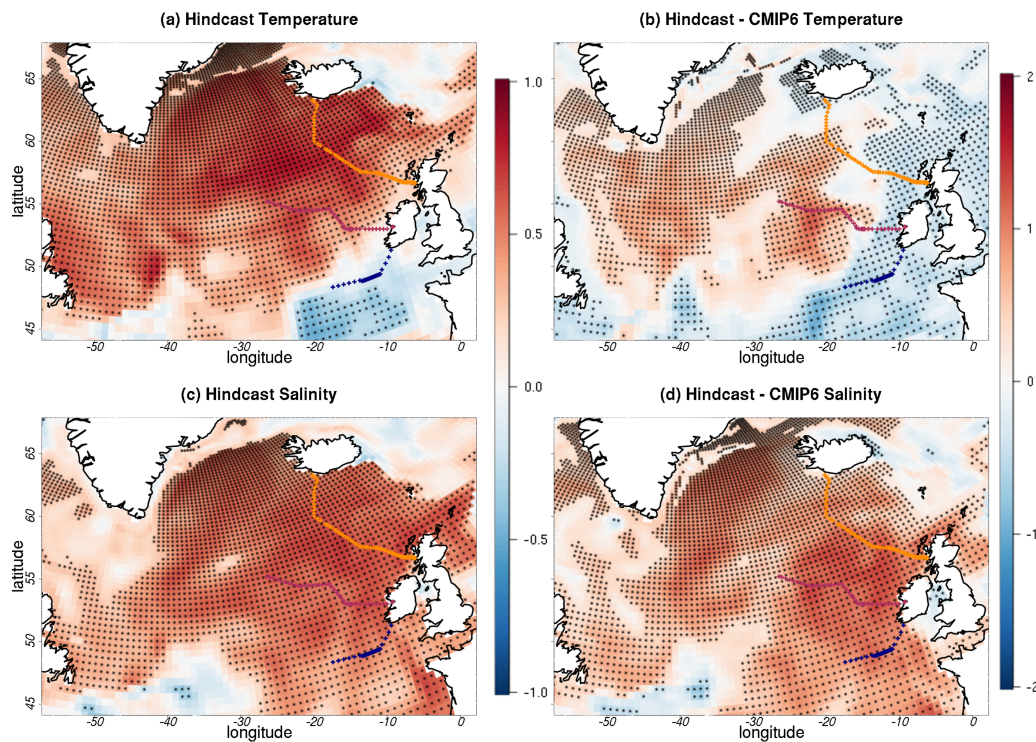


Fig. 2 Shows the anomaly correlation coefficient initialised hindcast against assimilation for potential temperature (6m) (a) and sea water salinity (6m) (c) for the North Eastern Atlantic and the difference between initialised hindcast ACC and uninitialised CMIP6 ACC for the North Eastern Atlantic for potential temperature (6m) (b) and sea water salinity (6m) (d). The areas shaded on red highlight the regions that have good predictability, the orange line is the Extended Ellet Line, the yellow line is the Porcupine Bank transect, and the navy line is the Goban Spur. The red areas show that there is positive skill, the blue shows that there is negative skill and the black dots show that they are significant. Generated from the MPI-ESM-LR; 1966-2013; initialised each November; 2 to 5 years lead time; 16 ensemble members.

the first draft of the manuscript. All authors read and approved the final manuscript.

References

- Andrews MB, Knight JR, Gray LJ (2015) A simulated lagged response of the north atlantic oscillation to the solar cycle over the period 1960-2009. *Environmental Research Letters* 10:054,022. <https://doi.org/10.1088/1748-9326/10/5/054022>
- Athanasiadis P, Bellucci A, Scaife A, et al (2017) A multisystem view of wintertime nao seasonal predictions. *Journal of Climate* 30:1461-1475. <https://doi.org/10.1175/JCLI-D-16-0153.1>
- Barcikowska M, Weaver S, Feser F, et al (2018) Euro-atlantic winter storminess and precipitation extremes under 1.5 c vs. 2 c warming scenarios. *Earth System Dynamics* 9:679-699. <https://doi.org/10.5194/esd-9-679-2018>

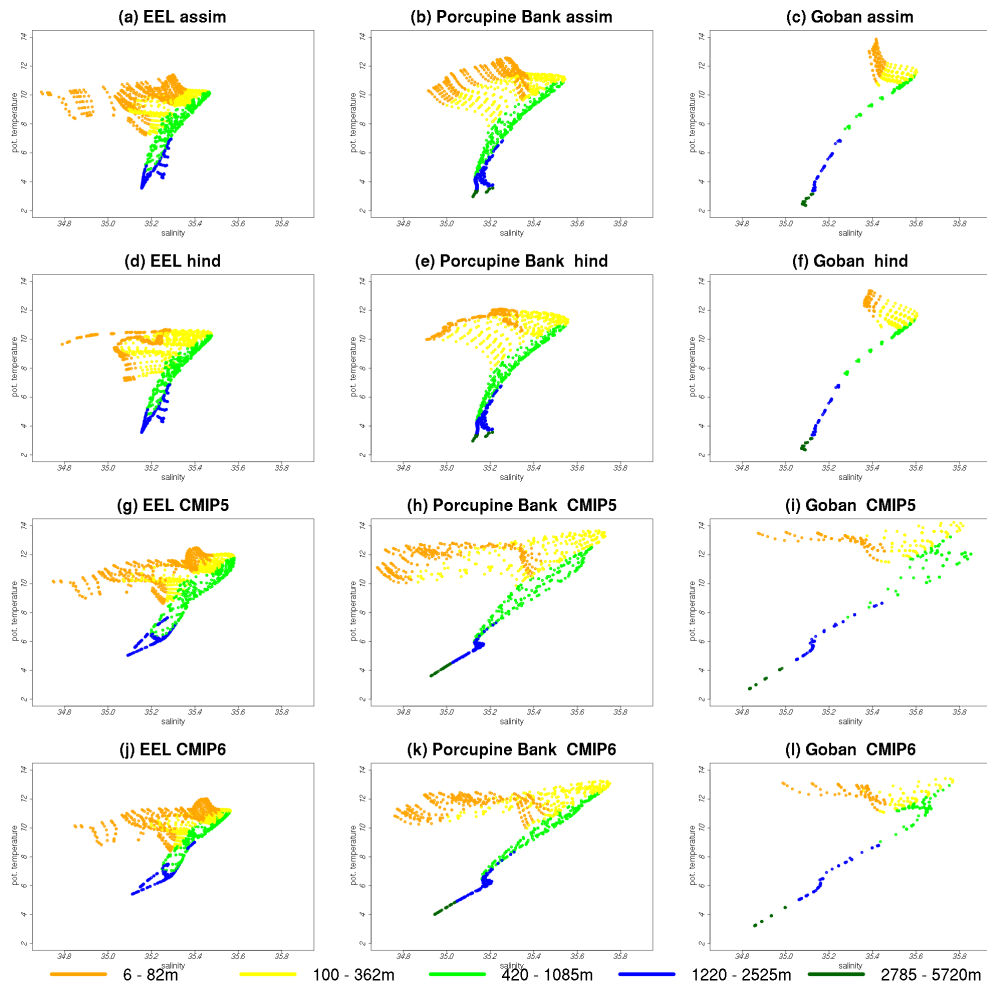


Fig. 3 Potential temperature-salinity diagram using the assimilation (a-c), initialised hindcast (d-f), uninitialised historical (CMIP5) (g-i), uninitialised historical (CMIP6) (j-l), for the EEL, Porcupine Bank, and Goban Spur. The colours on the diagram indicate the depth which Orange (6 - 82m), Orange (100- 362m), Green (420 - 1085m), Blue (1220 - 2525m), Darkgreen (2785 - 5720m). Generated from the MPI-ESM-LR; 1966-2013; initialised each November; 2 to 5 years led time; 16 ensemble members.

Borchert LF, Müller WA, Baehr J (2018) Atlantic ocean heat transport influences interannual-to-decadal surface temperature predictability in the north atlantic region. *Journal of Climate* 31:6763–6782. <https://doi.org/https://doi.org/10.1175/JCLI-D-17-0734.1>

Borchert LF, Düsterhus A, Brune S, et al (2019) Forecast-oriented assessment of decadal hindcast skill for north atlantic sst. *Geophysical Research Letters* 46:11,444–11,454. <https://doi.org/https://doi.org/10.1029/2019GL084758>

Borchert LF, Menary DM. B.and Swingedouw, Sgubin G, et al (2021) Improved decadal predictions of north atlantic subpolar gyre sst in cmip6. *Geophysical Research Letters* 48. <https://doi.org/https://doi.org/10.1029/2020GL091307>

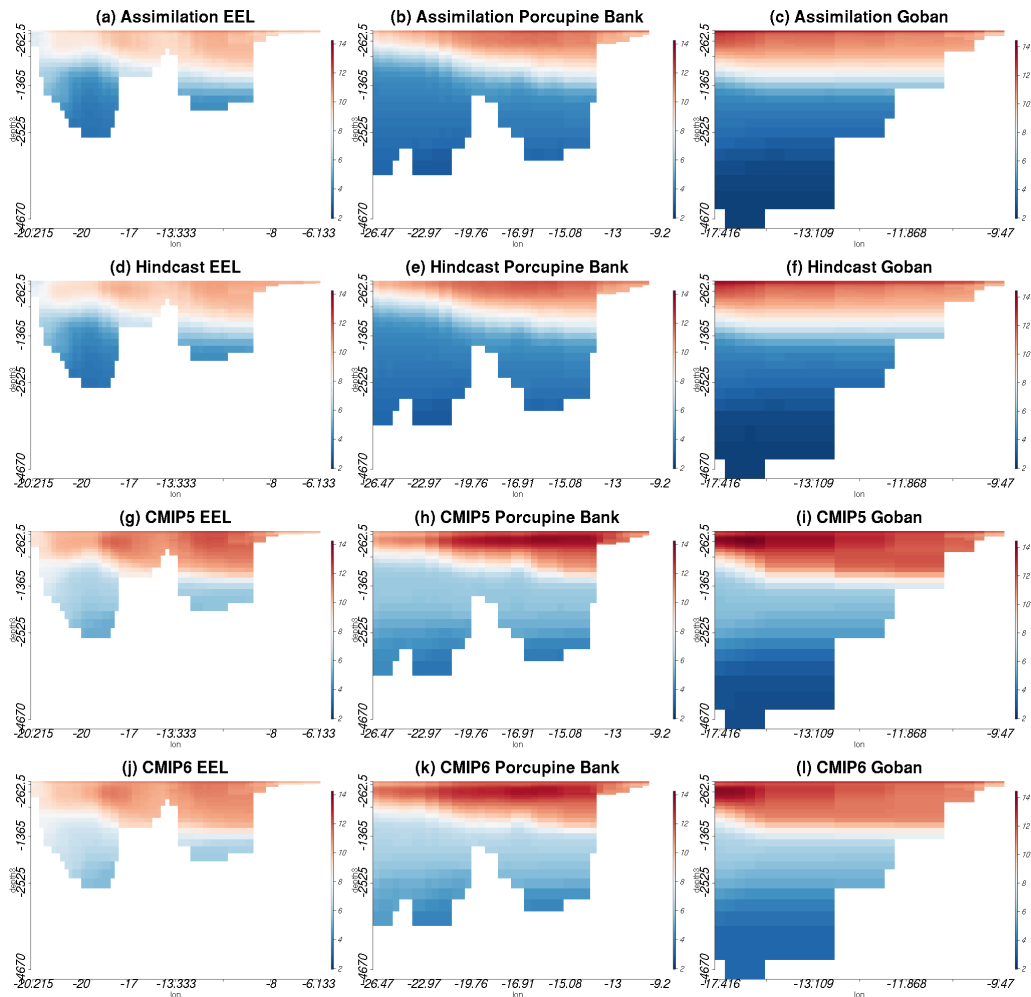


Fig. 4 Potential temperature values from the model for the assimilation (a-c), initialised hindcast (d-f), uninitialised historical (CMIP5) (g-i), uninitialised historical (CMIP6) (j-l) simulations along the EEL, Porcupine Bank, and Goban Spur transects. The red areas show that there is positive skill, the blue shows that there is negative skill and the black dots show that they are significant. Generated from the MPI-ESM-LR; 1966–2013; initialised each November; 2 to 5 years lead time; 16 ensemble members.

Brune S, Baehr J (2020) Preserving the coupled atmosphere–ocean feedback in initializations of decadal climate predictions. *Climate Change* 11:1–19. <https://doi.org/https://doi.org/10.1002/wcc.637>

Brune S, Nerger L, Baehr J (2015) Assimilation of oceanic observations in a global coupled Earth system model with the SEIK filter. *Ocean Model* 96, Part 2:254–264. <https://doi.org/https://doi.org/10.1016/j.ocemod.2015.09.011>

Brune S, Pohlmann H, Müller WA, et al (2021) MPI-ESM-LR 1.2.01 decadal prediction localEnKF monthly

Dee DP, Uppala SM, Simmons AJ, et al (2011) The ERA-Interim reanalysis: configuration and performance of the data assimilation system. *Quart J Roy Meteor Soc* 137(656):553–597. <https://doi.org/https://doi.org/10.1002/qj>

553
554
555
556
557
558
559
560
561
562
563
564
565
566
567
568
569
570
571
572
573
574
575
576
577
578
579
580
581
582
583
584
585
586
587
588
589
590
591
592
593
594
595
596
597
598

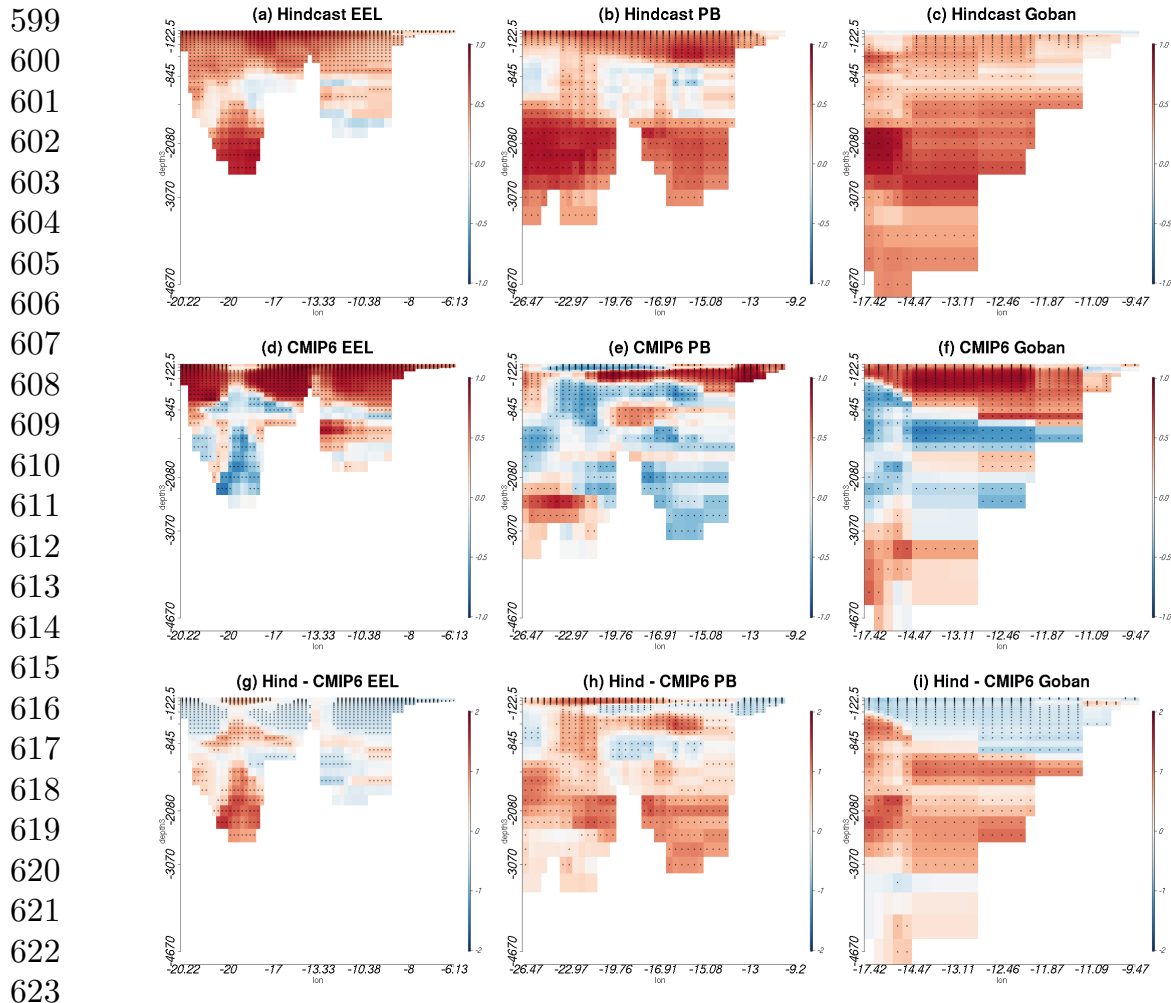


Fig. 5 Anomaly correlation coefficient against assimilation for potential temperature at lead years 2 to 5, using the initialised hindcast (a-c), uninitialised historical (CMIP6) (d-f), hindcast - uninitialised historical (g-i) for the EEL, Porcupine Bank, and Goban Spur. The red areas show that there is positive skill, the blue shows that there is negative skill and the black dots show that they are significant. Generated from the MPI-ESM-LR; 1966-2013; initialised each November; 2 to 5 years lead time; 16 ensemble members.

828

Dingle RV, Scrutton RA (1979) Sedimentary succession and tectonic history of a marginal plateau (goban spur, southwest of Ireland). *Marine Geology* 33(1–2):45–69. [https://doi.org/https://doi.org/10.1016/0025-3227\(79\)90132-4](https://doi.org/10.1016/0025-3227(79)90132-4)

Eyring V, Bony S, Meehl GA, et al (2016) Overview of the coupled model intercomparison project phase 6 (cmip6) experimental design and organization. *Geosci Model Dev* 9(5):1937–1958. [https://doi.org/https://doi.org/10.5194/gmd-9-1937-2016](https://doi.org/10.5194/gmd-9-1937-2016)

Giorgetta MA, et al (2013) Climate and carbon cycle changes from 1850 to 2100 in MPI-ESM simulations for the Coupled Model Intercomparison Project phase 5. *J Adv Mod Earth Sys* 5(3):572–597. [https://doi.org/https://doi.org/10.1002/jame.20038](https://doi.org/10.1002/jame.20038)

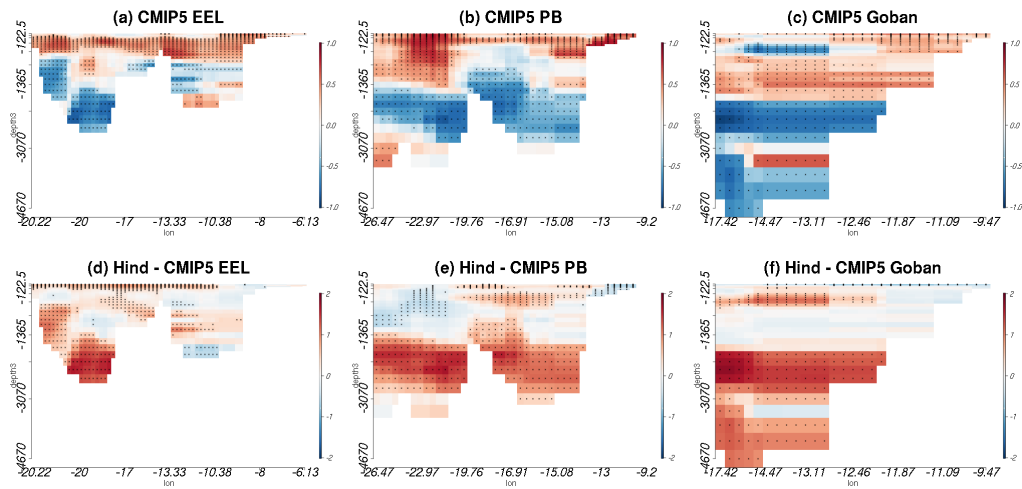


Fig. 6 Anomaly correlation coefficient against assimilation for potential temperature at lead years 2 to 5, using uninitialised historical (CMIP5) (a-c), hindcast - uninitialised historical (d-f) for the EEL, Porcupine Bank, and Goban Spur. The red areas show that there is positive skill, the blue shows that there is negative skill and the black dots show that they are significant. Generated from the MPI-ESM-LR; 1966-2013; initialised each November; 2 to 5 years lead time; 16 ensemble members.

Good SA, Martin MJ, Rayner NA (2013) EN4: Quality controlled ocean temperature and salinity profiles and monthly objective analyses with uncertainty estimates. *J Geophys Res* 118(12):6704–6716. <https://doi.org/https://doi.org/10.1002/2013JC009067>

de Graciansky P, Poag C (1985) Geologic history of goban spur, north-west europe continental margin. *Deep Sea Drilling Project Initial Reports* 80:1187–1216

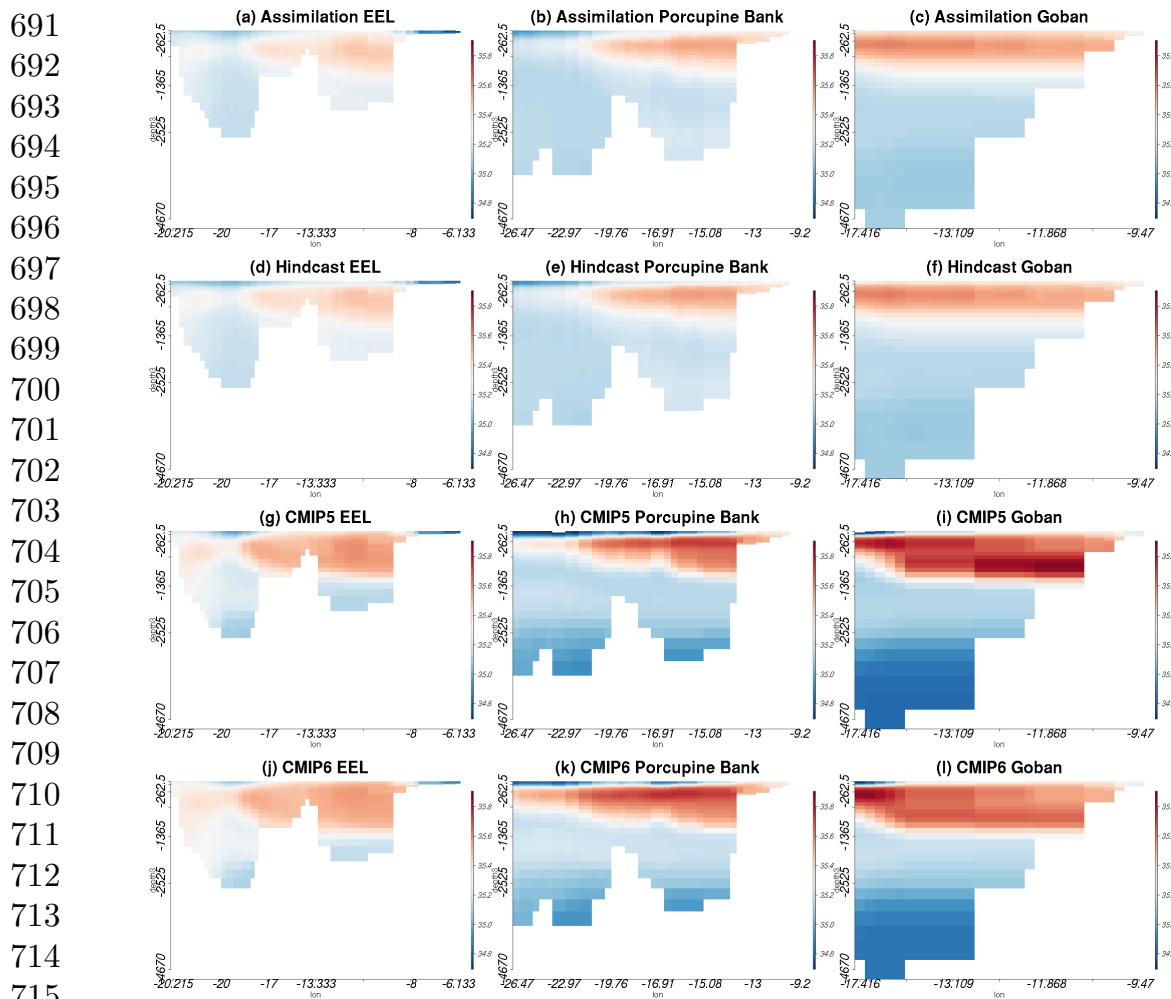
Hersbach H, Bell B, Berrisford P, et al (2020) The ERA5 global reanalysis. *Q J R Meteorol Soc* 146(730):1999–2049. <https://doi.org/https://doi.org/10.1002/qj.3803>

Holliday N, Bersch M, Berx B, et al (2020) Ocean circulation causes the largest freshening event for 120 years in eastern subpolar north atlantic. *Nat Commun* 11:585. <https://doi.org/https://doi.org/10.1038/s41467-020-14474-y>

Holliday NP, Cunningham SA, Johnson C, et al (2015) Multidecadal variability of potential temperature, salinity, and transport in the eastern subpolar north atlantic. *J Geophys Res Oceans* 120:5945–5967. <https://doi.org/https://doi.org/10.1002/2015JC010762>

Hövel L, Brune S, Baehr J (2022) Decadal Prediction of Marine Heatwaves in MPI-ESM. *Geophys Res Lett* 49(15):e2022GL099,347. <https://doi.org/https://doi.org/10.1029/2022GL099347>

645
646
647
648
649
650
651
652
653
654
655
656
657
658
659
660
661
662
663
664
665
666
667
668
669
670
671
672
673
674
675
676
677
678
679
680
681
682
683
684
685
686
687
688
689
690



716 **Fig. 7** Sea water salinity values from the model for the assimilation (a-c), hindcast (d-
717 f), uninitialised historical (CMIP5) (g-i), uninitialised historical (CMIP5) (j-l)
718 simulations along the EEL, Porcupine Bank, and Goban Spur. Generated from the MPI-ESM-LR; 1966-
2013; initialised each November; 2 to 5 years led time; 16 ensemble members.

720 Humphreys M, Griffiths A, Achterberg NE.P. Holliday, et al (2016) Multi-
721 decadal accumulation of anthropogenic and remineralized dissolved inor-
722 ganic carbon along the extended ellett line in the northeast atlantic ocean.
723 *Global Biogeochem Cycles* 30:293–310. [https://doi.org/https://doi.org/10.](https://doi.org/https://doi.org/10.1002/2015GB005246)
724 [1002/2015GB005246](https://doi.org/https://doi.org/10.1002/2015GB005246)

726 Huthnance J, Coelho H, Griffiths C, et al (2001) Physical structures, advec-
727 tion and mixing in the region of goban spur. *Deep Sea Research Part II:*
728 *Topical Studies in Oceanography* 48(14):2979–3021. [https://doi.org/https://](https://doi.org/https://doi.org/10.1016/S0967-0645(01)00030-3)
729 [doi.org/10.1016/S0967-0645\(01\)00030-3](https://doi.org/10.1016/S0967-0645(01)00030-3)

731 Jones S, Cottier F, Inall M, et al (2018) Decadal variability on the northwest
732 european continental shelf. *Progress in Oceanography* 161:131–151. [https://](https://doi.org/https://doi.org/10.1016/j.pocean.2018.01.012)
733 doi.org/https://doi.org/10.1016/j.pocean.2018.01.012

734
735
736

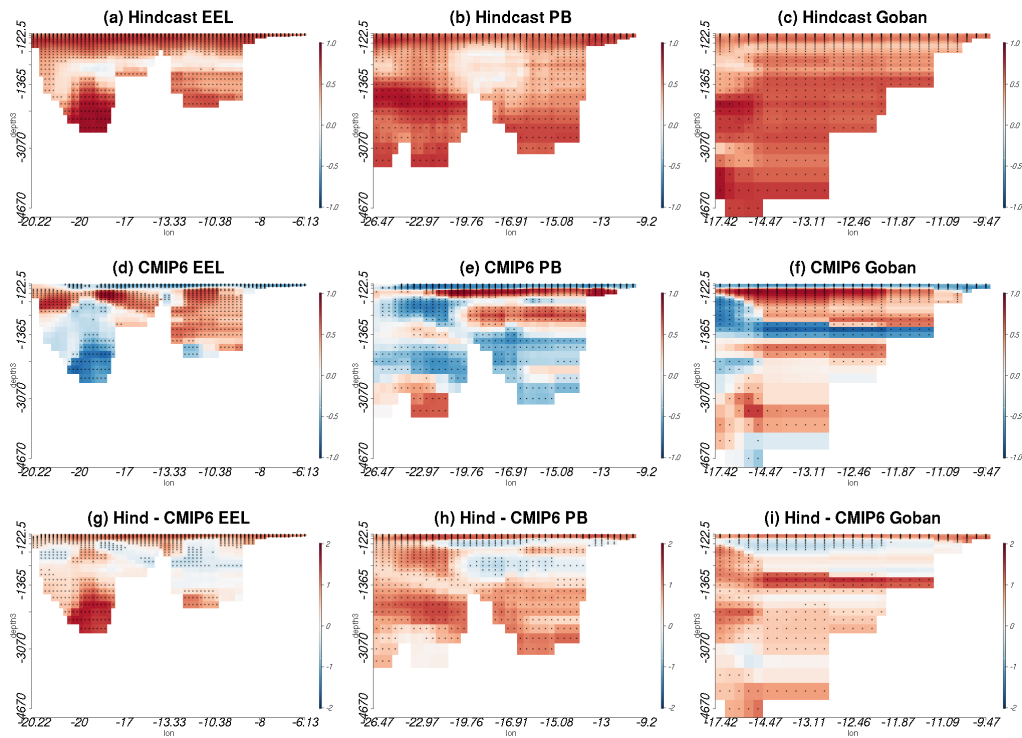


Fig. 8 Anomaly correlation coefficient against assimilation for sea water salinity at lead years 2 to 5, using the initialised hindcast (a-c), uninitialised historical (CMIP6) (d-f), hindcast - uninitialised historical (g-i) for the EEL, Porcupine Bank, and Goban Spur. The red areas show that there is positive skill, the blue shows that there is negative skill and the black dots show that they are significant. Generated from the MPI-ESM-LR; 1966-2013; initialised each November; 2 to 5 years lead time; 16 ensemble members.

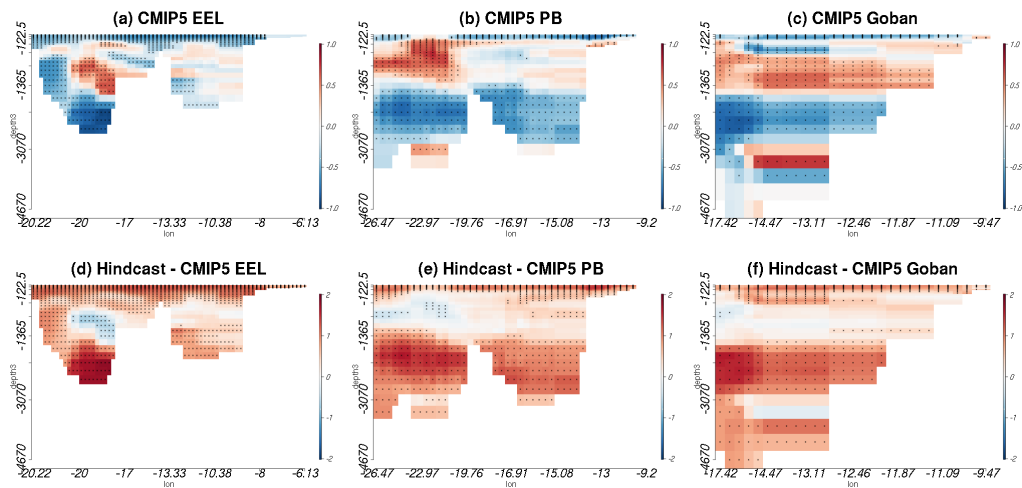


Fig. 9 Anomaly correlation coefficient against assimilation for sea water salinity at lead years 2 to 5, using uninitialised historical (CMIP5) (a-c), hindcast - uninitialised historical (d-f), for the EEL, Porcupine Bank, and Goban Spur. The red areas show that there is positive skill, the blue shows that there is negative skill and the black dots show that they are significant. Generated from the MPI-ESM-LR; 1966-2013; initialised each November; 2 to 5 years lead time; 16 ensemble members.

737
738
739
740
741
742
743
744
745
746
747
748
749
750
751
752
753
754
755
756
757
758
759
760
761
762
763
764
765
766
767
768
769
770
771
772
773
774
775
776
777
778
779
780
781
782

- 783 JungCLAUS JH, FISCHER N, HAAK H, et al (2013) Characteristics of the ocean
784 simulations in the Max Planck Institute Ocean Model (MPIOM) the ocean
785 component of the MPI-Earth system model. *Journal of Advances in Modeling
786 Earth Systems* 5(2):422–446. [https://doi.org/https://doi.org/10.1002/jame.
787 20023](https://doi.org/https://doi.org/10.1002/jame.20023)
788
- 789 Koul V, Schrum C, Düsterhus A, et al (2019) Atlantic inflow to the north sea
790 modulated by the subpolar gyre in a historical simulation with MPI-ESM.
791 *Journal of Geophysical Research: Oceans* 124:1807–1826. [https://doi.org/
792 https://doi.org/10.1029/2018JC014738](https://doi.org/https://doi.org/10.1029/2018JC014738)
793
- 794 Koul V, Tesdal J, Bersch M, et al (2020) Unraveling the choice of the north
795 atlantic subpolar gyre index. *Sci Rep* 10:1005. [https://doi.org/https://doi.
796 org/10.1038/s41598-020-57790-5](https://doi.org/https://doi.org/10.1038/s41598-020-57790-5)
797
- 798 Koul V, Sguotti C, Årthun M, et al (2021) Skilful prediction of cod stocks
799 in the north and barents sea a decade in advance. *COMMUNICATIONS
800 EARTH & ENVIRONMENT* 140(2). [https://doi.org/https://doi.org/10.
801 1038/s43247-021-00207-6](https://doi.org/https://doi.org/10.1038/s43247-021-00207-6)
802
- 803 Maher N, Milinski S, Suarez-Gutierrez L, et al (2019) The Max Planck
804 Institute Grand Ensemble: Enabling the Exploration of Climate System
805 Variability. *J Adv Model Earth Syst* 11(7):2050–2069. [https://doi.org/https://
806 //doi.org/10.1029/2019MS001639](https://doi.org/https://doi.org/10.1029/2019MS001639)
807
- 808 Mauritsen T, Bader J, Becker T, et al (2019) Developments in the MPI-M
809 Earth System Model version 1.2 (MPI-ESM1.2) and Its Response to Increas-
810 ing CO₂. *J Adv Model Earth Syst* 11(4):998–1038. [https://doi.org/https://
811 //doi.org/10.1029/2018MS001400](https://doi.org/https://doi.org/10.1029/2018MS001400)
812
- 813 Miesner AK, Payne MR (2018) Oceanographic variability shapes the spawning
814 distribution of blue whiting (*micromesistius poutassou*). *Fisheries Oceanog-
815 raphy* 27:623–638. <https://doi.org/https://doi.org/10.1111/fog.12382>
816
- 817 Moritz M, Jochumsen K, Kieke D, et al (2021) Volume transport time series
818 and variability of the north atlantic eastern boundary current at goban
819 spur. *Journal of Geophysical Research: Oceans* 126. [https://doi.org/https://
820 //doi.org/10.1029/2021JC017393](https://doi.org/https://doi.org/10.1029/2021JC017393)
821
- 822 NERGER L, HILLER W (2013) Software for ensemble-based data assimilation sys-
823 tems - Implementation strategies and scalability. *Comput Geosci* 55:110–118.
824 <https://doi.org/https://doi.org/10.1016/j.cageo.2012.03.026>
825
- 826 Olonscheck D, Suarez-Gutierrez L, Milinski S, et al (2023) The new Max
827 Planck Institute Grand Ensemble with CMIP6 forcing and high-frequency
828 model output. under review for JAMES [https://doi.org/https://doi.org/10.
22541/essoar.168319746.64037439/v1](https://doi.org/https://doi.org/10.22541/essoar.168319746.64037439/v1)

O'Reilly L, Fentimen R, Butschek F, et al (2022) Environmental forcing by submarine canyons: Evidence between two closely situated cold-water coral mounds (porcupine bank canyon and western porcupine bank, ne atlantic). <i>Marine Geology</i> 454:106,930. https://doi.org/https://doi.org/10.1016/j.margeo.2022.106930	829 830 831 832 833 834
Polkova I, Brune S, Kadow C, et al (2019) Initialization and Ensemble Generation for Decadal Climate Predictions: A Comparison of Different Methods. <i>J Adv Mod Earth Sys</i> 11(1):149–172. https://doi.org/https://doi.org/10.1029/2018MS001439	835 836 837 838 839
Stevens B, et al (2013) Atmospheric component of the MPI-M Earth System Model: ECHAM6. <i>J Adv Mod Earth Sys</i> 5(2):146–172. https://doi.org/https://doi.org/10.1002/jame.20015	840 841 842
Taylor KE, Stouffer RJ, Meehl GA (2012) An Overview of CMIP5 and the Experiment Design. <i>Bull Amer Meteor Soc</i> 93(4):485–498. https://doi.org/https://doi.org/10.1175/BAMS-D-11-00094.1	843 844 845 846
Uppala SM, Kållberg PW, Simmons AJ, et al (2005) The ERA-40 re-analysis. <i>Quart J Roy Meteor Soc</i> 131(612):2961–3012. https://doi.org/https://doi.org/10.1256/qj.04.176	847 848 849 850
Wang Y, Magnusdottir G, Stern H, et al (2014) Uncertainty estimates of the eof-derived north atlantic oscillation. <i>Journal of Cliamte</i> 27:1290–1301. https://doi.org/https://doi.org/10.1175/JCLI-D-13-00230.1	851 852 853 854
White PM.and Bowyer (1997) The shelf-edge current north-west of ireland. <i>Annales Geophysicae</i> 15:1076–1083. https://doi.org/https://doi.org/10.1007/s00585-997-1076-0	855 856 857 858
Wong APS, Wijffels SE, Riser SC, et al (2020) Argo Data 1999-2019: Two Million Temperature-Salinity Profiles and Subsurface Velocity Observations From a Global Array of Profiling Floats. <i>Front Mar Sci</i> 7. https://doi.org/https://doi.org/10.3389/fmars.2020.00700	859 860 861 862 863 864 865 866 867 868 869 870 871 872 873 874

Bibliography

- Allgaier, J. (2019). Science and environmental communication on youtube: strategically distorted communications in online videos on climate change and climate engineering. *Frontiers in communication*, page 36. [41](#)
- Andrews, M. B., Knight, J. R., and Gray, L. J. (2015). A simulated lagged response of the north atlantic oscillation to the solar cycle over the period 1960-2009. *Environmental Research Letters*, 10:054022. [10](#), [72](#)
- Athanasiadis, P., Bellucci, A., Scaife, A., Hermanson, L., Materia, S., Sanna, A., Borrelli, A., Maclachlan, C., and Gualdi, S. (2017). A multisystem view of wintertime nao seasonal predictions. *Journal of Climate*, 30:1461–1475. [10](#), [72](#)
- Barcikowska, M., Weaver, S., Feser, F., Russo, S., Schenk, F., Stone, D., Wehner, M., and Zahn, M. (2018). Euro-atlantic winter storminess and precipitation extremes under 1.5 c vs. 2 c warming scenarios. *Earth System Dynamics*, 9:679–699. [10](#), [72](#)
- Bartsch, J. (2005). The influence of spatio-temporal egg production variability on the modelled survival of the early life history stages of mackerel (*scomber scombrus*) in the eastern north atlantic. *ICES Journal of Marine Science*, 62:1049–1060. [29](#), [38](#), [39](#)
- Beare, D. J. and Reid, D. G. (2002). Investigating spatio-temporal change in spawning activity by atlantic mackerel between 1977 and 1998 using generalized additive models. *ICES Journal of Marine Science*, 59:711–724. [38](#), [55](#), [141](#)

- Beecher, B., O'Doherty, A., Goulao, B., Jalali, A., Salsberg, J., Dore, L., and Hannigan, A. (2023). Designing infographics in health research with patients and the public: A scoping review protocol. *Plos one*, 18(9):e0291066. 42
- Befort, D. J., Brunner, L., Borchert, L. F., O'Reilly, C. H., Mignot, J., Ballinger, A. P., Hegerl, G. C., Murphy, J. M., and Weisheimer, A. (2022). Combination of decadal predictions and climate projections in time: Challenges and potential solutions. *Geophysical Research Letters*, 49. 50, 51
- Befort, D. J., O'Reilly, C. H., and Weisheimer, A. (2020). Constraining projections using decadal predictions. *Geophysical Research Letters*, 47. 51
- Boer, G. J., Smith, D. M., Cassou, C., Doblas-Reyes, F., Danabasoglu, G., Kirtman, B., Kushnir, Y., Kimoto, M., Meehl, G. A., Msadek, R., et al. (2016). The decadal climate prediction project (dcpp) contribution to cmip6. *Geoscientific Model Development*, 9(10):3751–3777. xiii, 2, 3, 4, 50, 51, 70
- Borchert, L. F., Düsterhus, A., Brune, S., Müller, W. A., and Baehr, J. (2019). Forecast-oriented assessment of decadal hindcast skill for north atlantic sst. *Geophysical Research Letters*, 46:11,444–11,454. 5, 24, 52, 53, 74
- Borchert, L. F., Menary, M. B., Swingedouw, D., Sgubin, G., Hermanson, L., and Mignot, J. (2021). Improved decadal predictions of north atlantic subpolar gyre sst in cmip6. *Geophysical Research Letters*, 48(3). 27, 51, 52, 74, 96
- Borchert, L. F., Müller, W. A., and Baehr, J. (2018). Atlantic ocean heat transport influences interannual-to-decadal surface temperature predictability in the north atlantic region. *Journal of Climate*, 31:6763–6782. 5, 25, 52, 53, 74, 95
- Born, A., Mignot, J., and Stocker, T. F. (2015). Multiple equilibria as a possible mechanism for decadal variability in the north atlantic ocean. *Journal of Climate*, 28:8907–8922. 7, 22
- Born, A., Stocker, T. F., and Sandø, A. B. (2016). Transport of salt and freshwater in the atlantic subpolar gyre. *Ocean Dynamics*, 66:1051–1064. 9

- Bresnihan, P. (2019). Revisiting neoliberalism in the oceans: Governmentality and the biopolitics of ‘improvement’ in the irish and european fisheries. *Environment and Planning A: Economy and Space*, 50(1):156–177. [12](#), [32](#), [34](#)
- Brewer, J. F. (2013). Making an environmental market, unmaking adaptive capacity: Species commodification in the new england ground fishery. *Geoforum*, 50:172–181. [35](#)
- Brown, P. T., Lozier, M. S., Zhang, R., and Li, W. (2016). The necessity of cloud feedback for a basin-scale atlantic multidecadal oscillation. *Geophysical Research Letters*, 43:3955–3963. [1](#), [7](#), [21](#)
- Brox, O. (1996). Recent attempts at regulating the harvesting of norwegian arctic cod. *GeoJournal*, 39(2):203–210. [34](#)
- Bruge, A., Alvarez, P., Fontán, A., Cotano, U., and Chust, G. (2016). Thermal niche tracking and future distribution of atlantic mackerel spawning in response to ocean warming. *Frontiers in Marine Science*, 3(86). [29](#), [30](#), [39](#)
- Brune, S. and Baehr, J. (2020). Preserving the coupled atmosphere–ocean feedback in initializations of decadal climate predictions. *Climate Change*, 11:1–19. [5](#), [21](#), [46](#), [74](#), [75](#)
- Brune, S., Nerger, L., and Baehr, J. (2015). Assimilation of oceanic observations in a global coupled Earth system model with the SEIK filter. *Ocean Model.*, 96, Part 2:254–264. [75](#)
- Buckley, M. W. and Marshall, J. (2016). Observations, inferences, and mechanisms of the atlantic meridional overturning circulation: A review. *Reviews of Geophysics*, 54:5–63. [7](#), [22](#)
- Chen, S., Wu, R., and Chen, W. (2015). The changing relationship between interannual variations of the north atlantic oscillation and northern tropical atlantic sst. *Journal of Climate*, 28:485–504. [20](#)
- Coffin, A. B. (2021). Communicate your science: Engaging public audiences with acoustics. *Acoust. Today*, 17(4):12–19. [39](#), [41](#)

- Cropper, T., Hanna, E., Valente, M. A., and Jónsson, T. (2015). A daily azores–iceland north atlantic oscillation index back to 1850. *Geoscience Data Journal*, 2:12–24. [20](#)
- Curtis, J., Lynch, M., and Zubiate, L. (2016). The impact of the north atlantic oscillation on electricity markets: A case study on ireland. *Energy Economics*, 58:186–198. [1](#), [6](#), [19](#)
- Dahlke, F. T., Wohlrab, S., Butzin, M., and Pörtner, H.-O. (2020). Thermal bottlenecks in the life cycle define climate vulnerability of fish. *Science*, 369:65–70. [32](#)
- Dahlstrom, M. F. (2014). Using narratives and storytelling to communicate science with nonexpert audiences. *Proceedings of the national academy of sciences*, 111(supplement_4):13614–13620. [41](#)
- Dale, P., Sporne, I., Knight, J., Sheaves, M., Eslami-Andergoli, L., and Dwyer, P. (2019). A conceptual model to improve links between science, policy and practice in coastal management. *Marine Policy*, 103:42–49. [35](#)
- Dalelane, C., Dobrynin, M., and Fröhlich, K. (2020). Seasonal forecasts of winter temperature improved by higher-order modes of mean sea level pressure variability in the north atlantic sector. *Geophysical Research Letters*, 47. [54](#)
- Davini, P. and Cagnazzo, C. (2014). On the misinterpretation of the north atlantic oscillation in cmip5 models. *Climate Dynamics*, 43:1497–1511. [20](#)
- de Graciansky, P. and Poag, C. (1985). Geologic history of goban spur, northwest europe continental margin. *Deep Sea Drilling Project Initial Reports*, 80:1187–1216. [73](#)
- Dee, D. P., Uppala, S. M., Simmons, A. J., Berrisford, P., Poli, P., Kobayashi, S., Andrae, U., Balmaseda, M. A., Balsamo, G., Bauer, P., Bechtold, P., Beljaars, A. C. M., van de Berg, L., Bidlot, J., Bormann, N., Delsol, C., Dragani, R., Fuentes, M., Geer, A. J., Haimberger, L., Healy, S. B., Hersbach, H., Hólm, E. V., Isaksen, L., Kållberg, P., Köhler, M., Matricardi, M., McNally, A. P., Monge-Sanz, B. M., Morcrette, J.-J., Park, B.-K., Peubey, C., de Rosnay, P.,

- Tavolato, C., Thépaut, J.-N., and Vitart, F. (2011). The ERA-Interim reanalysis: configuration and performance of the data assimilation system. *Quart. J. Roy. Meteor. Soc.*, 137(656):553–597. 75
- Delworth, T. L., Manabe, S., and Stouffer, R. J. (1993). Interdecadal variations of the thermohaline circulation in a coupled ocean-atmosphere model. *J. Climate*, 6(11):1993–2011. 20
- Denis, V., Lejeune, J., and Robin, J. P. (2002). Spatio-temporal analysis of commercial trawler data using general additive models: patterns of loliginid squid abundance in the north-east atlantic. *ICES Journal of Marine Science*, 59:633–648. 33
- Dingle, R. V. and Scrutton, R. A. (1979). Sedimentary succession and tectonic history of a marginal plateau (goban spur, southwest of ireland). *Marine Geology*, 33(1–2):45–69. 73
- Dobrynin, M., Domeisen, D., Müller, W. A., Bell, L., Brune, S., Bunzel, F., Düsterhus, A., Fröhlich, K., Pohlmann, H., and Baehr, J. (2018). Improved teleconnection-based dynamical seasonal predictions of boreal winter. *Geophysical Research Letters*, 45:3605–3614. 1, 5, 6, 19, 20, 52, 53, 99
- Dobrynin, M., Kleine, T., Düsterhus, A., and Baehr, J. (2019). Skilful seasonal prediction of ocean surface waves in the atlantic ocean. *Geophysical Research Letters*, 46(3):1731–1739. 5, 21, 25, 52, 53, 99
- dos Santos Schmidt, T. C., Slotte, A., Olafsdottir, A. H., Nøttestad, L., Jansen, T., Jacobsen, J. A., Bjarnason, S., Lusseau, S. M., Ono, K., Hølleland, S., et al. (2023). Poleward spawning of atlantic mackerel (*scomber scombrus*) is facilitated by ocean warming but triggered by energetic constraints. *ICES Journal of Marine Science*, page fsad098. 38
- Dunstone, N., Lockwood, J., Solaraju-Murali, B., Reinhardt, K., Tsartsali, E. E., Athanasiadis, P. J., Bellucci, A., Brookshaw, A., Caron, L.-P., Doblas-Reyes, F. J., et al. (2022). Towards useful decadal climate services. *Bulletin of the American Meteorological Society*, 103(7):E1705–E1719. 2, 11, 12

- Düsterhus, A. (2020). Seasonal statistical–dynamical prediction of the north atlantic oscillation by probabilistic post-processing and its evaluation. *Climate Dynamics*, 27:121–131. [53](#), [99](#)
- Eyring, V., Bony, S., Meehl, G. A., Senior, C. A., Stevens, B., Stouffer, R. J., and Taylor, K. E. (2016). Overview of the coupled model intercomparison project phase 6 (cmip6) experimental design and organization. *Geosci. Model Dev.*, 9(5):1937–1958. [75](#), [76](#)
- Fan, K., Tiana, B., and Wanga, H. (2016). New approaches for the skillful prediction of the winter north atlantic oscillation based on coupled dynamic climate models. *International Journal of Climate*, 36:82–94. [1](#), [6](#), [19](#), [20](#)
- Fischhoff, B. and Scheufele, D. A. (2013). The science of science communication. *Proceedings of the National Academy of Sciences*, 110(supplement_3):14031–14032. [40](#), [41](#)
- Fitzpatrick, M., Maravelias, C. D., Eigaard, O. R., Hynes, S., and Reid, D. (2017). Fisher’s preferences and trade-offs between management options. *Fish and fisheries*, 18(5):795–807. [12](#)
- Foukal, N. P. and Lozier, M. S. (2016). No inter-gyre pathway for sea-surface temperature anomalies in the north atlantic. *Nature communications*, 7(1):11333. [9](#)
- Franconeri, S. L., Padilla, L. M., Shah, P., Zacks, J. M., and Hullman, J. (2021). The science of visual data communication: What works. *Psychological Science in the public interest*, 22(3):110–161. [42](#)
- Friedman, A. R., Reverdin, G., Khodri, M., and Gastineau, G. (2017). A new record of atlantic sea surface salinity from 1896 to 2013 reveals the signatures of climate variability and long-term trends. *Geophysical Research Letters*, 44:1866–1876. [7](#), [22](#), [23](#)
- García-Serrano, J., Frankignoul, C., Gastineau, G., and De La Cámara, A. (2015). On the predictability of the winter euro-atlantic climate: Lagged influence of autumn arctic sea ice. *Journal of Climate*, 28:5195–5216. [6](#), [21](#)

-
- Gastineau, G. and Frankignoul, C. (2014). Influence of the north atlantic sst variability on the atmospheric circulation during the twentieth century. *Journal of Climate*, 28:1396–1416. [21](#), [22](#)
- Ghosh, R., Müller, W. A., Baehr, J., and Jürgen, B. (2017). Impact of observed north atlantic multidecadal variations to european summer climate: a linear baroclinic response to surface heating. *Climate Dynamics*, 48:3547–3563. [23](#)
- Giorgetta, M. A. et al. (2013). Climate and carbon cycle changes from 1850 to 2100 in MPI-ESM simulations for the Coupled Model Intercomparison Project phase 5. *J. Adv. Mod. Earth Sys.*, 5(3):572–597. [52](#), [75](#)
- Good, S. A., Martin, M. J., and Rayner, N. A. (2013). EN4: Quality controlled ocean temperature and salinity profiles and monthly objective analyses with uncertainty estimates. *J. Geophys. Res.*, 118(12):6704–6716. [75](#)
- Guo, H., Zhan, C., Ning, L., Li, Z., and Hu, S. (2022). Evaluation and comparison of cmip6 and cmip5 model performance in simulating the runoff. *Theoretical and Applied Climatology*, 149(3):1451–1470. [51](#), [70](#)
- Halpern, B. S., Longo, C., Hardy, D., McLeod, K. L., Samhour, J. F., Katona, S. K., Kleisner, K., Lester, S. E., O’Leary, J., Ranelletti, M., et al. (2012). An index to assess the health and benefits of the global ocean. *Nature*, 488(7413):615–620. [1](#)
- Hamilton, L. C. (2007). Climate, fishery and society interactions: Observations from the north atlantic. *Deep Sea Research Part II: Topical Studies in Oceanography*, 54(23-26):2958–2969. [36](#)
- Hannesson, R. (1996). Exclusive rights to fish: Towards a rational fisheries policy. *GeoJournal*, 39:179–184. [33](#)
- Herceg-Bulić, I. and Kucharski, F. (2014). North atlantic ssts as a link between the wintertime nao and the following spring climate. *Journal of Climate*, 27:186–201. [20](#), [21](#)

- Hersbach, H., Bell, B., Berrisford, P., Hirahara, S., Horányi, A., Muñoz-Sabater, J., Nicolas, J., Peubey, C., Radu, R., Schepers, D., Simmons, A., Soci, C., Abdalla, S., Abellan, X., Balsamo, G., Bechtold, P., Biavati, G., Bidlot, J., Bonavita, M., De Chiara, G., Dahlgren, P., Dee, D., Diamantakis, M., Dragani, R., Flemming, J., Forbes, R., Fuentes, M., Geer, A., Haimberger, L., Healy, S., Hogan, R. J., Hólm, E., Janisková, M., Keeley, S., Laloyaux, P., Lopez, P., Lupu, C., Radnoti, G., de Rosnay, P., Rozum, I., Vamborg, F., Villaume, S., and Thépaut, J.-N. (2020). The ERA5 global reanalysis. *Q. J. R. Meteorolog. Soc.*, 146(730):1999–2049. [75](#)
- Holliday, N., Bersch, M., Berx, B., Chafik, L., Cunningham, S., Florindo-López, C., Hátún, H., Johns, W., Josey, S., Larsen, K., Mulet, S., Oltmanns, M., Reverdin, G., Rossby, T., Thierry, V., Valdmarsson, H., and Yashayaev, I. (2020). Ocean circulation causes the largest freshening event for 120 years in eastern subpolar north atlantic. *Nat Commun*, 11:585. [20](#), [73](#)
- Holliday, N. P., Cunningham, S. A., Johnson, C., Gary, S. F., Griffiths, C., Read, J. F., and Sherwin, T. (2015). Multidecadal variability of potential temperature, salinity, and transport in the eastern subpolar north atlantic. *J. Geophys. Res. Oceans*, 120:5945–5967. [73](#)
- Hövel, L., Brune, S., and Baehr, J. (2022). Decadal Prediction of Marine Heatwaves in MPI-ESM. *Geophys. Res. Lett.*, 49(15):e2022GL099347. [75](#), [76](#)
- Humphreys, M., Griffiths, A., Achterberg, E.P. Holliday, N., Rérolle, V., Barraqueta, J., Couldrey, M., Oliver, K., Hartman, S., Esposito, M., and Boyce, A. (2016). Multidecadal accumulation of anthropogenic and remineralized dissolved inorganic carbon along the extended ellett line in the northeast atlantic ocean. *Global Biogeochem. Cycles*, 30:293–310. [73](#)
- Hurrell, J. (1995). Decadal trends in the north atlantic oscillation:regional temperatures and precipitation. *Science*, 269:676–679. [20](#)
- Huthnance, J., Coelho, H., Griffiths, C., Knight, P., Rees, A., Sinha, B., Vangriesheim, A., White, M., and Chatwin, P. (2001). Physical structures, advec-

- tion and mixing in the region of goban spur. *Deep Sea Research Part II: Topical Studies in Oceanography*, 48(14):2979–3021. [73](#), [74](#), [82](#)
- Ibaibarriaga, L., Irigoien, X., Santos, M., Motos, L., Fives, J. M., Franco, C., Lago de Lanzós, A., Acevedo, S., Bernal, M., Bez, N., et al. (2007). Egg and larval distributions of seven fish species in north-east atlantic waters. *Fisheries Oceanography*, 16(3):284–293. [30](#), [36](#), [38](#), [55](#), [141](#)
- Jackson, L. C., Kahana, R., Graham, T., Ringer, M. A., Woollings, T., Mecking, J. V., and Wood, R. A. (2015). Global and european climate impacts of a slowdown of the amoc in a high resolution gcm. *Climate Dynamics*, 45:3299–3316. [7](#), [22](#)
- Jamieson, D. (1996). Scientific uncertainty: How do we know when to communicate research findings to the public? *Science of the total environment*, 184(1-2):103–107. [40](#)
- Jansen, T. and Gislason, H. (2013). Population structure of atlantic mackerel (*scomberscombrus*). *PloS one*, 8(5):e64744. [38](#)
- Johnsson, J. I., Höjesjö, J., and Fleming, I. A. (2001). Behavioural and heart rate responses to predation risk in wild and domesticated atlantic salmon. *Canadian Journal of Fisheries and Aquatic Sciences*, 58(4):788–794. [37](#)
- Jones, S., Cottier, F., Inall, M., and Griffiths, C. (2018). Decadal variability on the northwest european continental shelf. *Progress in Oceanography*, 161:131–151. [73](#)
- Jungclaus, J. H., Fischer, N., Haak, H., Lohmann, K., Marotzke, J., Matei, D., Mikolajewicz, U., Notz, D., and von Storch, J. S. (2013). Characteristics of the ocean simulations in the max planck institute ocean model (mpiom) the ocean component of the mpi-earth system model. *Journal of Advances in Modeling Earth Systems*, 5(2):422–446. [52](#), [75](#)
- Konefal, J. (2013). Environmental movements, market-based approaches, and neoliberalization: a case study of the sustainable seafood movement. *Organization & Environment*, 26(3):336–352. [12](#)

- Koul, V., Brune, S., Baehr, J., and Schrum, C. (2022). Impact of decadal trends in the surface climate of the north atlantic subpolar gyre on the marine environment of the barents sea. *Front. Mar.*, 8. [26](#), [27](#), [29](#)
- Koul, V., Schrum, C., Düsterhus, A., and Baehr, J. (2019). Atlantic inflow to the north sea modulated by the subpolar gyre in a historical simulation with mpi-esm. *Journal of Geophysical Research: Oceans*, 124:1807–1826. [10](#), [72](#), [73](#), [95](#), [96](#)
- Koul, V., Sguotti, C., Årthun, M., Brune, S., Düsterhus, A., Bogstad, B., Ottersen, G., Baehr, J., and Schrum, C. (2021). Skilful prediction of cod stocks in the north and barents sea a decade in advance. *COMMUNICATIONS EARTH & ENVIRONMENT*, 140(2). [1](#), [2](#), [30](#), [96](#), [142](#)
- Koul, V., Tesdal, J., Bersch, M., Hjálmar, H., Brune, S., Borchert, L., Haak, H., Schrum, C., and Baehr, J. (2020). Unraveling the choice of the north atlantic subpolar gyre index. *Sci Rep*, 10:1005. [xiii](#), [9](#), [74](#)
- Kröger, J., Pohlmann, H., Sienz, F., Marotzke, J., Baehr, J., Köhl, A., Modali, K., Polkova, I., Stammer, D., and Vamborg, F. S. (2018). Full-field initialized decadal predictions with the mpi earth system model: An initial shock in the north atlantic. *Climate Dynamics*, 51:2593–2608. [24](#), [25](#), [53](#)
- Kunze, K. N., Vadhera, A., Purbey, R., Singh, H., Kazarian, G. S., and Chahla, J. (2021). Infographics are more effective at increasing social media attention in comparison with original research articles: an altmetrics-based analysis. *Arthroscopy: The Journal of Arthroscopic & Related Surgery*, 37(8):2591–2597. [42](#)
- Lindegren, M. and Brander, K. (2018). Adapting fisheries and their management to climate change: a review of concepts, tools, frameworks, and current progress toward implementation. *Reviews in Fisheries Science & Aquaculture*, 26(3):400–415. [36](#)
- Luisi, M. L., Rodgers, S., and Schultz, J. C. (2019). Experientially learning how to communicate science effectively: A case study on decoding science. *Journal of Research in Science Teaching*, 56(8):1135–1152. [14](#), [39](#), [40](#), [43](#), [44](#)

- Lynam, C. P., Cusack, C., and Stokes, D. (2010). A methodology for community-level hypothesis testing applied to detect trends in phytoplankton and fish communities in irish waters. *Estuarine, Coastal and Shelf Science*, 87(3):451–462. 31
- Madrigal-González, J., Ballesteros-Cánovas, J. A., Herrero, A., Ruiz-Benito, P., Stoffel, M., Lucas-Borja, M. E., Andivia, Enrique and Sancho-García, C., and Zavala, M. A. (2017). Forest productivity in southwestern europe is controlled by coupled north atlantic and atlantic multidecadal oscillations. *Nature Communications*, pages 1–8. 20
- Maher, N., Milinski, S., Suarez-Gutierrez, L., Botzet, M., Dobrynin, M., Kornblueh, L., Kröger, J., Takano, Y., Ghosh, R., Hedemann, C., Li, C., Li, H., Manzini, E., Notz, D., Putrasahan, D., Boysen, L., Claussen, M., Ilyina, T., Olonscheck, D., Raddatz, T., Stevens, B., and Marotzke, J. (2019). The Max Planck Institute Grand Ensemble: Enabling the Exploration of Climate System Variability. *J. Adv. Model. Earth Syst.*, 11(7):2050–2069. 73, 76
- Mann, K. and Drinkwater, K. (1994). Environmental influences on fish and shellfish production in the northwest atlantic. *Environmental Reviews*, 2(1):16–32. 12, 13, 36, 37
- Mariotti, A., Baggett, C., Barnes, E. A., Becker, E., Butler, A., Collins, D. C., Dirmeyer, P. A., Ferranti, L., Johnson, N. C., Jones, J., et al. (2020). Windows of opportunity for skillful forecasts subseasonal to seasonal and beyond. *Bulletin of the American Meteorological Society*, 101(5):E608–E625. 3
- Marotzke, J., Müller, W. A., Vamborg, F. S. E., Becker, P., Cubasch, U., Feldmann, H., Kaspar, F., Kottmeier, C., Marini, C., Polkova, I., Prömmel, K., Rust, H. W., Stammer, D., Ulbrich, U., Kadow, C., Köhl, A., Kröger, J., Kruschke, T., Pinto, J. G., Pohlmann, H., Reyers, M., Schröder, M., Sienz, F., Timmreck, C., and Ziese, M. (2016). A national research project on decadal climate prediction. *American Meteorological Society*, 97:2379–2394. 6

- Marshall, J., Johnson, H., and Goodman, J. (2001). A Study of the Interaction of the North Atlantic Oscillation with Ocean Circulation. *J. Climate*, 14(7):1399 – 1421. [13](#), [20](#), [37](#)
- Mason, J. G., Woods, P. J., Thorlacius, M., Guðnason, K., Saba, V. S., Sullivan, P. J., and Kleisner, K. M. (2021). Projecting climate-driven shifts in demersal fish thermal habitat in iceland’s waters. *ICES Journal of Marine Science*, 78(10):3793–3804. [2](#), [30](#), [31](#), [33](#)
- Mauritsen, T., Bader, J., Becker, T., Behrens, J., Bittner, M., Brokopf, R., Brovkin, V., Claussen, M., Crueger, T., Esch, M., Fast, I., Fiedler, S., Fläschner, D., Gayler, V., Giorgetta, M., Goll, D. S., Haak, H., Hagemann, S., Hedemann, C., Hohenegger, C., Ilyina, T., Jahns, T., Jimenéz-de-la Cuesta, D., Jungclaus, J., Kleinen, T., Kloster, S., Kracher, D., Kinne, S., Kleberg, D., Lasslop, G., Kornbluh, L., Marotzke, J., Matei, D., Meraner, K., Mikolajewicz, U., Modali, K., Möbis, B., Müller, W. A., Nabel, J. E. M. S., Nam, C. C. W., Notz, D., Nyawira, S.-S., Paulsen, H., Peters, K., Pincus, R., Pohlmann, H., Pongratz, J., Popp, M., Raddatz, T. J., Rast, S., Redler, R., Reick, C. H., Rohrschneider, T., Schemann, V., Schmidt, H., Schnur, R., Schulzweida, U., Six, K. D., Stein, L., Stemmler, I., Stevens, B., von Storch, J.-S., Tian, F., Voigt, A., Vrese, P., Wieners, K.-H., Wilkenskjaeld, S., Winkler, A., and Roeckner, E. (2019). Developments in the MPI-M Earth System Model version 1.2 (MPI-ESM1.2) and Its Response to Increasing CO₂. *J. Adv. Model. Earth Syst.*, 11(4):998–1038. [52](#), [75](#)
- Meehl, G. A., Goddard, L., Boer, G., Burgman, R., Branstator, G., Cassou, C., Corti, S., Danabasoglu, G., Doblas-Reyes, F., Hawkins, E., et al. (2014). Decadal climate prediction: an update from the trenches. *Bulletin of the American Meteorological Society*, 95(2):243–267. [x](#), [2](#), [26](#)
- Meehl, G. A., Richter, J. H., Teng, H., Capotondi, A., Cobb, K., Doblas-Reyes, F., Donat, M. G., England, M. H., Fyfe, J. C., Han, W., et al. (2021). Initialized earth system prediction from subseasonal to decadal timescales. *Nature Reviews Earth & Environment*, 2(5):340–357. [46](#), [48](#), [49](#), [50](#), [51](#), [53](#)

- Menary, M. B. and Hermanson, L. (2018). Limits on determining the skill of north atlanticocean decadal predictions. *Nature Communications*, 9(1):1694. [26](#), [27](#)
- Menary, M. B., Mignot, J., and Robson, J. (2021). Skilful decadal predictions of subpolar north atlantic ssts using cmip model-analogues. *Environmental Research Letters*, 16(6):064090. [27](#)
- Merryfield, W. J., Baehr, J., Batté, L., Becker, E. J., Butler, A. H., Coelho, C. A., Danabasoglu, G., Dirmeyer, P. A., Doblas-Reyes, F. J., Domeisen, D. I., et al. (2020). Current and emerging developments in subseasonal to decadal prediction. *Bulletin of the American Meteorological Society*, 101(6):E869–E896. [23](#), [25](#), [26](#)
- Miesner, A. K. and Payne, M. R. (2018). Oceanographic variability shapes the spawning distribution of blue whiting (*micromesistius poutassou*). *Fisheries Oceanography*, 27:623–638. [32](#), [36](#), [96](#), [150](#)
- Moat, B. I., Sinha, B., Josey, S. A., Robson, J., Ortega, P., Sévellec, F., Holliday, P., McCarthy, G. D., New, A. L., and Hirschi, J. J. M. (2019). Insights into decadal north atlantic sea surface temperature and ocean heat content variability from an eddy-permitting coupled climate model. *Journal of Climate*, 32:6137–6161. [23](#)
- Moritz, M., Jochumsen, K., Kieke, D., Klein, B., Klein, H., Kollner, M., and Rhein, M. (2021). Volume transport time series and variability of the north atlantic eastern boundary current at goban spur. *Journal of Geophysical Research: Oceans*, 126. [20](#), [73](#)
- Muir, L. C. and Fedorov, A. V. (2015). How the amoc affects ocean temperatures on decadal to centennial timescales: the north atlantic versus an interhemispheric seesaw. *Climate Dynamics*, 45:151–160. [7](#), [21](#), [22](#)
- Müller, W. A., Baehr, J., Haak, H., Jungclaus, J. H., Kröger, J., Matei, D., Notz, D., Pohlmann, H., von Storch, J. S., and Marotzke, J. (2012). Forecast skill of multi-year seasonal means in the decadal prediction system of the max planck institute for meteorology. *Geophysical Research Letters*, 39(22). [28](#), [114](#)

-
- Negrete, A. and Lartigue, C. (2004). Learning from education to communicate science as a good story. *Endeavour*, 28(3):120–124. [41](#)
- Nelson, M., Zak, K., Davine, T., and Pau, S. (2016). Climate change and food systems research: current trends and future directions. *Geography Compass*, 10(10):414–428. [12](#), [13](#), [36](#)
- Nerger, L. and Hiller, W. (2013). Software for ensemble-based data assimilation systems - Implementation strategies and scalability. *Comput. Geosci.*, 55:110–118. [75](#)
- Olonscheck, D., Suarez-Gutierrez, L., Milinski, S., Beobide-Arsuaga, G., Baehr, J., Fröb, F., Hellmich, L., Ilyina, T., Kadow, C., Krieger, D., Li, H., Marotzke, J., Plésiat, É., Schupfner, M., Wachsmann, F., Wieners, K.-H., and Brune, S. (2023). The new Max Planck Institute Grand Ensemble with CMIP6 forcing and high-frequency model output. *under review for JAMES*. [76](#)
- Olson, J. (2011). Understanding and contextualizing social impacts from the privatization of fisheries: An overview. *Ocean & Coastal Management*, 54(5):353–363. [11](#), [35](#)
- Önskog, T., Franzke, C. L. E., and Hannachi, A. (2018). Predictability and non-gaussian characteristics of the north atlantic oscillation. *Journal of Climate*, 31:537–554. [20](#)
- O’Reilly, L., Fentimen, R., Butschek, F., J., T., Lim, A., Moore, N., O’Connor, O., Appah, J., Harris, K., Vennemann, T., and Wheeler, A. (2022). Environmental forcing by submarine canyons: Evidence between two closely situated cold-water coral mounds (porcupine bank canyon and western porcupine bank, ne atlantic). *Marine Geology*, 454:106930. [73](#), [74](#)
- Otten, J. J., Cheng, K., and Drewnowski, A. (2015). Infographics and public policy: using data visualization to convey complex information. *Health Affairs*, 34(11):1901–1907. [42](#)

- Paradis, A., Pepin, P., and Brown, J. (1996). Vulnerability of fish eggs and larvae to predation: review of the influence of the relative size of prey and predator. *Canadian Journal of Fisheries and Aquatic Sciences*, 53(6):1226–1235. [31](#), [37](#)
- Parker, T., Woollings, T., Weisheimer, A., O’Reilly, C., Baker, L., and Shaffrey, L. (2019). Seasonal predictability of the winter north atlantic oscillation from a jet stream perspective. *Geophysical Research Letters*, 46:10,159–10,167. [21](#)
- Pauly, D., Christensen, V., Gu enette, S., Pitcher, T. J., Sumaila, U. R., Walters, C. J., Watson, R., and Zeller, D. (2002). Towards sustainability in world fisheries. *Nature*, 418(6898):689–695. [35](#)
- Payne, M., Kudahl, M., Engelhar, G. H., Peck, M. A., and Pinnegar, J. K. (2021). Climate risk to european fisheries and coastal communities. *PNAS*, 118(40):e2018086118. [1](#), [2](#)
- Payne, M. R., Danabasoglu, G., Keenlyside, N., Matei, D., Miesner, A. K., Yang, S., and Yeager, S. G. (2022). Skilful decadal-scale prediction of fish habitat and distribution shifts. *Nature Communications*, 13(1):2660. [29](#), [30](#), [31](#), [50](#)
- Payne, M. R., Hobday, A. J., MacKenzie, B. R., Tommasi, D., Dempsey, D. P., F assler, S. M. M., Haynie, A. C., Ji, R., Liu, G., Lynch, P. D., Matei, D., Miesner, A. K., Mills, K. E., Strand, K. O., and Villarino, E. (2017). Lessons from the first generation of marine ecological forecast products. *Frontiers in Marine Science*, 4. [24](#), [25](#)
- Peings, Y., Simpkins, G., and Magnusdottir, G. (2016). Multidecadal fluctuations of the north atlantic ocean and feedback on the winter climate in cmip5 control simulations. *Journal of Geophysical Research: Atmospheres*, 121:2571–2592. [21](#), [22](#), [25](#), [26](#)
- Pitois, S. G., Lynam, C. P., Jansen, T., Halliday, N., and Edwards, M. (2012). Bottom-up effects of climate on fish populations: data from the continuous plankton recorder. *Marine Ecology Progress Series*, 456:169–186. [31](#)
- Pohlmann, H., Mueller, W. A., Kulkarni, K., Kameswarrao, M., Matei, D., Vamborg, F., Kadow, C., Illing, S., and Marotzke, J. (2013). Improved forecast

- skill in the tropics in the new mklip decadal climate predictions. *Geophysical Research Letters*, 40(21):5798–5802. [28](#), [114](#)
- Polkova, I., Köhl, A., and Stammer, D. (2019). Climate-mode initialization for decadal climate predictions. *Climate Dynamics*, 53:7097–7111. [75](#)
- Reid, D. G. (2001). Sefos—shelf edge fisheries and oceanography studies: an overview. *Fisheries Research*, 50(1-2):1–15. [38](#), [55](#), [141](#)
- Robson, J., Polo, I., Hodson, D. L., Stevens, D. P., and Shaffrey, L. C. (2018). Decadal prediction of the north atlantic subpolar gyre in the higem high-resolution climate model. *Climate dynamics*, 50:921–937. [23](#), [26](#), [27](#)
- Rose, G. A. and Leggett, W. C. (1990). The importance of scale to predator-prey spatial correlations: an example of atlantic fishes. *Ecology*, 71(1):33–43. [31](#), [37](#)
- Sandø, A. B., Johansen, G. O., Algen, A., Stiansen, J. E., and Renner, A. H. H. (2020). Climate change and new potential spawning sites for northeast arcticcod. *Frontiers in Marine Science*, 7:28. [2](#)
- Scheufele, D. A. and Krause, N. M. (2019). Science audiences, misinformation, and fake news. *Proceedings of the National Academy of Sciences*, 116(16):7662–7669. [43](#)
- Schuster, M., Grieger, J., Richling, A., Schartner, T., Illing, S., Kadow, C., Müller, W. A., Pohlmann, H., Pfahl, S., and Ulbrich, U. (2019). Improvement in the decadal prediction skill of the northern hemisphere extra-tropical winter circulation through increased model resolution. *Earth System Dynamics Discuss*, 10:171–187. [2](#), [3](#), [48](#), [50](#)
- Sgubin, G., Swingedouw, D., Borchert, L. F., Menary, M. B., Noël, T., Loukos, H., and Mignot, J. (2021). Systematic investigation of skill opportunities in decadal prediction of air temperature over europe. *Climate Dynamics*, 57(11-12):3245–3263. [3](#), [22](#), [26](#)
- Shaffrey, L. C., Hodson, D., Robson, J., Stevens, D. P., Hawkins, E., Polo, I., Stevens, I., Sutton, R. T., Lister, G., Iwi, A., Smith, D., and Stephens, A.

- (2017). Decadal predictions with the higem high resolution global coupled climate model: description and basic evaluation. *Climate Dynamics*, 48:297–311. [3](#)
- Silver, J. J. and Hawkins, R. (2017). “i’m not trying to save fish, i’m trying to save dinner”: Media, celebrity and sustainable seafood as a solution to environmental limits. *Geoforum*, 84:218–227. [33](#), [151](#)
- Smith, D., Eade, R., Scaife, A., Caron, L., Danabasoglu, G., DelSole, T., Delworth, T., Doblas-Reyes, F., Dunstone, N., Hermanson, L., et al. (2019). Robust skill of decadal climate predictions. *Climate and Atmospheric Science*. [2](#), [11](#), [14](#), [28](#)
- Stenseth, N. C., Mysterud, A., Ottersen, G., Hurrell, J. W., Chan, K.-S., and Lima, M. (2002). Ecological effects of climate fluctuations. *Science*, 297(5585):1292–1296. [37](#)
- Stevens, B. et al. (2013). Atmospheric component of the MPI-M Earth System Model: ECHAM6. *J. Adv. Mod. Earth Sys.*, 5(2):146–172. [52](#), [75](#)
- Sumby, J., Haward, M., Fulton, E. A., and Pecl, G. T. (2021). Hot fish: The response to climate change by regional fisheries bodies. *Marine Policy*, 123:104284. [11](#)
- Sun, C., Li, J., and Jin, F. (2015a). A delayed oscillator model for the quasi-periodic multidecadal variability of the nao. *Climate Dynamics*, 45:2083–2099. [20](#)
- Sun, C., Li, J., and Zhao, S. (2015b). Remote influence of atlantic multidecadal variability on siberian warm season precipitation. *Scientific Reports*, 5(1):16853. [20](#), [22](#), [23](#)
- Sutton, R., McCarthy, G. D., Robson, J., Sinha, B., Archibald, A., and Gray, L. (2018). Atlantic multidecadal variability and the uk acsis program. *Bulletin of the American Meteorological Society*, 99(2):415–425. [8](#), [22](#), [23](#)
- Symes, D., Phillipson, J., and Salmi, P. (2015). Europe’s coastal fisheries: Instability and the impacts of fisheries policy. *Sociologia Ruralis*, 55(3):245–257. [11](#), [12](#), [33](#)

- Taylor, K. E., Stouffer, R. J., and Meehl, G. A. (2012). An Overview of CMIP5 and the Experiment Design. *Bull. Amer. Meteor. Soc.*, 93(4):485–498. [72](#), [76](#)
- Thoma, M., Greatbatch, R. J., Kadow, C., and Gerdes, R. (2015). Decadal hindcasts initialized using observed surface wind stress: Evaluation and prediction out to 2024. *Geophysical Research Letters*, 42:6454–6461. [50](#), [51](#)
- Uppala, S. M., Kållberg, P. W., Simmons, A. J., Andrae, U., Bechtold, V. D. C., Fiorino, M., Gibson, J. K., Haseler, J., Hernandez, A., Kelly, G. A., Li, X., Onogi, K., Saarinen, S., Sokka, N., Allan, R. P., Andersson, E., Arpe, K., Balmaseda, M. A., Beljaars, A. C. M., Berg, L. V. D., Bidlot, J., Bormann, N., Caires, S., Chevallier, F., Dethof, A., Dragosavac, M., Fisher, M., Fuentes, M., Hagemann, S., Hólm, E., Hoskins, B. J., Isaksen, I., Janssen, P. A. E. M., Jenne, R., McNally, A. P., Mahfouf, J.-F., Morcrette, J.-J., Rayner, N. A., Saunders, R. W., Simon, P., Sterl, A., Trenberth, K. E., Untch, A., Vasiljevic, D., Viterbo, P., and Woollen, J. (2005). The ERA-40 re-analysis. *Quart. J. Roy. Meteor. Soc.*, 131(612):2961–3012. [75](#)
- Urquhart, J., Acott, T., and Zhao, M. (2013). Introduction: social and cultural impacts of marine fisheries. *Marine Policy*, 37:1–2. [32](#), [33](#)
- Van Der Bles, A. M., van der Linden, S., Freeman, A. L., and Spiegelhalter, D. J. (2020). The effects of communicating uncertainty on public trust in facts and numbers. *Proceedings of the National Academy of Sciences*, 117(14):7672–7683. [43](#)
- van Oldenborgh, G. J., Doblas-Reyes, F. J., Wouters, B., and Hazeleger, W. (2012). Decadal prediction skill in a multi-model ensemble. *Climate dynamics*, 38:1263–1280. [27](#), [28](#)
- Vecchi, G. A. and Delworth, Thomas, L. (2017). Origins of atlantic decadal swings. *Journal of Nature*, 548:284–285. [xiii](#), [8](#), [23](#)
- Vega, A., Miller, A. C., and O’Donoghue, C. (2014). Economic impacts of seafood production growth targets in ireland. *Marine Policy*, 47:39–45. [33](#)

- Volpi, D., Guemas, V., Doblas-Reyes, F. J., Hawkins, E., and Nichols, N. K. (2017). Decadal climate prediction with a refined anomaly initialisation approach. *Climate Dynamics*, 48:1841–1853. 3, 48
- Wang, Y., Magnúsdóttir, G., Stern, H., Tian, X., and Yu, Y. (2014). Uncertainty estimates of the eof-derived north atlantic oscillation. *Journal of Climate*, 27:1290–1301. 53, 76
- Weingart, P. and Guenther, L. (2016). Science communication and the issue of trust. *Journal of Science communication*, 15(05):C01. 41
- Wen, N., Frankignoul, C., and Gastineau, G. (2016). Active amoc-nao coupling in the ipsl-cm5a-mr climate model. *Climate Dynamics*, 47:2105–2119. 26
- Wetzel, P., Haak, H., Jungclauss, J., and Maier-Reimer, E. (2004). *The Max-Planck-institute global ocean/sea ice model*. Model MPI-OM Technical report. Retrieved From <http://www.mpimet.mpg.de> 47
- White, M. and Bowyer, P. (1997). The shelf-edge current north-west of ireland. *Annales Geophysicae*, 15:1076–1083. 73
- Wilder, M. (1995). Quota systems in international wildlife and fisheries regimes. *The Journal of Environment & Development*, 4(2):55–104. 11, 32, 34
- Wong, A. P. S., Wijffels, S. E., Riser, S. C., Pouliquen, S., Hosoda, S., Roemmich, D., Gilson, J., Johnson, G. C., Martini, K., Murphy, D. J., Scanderbeg, M., Bhaskar, T. V. S. U., Buck, J. J. H., Merceur, F., Carval, T., Maze, G., Cabanes, C., André, X., Poffa, N., Yashayaev, I., Barker, P. M., Guinehut, S., Belbéoch, M., Ignaszewski, M., Baringer, M. O., Schmid, C., Lyman, J. M., McTaggart, K. E., Purkey, S. G., Zilberman, N., Alkire, M. B., Swift, D., Owens, W. B., Jayne, S. R., Hersh, C., Robbins, P., West-Mack, D., Bahr, F., Yoshida, S., Sutton, P. J. H., Cancouët, R., Coatanoan, C., Dobbler, D., Juan, A. G., Gourrion, J., Kolodziejczyk, N., Bernard, V., Bourlès, B., Claustre, H., D’Ortenzio, F., Le Reste, S., Le Traon, P.-Y., Rannou, J.-P., Saout-Grit, C., Speich, S., Thierry, V., Verbrugge, N., Angel-Benavides, I. M., Klein, B., Notarstefano, G., Poulain, P.-M., Vélez-Belchí, P., Suga, T., Ando, K., Iwasaka, N., Kobayashi,

- T., Masuda, S., Oka, E., Sato, K., Nakamura, T., Sato, K., Takatsuki, Y., Yoshida, T., Cowley, R., Lovell, J. L., Oke, P. R., van Wijk, E. M., Carse, F., Donnelly, M., Gould, W. J., Gowers, K., King, B. A., Loch, S. G., Mowat, M., Turton, J., Rama Rao, E. P., Ravichandran, M., Freeland, H. J., Gaboury, I., Gilbert, D., Greenan, B. J. W., Ouellet, M., Ross, T., Tran, A., Dong, M., Liu, Z., Xu, J., Kang, K., Jo, H., Kim, S.-D., and Park, H.-M. (2020). Argo Data 1999-2019: Two Million Temperature-Salinity Profiles and Subsurface Velocity Observations From a Global Array of Profiling Floats. *Front. Mar. Sci.*, 7. 96
- Xin, X., Xue, W., Zhang, M., Li, H., Zhang, T., and Zhang, J. (2015). How much of the nao monthly variability is from ocean-atmospheric coupling: results from an interactive ensemble climate model. *Climate Dynamics*, 44:781–790. 20
- Yan, X., Zhang, R., and Knutson, T. R. (2019). A multivariate amv index and associated discrepancies between observed and cmip5 externally forced amv. *Geophysical Research Letters*, 46(8):4421–4431. 20, 22, 26
- Yeager, S. (2015). Topographic Coupling of the Atlantic Overturning and Gyre Circulations. *J. Phys. Oceanogr.*, 45(5):1258 – 1284. 20
- Yeager, S. G. and Robson, J. (2017). Recent progress in understanding and predicting atlantic decadal climate variability. *Current Climate Change Reports*, 3:112–127. 24, 28
- Zhai, X., Johnson, H. J., and Marshall, D. P. (2014). A simple model of the response of the atlantic to the north atlantic oscillation. *Journal of Climate*, 27:4052–4069. 21, 25
- Zimmermann, F., Claireaux, M., and Enberg, K. (2019). Common trends in recruitment dynamics of north-east atlantic fish stocks and their links to environment, ecology and management. *Fish and Fisheries*, 20(3):518–536. 32